REACTIVE AND ‘CLICKABLE’ HYDROPHILIC NANOFIBERS AS NOVEL BIOMATERIALS

by

Özlem İpek Kalaoğlu Altan

M.S., Polymer Science and Technology, Istanbul Technical University, 2010

B.S., Chemistry, Istanbul Technical University, 2008

Submitted to the Institute for Graduate Studies in
Science and Engineering in partial fulfillment of
the requirements for the degree of
Doctor of Philosophy

Graduate Program in Chemistry

Boğaziçi University

2017

REACTIVE AND ‘CLICKABLE’ HYDROPHILIC NANOFIBERS AS NOVEL BIOMATERIALS

APPROVED BY:

Prof. Rana Sanyal ……...
(Thesis Supervisor)

Prof. Amitav Sanyal ……
(Thesis Co-Supervisor)

Prof. İlknur Doğan ……

Assist. Prof. Oktay Demircan ……

Prof. Gürkan Hızal ……

Prof. E. Dilara Koçak ……

DATE OF APPROVAL:

To Doruk Kaan

ACKNOWLEDGMENTS

I owe my deepest gratitude to my thesis supervisor Prof. Rana Sanyal and my thesis co-advisor Prof. Amitav Sanyal for their kind interest, mentoring and support. Their scientific guidance improved my thesis projects and helped me to gain an innovative point of view towards science. I appreciate their encouraging attention and the way they prepared us to the future life. It is a pleasure to also acknowledge Prof. Karen De Clerck, Prof. Richard Hoogenboom and his group for their collaboration. I would like to extend my thanks to my committee members, Prof. İlknur Doğan, Assist. Prof. Oktay Demircan, Prof. Gürkan Hızal and Prof. Emine Dilara Koçak for their valuable time to review and evaluate my work. I am also thankful to Assoc. Prof. Stefan Fuss for his help in taking the confocal microscopy images.

I am deeply grateful to Tuğçe Nihal Gevrek for her contribution to my research, her valuable friendship and the unforgettable memories we collected during our PhD period which will increasingly continue for sure. I also thank to Burcu Sümer for cell culture studies and to Azize Kıraç for the synthesis of TEG-containing cyclic carbonate monomer.

I would like to extend my thanks to my current labmates Filiz Çalık, Merve Şimşek, Yavuz Öz, Laura Chambre, Büşra Cengiz, Merve Karaçivi, Elif Kağa, Duygu Aydin, Aysun Değirmenci, İsmail Altınbaşak, Bianca Golba, Rüveyda Kılıç and Nehir Kavak for the great time we spent and their friendship. I would also thank to my former labmates Özgül Gök, Melike Eceoğlu, Merve Coşar, Nergiz Cengiz, Sadık Kağa, Mehmet Arslan, Betül Bingöl, Merve Yaman and Yasemin Yüksekdağ for their friendship and particularly to Nazlı Böke and Pelin Ertürk for being among my best friends and the amazing time we are still spending together.

My special thanks are for my family for their great support and encouragement throughout my education life and for their endless love. I would like to thank in particular to my mother and husband for taking care of my son while I was working in the laboratory or on the computer and also for putting up with me at this stressful period. I am also grateful to my husband for his enormous help in formatting my thesis. My deepest thanks

are for my son, Doruk Kaan, for being so well-behaved and patient during this period and letting me steal from our precious time together.

This research has been supported by The Scientific and Technological Research Council of Turkey (TUBITAK, Project No. 114Z139) and Ministry of Development of Turkey, Grant No. 2009K120520. I would also like to thank to the graduate scholarship program of TUBITAK BIDEB 2211-A for the financial support during my PhD program.

ABSTRACT

REACTIVE AND 'CLICKABLE' HYDROPHILIC NANOFIBERS AS NOVEL BIOMATERIALS

Among many other nanomaterials, polymeric nanofibers have gained attraction in biomedical applications due to their unique properties such as high surface area, porosity and physical resemblance to the extracellular matrix. Electrospinning is the most commonly used method for producing nanofibers due to its low-cost, simplicity and efficiency. These nanofibers usually need to be modified with a biological material for bioapplications in order to enhance their biocompatibility, cell-adhesivity and stimuli-responsivity. Recently, 'click' chemistry, in particular metal-free click reactions, has emerged as a preferred method for the functionalization of electrospun nanofibers as it enables efficient and orthogonal functionalization under mild reaction conditions. In this thesis, clickable polymers with various reactive groups were designed and electrospun into reactive nanofibers which were aimed to be used for the reagent-free (bio)functionalization of nanofibers under mild reaction conditions. In the first project, furan-bearing acrylate-based non-biodegradable nanofibers were produced and modified with maleimide-containing fluorescent dye and biotin ligand via Diels-Alder reaction. In the second project, maleimide-containing acrylate-based non-biodegradable nanofibers were obtained and photo-patterned. The patterned nanofibers were biofunctionalized with a thiol-bearing oligonucleotide via Michael reaction, followed with hybridization with its complementary sequence. The third project involved the *in situ* crosslinking of polyoxazoline-based nanofibers. The alkene unit on the polymer was used for modification of the crosslinked nanofibers via thiol-ene reaction. In the fourth project, furan-bearing biodegradable polylactide nanofibers were produced and modified with a maleimide-containing RGD peptide via Diels-Alder reaction, followed by cell culture on the modified nanofibers. In the last project, dual-functional biodegradable polylactide nanofibers were obtained and modified with fluorescent dyes and biomolecules using strain-promoted azide-alkyne cycloaddition and inverse electron-demand Diels-Alder reaction.

ÖZET

YENİ BİYOMATERYALLER OLARAK REAKTİF VE KLİK KİMYASINA UYGUN HİDROFİLİK NANOLİFLER

Polimerik nanolifler yüksek yüzey alanı, porozite, ve doğal ekstraselülar matrikse olan fiziksel benzerlik gibi eşsiz özellikleri nedeniyle, diğer nanomalzemelere kıyasla biyomedikal uygulamalarda ilgi odağı olmaktadırlar. Nanolif üretiminde basit, düşük maliyetli ve verimli olması sebebiyle yaygın olarak elektroçekim yöntemi kullanılmaktadır. Elde edilen nanoliflerin biyouygulamalarda kullanılabilmeleri için biyouyumluluk, hücre yapışkanlığı gibi özelliklerini arttırabilecek biyolojik materyaller ile modifiye edilmeleri gerekmektedir. Son zamanlarda özellikle metal-kataliz içermeyen klik kimyası hafif reaksiyon koşulları altında yüksek verim gösterdiğinden nanoliflerin işlevselleştirilmesi için sıklıkla kullanılan bir method haline gelmiştir. Bu tezde, klik kimyasına uygun çeşitli reaktif gruplar içeren hidrofilik polimerler sentezlenmiş ve bu polimerlerden biyouygulamalarda kullanılmak üzere herhangi bir ayıraç kullanmadan işlevselleştirilebilecek reaktif gruplar içeren nanolifler elde edilmiştir. İlk projede, furan grubu içeren ve biyobozunur olmayan akrilat türevi nanolifler elde edilmiş ve maleimid grubu içeren floresan boya ve biotin ligandı ile Diels-Alder reaksiyonu kullanılarak fonksiyonelleştirilmiştir. İkinci projede, maleimid grubu içeren ve biyobozunur olmayan akrilat türevi nanolifler elde edilmiş, UV ışını altında bir maske ile desenlendirilmiş ve üzerine Michael reaksiyonu aracılığı ile tiyol gubu içeren bir oligonükleotid dizisi bağlanmıştır. Üçüncü projede poliokzazolin bazlı nanolifler *in situ* olarak çapraz bağlanmış, polimerin yan dallarındaki alken üniteleri kullanılarak tiyol-en rekasiyonu ile floresan boya bağlanmıştır. Dördüncü projede, furan grubu içeren biyobozunur nanolifler elde edilmiş, maleimid içeren RGD peptidi ile Diels-Alder reaksiyonu ile modifiye edilerek nanoliflerin üzerinde hücre kültürü çalışmaları yapılmıştır. Son projede, zincir uçlarında çift reaktif grup içeren biyobozunur polilaktid nanofiberleri elde edilmiş, iki ucuna farklı (biyo)moleküller bağlanarak işlevsellik kazandırılmıştır.

TABLE OF CONTENTS

ACKNOWLEDGMENTS iv
ABSTRACT vi
ÖZET vii
LIST OF FIGURES xiv
LIST OF TABLES xxv
LIST OF ACRONYMS/ABBREVIATIONS xxvi
1. INTRODUCTION 1
1.1. Nanofibers and Electrospinning 1
1.2. Electrospinning Parameters 4
1.2.1 Solution Parameters 4
1.2.1.1. Concentration. 4
1.2.1.2. Molecular weight. 5
1.2.1.3. Viscosity of the solution. 5
1.2.1.4. Surface tension. 6
1.2.1.5. Conductivity/surface charge density. 6
1.2.2. Processing Parameters 7
1.2.2.1. Applied voltage. 7
1.2.2.2. Feed rate/flow rate. 7
1.2.2.3. Types of collectors. 8
1.2.2.4. Tip to collector distance. 8
1.2.3. Ambient Parameters 9
1.3. Applications of Nanofibers 10
1.3.1. Scaffolds For Tissue Engineering 11
1.3.2. Wound Healing 12
1.3.3. Drug Delivery 13
1.3.4. Filtration 14
1.3.5. Biosensors 15
1.3.6. Protective Clothing Applications 16
1.3.7. As Affinity Membrane 16
1.3.8. In Cosmetics 17

1.3.9. Energy Generation Applications 17
1.4. Click Chemistry 17
1.4.1. Copper(I)-Catalyzed Azide/Alkyne Cycloaddition 18
1.4.2. Metal-Free Click Reactions 19
1.4.2.1. Copper-free [3+2] cycloaddition reactions of azides with substituted cyclooctyne. 20
1.4.2.2. Thiol-ene reaction. 21
1.4.2.3. Michael addition of thiols. 23
1.4.2.4. Diels–Alder reactions. 25
1.4.2.5. Activated esters. 29
1.5. Surface Modification Techniques of Nanofiber Mesh 30
1.5.1. Plasma Treatment 31
1.5.2. Wet Chemical Method 31
1.5.3. Surface Graft Polymerization 32
1.5.4. Co-electrospinning Of Surface Active Agents And Polymers 32
1.5.5. Physical Adsorption 32
1.5.5.1. Simple physical adsorption. 32
1.5.5.2. Nanoparticles assembly on the surface. 33
1.5.5.3. Layer-by-layer multilayer assembly. 34
1.5.6. Click Chemistry For The Chemical Immobilization Of Nanofibers 34
2. RESEARCH OVERVİEW 41
3. BIOFUNCTIONALIZATION OF FURAN-CONTAINING NON-BIODEGRADABLE NANOFIBERS VIA DIELS-ALDER REACTION 42
3.1. Introduction 42
3.2. Experimental 45
3.2.1. Materials 45
3.2.2. Instrumentation 45
3.2.3. Copolymerization of Furan-Containing Copolymers 46
3.2.3.1. Synthesis of furan-containing copolymer (Poly($PEGMEMA_{20}$-MMA_{45}-$FuMA_{35}$)) 46
3.2.3.2. Synthesis of furan-containing copolymer (Poly($PEGMEMA_{30}$-MMA_{30}-$FuMA_{40}$)) 46

3.2.3.3. Synthesis of furan-containing copolymer (Poly(PEGMEMA$_{40}$-MMA$_{35}$-FuMA$_{25}$))....47
3.2.3.4. Synthesis of furan-containing copolymer (Poly(PEGMEMA$_{50}$-FuMA$_{50}$))....47
3.2.3.5. Synthesis of furan-containing copolymer (Poly(MMA$_{60}$-FuMA$_{40}$))....47
3.2.4. Electrospinning of Furan-Containing Copolymers....48
3.2.5. Fluorescent Dye Conjugation On Furan-Containing Nanofibers....48
3.2.6. Biofunctionalization of Furan-Containing Nanofibers....48
3.2.7. Nanoparticle Immobilization on Furan-Containing Nanofibers....49
3.3. Results and Discussion....49
3.3.1. Fabrication and Characterization of Furan-Containing Hydrophilic Non-Biodegradable Polymers....49
3.3.2. Fabrication and Characterization of Furan-Containing Hydrophilic Non-Biodegradable Nanofibers....52
3.3.3. (Bio)Functionalization of Furan Containing Nanofibers....60
4. BIOFUNCTIONALIZATION OF PATTERNED MALEIMIDE-CONTAINING NON-BIODEGRADABLE NANOFIBERS....64
4.1. Introduction....64
4.2. Experimental....66
4.2.1. Materials....66
4.2.2. Instrumentation....67
4.2.3. Copolymerization of Reactive Copolymers....67
4.2.3.1. Synthesis of furan protected maleimide-containing copolymer (poly(PEGMEMA-MMA-FuMaMA))....67
4.2.3.2. Synthesis of maleimide-containing copolymer (poly(PEGMEMA-MMA-MaMA))....68
4.2.3.3. Synthesis of furan protected maleimide-containing copolymer (poly(MMA-FuMaMA))....68
4.2.3.4. Synthesis of maleimide-containing copolymer (poly(MMA-MaMA))....68
4.2.4. Electrospinning of Maleimide-Containing Copolymers....68
4.2.5. Photo-Patterning and Crosslinking of Maleimide-Containing Nanofibers....69

4.2.6. Dye Conjugation on Maleimide-Containing Patterned Nanofibers 69
4.2.7. Biofunctionalization of Maleimide-Containing Patterned Nanofibers 69
4.3. Results and Discussion 70
4.3.1. Synthesis and Characterization of Maleimide-Containing Hydrophilic Non-Biodegradable Polymers 70
4.3.2. Fabrication and Photo-Patterning of Maleimide-Containing Nanofibers 74
4.3.3. (Bio)Functionalization of Patterned Nanofibers 75
5. MODIFICATION OF *IN SITU* CROSSLINKED POLYOXAZOLINE NANOFIBERS 81
5.1. Introduction 81
5.2. Experimental 84
5.2.1. Materials 84
5.2.2. Instrumentation 84
5.2.3. Synthesis of P(EtOx-co-ButEnOx) 84
5.2.4. Electrospinning and *In Situ* Crosslinking of P(EtOx-co-ButEnOx) Nanofibers 85
5.2.5. Determination of Sulfhydryl Content 85
5.2.6. Fluorescent Dye Immobilization on Crosslinked P(EtOx-co-ButEnOx) Nanofibers via Thiol-Ene Reaction 86
5.2.7. Fluorescent Dye Immobilization on Crosslinked P(EtOx-co-ButEnOx) Nanofibers via Michael Addition 86
5.3. Results and Discussion 86
5.3.1. Fabrication of Crosslinked P(EtOx-co-ButEnOx) Nanofibers 86
5.3.2. Fluorescent Dye Immobilization on Crosslinked P(EtOx-co-ButEnOx) Nanofibers 89
6. BIOFUNCTIONALIZATION OF FURAN-CONTAINING BIODEGRADABLE NANOFIBERS VIA DIELS-ALDER REACTION 94
6.1. Introduction 94
6.2. Experimental 97
6.2.1. Materials 97
6.2.2. Instrumentation 97
6.2.3. Synthesis of TEG-containing Cyclic Carbonate Monomer (MTC-TEG) 98
6.2.3.2. Synthesis of TEG containing diol. 98

6.2.3.3. Synthesis of TEG containing cyclic carbonate monomer (MTC-TEG).....99
6.2.4. Synthesis of Furan-Containing Cyclic Carbonate Monomer (MTC-F).....99
6.2.4.1. Synthesis of furan containing acetal. 99
6.2.4.2. Synthesis of furan containing diol.....99
6.2.4.3. Synthesis of furan containing cyclic carbonate monomer (MTC-F).....100
6.2.5. Synthesis of Furan and TEG-Containing PLLA Copolymers 100
6.2.6. Electrospinning of Furan and TEG-Containing PLLA Copolymers 100
6.2.7. Conjugation of Fluorescent Dye to Furan and TEG-Containing PLLA Nanofibers.....101
6.2.8. Ligand-Directed Immobilization of Protein on Furan and TEG-Containing PLLA Nanofibers 101
6.2.9. Degradation Studies of Furan and TEG-Containing PLLA Nanofibers.....101
6.2.10. Bicinchoninic Acid Protein Quantification of Furan and TEG-Containing PLLA Nanofibers 102
6.2.11. Cell Culture on Furan and TEG-Containing PLLA Nanofibers 102
6.2.12. Cytotoxicity of Furan and TEG-Containing PLLA Nanofibers.....102
6.3. Results and Discussions 103
6.3.1. Synthesis of TEG-Containing Cyclic Carbonate Monomer 103
6.3.2. Synthesis of Furan-Containing Cyclic Carbonate Monomer.....105
6.3.3. Synthesis of Furan and TEG-Containing PLLA Copolymers 106
6.3.4. Fabrication of Furan and TEG-Containing PLLA Nanofibers 110
6.3.5. (Bio)Functionalization, Degradation and Cell Culture Studies of Furan and TEG-Containing PLLA Nanofibers 112
7. MODIFICATION OF DUAL FUNCTIONAL BIODEGRADABLE POLYLACTIDE NANOFIBERS.....118
7.1. Introduction.....118
7.2. Experimental 120
7.2.1. Materials.....120
7.2.2. Instruments.....121
7.2.3. Synthesis of Alkene-Ended PLA (A-PLA) Polymers.....121
7.2.4. Synthesis of Maleimide-Ended PLA (M-PLA) Polymers 122

7.2.5. Synthesis of Alkene-PLA-Azide (A-PLA-N_3) Bifunctional Polymers.....122
7.2.6. Electrospinning of PLA Polymers 122
7.2.7. Fluorescent Dye Conjugation on A-PLA Nanofibers via Thiol-ene Reaction.....123
7.2.8. Fluorescent Dye Conjugation on M-PLA Nanofibers via Michael Reaction.....123
7.2.9. Dual Fluorescent Dye Conjugation on A-PLA-N_3 Nanofibers.....123
7.2.10. PEGylation and Enzyme Immobilization on A-PLA-N_3 Nanofibers 123
7.3. Results and Discussions 124
7.3.1. Synthesis of (Dual)Functional PLA Polymers.....124
7.3.2. Fabrication of (Dual)Functional Nanofibers.....124
7.3.3. Fluorescent Dye Immobilization on (Dual)Functional Nanofibers 129
7.3.4. PEGylation and Biomolecule Immobilization on Dual Functional Nanofibers.....131
8. CONCLUSIONS 134
REFERENCES 136
APPENDIX A: COPYRIGHT NOTICES.....163

LIST OF FIGURES

Figure 1.1. Scanning electron microscope (SEM) image of electrospun fibers enclosing a single human hair (Reproduced with permission from Ref [3]). 1

Figure 1.2. Effect of the applied voltage on the formation of the Taylor cone. 2

Figure 1.3. Schematic illustration of a typical electrospinning apparatus. 3

Figure 1.4. Schematic illustration of the main types of electrospinning collectors (Reproduced with permission from Ref [6]). 4

Figure 1.5. SEM images of concentrations of a) 10% wt, b) 20% wt, c) 25% wt of polystyrene electrospun nanofibers keeping the other parameters the same [9]. 5

Figure 1.6. The effect of solution viscosity on the morphology of fibers. The horizontal edge of each image is 20 μm (Adapted with permission from Ref [13]). 6

Figure 1.7. SEM images of PVA nanofibers with applied voltages (a) 10 kV, (b) 15 kV, (c) 20 kV, having a tip-to-collector distance of 10 cm and concentration of 7 wt % (Reproduced with permission from Ref [17]). 8

Figure 1.8. Different collectors for electrospinning a) static plate b) split electrodes c) rotating drum d) rotating disc e) rotating disc (sharp edge) f) conveyor (Reproduced with permission from Ref [6]). 8

Figure 1.9. SEM images of electrospun polysulfone nanofibers at a tip-to-collector distance of a) 5, b) 10, c) 15 cm [20]. 9

Figure 1.10. Field emission scanning electron microscopy images of electrospun polystyrene fibers under various humidity (a) <25 %, (b) 40-45 %, (c) 60-72 % [22]. 10

Figure 1.11. (a) Percental distribution of the application fields of electrospun nanofibers according to US patents, (b) Application areas of electrospun polymeric nanofibers (Reproduced with permission from Ref [26]). 11

Figure 1.12. An example to a tissue engineering concept which involves cell seeding into porous biomaterial scaffolds (Reproduced with permission from Ref [30]). 12

Figure 1.13. Schematic illustration of (a) main biomolecules present in the wound bed and the healing process, (b) fabrication of nanofibers by electrospinning process, (c) main approaches to prepare electrospun fibers as wound healing scaffolds (Reproduced with permission from Ref [26]). 13

Figure 1.14. Schematic illustration of different methods for drug-loaded nanofiber preparation. (a) Post-treatment (b) Immobilization of drug-loaded nanocarriers (c) Co-electrospinning of drug–polymer blends (d) Coaxial electrospinning (Reproduced with permission from Ref [35]). 14

Figure 1.15. Schematic illustration of fabrication and oligonucleotide sensing mechanisms of a nanocomposite membrane composed of nanofibers and nanoparticles (Reproduced with permission from Ref [44]). 15

Figure 1.16. An example to protective clothing with a nanofibrous breathable barrier membrane [46]. 16

Figure 1.17. Copper-catalyzed azide-alkyne click reaction mechanism (Reproduced with permission from Ref [59]). 18

Figure 1.18. Preparation of hydrophobic polyester-camptothecin conjugate by 'click' cycloaddition (Adapted with permission from Ref [60,61]). 19

Figure 1.19. a) Examples to cyclooctyne derivatives b) The SPAAC click reaction (Adapted with permission from Ref [62]).....20

Figure 1.20. Synthesis of triblock copolymers (Adapted with permission from Ref [67]).....21

Figure 1.21. Mechanism for photoinitiated thiol-ene reaction (Reproduced with permission from Ref [68]). 22

Figure 1.22. Organocatalyzed radical ROP of MAC and thiol-ene modification(Reproduced with permission from Ref [70]). 23

Figure 1.23. a) Base-catalyzed b) Nucleophile-catalyzed Michael addition reaction mechanism (Reproduced with permission from Ref [71]).....24

Figure 1.24. Synthesis of maleimide functional homo- and copolymers and functionalization (Reproduced with permission from Ref [74]).....25

Figure 1.25. Examples to well-known Diels-Alder reactions in polymer and material science (Adapted with permission from Ref [77]).....27

Figure 1.26. One-pot functionalizations of norbornene-functional poly(carbonate)s (Reproduced with permission from Ref [82]).....28

Figure 1.27. Synthetic route for the synthesis of polycarbonate graft copolymers via Diels-Alder reaction (Reproduced with permission from Ref [83]).....29

Figure 1.28. (a) Examples to activated esters (b) activated ester-amine reaction. 30

Figure 1.29. Schematic illustration for the surface modification of nanofibers via (a) plasma treatment/wet chemical methods (b) surface graft polymerization (c) co-electrospinning. 33

Figure 1.30. Schematic illustration for the modification of nanofibers via (a) simple physical adsorption (b) nanoparticle assembly (c) layer-by-layer assembly. ...34

Figure 1.31. Modification of side-chain alkyne-containing PLA nanofibers with an azide-containing biomarker via CUAAC (Adapted with permission from Ref [95]).....36

Figure 1.32. Modification of azide and alkyne-containing PEU nanofibers with alkyne and azide-containing fluorescent dyes, respectively via CUAAC (Adapted with permission from Ref [96,97]). 37

Figure 1.33. Modification of chain-end DIBO-containing (a) PLA with azide-containing peptide, (b) PCL nanofibers with azide-containing fluorcent dye, via SPAAC reaction (Adapted with permission from Ref [98,100]).....38

Figure 1.34. Modification of alkene-containing PEU nanofibers with thiol-containing RGD peptide via thiol-ene reaction (Adapted with permission from Ref [96]).....39

Figure 1.35. Synthesis and modification of active ester containing amine- reactive porous electrospun fibers (Adapted with permission from Ref[102]]…….40

Figure 3.1. Scheme illustrating fabrication and functionalization of nanofibers via Diels-Alder reaction.....44

Figure 3.2. Furan-containing non-biodegradable copolymer synthesis.....50

Figure 3.3. a)^{1}H-NMR spectrum b) Size exclusion chromatography trace of poly(PEGMEMA$_{50}$-FuMA$_{50}$). 50

Figure 3.4. a)^{1}H-NMR spectrum b) Size exclusion chromatography trace of poly(PEGMEMA$_{40}$-MMA$_{35}$-FuMA$_{25}$). 51

Figure 3.5. a)^{1}H-NMR spectrum b) Size exclusion chromatography trace of poly(PEGMEMA$_{30}$-MMA$_{30}$-FuMA$_{40}$). 51

Figure 3.6. a)^{1}H-NMR spectrum b) Size exclusion chromatography trace of poly(PEGMEMA$_{20}$-MMA$_{45}$-FuMA$_{35}$). 52

Figure 3.7. a)^{1}H-NMR spectrum b) Size exclusion chromatography trace of poly(MMA$_{60}$-FuMA$_{40}$). 52

Figure 3.8. SEM images showing the effects of increasing tip-to-collector distance on the average fiber diameter. 54

Figure 3.9. SEM images showing the effects of increasing applied voltage on the average fiber diameter. 55

Figure 3.10. SEM images showing the effects of increasing flow rate on the average fiber diameter. 56

Figure 3.11. SEM images of poly(PEGMEMA20-MMA45-FuMA35) nanofibers obtaining under optimal electrospinning conditions: (a) dry nanofibers and (b) after immersion in water for 3 days. 57

Figure 3.12. SEM images of nanofibers at dry state with compositional ratio of (a) PEGMEMA$_{50}$-FuMA$_{50}$ (b) PEGMEMA$_{40}$-MMA$_{35}$-FuMA$_{25}$ (c) PEGMEMA$_{30}$-MMA$_{30}$-FuMA$_{40}$, after immersion in water with compositional ratio (d) PEGMEMA$_{50}$-FuMA$_{50}$ (e) PEGMEMA$_{40}$-MMA$_{35}$-FuMA$_{25}$ (f) PEGMEMA$_{30}$-MMA$_{30}$-FuMA$_{40}$. 58

Figure 3.13. DSC measurements of MMA$_{60}$-FuMA$_{40}$, PEGMEMA$_{40}$-MMA$_{35}$-FuMA$_{25}$ and PEGMEMA$_{20}$-MMA$_{45}$-FuMA$_{35}$. 59

Figure 3.14. Contact angle measurement and elemental composition via XPS analysis on surface for (a) MMA_{60}-$FuMA_{40}$ nanofibers without PEG-based monomer and (b) $PEGMEMA_{20}$-MMA_{45}-$FuMA_{35}$ nanofibers containing PEG-based monomer. 59

Figure 3.15. Fluorescence microscopy images for the functionalization of furan-containing nanofibers with maleimide-appended fluorescein (inset shows fibers after treatment with fluoresceinamine). 60

Figure 3.16. Fluorescence microscopy images for the functionalization of furan-containing nanofibers with maleimide-appended biotin followed by FITC-Streptavidin immobilization (inset shows fibers without biotinylation). 61

Figure 3.17. Fluorescence microscopy images of FITC-streptavidin exposed (a) non-biotinylated poly($PEGMEMA_{20}$-MMA_{45}-$FuMA_{35}$) nanofibers (b) non-biotinylated poly(MMA_{60}-$FuMA_{40}$) nanofibers to demonstrate anti-biofouling due to presence of PEG. 61

Figure 3.18. (a) Fluorescence microscopy images (b) STEM images for for the functionalization of furan-containing nanofibers with maleimide-appended biotin followed by avidin-coated qdots immobilization (inset shows fibers without biotinylation). 62

Figure 4.2. Synthesis of furan-protected maleimide-containing copolymer (poly(PEGMEMA-MMA-FuMaMA)). 71

Figure 4.3. ^{1}H-NMR spectrum of poly(PEGMEMA-MMA-FuMaMA). 71

Figure 4.4. Synthesis of maleimide-containing copolymer (poly(PEGMEMA-MMA-MaMA)). 72

Figure 4.5. ^{1}H-NMR spectrum of poly(PEGMEMA-MMA-MaMA). 72

Figure 4.6. Synthesis of (poly(MMA-FuMaMA)).....73

Figure 4.7. ^{1}H-NMR spectrum of poly(MMA-FuMaMA). 73

Figure 4.8. Synthesis of (poly(-MMA-MaMA)). 74

Figure 4.9. ^{1}H-NMR spectrum of poly(MMA-MaMA). 74

Figure 4.10. Average water contact angles of (a) poly(MMA-MaMA) (b) poly(PEGMEMA-MMA-MaMA) nanofibers. 75

Figure 4.11. SEM images of poly(PEGMEMA-MMA-MaMA) nanofibers (a) before crosslinking (b) after crosslinking (c) after patterning. 76

Figure 4.12. Fluorecence microscopy images of (a) thiol-containing fluorescent dye (b) amine-containing fluorescent dye immobilization on patterned nanofibers.....77

Figure 4.13. Fluorecence microscopy images of TRITC-Extravidin immobilization on (a) biotinylated (b) non-biotinylated patterned nanofibers. 78

Figure 4.14. Fluorecence microscopy images of fluorescently-labeled DNA immobilization on patterned nanofibers. 79

Figure 4.15. Fluorecence microscopy images of (a) Cy5S1 (b) Cy5-mismatch hybridization on ThiolS1 immobilized patterned nanofibers. 79

Figure 4.16. Confocal microscopy images of Cy5S1 hybridization with a concentration of (a) 2 ng/μL (b) 1/10 dilution (c) 1/100 diution on ThiolS1 immobilized patterned nanofibers (scalebar 50 μm).....80

Figure 5.1. Schematic illustration showing the *in situ* crosslinking and functionalization of P(EtOx-co-ButEnOx) nanofibers. 83

Figure 5.2. SEM images of nanofibers: (a) dry, (b) after immersion in water for 48 h, and (c) change in water contact angle, (d) graph showing the thermoresponsive behavior of the nanofibers probed with change in water contact angle with temperature. 88

Figure 5.3. FT-IR spectra of (a) non-crosslinked (in black) and (b) crosslinked P(EtOx-co-ButEnOx) nanofibers. 88

Figure 5.4. UV spectrum of Ellman's analysis. 89

Figure 5.5. Functionalization of P(EtOx-co-ButEnOx) nanofibers. 90

Figure 5.6. Fluorescence microscopy images of BODIPY-SH treated nanofibers (a) via thiol−ene reaction after, (b) without UV exposure, before N-ethylmaleimide conjugation and (c) rhodamine-maleimide treated nanofibers (insets are controls. 91

Figure 5.7. Photo-patterning of P(EtOx-co-ButEnOx) nanofibers with BODIPY-SH..... 92

Figure 5.8. (a) Step-wise dual functionalization. Fluorescence images of sequentially functionalized nanofibers with (b) rhodamine maleimide, (c) BODIPY-SH, and (d) dual-functionalized (merged image) conditions. 93

Figure 6.1. General scheme for the modification of furan-containing biodegradable nanofiber. 97

Figure 6.2. General scheme for the synthesis of the TEG-containing cyclic carbonate.... 103

Figure 6.3. ^{1}H-NMR spectrum of TEG-containing cyclic carbonate. 104

Figure 6.4. ^{13}C-NMR spectrum of TEG-containing cyclic carbonate 104

Figure 6.5. General scheme for the synthesis of the furan-containing cyclic carbonate. .. 105

Figure 6.7. ^{13}C-NMR spectrum of furan-containing cyclic carbonate. 106

Figure 6.8. Synthesis of TEG and furan-containing hydrophilic biodegradable PLA copolymers. 107

Figure 6.9. ^{1}H-NMR spectrum of furan-containing copolymer.....108

Figure 6.10. ^{1}H-NMR spectrum of furan and 5% TEG-containing copolymer.....108

Figure 6.11. ^{1}H-NMR spectrum of furan and 7.5% TEG-containing copolymer.....109

Figure 6.12. ^{1}H-NMR spectrum of furan and 10 % TEG-containing copolymer.....109

Figure 6.13. SEM images of (a) 0% (b) 5% (c) 7.5% (d) 10% TEG-containing MTC-F/PLA nanofibers. 110

Figure 6.14. DSC thermograms of furan-containing PLLA copolymers with various TEG comonomer ratios. 111

Figure 6.15. Fluorescence microscopy images of FITC-labelled Streptavidin immobilization on non-biotinylated (a) 0 % TEG-containing (b) 5 % TEG-containing (c) 7.5 % TEG-containing MTC-F/PLA nanofibers. 112

Figure 6.16. XPS and water contant angle measurements of (a) MTC-F/PLA (b) MTC-$TEG_{7.5}$-F/PLA nanofibers. 112

Figure 6.17. Fluorescence microscopy images of MTC-$TEG_{7.5}$-F/PLA nanofibers treated with maleimide-containing fluorescent dye (inset shows fibers after treatment with fluoresceinamine). 113

Figure 6.18. Ligand-directed TRITC-Extravidin immobilization on MTC-$TEG_{7.5}$-F/PLA nanofibers and fluorescence microscopy images (Control experiment on non-biotinylated nanofibers is shown as inset). 114

Figure 6.19. SEM micrographs indicating change in morphology of nanofibers with and without TEG units after immersion in PBS at 37 °C for 20 days. 115

Figure 6.20. (a) UV-vis spectra of BCA assay standards and cRGD conjugated MTC-$TEG_{7.5}$-F/PLA nanofibers (b) BCA assay calibration curve. 115

Figure 6.21. (a) Confocal microscopy images of scaffolds showing L929 mouse fibroblasts after 1 and 3 days on (scalebar 50 μm); (b) Cytotoxicity of, non-functionalized and RGD-functionalized nanofibers. 117

Figure 7.1. Schematic illustration of dual functionalization of nanofibers. 120

Figure 7.2. Synthesis of PLA polymers. 125

Figure 7.3. ^{1}H-NMR spectrum of A-PLA. 125

Figure 7.4. ^{1}H-NMR spectrum of M-PLA. 126

Figure 7.5. ^{1}H-NMR spectrum of A-PLA-N_3. 126

Figure 7.6. FT-IR spectra of A-PLA and A-PLA-N_3. 127

Figure 7.7. SEM images of (a) A- PLA (b) M-PLA (c) A-PLA-N_3 nanofibers. 128

Figure 7.8. Fluorescence microscopy images of SAMSA dye conjugation on (a) A-PLA nanofibers via thiol-ene (b) M-PLA nanofibers via Michael reaction (control experiments are shown as insets). 130

Figure 7.9. Fluorescence microscopy images of (a) Cy5-tetrazine immobilized via iedDA (b) DBCO-appended dye conjugation on Cy5-tetrazine immobilized via SPAAC on A-PLA-N3 nanofibers (c) Merged image of A and B. 130

Figure 7.10. Fluorescence microscopy images of FITC-Streptavidin immobilization on non-biotinylated (a) non-PEGylated (b) PEGylated A-PLA-N_3 nanofibers Water contact angles of (c) non-PEGylated (d) PEGylated A-PLA-N_3 nanofibers.....131

Figure 7.11. Fluorescence microscopy images of (a) FITC-streptavidin immobilization on biotinylated (b) Cy5-Biotin conjugation on FITC-streptavidin immobilized, A-PLA-N_3 nanofibers (c) Merged image of A and B. 133

Figure A.1. Copyright permission……..164

LIST OF TABLES

Table 1.1. Properties Of Different Solvents Used İn Electrospinning Process [5].....7

Table 6.1. Summary Of Size Exclusion Chromatography Results For Synthesized Furan-Containing Plas.....107

LIST OF ACRONYMS/ABBREVIATIONS

BODIPY	Boron-dipyrromethene
CCK-8	Cell counting kit-8
$CDCl_3$	Deuterated chloroform
CH_2Cl_2	Dichloromethane
cRGDfK	Cyclic Arginine-Glycine-Aspartic acid-D-Phenyl alanine-Lysine)
CuAAC	Copper-catalyzed Azide-Alkyne Cycloaddition
Da	Dalton
DA	Diels-Alder
DAPI	4',6-diamidino-2-phenylindole
DBU	1,8-Diazabicyclo(5.4.0)undec-7-ene
DCC	*N*,*N'*-Dicyclohexylcarbodiimide
DIBO	Dibenzocyclooctyne
DSC	Differential Scanning Calorimeter
DMAP	4-Dimethylaminopyridine
DMPA	2,2-dimethoxy-2-phenylacetophenone
DMF	Dimethyformamide
ECM	Extracellular Matrix
EDCI	1-Ethyl-3-(3-dimethylaminopropyl)carbodiimide
EtOAc	Ethyl Acetate
FITC	Fluorescein Isothiocynate
FT-IR	Fourier Transform Infrared
FuMA	Furfuryl Methacrylate
FuMaMA	Furan-Protected Maleimide Methacrylate Monomer
GPC	Gel Permeation Chromatography

iedDA	Inverse Electron-Demand Diels-Alder
MeOH	Methanol
MHz	Mega Hertz
MMA	Methyl Methacrylate
NMR	Nuclear Magnetic Resonance
PBS	Phosphate Buffer Saline
PEG	Poly(ethylene glycol)
PEGMEMA	Poly(ethylene glycol) methyl ether methacrylate
PLLA	Polylactide
rDA	Retro Diels-Alder
RGD	Arginylglycylaspartic Acid
ROP	Ring-Opening Polymerization
SAMSA	5-((2(and-3-)-S-(acetylmercapto)succinoyl)amino)
SEC	Size-Exclusion Chromatograpy
SEM	Scanning Electron Microscope
SPAAC	Strain-Promoted Alkyne-Azide Cycloaddition
STEM	Scanning Transmission Electron Microscope
TEA	Triethylamine
TEG	Triethylene glycol
TGA	Thermogravimetric Analysis
THF	Tetrahydrofuran
TLC	Thin Layer Chromatography
TRITC	Tetramethylrhodamine
TU	1-(3,5-bis(trifluoromethyl)phenyl)-3-cyclohexylthiourea
UV	Ultraviolet
V-501	4,4 -Azobis(4-cyanopentanoic acid)
XPS	X-ray Photoelectron Spectroscopy

1. INTRODUCTION

1.1. Nanofibers and Electrospinning

Nanofibers are a unique class among various nanomaterials with diameters in the sub-micron range with several particular properties (Figure 1.1). They have much higher surface area and surface energy compared to bulk materials which enables the enhanced attachment of various (bio)molecules, cells, drugs, etc. The composition of the nanofibers can be varied according to the desired properties and applications from a wide range of polymers. The physical resemblance of the nanofibers to the naturally occuring extracellular matrix is important especially for biomedical applications. Together with high surface-to-volume ratio, nanofibers also have higher porosity than bulk materials which is useful for cell activities easing the cell attachment and nutrient transportation [1,2].

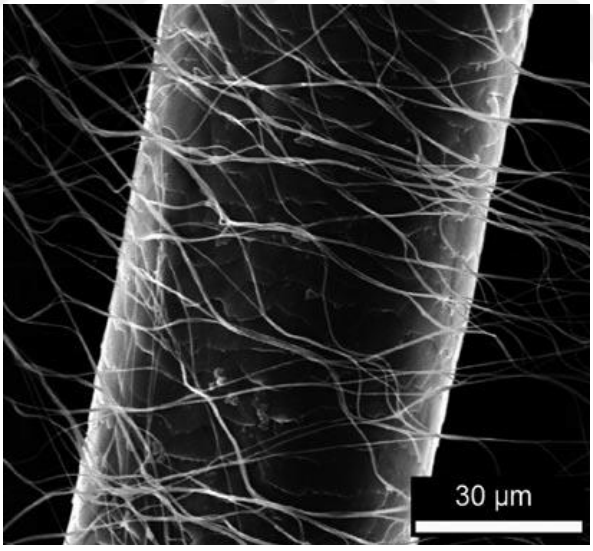

Figure 1.1. Scanning electron microscope (SEM) image of electrospun fibers enclosing a single human hair (Reproduced with permission from Ref [3]).

Among the various processing methods such as drawing, template synthesis and phase separation, electrospinning is the simplest and the most common technique which uses electrical forces to fabricate continuous polymeric fibers with diameters ranging from 2 nm to several micrometers using solutions of both synthetic and natural polymers. Electrospinning is a straight-forward method that allows control over fiber diameter which

can also be scaled up for mass production [4,5]. The term “electrospinning” was derived from “electrostatic spinning". The electrospinning technique was first observed in 1897 by Rayleigh and developed by Zeleny in 1914 on electrospraying. The first patent electrospinning was taken for the electrospinning of cellulose acetate with acetone and monomethyl ether of ethylene glycol as solvents and a voltage of 57 kV by Formhals in 1934, who published a series of other patents from 1934 to 1944. In 1969, Taylor described the conical deformation of the droplet due to electrically driven jet, known as the Taylor cone, which constitutes the basis of the electrospinning. A basic electrospinning setup is composed of a high voltage power supply, a spinneret, a grounded collector (usually a metal plate) and a syringe pump and it can be vertical or horizontal. In the electrospinning process, an electric field of several tens of kVs is applied to a polymer solution or melt held by its surface tension at the end of the spinneret to inject charge of a certain polarity, causing the surface of the droplet to deform into a conical shape, which is known as the Taylor Cone (Figure 1.2).

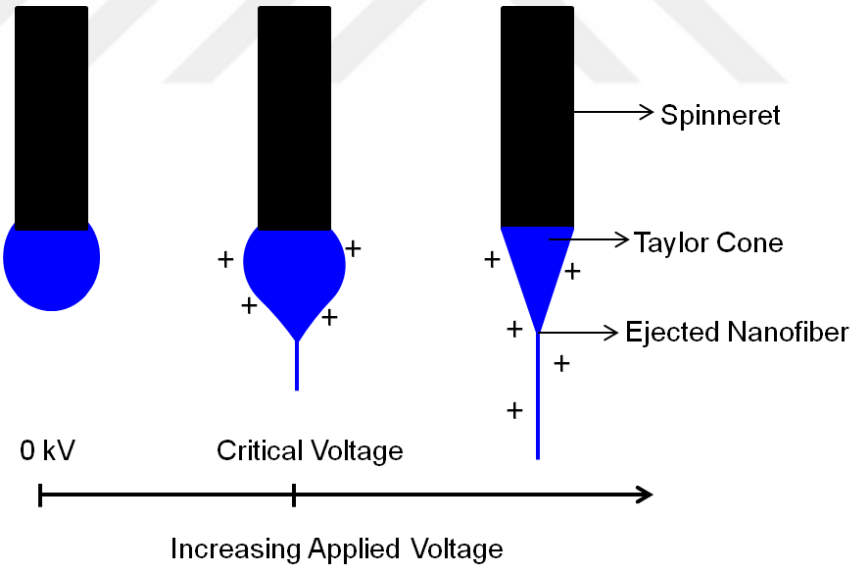

Figure 1.2. Effect of the applied voltage on the formation of the Taylor cone.

When the applied electrical field reaches a critical value, the strong electrical repulsive forces overcome the weaker surface tension forces in the charged polymer solution or melt. Hereafter, a charged jet of the solution or melt is ejected from the tip of the Taylor cone towards the oppositely charged collector with an unstable and a rapid whipping (Figure 1.3). The evaporation of the solvent in the polymer solution occurs in the

distance between the spinneret and the collector leading to the formation of polymeric nanofibers. Electrospinning is conducted at room temperature with atmosphere conditions.

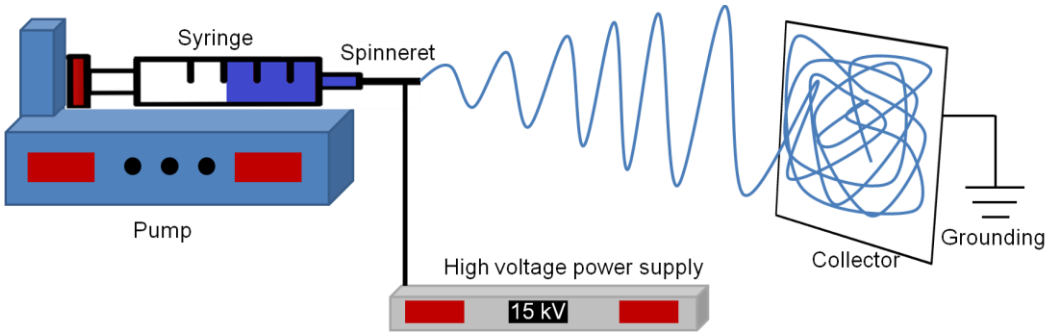

Figure 1.3. Schematic illustration of a typical electrospinning apparatus.

A basic electrospinning setup usually contains a single spinneret (Figure 1.4). In order to increase the volume of production, multi-spinneret components can be inserted to the polymer injection system which can be arranged either in a uniaxial configuration or in a circular geometry [6]. Multi-spinnerets are useful for increasing the overall production, thickness of the mats and deposition area. In this case, the two immiscible solutions can be electrospun from separate spinnerets, resulting in a composite nanofiber. Recently, co-axial electrospinning have also been developed which has potential in biomedical applications [1]. In co-axial electrospinning, a co-axial spinneret with one nozzle inside a larger nozzle is used which delivers two seperate polymer solutions, resulting in core-shell nanofibers. In core-shell nanofibers, biomolecules can be incorporated into the core while the shell can be composed of a more mechanically stable or less degradable polymer which also provides an extra layer of control for a more sustained release profile. The core solution does not need to be electrospinnable as long as the shell solution can provide fibers capable of carrying the core solution.

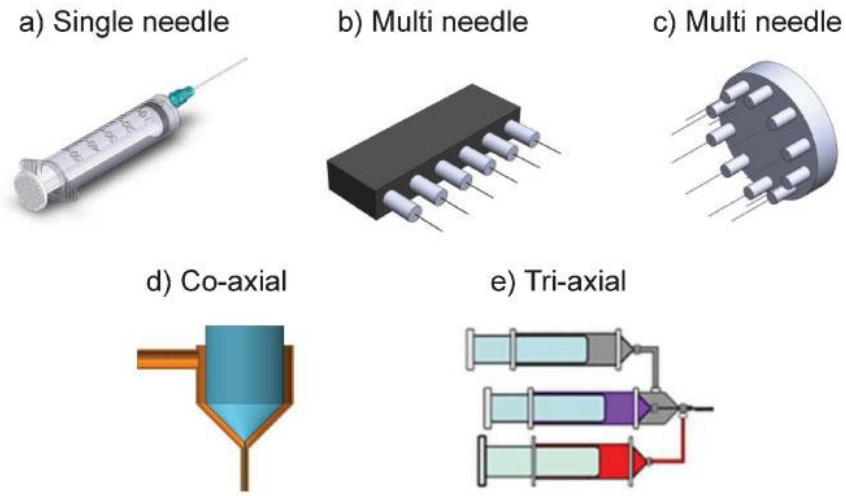

Figure 1.4. Schematic illustration of the main types of electrospinning collectors (Reproduced with permission from Ref [6]).

1.2. Electrospinning Parameters

The electrospinning process is affected by several parameters which can be mainly classified as solution parameters, process parameters, and ambient parameters. Solution parameters include viscosity, conductivity, molecular weight, and surface tension while process parameters are flow rate, applied electric field and tip-to-collector distance. Ambient parameters contain variables such as temperature and humidity. Each of these parameters play a significantly role on the fiber morphology and diameter.

1.2.1 Solution Parameters

1.2.1.1. Concentration. In electrospinning, an optimum solution concentration is necessary for the formation of fibers. It has been shown that beads or a mixture of beads and fibers occur at low solution concentration and the spherical shape of the beads transform into spindle-like fibers as the solution concentration increases and eventually fibers with increased diameters as a result of the higher viscosity resistance (Figure 1.5). There is research which indicates a power law relationship between solution concentration and fiber diameter [7,8].

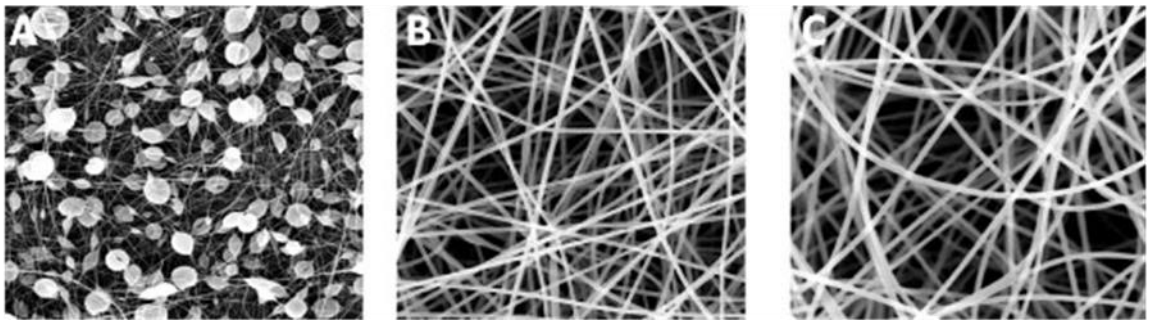

Figure 1.5. SEM images of concentrations of a) 10% wt, b) 20% wt, c) 25% wt of polystyrene electrospun nanofibers keeping the other parameters the same [9].

1.2.1.2. Molecular weight. Molecular weight is another important solution parameter as it affects the solution viscosity with the number of entanglements of polymer chains in a solution which plays an important role in electrospinning [10]. In general, higher molecular weights provide better viscosity which enables the fiber formation. A low molecular weight polymer solution tends to form beads as the desired viscosity can not be reached while a too high molecular weight can result in fibers with very large diameters. It has also been demonstrated that if sufficient intermolecular interactions can be provided, high molecular weights are not always crucial for the electrospinning process. Uyar and coworkers have shown that nanofibers can be obtained from a solution of cyclodextrins [11]. Intermolecular hydrogen bonding and other related interactions hold these molecules that possess no entanglement efficiency in nanofibrous form.

1.2.1.3. Viscosity of the solution. Viscosity is a parameter in relation with polymer concentration and molecular weight. Researchers have found that continuous fiber formation can not be achieved with very low viscosity, only beads or beaded fibers can be obtained (Figure 1.6). On the other hand, very high viscosities also prevents the formation of uniform fibers with very high viscosity as a result of the difficulty in jet ejection from polymer solution. Eventually, there is an optimal viscosity for each polymer solution that gives uniform fibers with the desired diameter [12].

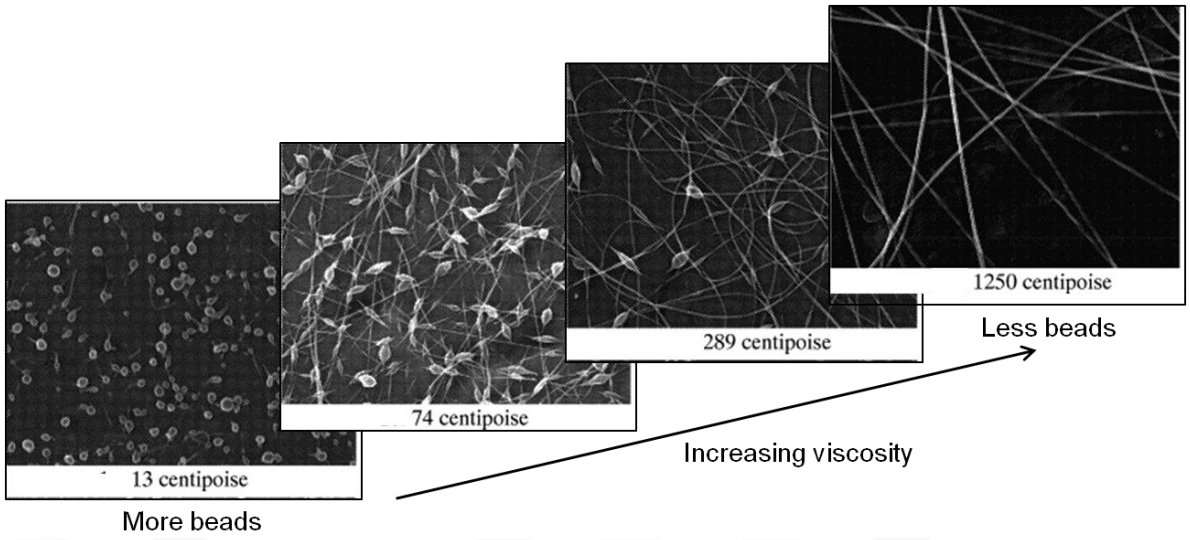

Figure 1.6. The effect of solution viscosity on the morphology of fibers. The horizontal edge of each image is 20 μm (Adapted with permission from Ref [13]).

1.2.1.4. Surface tension. Surface tension is more likely a property of the solvent, and generally uniform fibers without beads can be obtained by reducing the surface tension of a polymer solution. However, a lower surface tension is not always necessary for electrospinning [10,14,15]. The solvent has an important influence on the spinnability since the first step of the electrospinning is preparing a suitable polymer solution. The intermolecular interaction is either repulsive or attractive in a polymer–solvent system which only depends on the solvent. Additionaly, solvent vapour pressure is important in determining the evaporation rate and the drying time which also affects the phase separation process. Some common solvents used in the electrospinning process include chloroform, ethanol, dimethylformamide (DMF), tetrahydrofuran (THF), dichloromethane, water, etc. (Table 1.1).

1.2.1.5. Conductivity/surface charge density. Most of the polymers are conductive except some dielectric materials. It is known that the diameter of nanofibers decreases with the increase of electrical conductivity of the solution while beaded structures occur with low conductivity of the solution as a result of insufficient elongation of the jet [10,16]. However, it was also observed that highly conductive solutions result in a broad diameter distribution under strong electric fields because of bending instability.

Table 1.1. Properties of different solvents used in electrospinning process (Adapted with permission from Ref [5]).

Solvents	Surface tension (mN/m)	Dielectric constant	Boiling point (°C)	Density (g/mL)
Chloroform	26.5	4.8	61.6	1.498
Dimethylformamide	37.1	38.3	153	0.994
Hexafluoroisopropanol	16.1	16.7	58.2	1.596
Tetrahydrofuran	26.4	7.5	66	0.886
Trifluoroethanol	21.1	27	78	1.393
Acetone	25.2	21	56.1	0.786
Water	72.8	80	100	1
Methanol	22.3	33	64.5	0.791
Acetic acid	26.9	6.2	118.1	1.049
Formic acid	37	58	100	1.21
Dichloro methane	27.2	9.1	40	1.326
Ethanol	21.9	24	78.3	0.789
Trifluoroacetic acid	13.5	8.4	72.4	1.525

1.2.2. Processing Parameters

1.2.2.1. Applied voltage. Applied voltage is an essential element in the electrospinning process a crucial element since fiber formation occurs only after sufficient voltage is applied to form the necessary charges on the solution. In general, a higher applied voltage results in a reduction in the fiber diameter because greater columbic forces result in greater stretching of the solution and also rapid evaporation of the solvent (Figure 1.7).

1.2.2.2. Feed rate/flow rate. The flow rate of the polymer solution from the syringe is another important process parameter. The polymer solution has to be fed at a minimum flow rate. A lower feed rate will give enough time to the solvent for evaporation giving fibers with small diameters. High flow rates result in increased fiber and pore diameter and also beaded fibers due to lack of time for proper drying before reaching the collector.

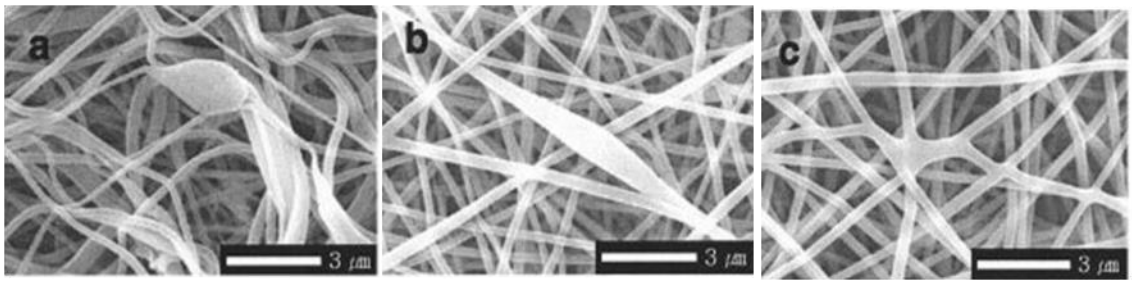

Figure 1.7. SEM images of PVA nanofibers with applied voltages (a) 10 kV, (b) 15 kV, (c) 20 kV, having a tip-to-collector distance of 10 cm and concentration of 7 wt % (Reproduced with permission from Ref [17]).

1.2.2.3. Types of collectors. In electrospinning process, a grounded collector is used to collect the nanofibers. In general, aluminium foil is used as a collector but other collectors such as, conductive paper, conductive cloth, wire mesh, pin, parallel or grided bar, rotating rod, rotating wheel, liquid non solvent such as methanol coagulation bath can also be used according to application area (Figure 1.8). The fiber alignment can be achieved by using a rotating drum or a rotating wheel-like bobbin, metal frame or split electrodes [18,19].

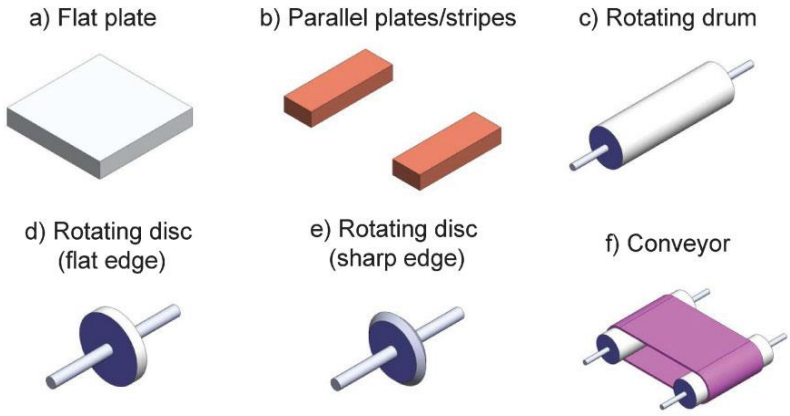

Figure 1.8. Different collectors for electrospinning a) static plate b) split electrodes c) rotating drum d) rotating disc e) rotating disc (sharp edge) f) conveyor (Reproduced with permission from Ref [6]).

1.2.2.4. Tip to collector distance. The distance between the tip of the spinneret and the collector is another parameter which influences the fiber diameters and morphology. There should be a minimum distance which allows enough time to the solvent for evaporation. It

was observed that the fibers became rounder than flatter and the fiber diameter decreased with increased distance (Figure 1.9) [5].

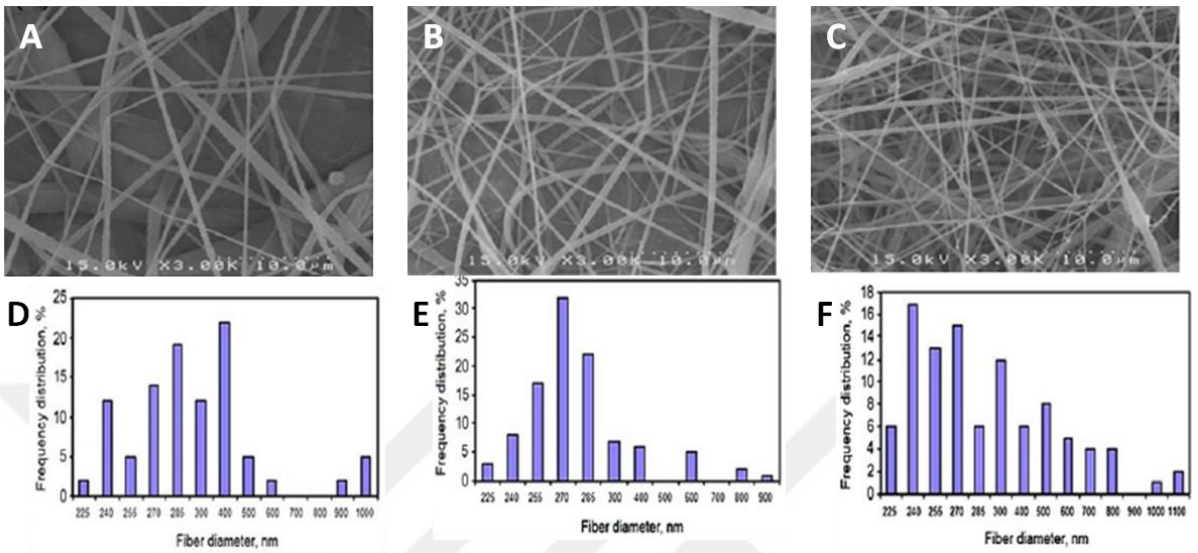

Figure 1.9. SEM images of electrospun polysulfone nanofibers at a tip-to-collector distance of a) 5, b) 10, c) 15 cm [20].

1.2.3. Ambient Parameters

Ambient parameters such as humidity and temperature also affect the fiber morphology (Figure 1.10). There are researches which shows that with increase in temperature, the viscosity decreases also decreasing the fiber diameter. Low humidity causes the rapid evaporation of a volatile solvent which can also create a problem with electrospinning with clogging in the needle. It has also been suggested that the high humidity can help the discharge of the electrospun fibers [21].

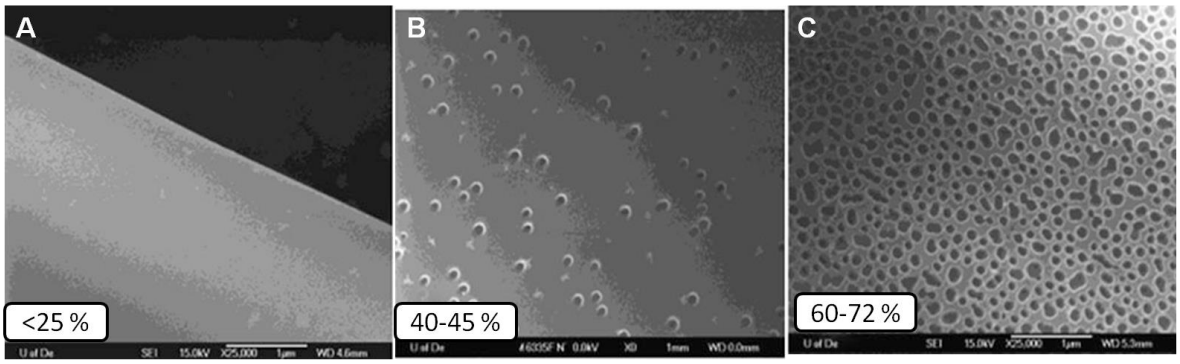

Figure 1.10. Field emission scanning electron microscopy images of electrospun polystyrene fibers under various humidity (a) <25 %, (b) 40-45 %, (c) 60-72 % [22].

1.3. Applications of Nanofibers

Nanofibers have become promising materials for various application areas due to their several unique properties such as high surface to volume ratio, high porosity and compositional flexibility [1,15,23-25]. Additionally, the required electrospun fibers are in small amount and can be electrospun into any shape using various polymers. Some application areas of electrospun nanofibers include biomedical applications, tissue engineering scaffolds, wound healing, drug delivery, filtration, affinity membrane, immobilization of enzymes, vascular graft implants, healthcare, biotechnology, environmental engineering, defense and security, and energy storage and generation, catalysis, etc (Figure 1.11). Among other applications, nanofibers are especially ideal scaffolds for bioapplications. Nanofibers have advantages such as mimicing the extracellular matrix, desirable topography and surface functionalization.

There are a wide range of polymers used in electrospinning including synthetic polymers, natural polymers or a blend of both with also proteins, nucleic acids and polysaccharides which are able to produce fine nanofibers.

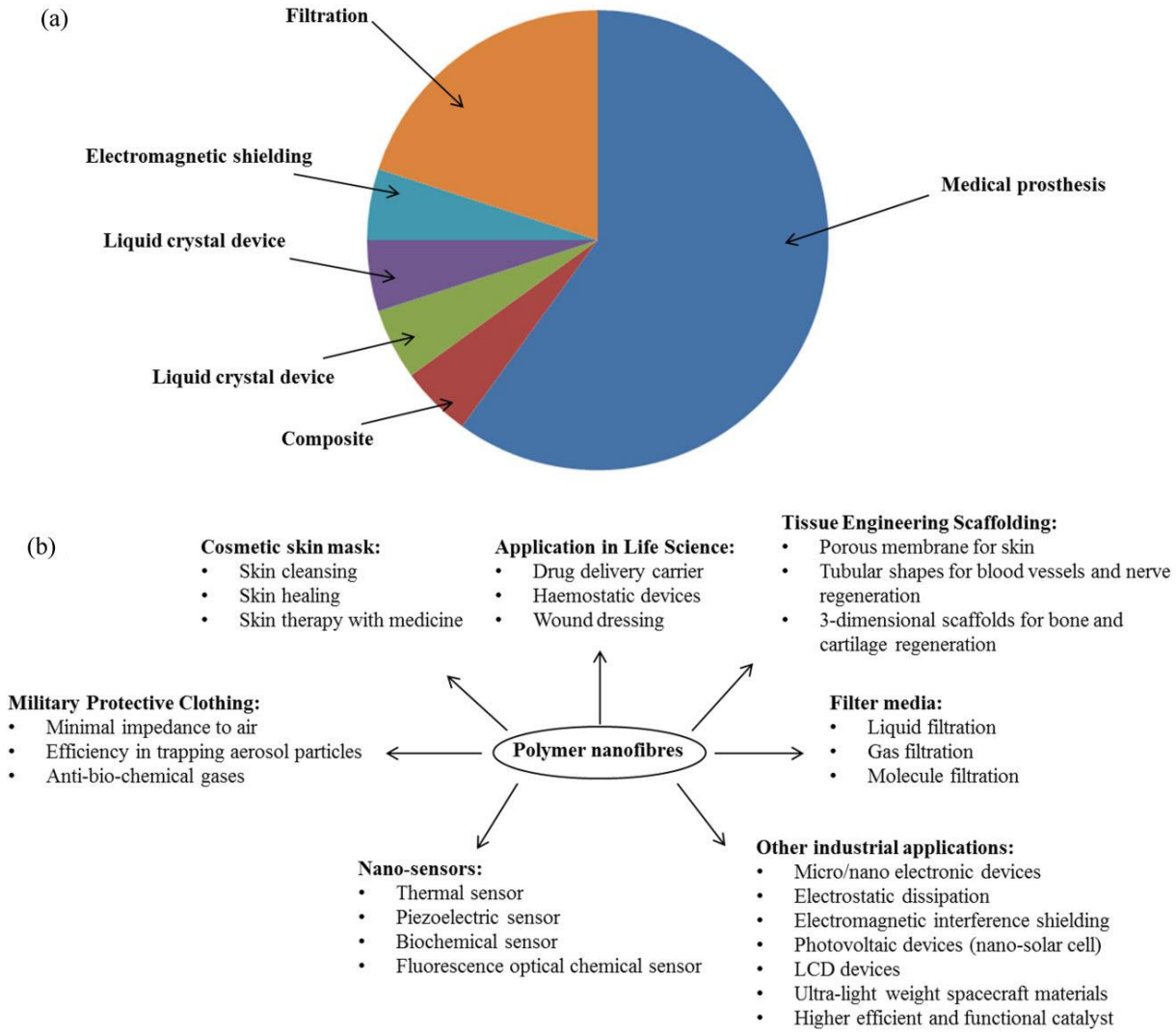

Figure 1.11. (a) Percental distribution of the application fields of electrospun nanofibers according to US patents, (b) Application areas of electrospun polymeric nanofibers (Reproduced with permission from Ref [26]).

1.3.1. Scaffolds For Tissue Engineering

Electrospun nanofibrous scaffolds are of special important for biomedical applications as a result of their ability to mimic the 3D network of natural collagen fibers with an average diameter of 50–500 nm composing the naturally occuring extracellular matrix. They are ideal networks for cell seeding, invasion, proliferation, and differentiation as they can enhance cell–matrix and cell–cell interactions and allow nutrient transportation [27-29]. Moreover, the electrospun nanofibers have other advantages for tissue regeneration such as desirable topography including porosity, nano-scale size, alignment),

encapsulation and local sustained release of growth factors, and surface functionalization with bioactive molecules (Figure 1.12).

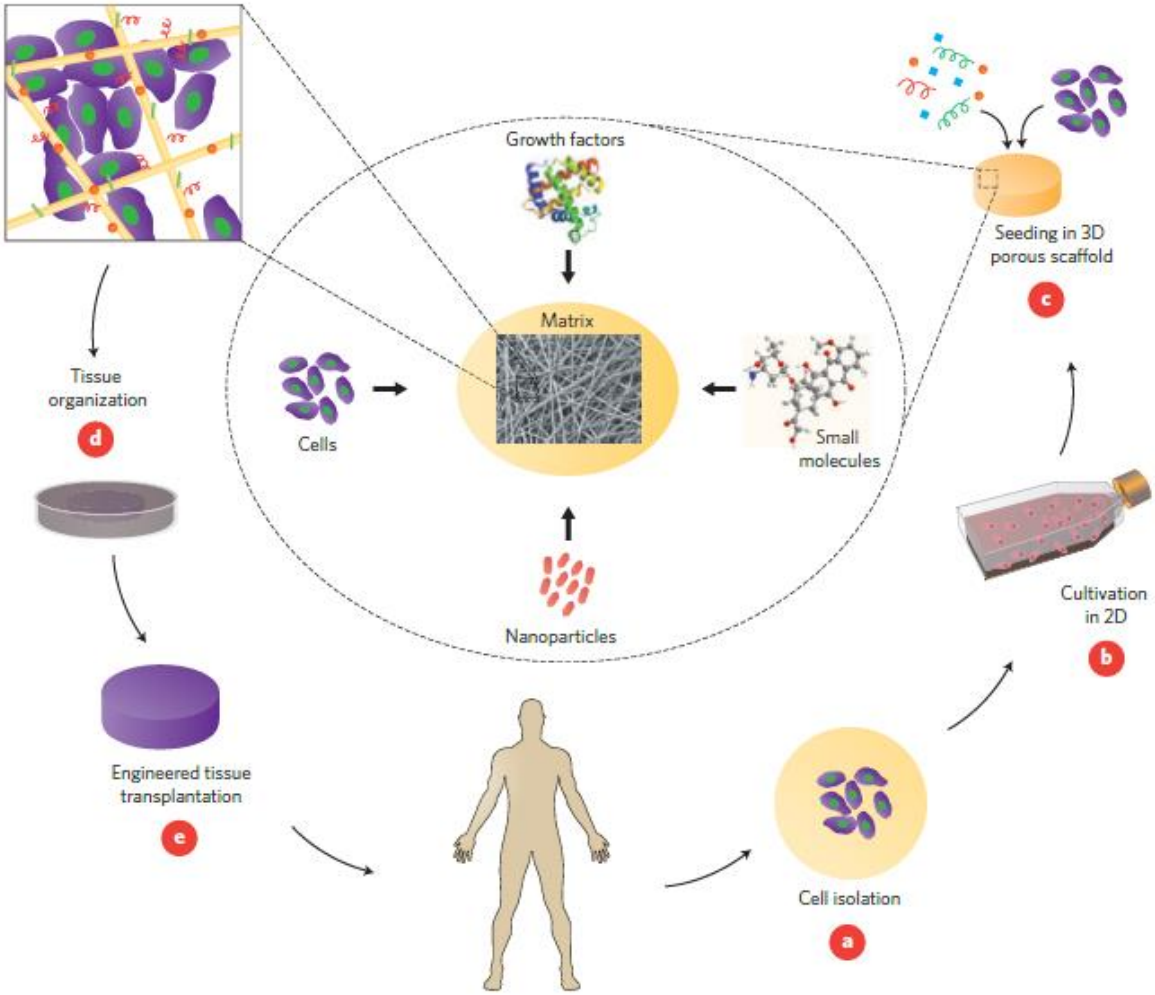

Figure 1.12. An example to a tissue engineering concept which involves cell seeding into porous biomaterial scaffolds (Reproduced with permission from Ref [30]).

1.3.2. Wound Healing

An ideal wound healing dressing should have some properties such as astringent ability, excess exudates absorption ability, bacterial barrier, sufficient gaseous exchange ability, proper water vapour transmission rate, functional and comfortable adhesion to the wound area, painless to patient and easy removal, and finally low cost. Electrospun materials are promising in this area as they meet most of these requirements with their porosity, functionality with drugs and low cost (Figure 1.13) [31,32].

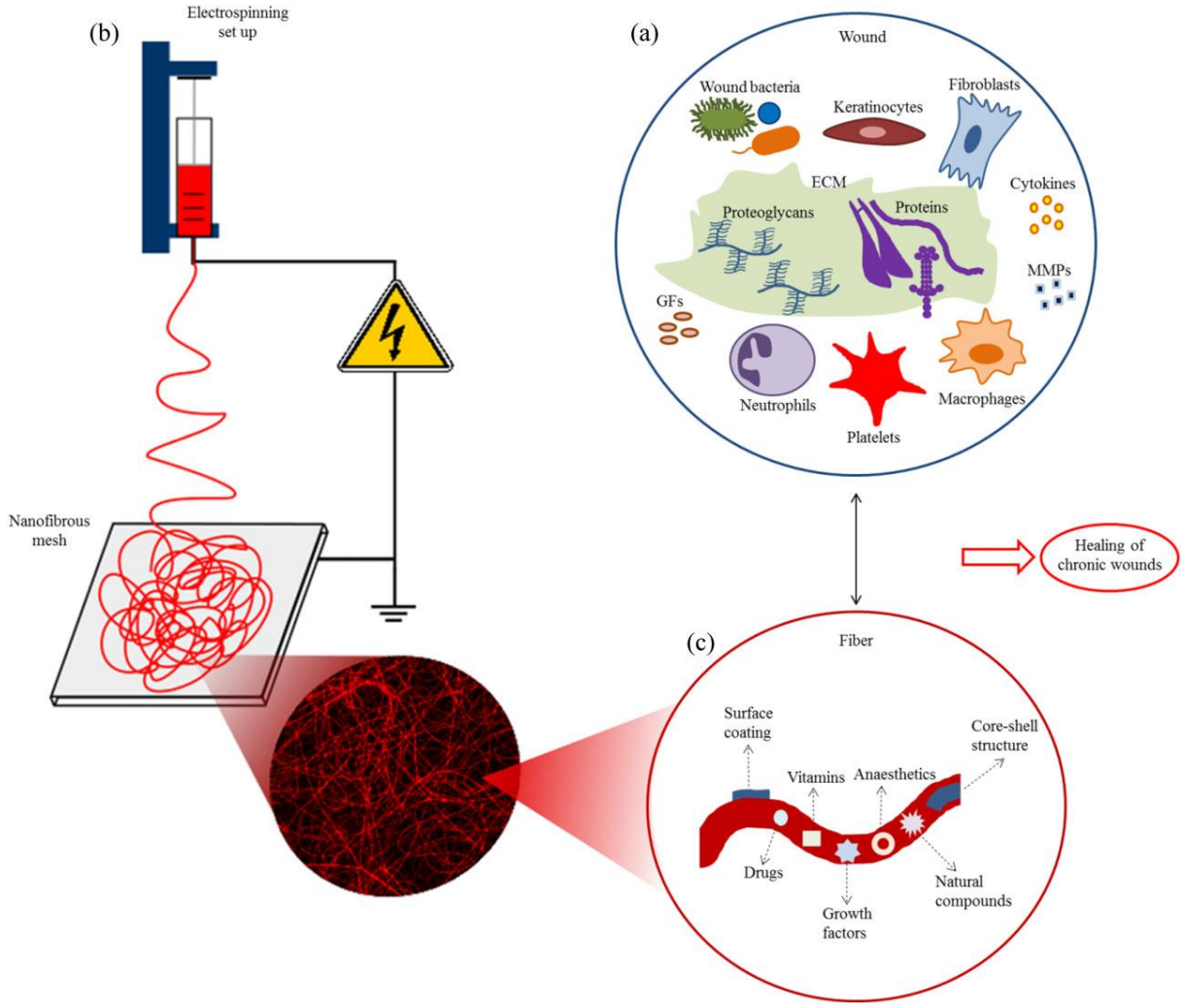

Figure 1.13. Schematic illustration of (a) main biomolecules present in the wound bed and the healing process, (b) fabrication of nanofibers by electrospinning process, (c) main approaches to prepare electrospun fibers as wound healing scaffolds (Reproduced with permission from Ref [26]).

1.3.3. Drug Delivery

Various nanoscale delivery systems such as liposomes, polymeric micelles, and nanofibers have been investigated in order to improve the therapeutic effect and to decrease the toxicity of drugs. Nanofibrous scaffolds attracted special attention are also suitable networks for drug delivery systems because of their high surface area and funcitonality which allow high loading and dissolution rate of a drug, besides ease of operation, and low-cost [24]. Biocompatible polymers are preferred for drug delivey

applications. There are several researches varying from encapsulation of a drug in the nanofiber to covalently binding the drug on the polymer followed by electrospinning (Figure 1.14) [33,34]. Drugs ranging from antibiotics, various antibacterial agents, DNA, RNA and growth factors, anticancer agents have been integrated into nanofibers and the nanofibers are seen as promising materials especially for cancer therapy.

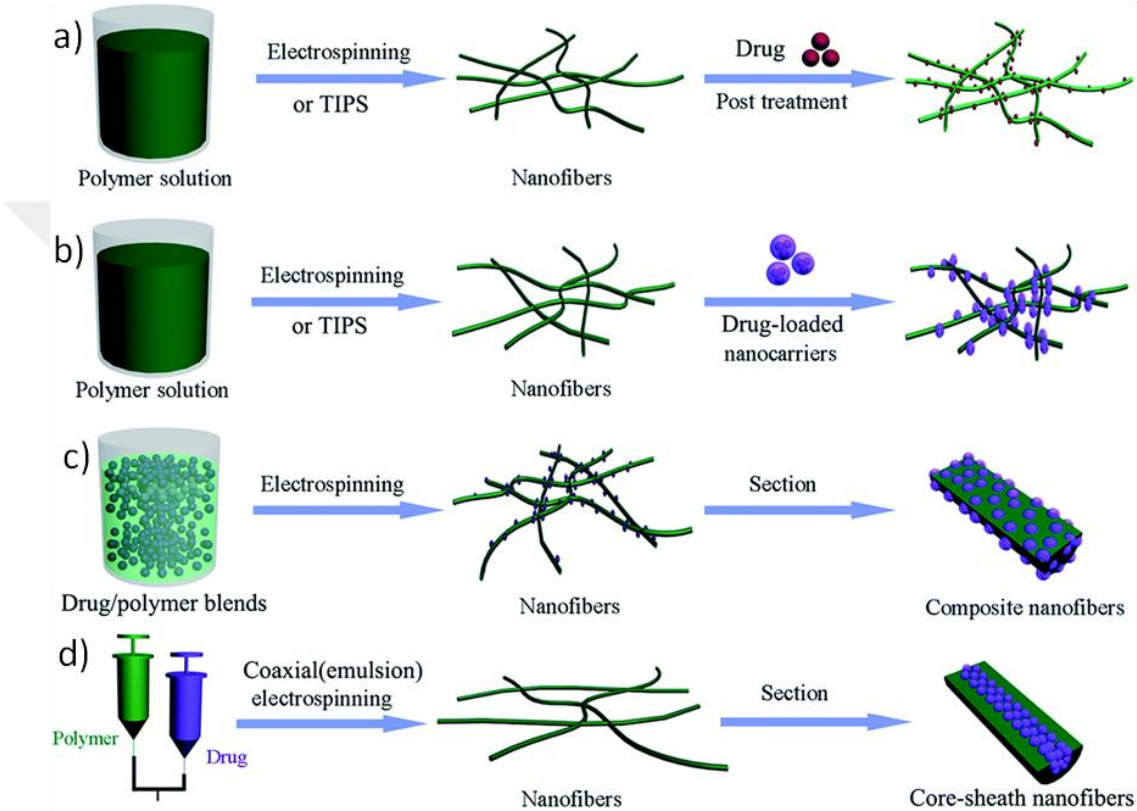

Figure 1.14. Schematic illustration of different methods for drug-loaded nanofiber preparation. (a) Post-treatment (b) Immobilization of drug-loaded nanocarriers (c) Co-electrospinning of drug–polymer blends (d) Coaxial electrospinning (Reproduced with permission from Ref [35]).

1.3.4. Filtration

Fibrous materials have been widely used for high efficiency filtration applications such as filtration of water, beverages, bio-pharma materials, blood, chemicals, oils, diesel, petrol and others. A filter must match the size of the particles or droplet which are aimed to be enclosed in the filter. Polymeric nanofibers fulfil this requirement with their very small diameter size, high interfacial ratio and high surface cohesion, good interconnectivity of

pores and wide material selection with tunable functionality. They can trap small particles with a size of submicron ranges [36-38]. A wide range of filter design can also be made for optimizing the interaction between flow, efficiency and filter life.

1.3.5. Biosensors

The nanofibers produced by electrospinning provide an ideal platform for sensing applications as they possess several advantages such as uniformity, porosity, reproducibility, mechanical strength, and high surface areas [39-43]. The high surface area increases the amount of sensing sites whereas the porous structure allows easy access of the target molecules to the sensing sites. The electrospun nanofibers can be obtained from a variety of both synthetic and natural polymers which enables the sensing of various materials such as such as glucose, protein, DNA, cells as well as volatile organic compounds, heavy metals and organic small molecules (Figure 1.15).

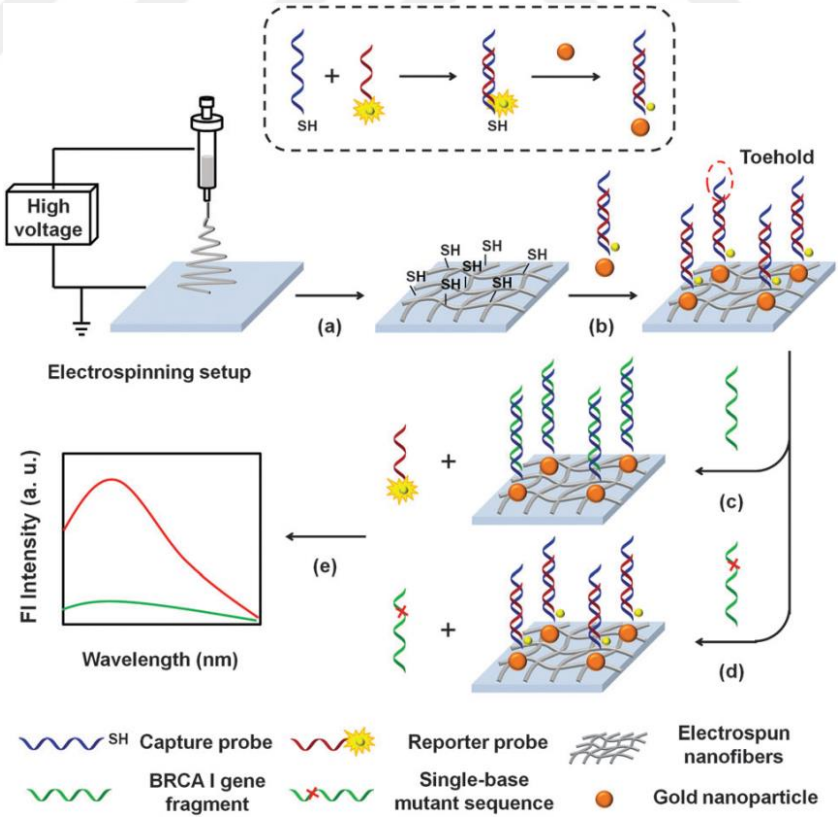

Figure 1.15. Schematic illustration of fabrication and oligonucleotide sensing mechanisms of a nanocomposite membrane composed of nanofibers and nanoparticles (Reproduced with permission from Ref [44]).

1.3.6. Protective Clothing Applications

Protective clothing should possess some properties such as, light weight, breathable fabric, air and water vapour permeability, enhanced toxic chemical resistance, insolubility in solvents, etc. Electrospun nanofibers meet most these requirements with their light weight, high surface area, porosity and filtration capability and resistance towards the penetration of toxic chemicals in aerosol form. Protection against toxins can be enhanced with surface modification with groups like oximes, cyclodextrins, and chloramines which bind and detoxify warfare agents (Figure 1.16) [45].

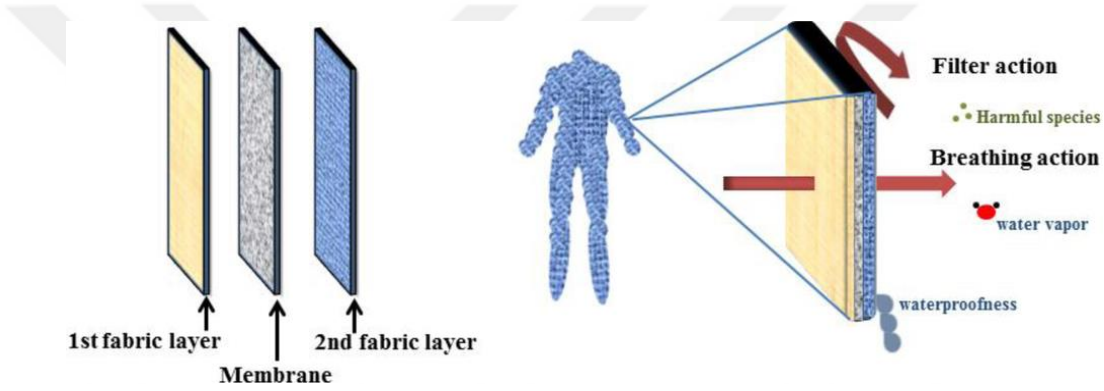

Figure 1.16. An example to protective clothing with a nanofibrous breathable barrier membrane [46].

1.3.7. As Affinity Membrane

Affinity or adsorptive membranes are used for purification of proteins and other molecules by selectively catching specific target molecules through immobilization of specific ligands on the membrane surface. Mostly the ligand molecules must be attached on the membrane covalently to prevent extracting of the ligands. The affinity membranes should be made of hydrophilic materials for protein purification which have lower non-specific protein adsorption and they also provide another way for organic molecule removal from waste water [47].

1.3.8. In Cosmetics

Electrospun polymeric nanofibers are also promising in cosmetic skin care mask for the treatment of skin healing, skin cleansing, or other therapeutical or medical properties with or without various additives [4]. The high surface area and small pore sizes of the nanofibers facilitates and accelerates the rate of transfer of the skin-revitalizing factors of the additives to the skin for the fullest potential. The cosmetic skin mask composed of the electrospun nanofibers can be directly applied gently and painlessly to the three-dimensional profileof the skin to provide healing or care treatment.

1.3.9. Energy Generation Applications

Polymeric conductive nanofibers are also suitable materials for applications such as, corrosion protection, photovoltaic devices, electrostatic dissipation, electro-magnetic interference shielding, fabrication of small electronic devices as Schottky junctions, sensors and actuators, because the surface area of the electrode is proportional to the rate of electrochemical reactions [48-50]. The high surface area and porosity of conductive nanofibrous scaffolds also allow them to be used as high performance batteries, polymer electrolyte membranes, fuel cells and polymer batteries [51].

1.4. Click Chemistry

Click chemistry has been widely used in polymer modification since its introduction by Sharpless and coworkers in 2001 [52]. The requirements for the click reactions were defined as being modular, wide in scope, stereospecific, giving very high yields, generating no or inoffensive byproducts, simple reaction conditions, readily available starting materials and reagents, the use of no or a benign solvent which is easily removed, simple purification and stability under physiological conditions.

1.4.1. Copper(I)-Catalyzed Azide/Alkyne Cycloaddition

The first examples of click chemistry were via copper(I)-catalyzed azide/alkyne cycloaddition (CuAAC) which was introduced by Sharpless and Meldal and has been broadly used to construct advanced functional (macro)molecules [53,54]. In a typical azide/alkyne click reaction, a metal-catalyzed Huisgen-type 1,3-dipolar cycloaddition reaction occurs between C–C triple, C–N triple bonds and alkyl-/aryl-/sulfonyl azides forming tetrazoles, 1,2,3-triazoles, or 1,2-oxazoles, respectively (Figure 1.17) [55]. The CuAAC is a highly chemoselective reaction with high efficiency known to be inexpensive and easy with the usage of Cu(I) among other metal-catalyzed reactions. Cu(I) is obtained either by the reduction of a Cu(II) source such as $CuSO_4$ with sodium salts or by the comproportionation of Cu(II)/Cu(0) species [56,57]. The CuAAC tolerates a variety of pH values, and a broad temperature range and can proceed in various solvents including water which allows to perform the reaction under physiological conditions. The reaction also possesses the advantage of the possibility of incorporating a wide scope of both alkyne and azide functional groups into various compounds. While widely applied in polymer science, the drawback of CuAAC is the presence of toxic Cu resiual and the need for additional purification which is especially unfavored in biomedical applications [58]. Consequently, there has been rose a strong interest for the development of metal-free click reactions which will encourage the modifications in biological applications.

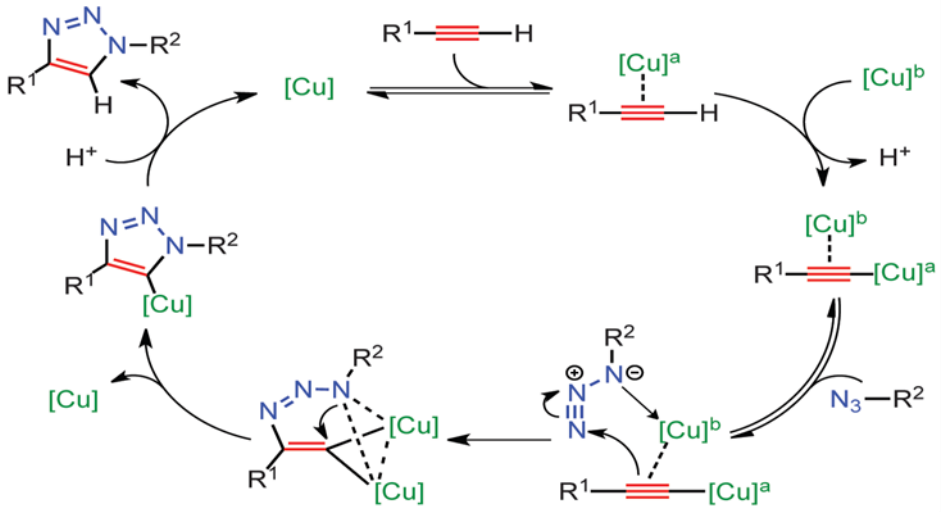

Figure 1.17. Copper-catalyzed azide-alkyne click reaction mechanism (Reproduced with permission from Ref [59]).

Emrick and coworkers prepared PEG-and peptide-grafted aliphatic polyesters using CUAAC reaction [60,61]. An alkyne functionalized polyester was synthesized through the ring opening polymerization of α-propargyl-δ-valerolactone and ϵ-caprolactone using $Sn(OTf)_2$ as the catalyst and ethanol as the initiator (Figure 1.18). An azide-ended GRGDS oligopeptide and α,ω-PEG-1100-monomethyl ether azide were reacted with acetylene-pendant polyester in the presence of sodium ascorbate and copper (II) sulfate. This alkyne functional PEG-grafted polyester was further used for the conjugation of water-soluble camptothecin using N,N-diisopropylethylamine and bromotris(triphenylphosphine) copper(I). PEG grafting was found to enhance solubility and biocompatibility of these polymer-drug conjugates enabling their usage for polymer therapeutics applications.

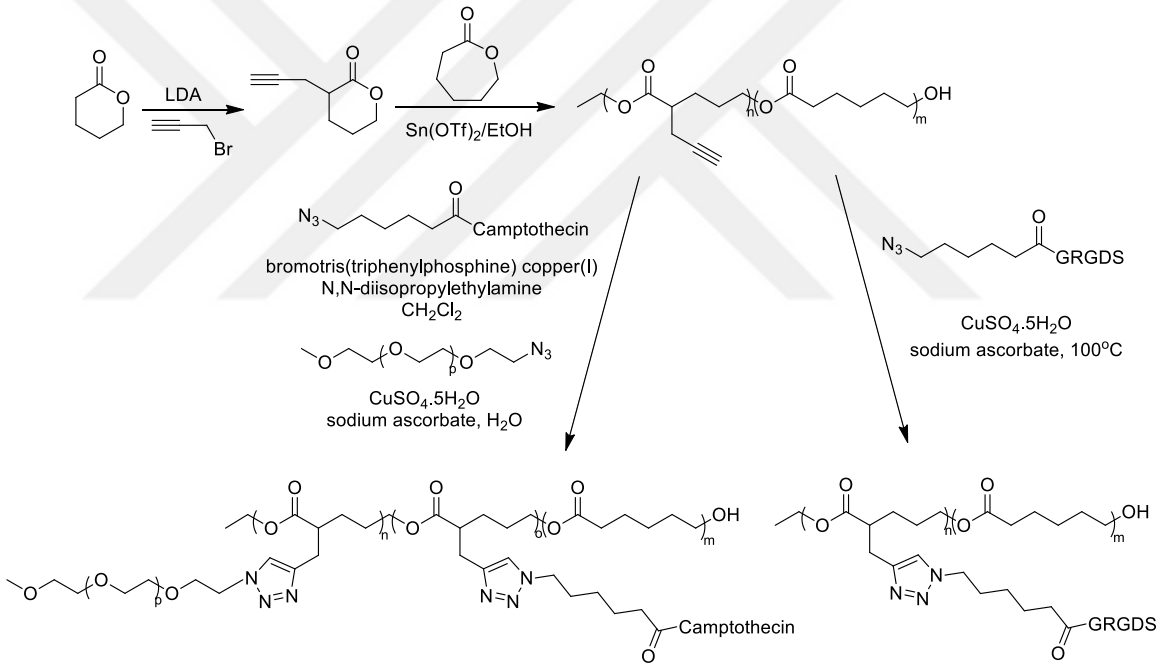

Figure 1.18. Preparation of hydrophobic polyester-camptothecin conjugate by 'click' cycloaddition (Adapted with permission from Ref [60,61]).

1.4.2. Metal-Free Click Reactions

Metal-free click reactions have been of significant importance as metal catalysts such as the trace copper in CuAAC reaction can cause problems in biological applications.

1.4.2.1. Copper-free [3+2] cycloaddition reactions of azides with substituted cyclooctyne.

Azides have received great attraction in recent years as a result of their success in CuAAC click reactions. However, as they are not very strong 1,3-dipolar acceptors, they do not readily react with an alkyne-bearing moiety without a metal catalyst. Hence, recent studies on this topic have focused on increasing the reactivity of the alkyne groups in order to achieve metal-free azide-alkyne cycloadditions under mild conditions [62]. Bertozzi and coworkers reported the strain-promoted azide-alkyne [3+2] cycloaddition (SPAAC) reaction between azides and cyclooctyne derivatives which was improved from the initial study of Wittig and Krebs (Figure 1.19) [63-66]. However, the rate of SPAAC reactions using the first generation of cyclooctyne is not as fast as CuAAC reactions. Therefore, mono and difluorinated cyclooctyne derivatives were prepared in order to increase the second order rate constants by decreasing the lowest unoccupied molecular level (LUMO) level of the alkyne using electron-withdrawing groups. 4-dibenzocyclooctynol (DIBO) derivatives were also used with similar reasons for increasing the ring strain.

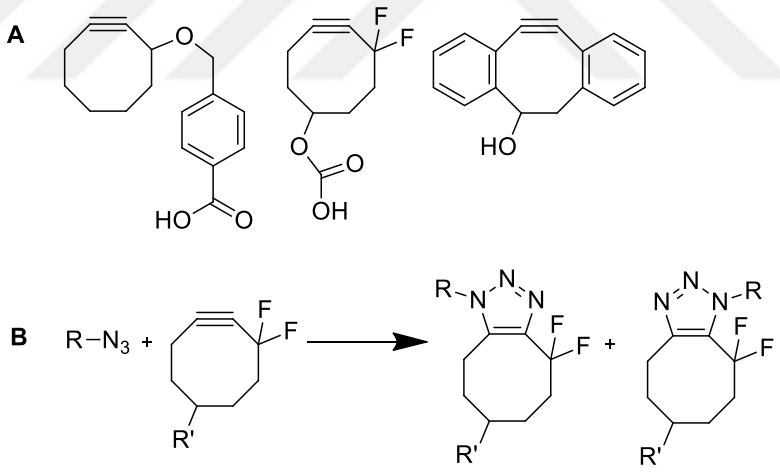

Figure 1.19. a) Examples to cyclooctyne derivatives b) The SPAAC click reaction (Adapted with permission from Ref [62]).

In a study by Theogarajan and coworkers, hydrophilic poly(oxazoline) (POX) or poly(ethylene glycol) (PEG) blocks were coupled with a hydrophobic poly(siloxane) block in order to obtain provide self-assembled triblock vesicular nanostructures, both via CuAAC and SPAAC reactions (Figure 1.20) [67]. Cyclooctyne-containing POX and PEG polymers were prepared and coupled with a hydrophobic bis-azide poly-(dimethylsiloxane) via SPAAC reaction for 12 h at room temperaure and 50 °C,

respectively. For CuAAC reaction, alkyne-terminated POX and PEG polymers were prepared and conjugated to bis-azide poly-(dimethylsiloxane) using copper nanoparticles as the catalyst at 60 °C. Dynamic light scattering (DLS) results showed that polymersomes formed via SPAAC are considerably smaller than those formed via CuAAC due to the chelation of copper metal ions by the ether oxygens in the PEG blocks, or the amide nitrogens in the POX blocks. The in vitro stealth attributes and biocompatibility of polymersomes synthesized via SPAAC versus CuAAC were compared via a standard complement activation assay using sheep red blood cells (RBCs) coated with rabbit antisheep erythrocyte IgM antibodies. Biocompatibility of the polymersomes obtained via SPAAC was found to be superior than those formed via CuAAC and purified by simple filtration of the copper nanoparticle catalyst as the PEG containing polymersomes demonstrated up to 2% cell lysis, while POX containing polymersomes showed up to 28% cell lysis. For the polymersomes coupled with SPAAC reaction, lysis of RBCs was not observed.

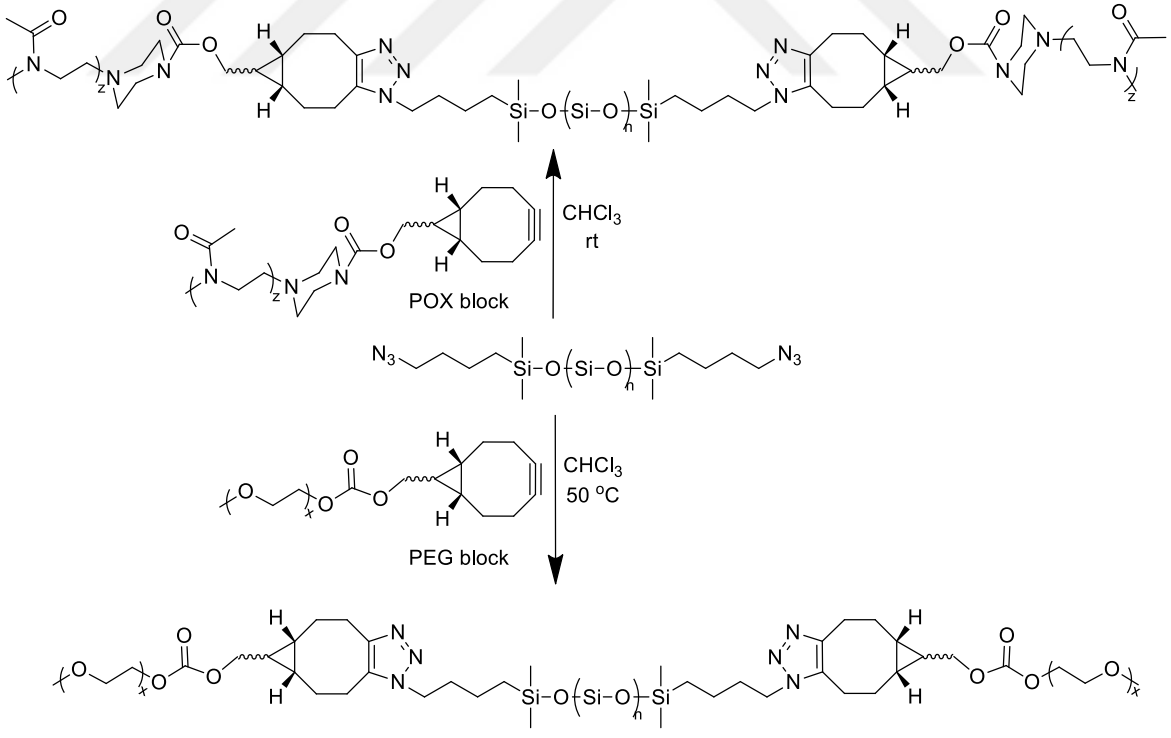

Figure 1.20. Synthesis of triblock copolymers (Adapted with permission from Ref [67]).

1.4.2.2. Thiol-ene reaction. The thiol-ene reaction known for over 100 years is basically the hydrothiolation of a C=C bond. There are several features associated with the thiol-ene

reaction that make it a particularly attractive, facile and versatile process [58,68,69]. Hydrothiolation reactions can proceed through radicalic and catalytic processes by nucleophiles, acids, bases, or via supramolecular catalysis. Thiol-ene reactions has attracted attention in polymerizations, modification of polymers, curing reactions, as they are simple, highly reactive, versatile, fast, tolerant to air/oxygen and moisture and can proceed under mild conditions with various reagents. Mostly, the thiol-ene reaction has been performed via radicalic conditions, often through photoinitiation (Figure 1.21). The reaction proceeds via a typical chain process with initiation, propagation and termination steps. A thiyl radical is formed using a photoinitiator under UV irradiation, followed by its addition to C=C bond as the propagation step to give the thiol-ene addition product forming a new thiyl radical with anti-Markovnikov orientation. Termination step is generally via radical–radical coupling.

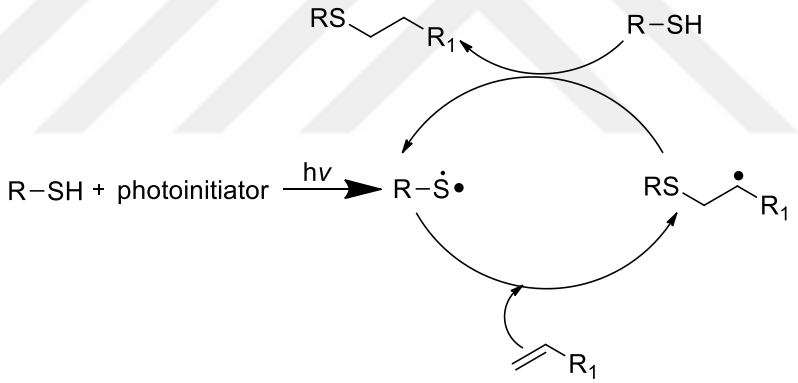

Figure 1.21. Mechanism for photoinitiated thiol-ene reaction (Reproduced with permission from Ref [68]).

In a study by Dove and coworkers, the ROP of the allyl ester-functional cyclic carbonate (MAC) and the post-polymerization functionalization via thiol-ene reaction were reported (Figure 1.22) [70]. For the organocatalyzed ROP, 1-(3,5-bis(trifluoromethyl)phenyl)-3-cyclohexylthiourea and (-)-sparteine were used as the cocatalysts and benzyl alcohol as the initiator. Postfunctionalization of PMAC homopolymer was studied using 1-dodecanethiol, benzyl mercaptan, 1-thioglycerol and mercaptoethanol via radical thiol-ene reaction using AIBN as the radical initiator at 90 °C for 24 h, demonstrating the versatility of the methadology for the synthesis of various functional aliphatic poly(carbonates).

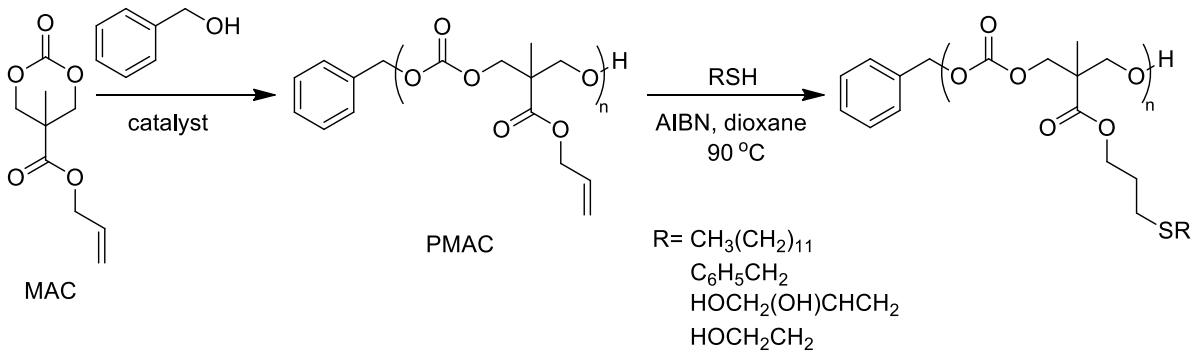

Figure 1.22. Organocatalyzed radical ROP of MAC and thiol-ene modification(Reproduced with permission from Ref [70]).

1.4.2.3. Michael addition of thiols. The Michael addition reaction discovered by Arthur Michael in the 1880s is a special type of (1,4) conjugate addition. In Michael reaction, the β-carbon of an α,β-unsaturated carbonyl is attacked by a strong nucleophile forming a negatively charged enolate intermediate which subsequently yields the Michael adduct in the presence of a catalyst, generating C−C, C−N, C−S, C−O, and other C−X bonds (Figure 1.23). A more specific Michael addition reaction between thiols and activated alkenes has gained great interest in bimolecular synthesis, surface modification, engineering adhesives, dendrimer synthesis and block polymer conjugation since the first report by Allen et al. in the 1960s [71]. The thiol-Michael addition reaction is an effective method due to mild reaction conditions, high efficiency, solventless or aqueous environment and modularity [72]. The thiol-maleimide Michael addition has distinguished among others especially in biological applications due to selectivity of the thiol-maleimide reaction in aqueous environments, the rapid kinetics of the reaction, and the stability of the thiol-maleimide product in biological systems, primarily. The thiol-maleimide reaction can also proceed without a catalyst in highly polar solvents. This reaction has been used widely in fluorescent labeling of molecules, cross-linking of hydrogels, as well as for its ability to undergo retro reactions at high temperatures due to the succinimide thioether bonds [73]

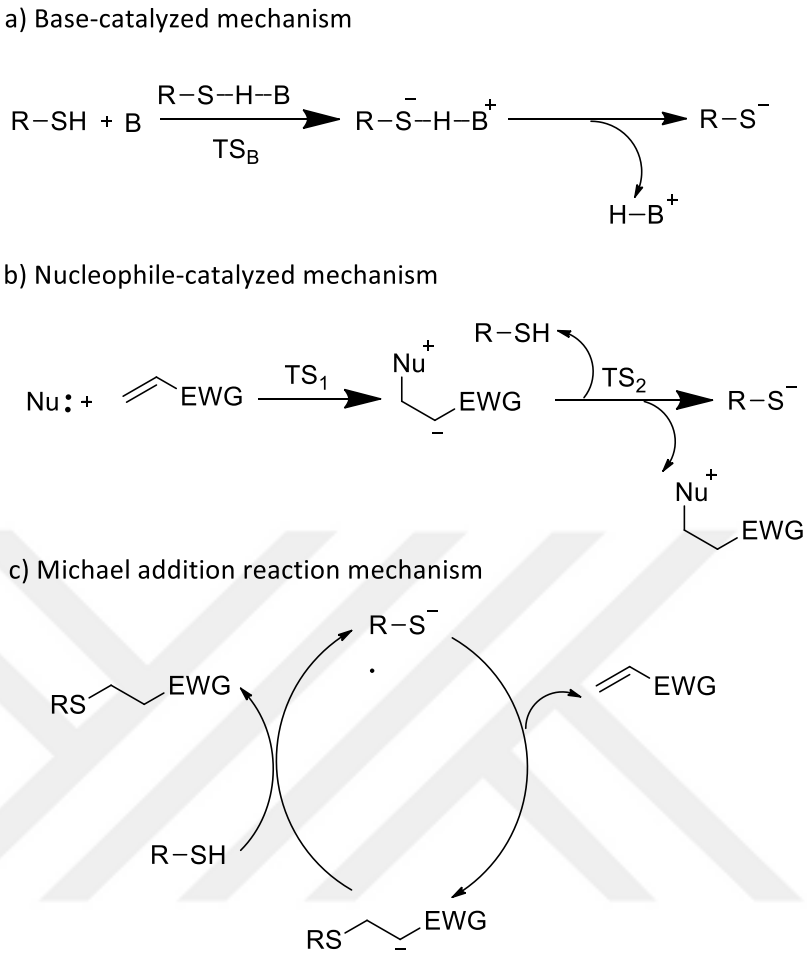

Figure 1.23. a) Base-catalyzed b) Nucleophile-catalyzed Michael addition reaction mechanism (Reproduced with permission from Ref [71]).

Sanyal, Dove and coworkers introduced a side chain maleimide functional copolymer using a novel furan-protected maleimide-functional carbonate monomer (Figure 1.24). The carbonate monomer was copolymerized with lactide via ring opening polymerization using with 1,8-diazabicycloundec-7-ene (DBU) as the catalyst and benzyl alcohol as the initiator. The maleimide functionality was obtained through the removal of furan protection via retro Diels-Alder reaction. The reactivity of the maleimide-containing copolymer was investigated via Michael reaction using thiol-containing molecules such as 6-(ferrocenyl)hexanethiol and 1-hexanethiol [74].

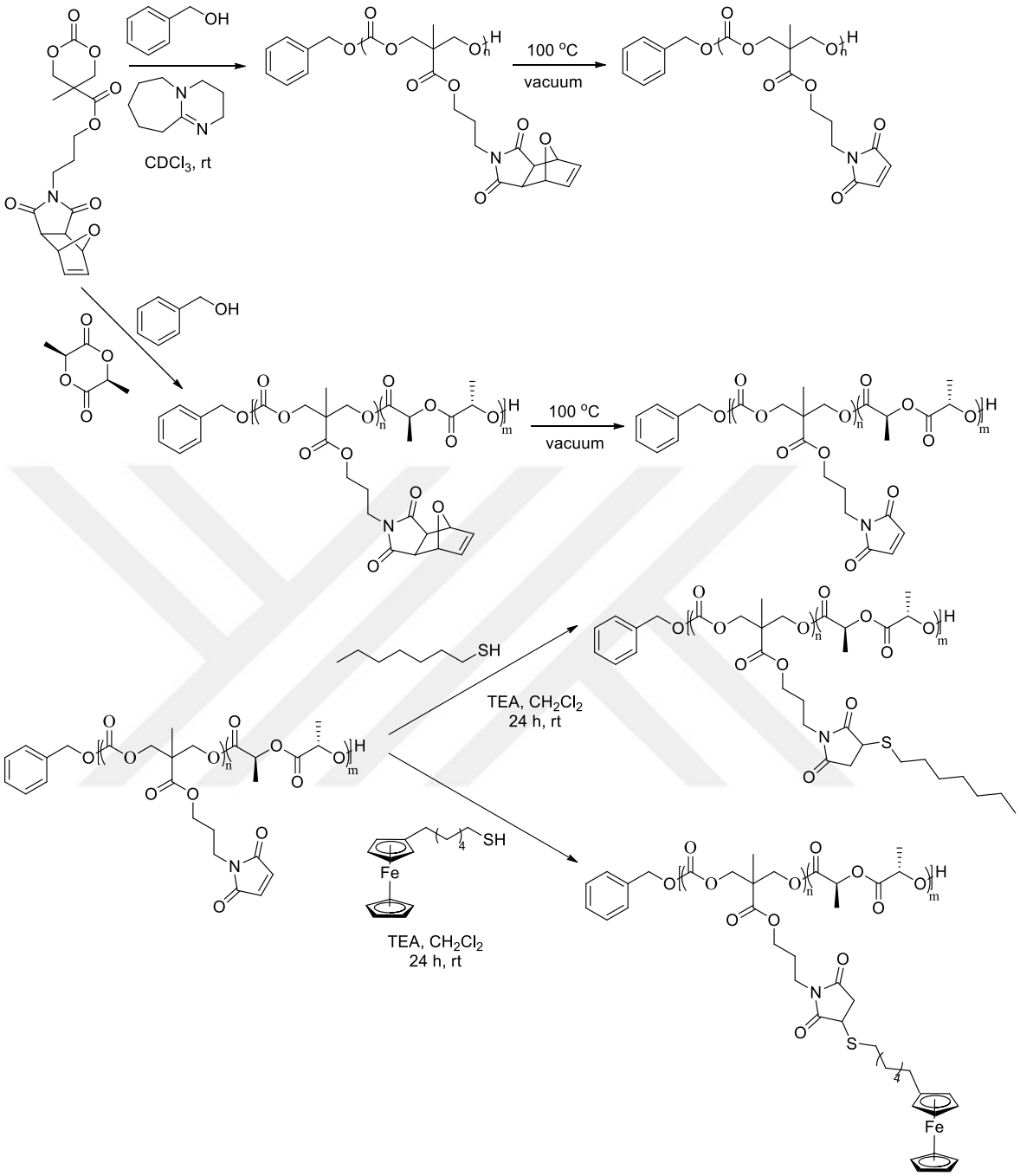

Figure 1.24. Synthesis of maleimide functional homo- and copolymers and functionalization (Reproduced with permission from Ref [74]).

1.4.2.4. Diels–Alder reactions. [4+2] cycloaddition reaction between an electron rich diene and an electron deficient dienophile, known as Diels-Alder reaction was revealed by Otto Diels and Kirk Alder in 1928 [75-78]. This electrocyclıc reaction causes the formation of a six membered ring formation, namely an adduct by forming new σ-bonds which are energetically more stable than the π-bonds. This reaction has been widely used in polymer

and materials science recently, as a result of its high yield, thermoreversibility, mild and reagent-free reaction conditions. These properties encourage the use of Diels-Alder reaction in the design and (bio)functionalization of dendrimers, polymers, dendronized polymer. The Diels-Alder reaction gives two stereoisomers, namely endo and exo products. In the endo transition, the substituent on the dienophile is positioned towards the π system in the diene. The endo product is kinetically controlled. The exo product is thermodynamically controlled and it is a more stable conformation sterically which is favored at high temperatures. In the exo transition, the substituent on the dienophile is positioned away from the π system. Although it is more sterically hindered, the *endo* transition state is usually preferred, known as the Alder rule.

Commonly used dienes include furan, anthracene, cyclopentadiene, butadiene and isoprene while the dienophile has been mainly limited to maleimide due to its high stability, reactivity, and ease of incorporation in polymeric materials (Figure 1.25). Mostly the furan-malemide pair is used in the fabrication of thermoreversible materials because the furan-based cycloadducts are thermoreversible at around 100 °C while the other cycloadducts can need up to 200 °C [79]. This reverse reaction is called retro Diels-Alder reaction. Although the furan-maleimide pair is advantageous for the fabrication of easily thermocleavable materials, a more reactive diene may be needed for the sterically demanding conjugation of two high molecular weight macromolecular building blocks. Anthracene-based polymers have been widely used for this purpose due to its high reactivity with maleimide and irreversibility of the cycloadduct at temperatures around 110 °C [80]. Dienes and dienofils can also be appended in the polymer side chains for postpolymerization functionalization which may alternatively masked through protection–deprotection strategy during polymerization.

For more more demanding systems such as in vitro/vivo modification of biomolecules that require a fast and clean reaction in very dilute conditions, the inverse-electron-demand Diels−Alder (iedDA) reaction between a tetrazine group and different types of double bonds is a promising example. The combination of tetrazine with highly reactive norbornene has already been studied as a fast, reagent-free, and irreversible conjugation method, which allowed for the effective synthesis of block copolymers [81,82].

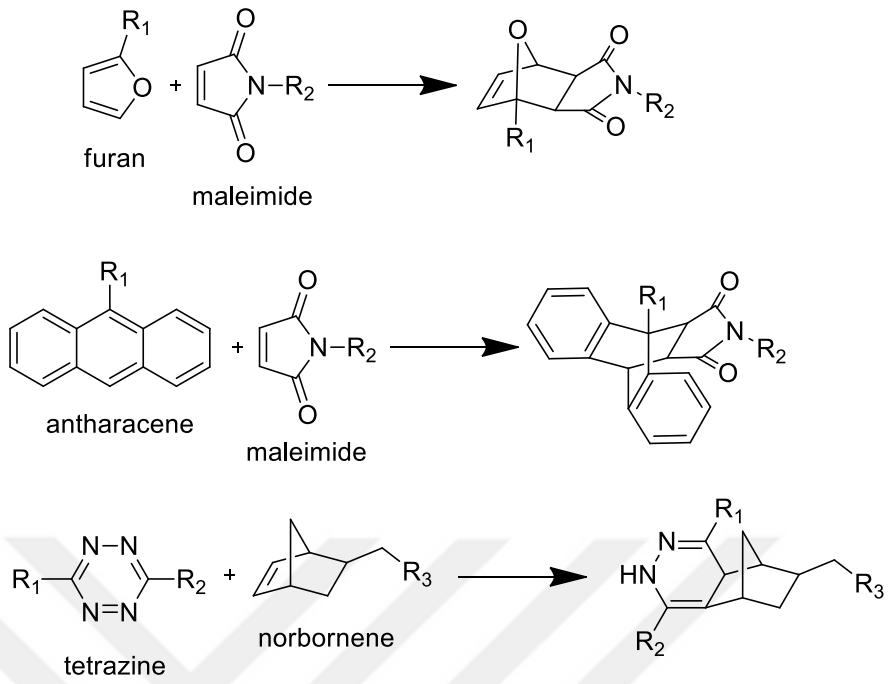

Figure 1.25. Examples to well-known Diels-Alder reactions in polymer and material science (Adapted with permission from Ref [77]).

Dove and coworkers investigated the ring opening polymerization of a novel norbornene functional cyclic carbonate monomer followed by further functionalization using heat promoted 1,3-dipolar cycloaddition reaction with azides, the inverse electron demand Diels−Alder (iedDA) reaction with tetrazines and the radical addition of thiols promoted by UV irradiation both individually and in a sequential one-pot reaction (Figure 1.26) [82]. Ring-opening polymerizations were performed using 1,8-diazabicycloundec-7-ene (DBU) and 1-(3,5-bis(trifluoromethyl)phenyl)-3-cyclohexylthiourea as cocatalysts, benzyl alcohol as an initiator and $CHCl_3$ or DCM as the solvent. The norbornene-containing polymer was functionalized with benzyl azide and triethyleneglycol monomethyl ether (TEG) azide via 1,3-dipolar cycloaddition between norbornenes and azides. The iedDA reaction was performed using an equimolar amount of 3,6-di-2-pyridyl-1,2,4,5-tetrazine. The radical addition of excess 1-dodecanethiol and pro-fluoroscent 7-mercapto-4-methylcoumarin to the norbornene-functional scaffolds was also carried out in the presence of a photoinitiator under UV irradiation. After these successful individual modifications, all three of the modifications were performed successively in the order of 1,3-dipolar cycloaddition, iedDA reaction and radical addition.

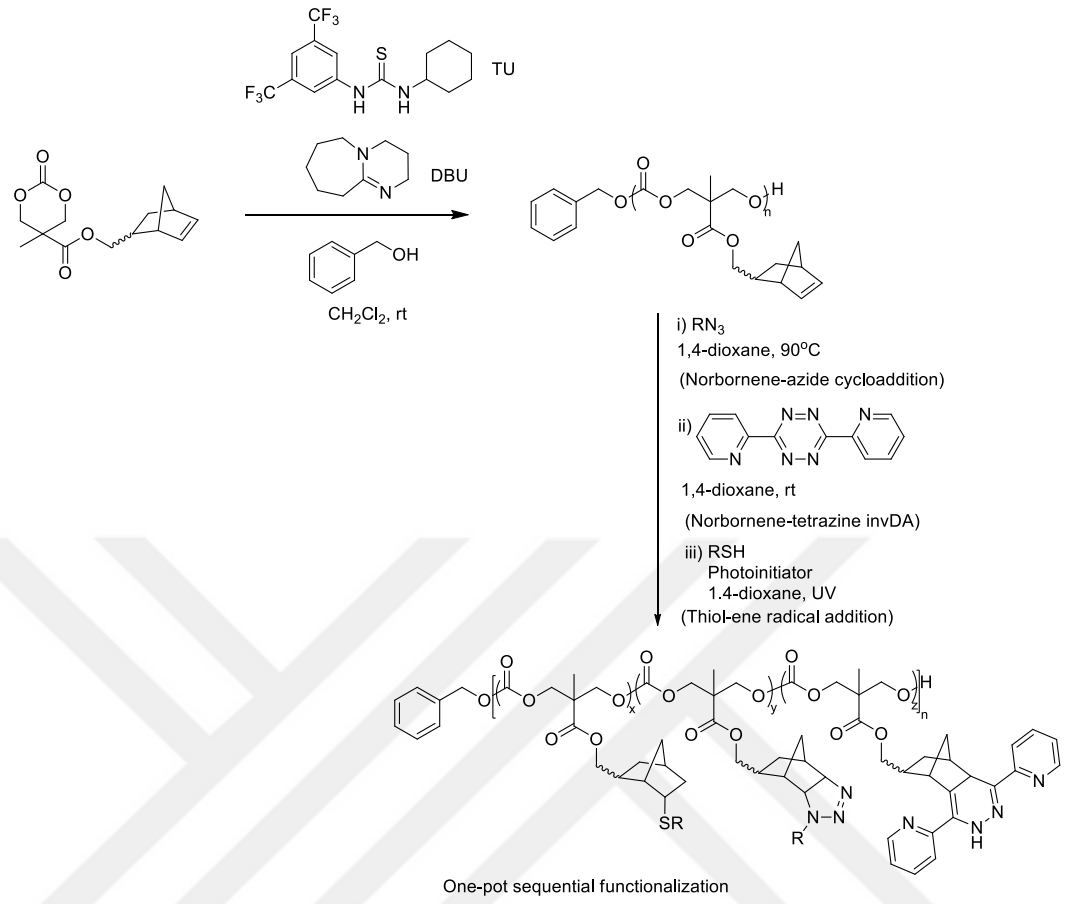

Figure 1.26. One-pot functionalizations of norbornene-functional poly(carbonate)s (Reproduced with permission from Ref [82]).

Tunca and Hizal group introduced a novel anthracene-containing cyclic carbonate monomer and prepared a polycarbonate with side-chain anthracene groups (PC-anthracene) via ring opening polymerization using benzyl alcohol as an initiator, DBU/TU as the catalyst in DCM (Figure 1.27). The obtained PC-anthracene was grafted to various chain-end furan protected-maleimide-containing polymers such as poly(methyl methacrylate), poly(ethylene glycol) or a mixture of them via Diels-Alder chemistry in toluene for 36 h [83].

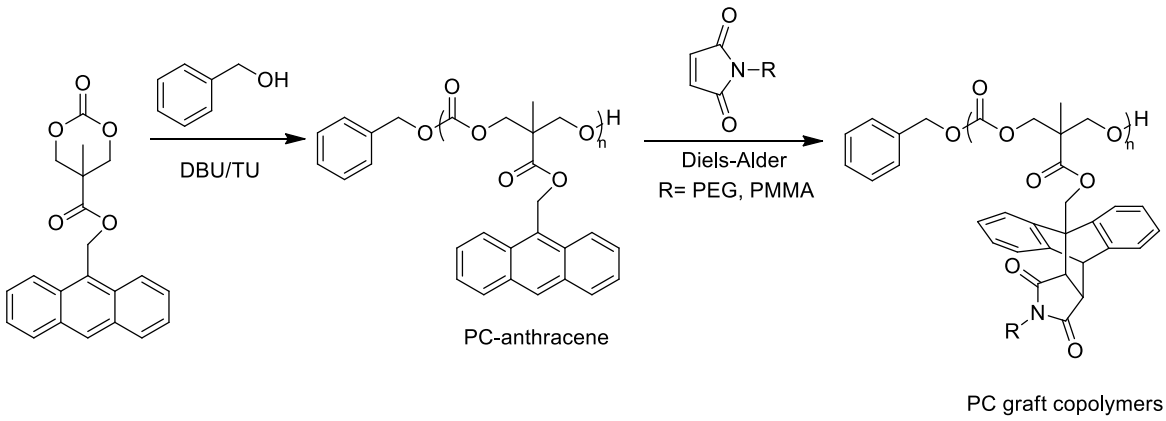

Figure 1.27. Synthetic route for the synthesis of polycarbonate graft copolymers via Diels-Alder reaction (Reproduced with permission from Ref [83]).

1.4.2.5. Activated esters. Polymeric activated esters have been widely used in materials and life sciences since the pioneering works of Ringsdorf and coworkers [84] and Fere and coworkers [85] in 1972. They are important as they can covalently bind to amines due to their good nucleophilicity to form amides which provides selectivity without a protecting group and so find broad application in peptide chemistry [72,86]. The conversion of polymeric activated esters are quantitative, fast under mild conditions without any side reactions. Another advantage of this reaction is that it can proceed without a metal catalyst. N-hydroxysuccinimide (NHS) esters are suitable candidates for the biofunctionalization of polymers in aqueous or mixed aqueous media as they have good hydrolytic stability. The most commonly used monomers in order to prepare side-chain NHS ester polymers are N-acryloxysuccinimide (NAS) and N-methacryloxysuccinimide (NMAS) which can be be polymerized via various controlled polymerization methods such as ATRP, NMP or RAFT polymerization (Figure 1.28). However, polyNAS and polyNMAS are only soluble in DMF and DMSO. The solubility of activated-ester-based polymer precursors can be enhanced by copolymerization or using other activating groups, such as 2,4,5-trichlorophenol ester, bicyclo[2.2.1]hept-5-ene-exo-2-carboxylic acid N-hydroxy succinimide ester (NHSNorb) or pentafluorophenol ester groups.

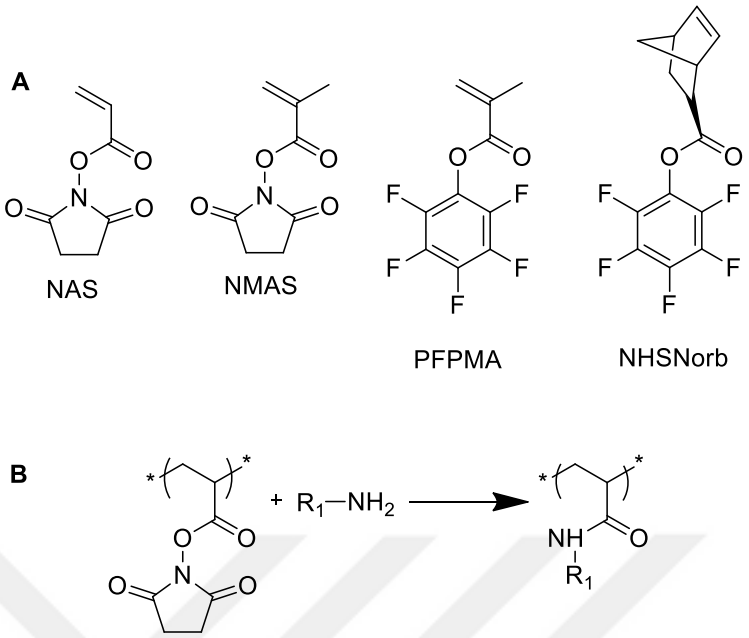

Figure 1.28. (a) Examples to activated esters (b) activated ester-amine reaction.

1.5. Surface Modification Techniques of Nanofiber Mesh

A variety of degradable and non-degradable synthetic polymers have been used for nanofiber production due to the processing benefits [87,88]. The surfaces of these nanofibers have been modified with various bioactive species for further biological and therapeutic applications. These biologically modified synthetic nanofibers have enhanced cellular activities such as migration, proliferation, differentiation, gene expression due to the increase in biocompatibility and specific biological responses from attached cells. The nanofibers have also been modified with various hydrophobic therapeutic agents for sustained drug delivery applications as well as the covalent and physical attachment of a variety of hydrophilic and charged macromolecular drugs. Various natural polymers with unique biological properties can also be used to cover the surface of the synthetic nanofibers without losing bulk properties. Several surface modification techniques have been used for the modification of synthetic polymer nanofibers to tissue engineering and drug delivery.

1.5.1. Plasma Treatment

Plasma treatment has been used widely to change the surface chemical composition of polymeric nanofibers in order to improve surface wetting, adhesion, biocompatibility. Typical plasma sources include oxygen, ammonia and air which will produce carboxyl groups or amine groups on the surface allowing covalent immobilization of various bio molecules (Figure 1.29a). Chen and Su modified the electrospun poly(lactic acid) nanofibers with cationized gelatin in order to enhance their compatibility with chondrocytes and indicated the potential use of cationized gelatin grafted poly(lactic acid) nanofibers as a cartilage tissue engineering scaffold [89]. At first, –COOH groups were introduced onto the surface of poly(lactic acid) nanofibers with oxygen plasma, followed by covalent surface grafting of cationized gelatin molecules in the presence of a water-soluble coupling agent which provided enhanced chondrocytic activities.

1.5.2. Wet Chemical Method

Plasma treatment of the nanofibers allows limited modification of the nanofibers due to the unsufficient penetration of plasma to the deeper regions, so wet chemical method is preferred for thicker scaffolds. In wet chemical methods, modification is obtained through the partial surface hydrolysis of biodegradable aliphatic polyester scaffolds under acidic or basic conditions resulting random carboxylic and hydroxyl groups (Figure 1.29a). The hydrolysis time and the concentration of hydrolyzing agents are important parameters to produce surface functional groups without changing the bulk property. In a recent study, Li and coworkers mineralized chitosan nanofibers by hydroxyapatite through a wet chemical method [90]. The electrospun chitosan nanofibers were firstly crosslinked with glutaraldehyde and then treated with calcium nitrate, ammonium phosphate and ammonium hydroxide solutions respectively, for four cycles. It was shown that this method was efficient for the production of biomimetic and osteoconductive chitosan/ hydroxyapatite composite nanofibers which is promising for bone tissue engineering.

1.5.3. Surface Graft Polymerization

Synthetic biodegradable polymers generally need hydrophilic surface modification for biological applications. Surface graft polymerization has been used for introducing both surface hydrophilicity and functional groups on the surface via initiation with plasma and UV radiation in order to generate free radicals for the polymerization (Figure 1.29b). Hereby, covalent binding of biomolecules will allow enhanced cell adhesion, proliferation, and differentiation. Carbonell and coworkers grafted poly glycidyl methacrylate on polybutylene terephthalate nonwoven surface via photo-induced graft polymerization followed by diethylene glycol and diol attachment which decreased the amount of nonspecific protein binding onto the nonwoven [91].

1.5.4. Co-electrospinning Of Surface Active Agents And Polymers

Fibers with reactive groups on the surfaces can also be fabricated with co-electrospinning of a bulk polymer with nanoparticles, functional polymer segments (Figure 1.29c). Börner and coworkers electrospun a homogeneous mixture of poly(L-lactic-co-glycolic acid), as the bulk fiber-forming polymer and poly(L-lactic acid)-b-CGGRGDS), as the bioactive polymer-peptide conjugate. They reported that the GRGDS-functionalized nanofibers showed an enhanced cell adhesion as compared to pure PLGA fibers [92].

1.5.5. Physical Adsorption

1.5.5.1. Simple physical adsorption. Physical surface adsorption for the loading on nanofibrous scaffolds is generally obtained through electrostatic interactions, hydrogen bonding, hydrophobic interactions or van der Waals interactions (Figure 1.30a). A typical example is the use of specific interaction between heparin and growth factor. In a study of Rabolt and coworkers, a poly(ethylene glycol) functionalized with low molecular weight heparin was mixed with poly(ethylene oxide) and poly(lactide-*co*-glycolide) carrier polymers and was electrospun into nanofibers with a heparin concentration between 3.5 to 85 μg per milligram [93]. The retention of heparin in the nanofibers was 14 days. Fibroblast growth factor was bound on the heparin-containing nanofibers through electrostatic interactions.

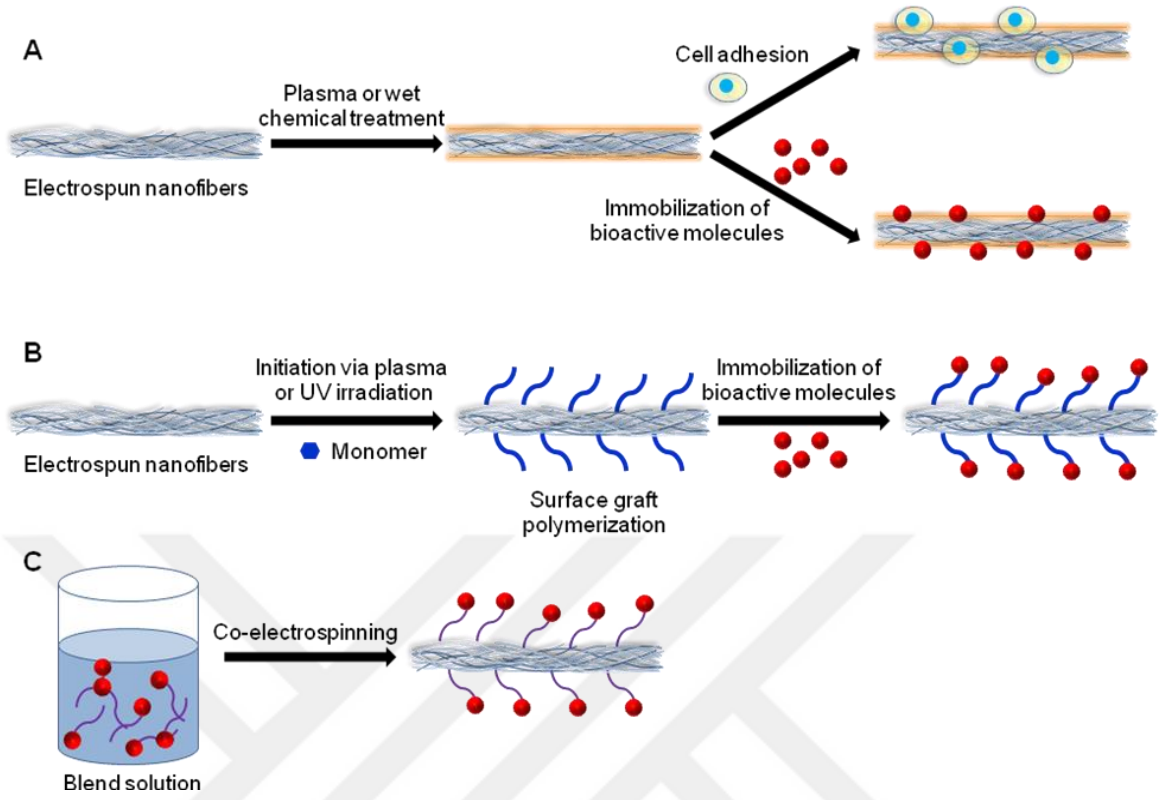

Figure 1.29. Schematic illustration for the surface modification of nanofibers via (a) plasma treatment/wet chemical methods (b) surface graft polymerization (c) co-electrospinning.

1.5.5.2. Nanoparticles assembly on the surface. The accumulation of nanoparticles on nanofibers' surfaces has been used for various applications such as electronic, catalysis, drug loading and sensor devices. The large interfacial area of the nanofibers enables the attachment of a high number of nanoparticles which are usually loaded by therapeutic and biological materials (Figure 1.30b). Liu and coworkers proposed a strategy for biosensing applications via DNA-functionalized gold nanoparticle immobilization on electrospun cellulose acetate nanofibers for the detection of specific nucleic acids through fluorescent sensing [44]. Cellulose acetate was coelectrospun with n-dodecanethiol and DNA oligonucleotide probe-containing gold nanoparticles were immobilized on the nanofibers through the thiol-gold assembly. The complementary BRCA I gene acticates a strand displacement, releasing a reporter probe tagged with 5-carboxyfluorescein from the DNA–AuNP–CANF membrane.

1.5.5.3. Layer-by-layer multilayer assembly. Another surface adsorption technique is layer-by-layer (LbL) polyelectrolyte multilayer assembly which is based on the alternative layer-by-layer deposition of polyanions and polycations driven by an electrostatic force on charged substrates (Figure 1.30c). This method enables surface coating with a thickness varying from a few nano to several micrometers. Charged therapeutic components can easily be integrated in the multilayer assembly, while the insoluble and uncharged drugs can not be incorporated so simply. Some studies have also shown the possibility of the multilayer assembly of many bioactive agents and chemical drugs via other intermolecular forces including hydrogen bonding, metal-ligand complexation, covalent bonding, hydrophobic interaction, and molecular recognition. Du and coworkers immobilized quaternized carboxymethyl chitosan and sodium alginate on cellulose nanofibers via layer-by-layer technique [94]. They produced negatively charged cellulose nanofibers from the hydrolysis of electrospun cellulose acetate. Then, positively charged quaternized carboxymethyl chitosan with organic rectorite and negatively charged sodium alginate were immobilized alternately on these negatively charged nanofibers.

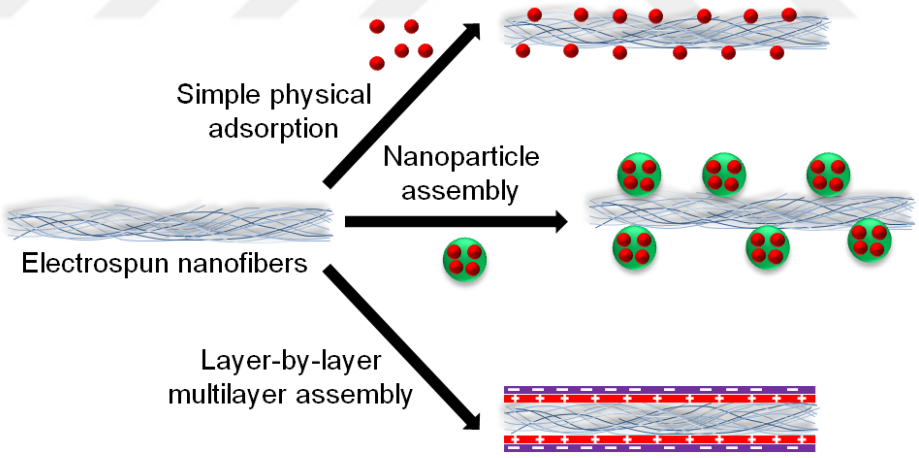

Figure 1.30. Schematic illustration for the modification of nanofibers via (a) simple physical adsorption (b) nanoparticle assembly (c) layer-by-layer assembly.

1.5.6. Click Chemistry For The Chemical Immobilization Of Nanofibers

For particularly biomedical applications, electrospun nanofibers usually need the immobilization or encapsulation of various bioactive molecules and cell recognizable ligands such as enzymes, proteins, growth factors, nucleic acids, carbohydrates or drugs

that would guide or direct specific biological functions. These biologically modified nanofibers offer enhanced biomimetic microenvironments to contacting cells and tissues with increased cell−material interactions. Chemical immobilization is generally preferred over physical immobilization as in chemical immobilization the biomolecules are covalently attached to the nanofibers which prevents the easy release compared to the physical immobilization. Methods like surface modification techniques and physical adsorption can be time- and resource consuming with multistep processes and can also cause immune specific reactions and biocompatibility problems. On the other hand, chemical conjugation can also need multi-step procedures and purification in harsh conditions. Recently, 'click' chemistry has become popular for fiber modification due to its robust, selective, bio-friendly, orthogonal, efficient, and high yielding nature. Although copper-catalysed click chemistry (CuAAC) has been pioneering in this area, metal-free click reactions such as SPAAC, Diels-Alder, thiol-ene, etc. have been preffered lately due to the toxic residual copper ions which can cause biocompatibility problems.

In an early example of the usage of "click chemistry" for the functionalization of electrospun nanofibers, Jing and coworkers prepared alkyne side chain containing polylactide-based fibers which were functionalized through copper-catalyzed azide-alkyne cycloaddition (Figure 1.31) [95]. The reactive nanofibers were electrospun from a chloroform solution of an alkyne bearing-copolymer composed of a propargyl functional cyclic carbonate monomer and l-lactide via ring-opening polymerization P(LA-co-MPC). These alkyne-functional fibers were immobilized with an azide-containing testis-specific protease-50 (TSP50), a biomarker for breast cancer, through CuAAC using $CuSO_4$ and metallic Cu in aqueous media. TSP50-immobilized fibers could selectively identify the antibody, anti-TSP50, which proposes that these fibers are promising materials for the immobilization and detection of an antigen/antibody pair.

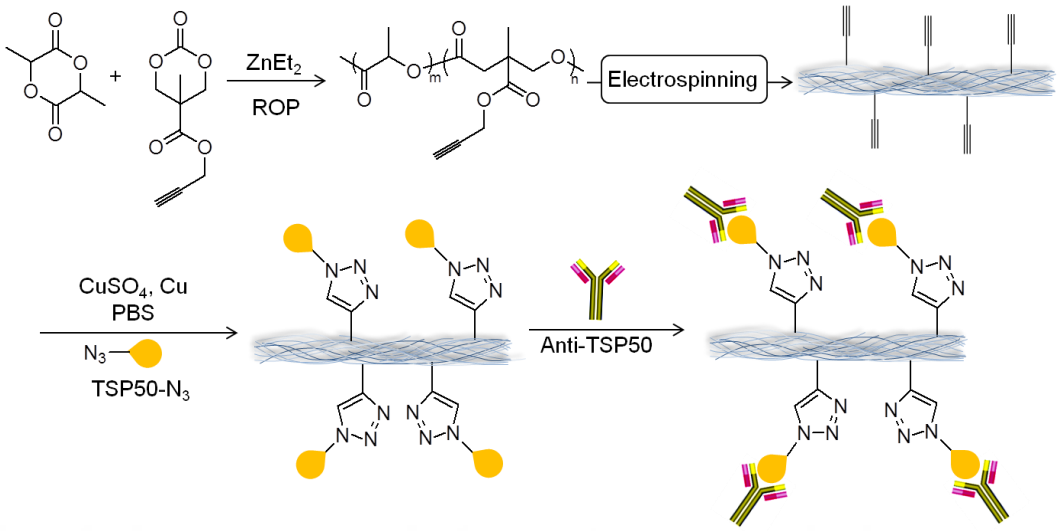

Figure 1.31. Modification of side-chain alkyne-containing PLA nanofibers with an azide-containing biomarker via CUAAC (Adapted with permission from Ref [95]).

Modifications on nanofibers through CuAAC were also studied by Becker and coworkers on poly(ester urea)(PEU) nanofibers [96]. Azide and alkyne containing poly(ester urea) copolymers were synthesized via interfacial polycondensation polymerization and nanofibers were prepared by electrospinning the PEU solutions in hexafluoroisopropanol (Figure 1.32). Alkyne-PEU nanofibers were functionalized with Chromeo 488 azide in PBS buffer solution while azide-PEU nanofibers were modified with alkyne-RGD-biotin followed by rhodamine (TRITC)-conjugated streptavidin immobilization in aqueous environment, both via CuAAC. In a more recent study of Becker group, sequential "triclick" modifications of DIBO-(P(CL-co-OPD)) based nanofibers including SPAAC, oxime ligation and CuAAC were investigated [97]. DIBO-(P(CL-co-OPD)) was synthesized through the ring-opening copolymerization of ε-caprolactone and 1,4,8-trioxaspiro[4.6]-9-undecanone initiated by 4-dibenzocyclooctynol (DIBO). Gly-Arg-Gly-Asp-Ser (N_3-GRGDS), NH_2O-dopamine, and bone morphogenetic protein 2 (N_3-BMP-2) peptide were attached to the nanofibers sequentially via SPAAC, oxime, and CuAAC reactions.

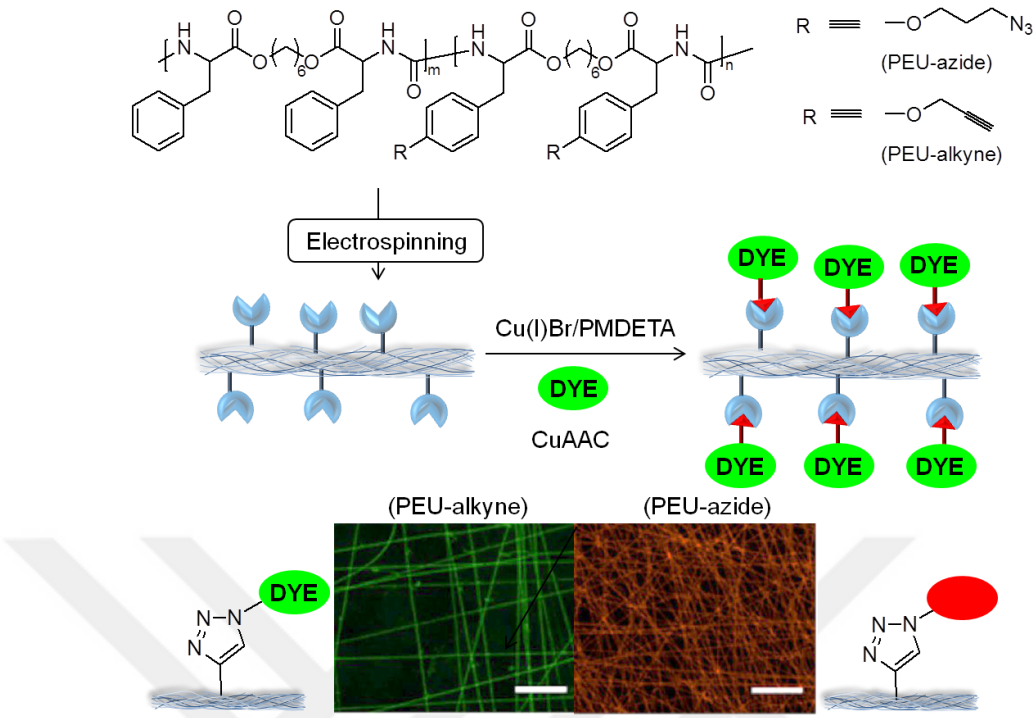

Figure 1.32. Modification of azide and alkyne-containing PEU nanofibers with alkyne and azide-containing fluorescent dyes, respectively via CUAAC (Adapted with permission from Ref [96,97]).

Becker and coworkers used a DIBO initiator for the ring opening polymerizations of poly(ε-caprolactone) [98], poly(γ-benzyl-L-glutamate)[99] and polylactide [100] which were electrospun into nanofibers (Figure 1.33). Ring-opening polymerization of ε-caprolactone was studied using DIBO as the initiator and stannous octoate as the catalyst. The resulting DIBO-PCL was electrospun into chain-end DIBO functional PCL nanofibers by dissolving the polymer in DCM:DMF (4:1). The DIBO-PCL nanofibers were functionalized with an aqueous solution of an azide-containing fluorescence probe (Chremo 488 azide) via SPAAC. In a similar way, DIBO-initiated poly(γ-benzyl-L-glutamate) (DIBO-PBLG) was reported by ring opening polymerization. DIBO-PBLG was dissolved in 12 wt % 1,4-dioxane solution and electrospun into nanofibers. The DIBO-PBLG nanofibers were modified with Chremo 488 azide and azide-containing gold nanoparticles in a reagent-free way. DIBO-PLLA was also prepared through organocatalyzed ring opening polymerization of l-lactide. A solution of DIBO-PLLA in DCM:DMF (4:1) was electrospun into DIBO-terminated polylactide nanofibers which were modified with an azidized peptide, Tyr-Ile-Gly-Ser-Arg (YIGSR).

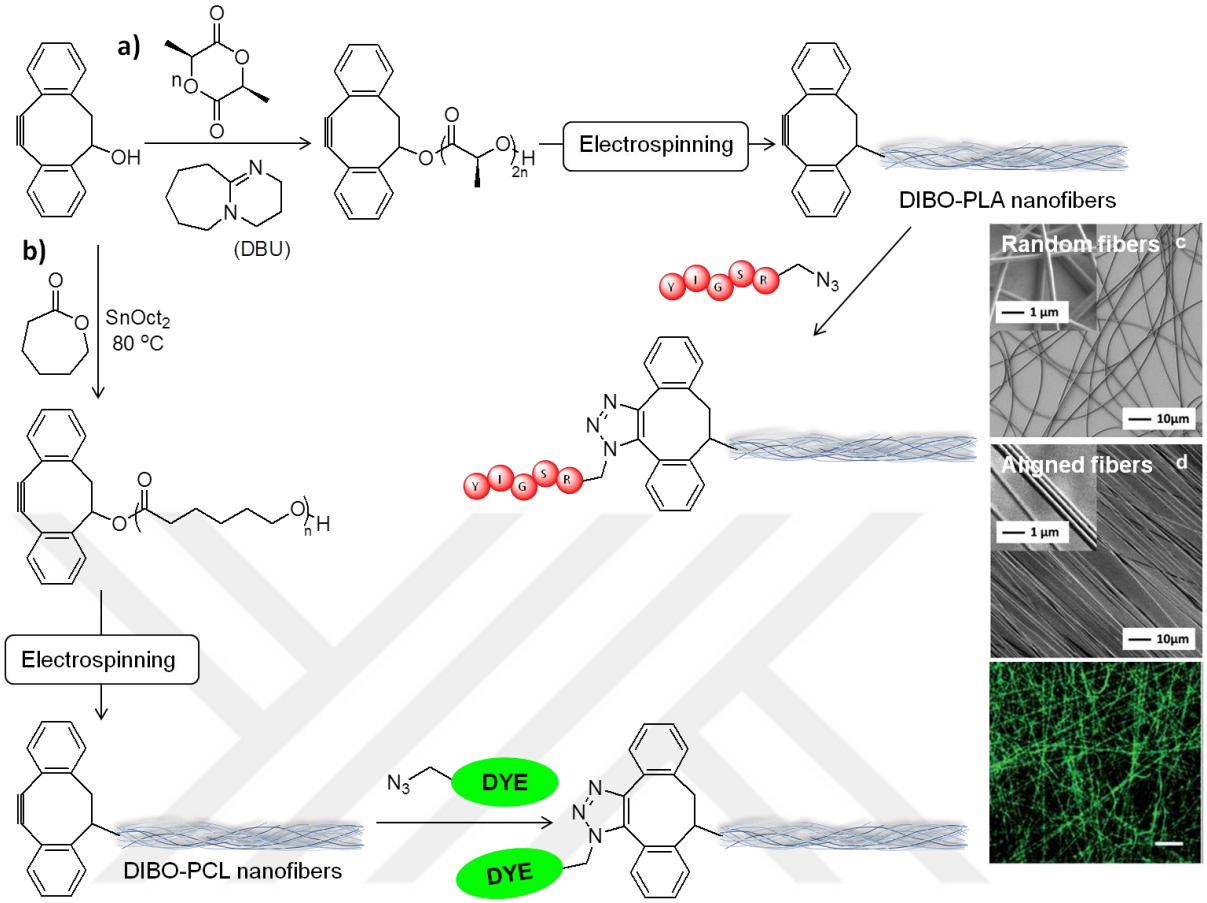

Figure 1.33. Modification of chain-end DIBO-containing (a) PLA with azide-containing peptide, (b) PCL nanofibers with azide-containing fluorcent dye, via SPAAC reaction (Adapted with permission from Ref [98,100]).

Becker and coworkers also synthesized an alkene-containing poly(ester urea) via interfacial polymerization and produced alkene-functional nanofibers by electrospinning a solution of alkene-PEU in hexafluoroisopropanol (Figure 1.34) [96]. These alkene-PEU nanofibers were functionalized with FITC-RGD-thiol and Fmoc-RGD-thiol via thiol-ene reaction in the presence of a photoinitiator, Irgacure- 2959, in PBS solution under UV light for 2 min (365 nm, intensity 10 mW/cm^2).

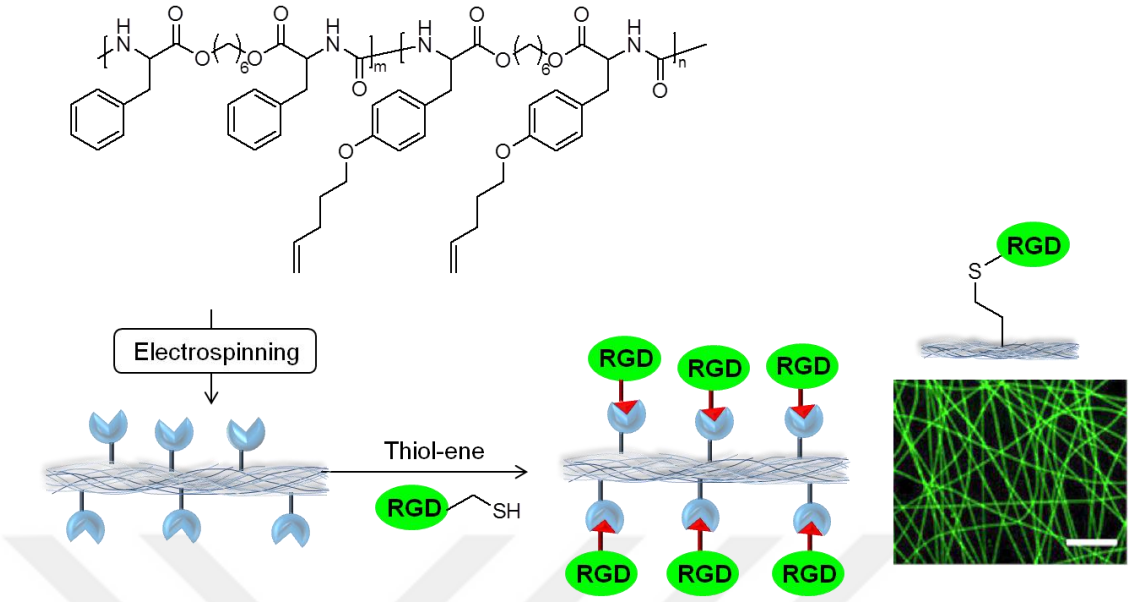

Figure 1.34. Modification of alkene-containing PEU nanofibers with thiol-containing RGD peptide via thiol-ene reaction (Adapted with permission from Ref [96]).

In another study, Guo and coworkers prepared crosslinked poly((3-mercaptopropyl)methylsiloxane) (PMMS)-based fibers via radical thiol-ene reaction [101]. PMMS was dissolved in THF with 2,2-dimethoxy-2-phenylacetophenone as the photoinitiator and crosslinked under UV light during electrospinning. A maleimide-containing poly(N-isopropylacrylamide) was grafted on the remaining free thiols via nucleophilic Michael addition in the presence of a small amount of triethylamine in aqueous environment, which brought thermo-responsiveness to the PMMS nanofibers.

An example to activated-ester based nanofiber functionalization was reported by Theato, Coughlin and coworkers [102]. An amine-reactive poly(ethylene oxide)-block-poly(pentafluorophenyl (methyl)acrylate) (PEO-hv-PPfpMA) diblock copolymer was synthesized via RAFT polymerization using pentafluorophenyl methacrylate (PfpMA) as monomer in the presence of a PEO-based Macro-CTA (Figure 1.35). The photocleavable diblock copolymer was electrospun into nanofibers with diameters between 800 nm to 2 μm which were exposed to UV irradiation (λ = 365 nm) to cleave the o-nitrobenzyl functional group junction between the two blocks, followed by treatment with a diamine to induce crosslinking. The porous nanofibers were functionalized with an amine-containing fluorescent dye, 4-nitro-7-(piperazin-1-yl)benzo-[c][1,2,5]oxadiazole (NBD).

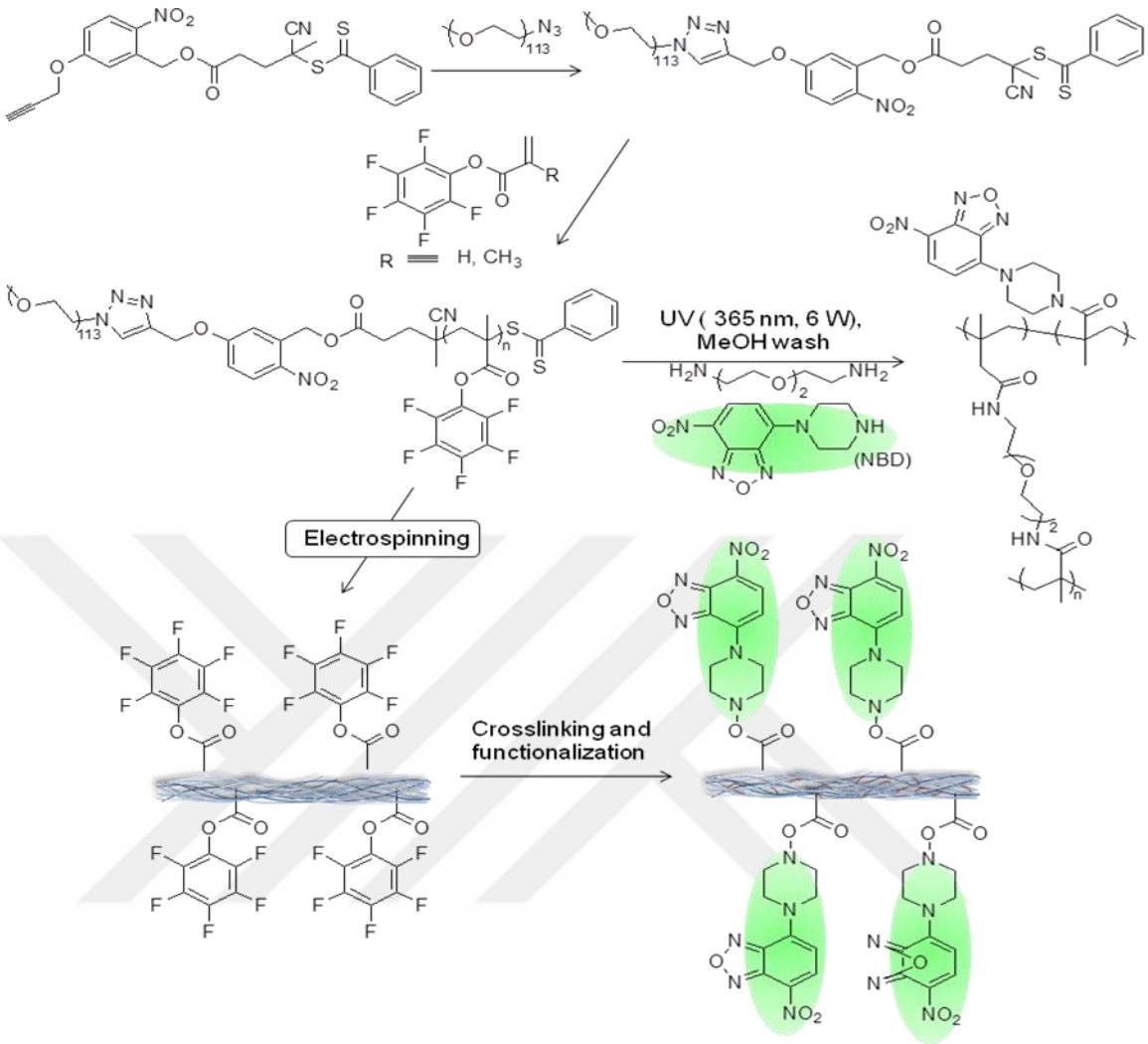

Figure 1.35. Synthesis and modification of active ester containing amine- reactive porous electrospun fibers (Adapted with permission from Ref [102]).

2. RESEARCH OVERVIEW

The main objective of this thesis is to synthesize novel functional nanofibers for biomedical applications. For this purpose, novel clickable group bearing nanofibers were obtained using electrospinning method and reagent-free functionalized with various (bio)molecules such as fluorescent dyes, enzymes, nanoparticles, peptides, oligonucleotides via click chemistry and evaluated as suitable candidates to enhance the (bio)molecule loading, sensing, cell attachment.

To achieve this goal, various biodegradable and non-biodegradable copolymers with side chain or chain-end clickable groups were synthesized. The biodegradable copolymers were synthesized with organo-catalyzed ring-opening polymerization while the non-biodegradable copolymers were synthesized with free radical polymerization. Antibiofouling property was also brought in using poly(ethylene glycol) based comonomers as it is commonly known that antibiofouling prevent non-specific binding of the (bio)molecules. It is well known that nanofibers are promising materials for biomedical applications as the high surface area allows high loading, porosity and fibrillar structure enhances cell attachment. Therefore, the synthesized copolymers were electrospun into clickable nanofibers using the solution electrospinning method. Some types of nanofibers were also crosslinked and patterned. An important achievement in this thesis is that the biomolecules were immobilized on the clickable nanofibers in aqueous environment at room temperature without using any catalysts.

In short, novel clickable polymeric nanofibers were synthesized using a combination of synthetic organic and polymer chemistries. Both biodegradable and non-biodegradable nanofibers were functionalized with a variety of (bio)molecules including fluorescent dyes, enzymes, nanoparticles, peptides and oligonucleotides under mild reaction conditions and they were evaluated as promising candidates for biomedical applications.

3. BIOFUNCTIONALIZATION OF FURAN-CONTAINING NON-BIODEGRADABLE NANOFIBERS VIA DIELS-ALDER REACTION

Published as the following paper: Kalaoglu-Altan, O.I., R. Sanyal, and A. Sanyal, "'Clickable' Polymeric Nanofibers Through Hydrophilic−Hydrophobic Balance : Fabrication Of Robust Biomolecular Immobilization Platforms." *Biomacromolecules,* Vol. 16, pp. 1590−1597, 2015.

3.1. Introduction

In recent years polymeric nanofibers have emerged as attractive functional scaffolds for various materials and biomedical applications. Particular areas of interest in the biomedical arena include utilization of polymeric nanofibers in tissue engineering and regenerative medicine where functional biomaterials capable of promoting cellular attachment, their growth and controlled *in vitro* differentiation and scaffolds capable of regenerating damaged tissue *in vivo* [103-105]. Nanofibrous scaffolds are also of interest in biomolecular immobilization to support proteins and enzymes for purposes like catalysis and detection due to their enhanced surface area [106-108]. The interest in utilization of polymeric nanofibers in biomedical applications arise due to their unique properties such as high surface to volume ratio, tunable porosity and physical resemblance to the fibrillar structure of the collagen fibers in the natural extracellular matrix [2, 109]. Among many methods of producing polymers nanofibers, electrospinning has emerged as a method of choice due to its simplicity, low cost and high turnover [3-5]. A wide variety of polymeric fibers with different physical and chemical properties desirable for a particular application can be obtained by selecting appropriate polymeric precursors. Oftentimes, electrospun polymeric nanofibers require modifications by inclusion of bioactive molecules such as extra cellular matrix (ECM) proteins, ECM carbohydrates, ECM-derived peptides, and growth factors for biomedical applications. Until recently, majority of the polymeric fibers utilized for such applications lacked specific binding sites which are necessary to decorate the fibers with biological cues to mimic microenvironment of cells and regulate cellular functions [15,110]. Traditionally, functionalization of nanofibers is usually carried out via multiple time and resource-consuming procedures like plasma treatment, wet chemical

methods, surface graft polymerization, co-electrospinning of surface active agents with polymers, physical adsorption and conjugation chemistry [87,111]. In recent years, 'click' reactions have emerged as a powerful post-polymerization functionalization methodology due to their high efficiency under mild reaction conditions [52,72]. While initial reports focused on modification of electrospun fibers using the copper catalyzed Huisgen-type [3+2] azide-alkyne cycloaddition, focus has shifted towards utilization of metal-free modification [58,62,95,112-114]. Recently, Becker and coworkers demonstrated poly(ester urea) (PEU) based nanofibers with various types of pendent groups such as alkyne, azide, alkene, tyrosine-based phenol, and ketone [96]. Alkyne-bearing PEU nanofibers were functionalized with an azide-containing fluorescent dye via copper-catalyzed click chemistry while RGD-thiol was immobilized on alkene functional nanofibers using thiol-ene reaction. Another recent example by the same group utilized metal-free azide-alkyne click reaction for nanofiber functionalization. Poly(γ-benzyl-L-glutamate) (PBLG) and poly lactide (PLA) copolymers initiated using 4-dibenzyocyclooctynol (DIBO) were functionalized through metal-free click reaction with azide-appended gold nanoparticles and azide-ended GYIGSR peptide, respectively [98,100]. Although the methodology is attractive since no reagents are required to promote the strain-release induced azide-alkyne cycloaddition, the alkyne bearing cyclooctyne entails multistep synthesis. The thiol-ene and thiol-yne reactions provide an attractive and effective method for functionalization, albeit, the reaction involves thermal or photochemical generation of free-radicals. A quick survey of the 'click' chemistry tool-box reveals that Diels-Alder reactions provide another alternative for metal-free conjugations. To date, the Diels-Alder cycloaddition has been employed as reagent-free 'click' reaction to obtain various macromolecular architectures with high yields by incorporation of appropriate diene and dienophile into polymeric structures [76,77,80,115]. Additionally, this facile conjugation chemistry has been employed for attachment of drugs, ligands and biomolecules to polymeric materials for applications such as drug delivery, biomolecular immobilization and tissue engineering [79,116,117].

Utilization of furan as a dienophile component is attractive since it undergoes efficient conjugation with maleimide-containing molecules at ambient temperatures [118,119]. Furthermore, several studies have shown that the Diels-Alder cycloaddition reaction is accelerated under aqueous conditions.

Herein we report the fabrication and functionalization of polymeric nanofibers that can be functionalized under benign conditions using metal-free Diels-Alder 'click' cycloaddition reaction [120]. Nanofibers containing pendant furan groups can be obtained via electrospinning of furan-containing copolymers. Due to the high reactivity of furan and maleimide groups in aqueous environment these fibers can be expected to undergo efficient functionalization at room temperature. In particular, we present the synthesis of copolymers possessing furan moieties as reactive groups, polyethylene glycol pendant side chains for rendering these fibers hydrophilic and anti-biofouling, and methyl methacrylate units to provide hydrophobic domains that lead to stability of the fibrous core in aqueous medium. Following, a variety of electrospinning conditions are studied to obtain furan reactive nanofibers. Thereafter, functionalization of the nanofibrous scaffolds with maleimide-appended fluorescent dye and biotin is performed via the Diels-Alder reaction. Successful immobilization of FITC-streptavidin and streptavidin-coated CdSe based quantum dots on biotinylated nanofibers was demonstrated (Figure 3.1.).

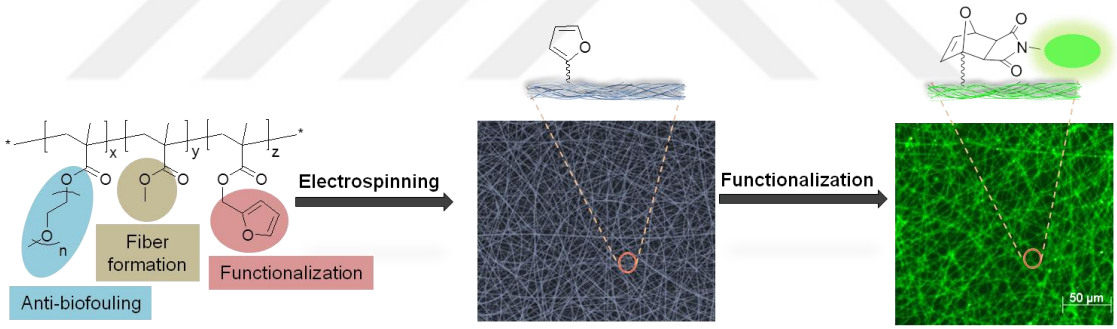

Figure 3.1. Scheme illustrating fabrication and functionalization of nanofibers via Diels-Alder reaction.

3.2. Experimental

3.2.1. Materials

Furfuryl methacrylate (FuMA), poly(ethylene glycol) monomethyl ether methacrylate (PEGMEMA) (average M_n=300 $gmol^{-1}$), N-(5-fluoresceinyl)-maleimide, and fluoresceinamine isomer I were obtained from Aldrich. Methyl methacrylate (MMA), dimethylformamide (DMF), and tetrahydrofuran (THF) were obtained from Merck and solvents were used as received. PEGMEMA, MMA and FuMA were used after passing through neutral Al_2O_3 in order to remove inhibitors prior to use. 4,4′-Azobis(4-cyanovaleric acid) (V-501) was purchased from Fluka. Biotin-PEG2-maleimide and FITC-conjugated streptavidin were purchased from ThermoScientific and Pierce, respectively. Qdot 605 streptavidin conjugate was purchased from Life Sciences.

3.2.2. Instrumentation

The NMR spectra were recorded on a Varian 400 MHz spectrometer with deuterated chloroform ($CDCl_3$) as the solvent at 25 ^oC. The molecular weights of the copolymer were estimated by gel permeation chromatography analysis using a Shimadzu PSSSDV (length/ID 8 × 300 mm, 10 μm particle size) mixed-C column calibrated with polystyrene standards (1−400 kDa) using a refractiveindex detector. THF was used as eluent at a flow rate of 1 mL/min at 30 °C. The morphology of electrospun nanofibers were observed with Jeol Neoscope JCM-5000 scanning electron microscopy and Philips XL30 ESEM-FEG/EDAX system SEM and scanning transmission electron microscopy. Fluorescence images of the functionalized samples were recorded on a Zeiss Observer Z1 fluorescence microscope connected to Axiocam MRc5 using a Zeiss Filter set 38 (Excitation BP 470/40, Emission BP 525/50) for imaging the functionalized nanofibers. Static water contact angle were measured in air via the sessile-drop method using a goniometer (CAM 101 KSV instruments). Approximately 5 μL of deionized water was deposited on the surface and images were taken by an integrated digital camera. The software CAM2008 was used for image processing to determine the contact angle. Contact angle value for each sample was independently measured at three different locations and average values were measured. XPS measurements were carried out using a K-Alpha

instrument from Thermo Scientific. The X-ray source employed was a monochromatic Al Kα (1486.6 eV) at 72 W and 10^{-9} mbar. All XPS spectra were calibrated on the aliphatic carbon signal at 285.0 eV. DSC experiments were performed on a TA Instruments Q-2000 DSC apparatus at a heating rate of 10 °C/min.

3.2.3. Copolymerization of Furan-Containing Copolymers

3.2.3.1. Synthesis of furan-containing copolymer (Poly(PEGMEMA$_{20}$-MMA$_{45}$-FuMA$_{35}$)). PEGMEMA (average M_n = 300 g mol^{-1}), FuMA, and MMA were passed through an aluminum oxide column in order to remove inhibitors. PEGMEMA (1.00 mL, 3.5 mmol), FuMA (1.08 mL, 7 mmol), MMA (0.74 mL, 7 mmol), and V-501 (19.6 mg, 0.07 mmol) were dissolved in DMF (10 mL) in a 25 mL round-bottom flask equipped with a magnetic stir bar and degassed by bubbling nitrogen. Thereafter, the roundbottom flask was sealed and placed in a 80 °C oil bath and stirred for 20 h. At the end of the reaction, the solvent was evaporated under reduced pressure. The residue was dissolved in minimum amount of dichloromethane and purified by precipitation in cold diethyl ether. The polymer was obtained as a white powder (2.5 g, conversion 86%). ^{1}H-NMR (400 MHz, $CDCl_3$,δ): 7.40 (s, 1H furan), 6.37 (s, 1H furan), 6.32 (s, 1H furan), 4.93 (br s, 2H, –OC*H*$_2$–furan), 4.05 (br s, 2H, –COOC*H*$_2$–PEG), 3.63-3.53 (m, 15H,–OC*H*$_2$C*H*$_2$O– and–COOC*H*$_3$), 3.35 (s, 3H, OC*H*$_3$).

3.2.3.2. Synthesis of furan-containing copolymer (Poly(PEGMEMA$_{30}$-MMA$_{30}$-FuMA$_{40}$)). PEGMEMA (average M_n = 300 g mol^{-1}), FuMA, and MMA were passed through an aluminum oxide column in order to remove inhibitors. PEGMEMA (0.5 mL, 1.75 mmol), FuMA (0.27 mL, 1.75 mmol), MMA (0.1 mL, 0.875 mmol), and V-501 (4.9 mg, 0.07 mmol) were dissolved in DMF (4 mL) in a 25 mL round-bottom flask equipped with a magnetic stir bar and degassed by bubbling nitrogen. Thereafter, the roundbottom flask was sealed and placed in a 80 °C oil bath and stirred for 20 h. At the end of the reaction, the solvent was evaporated under reduced pressure. The residue was dissolved in minimum amount of dichloromethane and purified by precipitation in cold diethyl ether. The polymer was obtained as a white powder (0.76 g, conversion 84%). ^{1}H-NMR (400 MHz, $CDCl_3$,δ): 7.42 (s, 1H furan), 6.36 (s, 1H furan), 6.32 (s, 1H furan), 4.92 (br s, 2H, –

OCH_2–furan), 4.05 (br s, 2H, –COOCH_2–PEG), 3.64-3.53 (m, 15H,–OCH_2CH_2O– and–COOCH_3), 3.35 (s, 3H, OCH_3).

3.2.3.3. Synthesis of furan-containing copolymer (Poly(PEGMEMA$_{40}$-MMA$_{35}$-FuMA$_{25}$)). PEGMEMA (average M_n = 300 g mol^{-1}), FuMA, and MMA were passed through an aluminum oxide column in order to remove inhibitors. PEGMEMA (0.5 mL, 1.75 mmol), FuMA (0.135 mL, 0.875 mmol), MMA (0.1 mL, 0.875 mmol) and V-501 (4.9 mg, 0.07 mmol) were dissolved in DMF (4 mL) in a 25 mL round-bottom flask equipped with a magnetic stir bar and degassed by bubbling nitrogen. Thereafter, the roundbottom flask was sealed and placed in a 80 °C oil bath and stirred for 20 h. At the end of the reaction, the solvent was evaporated under reduced pressure. The residue was dissolved in minimum amount of dichloromethane and purified by precipitation in cold diethyl ether. The polymer was obtained as a white powder (0.55 g, conversion 72%). ^{1}H-NMR (400 MHz, $CDCl_3$,δ): 7.41 (s, 1H furan), 6.37 (s, 1H furan), 6.32 (s, 1H furan), 4.92 (br s, 2H, –OCH_2–furan), 4.05 (br s, 2H, –COOCH_2–PEG), 3.63-3.53 (m, 15H,–OCH_2CH_2O– and–COOCH_3), 3.35 (s, 3H, OCH_3).

3.2.3.4. Synthesis of furan-containing copolymer (Poly(PEGMEMA$_{50}$-FuMA$_{50}$)). PEGMEMA (average M_n = 300 g mol^{-1}), and FuMAwere passed through an aluminum oxide column in order to remove inhibitors. PEGMEMA (0.5 mL, 1.75 mmol), FuMA (0.18 mL, 1.17 mmol), and V-501 (3.28 mg, 0.017 mmol) were dissolved in DMF (4 mL) in a 10 mL round-bottom flask equipped with a magnetic stir bar and degassed by bubbling nitrogen. Thereafter, the roundbottom flask was sealed and placed in a 80 °C oil bath and stirred for 20 h. At the end of the reaction, the solvent was evaporated under reduced pressure. The residue was dissolved in minimum amount of dichloromethane and purified by precipitation in cold diethyl ether. The polymer was obtained as a white powder (0.43 g, conversion 60%). ^{1}H-NMR (400 MHz, $CDCl_3$,δ): 7.41 (s, 1H furan), 6.37 (s, 1H furan), 6.32 (s, 1H furan), 4.91 (br s, 2H, –OCH_2–furan), 4.05 (br s, 2H, –COOCH_2–PEG), 3.64-3.53 (m, 12H,–OCH_2CH_2O–), 3.35 (s, 3H, OCH_3).

3.2.3.5. Synthesis of furan-containing copolymer (Poly(MMA$_{60}$-FuMA$_{40}$)). FuMA, and MMA were passed through an aluminum oxide column in order to remove inhibitors. FuMA (0.5 mL, 3.24 mmol), MMA (0.51 mL, 4.86 mmol), and V-501 (7.56 mg, 0.027

mmol) were dissolved in DMF (5 mL) in a 25 mL round-bottom flask equipped with a magnetic stir bar and degassed by bubbling nitrogen. Thereafter, the roundbottom flask was sealed and placed in a 80 °C oil bath and stirred for 20 h. At the end of the reaction, the solvent was evaporated under reduced pressure. The residue was dissolved in minimum amount of dichloromethane and purified by precipitation in cold diethyl ether. The polymer was obtained as a white powder (0.9 g, conversion 90%). ^{1}H-NMR (400 MHz, $CDCl_3$,δ): 7.40 (s, 1H furan), 6.37 (s, 1H furan), 6.32 (s, 1H furan), 4.93 (br s, 2H, –OCH_2–furan), 3.55 (s, 3H, COOCH_3).

3.2.4. Electrospinning of Furan-Containing Copolymers

A copolymer solution was prepared with a concentration of 35 wt % using 3:2 (v/v) DMF/THF solvent mixture. In a typical experiment, the solution was delivered at a constant flow rate of 0.008 mL/min (KDScientific 101 syringe pump) to a needle connected to a high voltage power supply (Matsusada Precision Inc.) with an applied voltage of 11 kV and a the tip to collector distance of 20 cm. Fibers were collected on 22 × 22 mm glass slides sticked onto a grounded aluminum collector.

3.2.5. Fluorescent Dye Conjugation On Furan-Containing Nanofibers

A solution of N-(5-Fluoresceinyl)maleimide (1 mg/mL) was prepared in 1×PBS and 50 μL of this solution was dropped onto the furan-containing nanofibers. After 4 h in the dark, the excess dye was rinsed with copious amounts of PBS solution. As a control experiment, fluoresceinamine isomer I solution was also prepared in 1×PBS (1 mg/mL) and 50 μL of this solution was also dropped on the furan-containing nanofibers. The nanofibers were After 4 h in the dark, the nanofibers were washed with excess PBS solution. Modified nanofibers were investigated with fluorescence microscope.

3.2.6. Biofunctionalization of Furan-Containing Nanofibers

An aqueous biotin-PEG2-maleimide solution (1 mg/mL) was prepared and 50 μL of this solution was dropped onto the furan-containing nanofibers. The reaction was carried out in the dark for 4 h at room temperature. Then, the fiber-coated surfaces were rinsed

with copious amount of water in order to remove any unbound biotin. An aqueous solution of FITC-streptavidin (0.1 mg/mL) was prepared and 10 μL of this solution was dropped onto the biotinylated fibers. After 30 min in the dark, the fibers were washed with ample water to remove any unbound protein. The conjugation was analyzed with fluorescence microscopy.

3.2.7. Nanoparticle Immobilization on Furan-Containing Nanofibers

Nanofibers were biotinylated as explained previously. For the immobilization of Qdots, 3 μL of Qdot solution (1 μM) was dropped onto the biotinylated nanofibers. The nanofibers were washed with ample water to remove any unbound protein after 30 min in the dark. The conjugation was analyzed under fluorescence microscopy and scanning transmission electron microscopy.

3.3. Results and Discussion

Various furan-bearing copolymers were synthesized with varying hydrophilic:hydrophobic comonomer ratios. These copolymers were electrospun into furan-containing non-biodegradable nanofibers and the effect of hydrophilicity on fiber morphology was investigated. Maleimide-bearing fluorescent dye and biotin was conjugated on the furan-containing nanofibers using Diels-Alder reaction. FITC-labeled streptavidin and CdSe qdots were immobilized onto the biotinylated nanofibers.

3.3.1. Fabrication and Characterization of Furan-Containing Hydrophilic Non-Biodegradable Polymers

Various furan-containing reactive copolymers were synthesized by conventional free radical polymerization named as poly(PEGMEMA$_x$-MMA$_y$-FuMA$_z$) where x, y, and z stand for experimental percentage comonomer ratios. FuMA was used as the diene-based reactive group for functionalization, PEGMEMA was used to introduce antibiofouling characteristics to the nanofibers and MMA was integrated to increase the atmosphere. The free radical polymerizations were performed using V-501 as the initiator and DMF as the solvent at 80 °C and the obtained copolymers were purified by precipitation in cold diethyl

ether (Figure 3.2). Polymerizations were confirmed by ^{1}H-NMR spectroscopy (Figure 3.3-3.7).

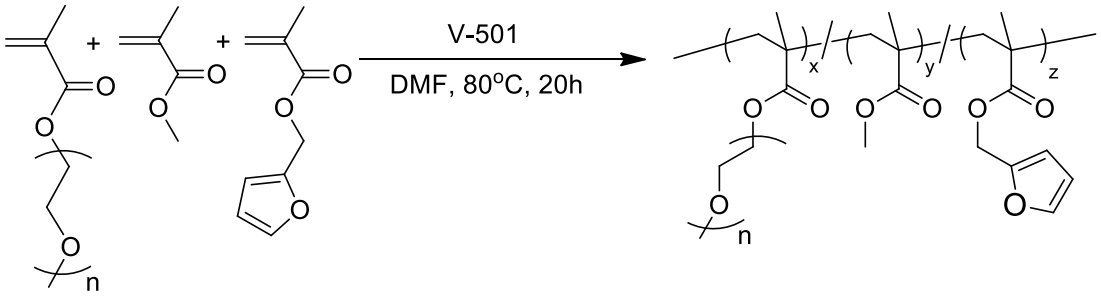

Figure 3.2. Furan-containing non-biodegradable copolymer synthesis.

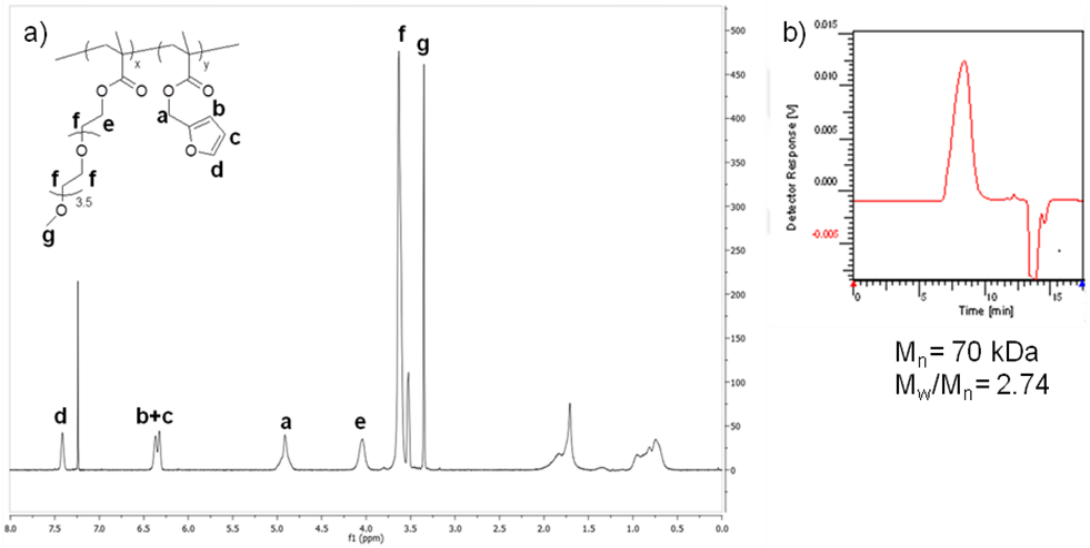

Figure 3.3. a)^{1}H-NMR spectrum b) Size exclusion chromatography trace of poly(PEGMEMA$_{50}$-FuMA$_{50}$).

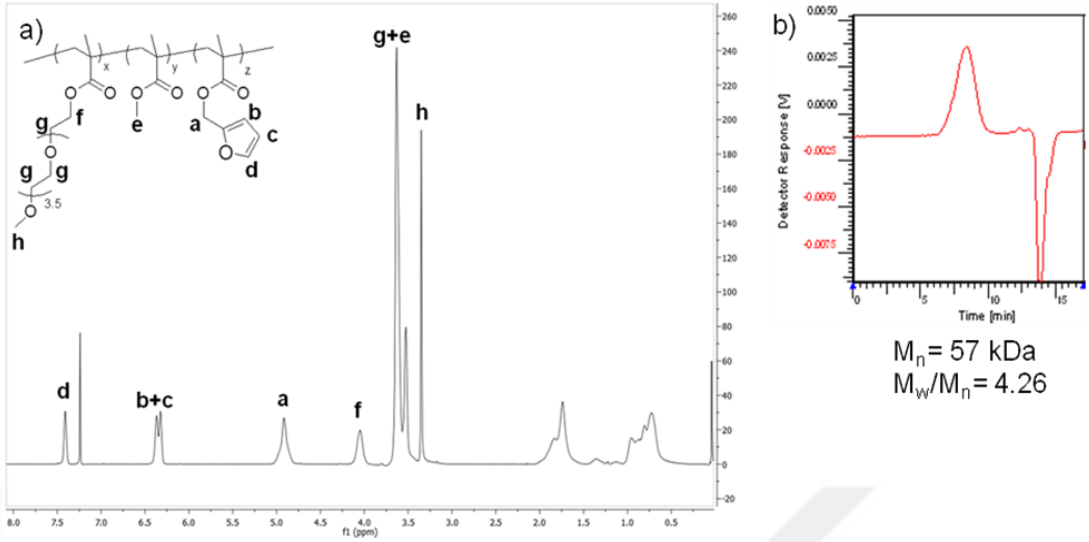

Figure 3.4. a)^{1}H-NMR spectrum b) Size exclusion chromatography trace of poly(PEGMEMA$_{40}$-MMA$_{35}$-FuMA$_{25}$).

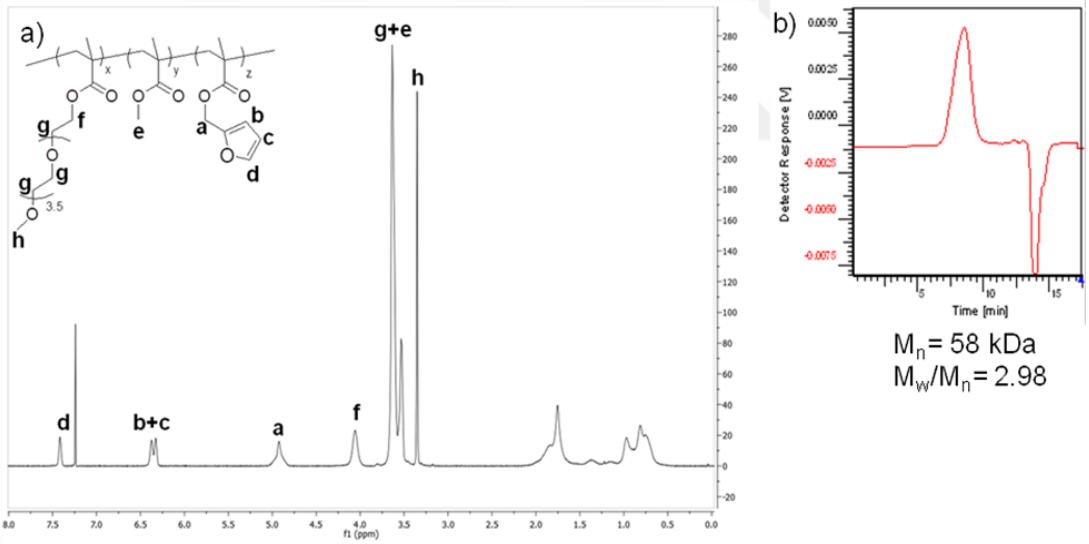

Figure 3.5. a)^{1}H-NMR spectrum b) Size exclusion chromatography trace of poly(PEGMEMA$_{30}$-MMA$_{30}$-FuMA$_{40}$).

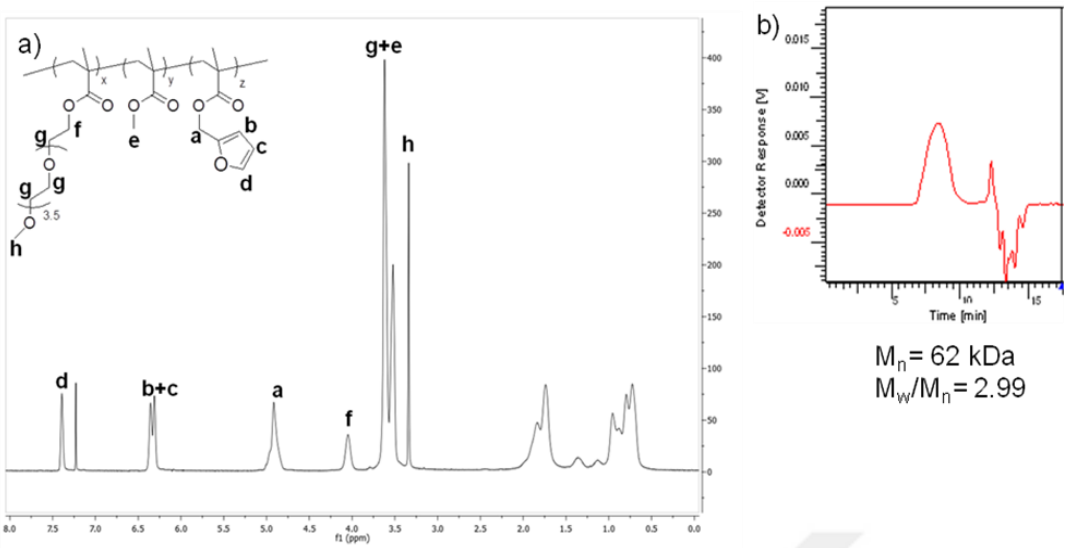

Figure 3.6. a)^{1}H-NMR spectrum b) Size exclusion chromatography trace of poly(PEGMEMA$_{20}$-MMA$_{45}$-FuMA$_{35}$).

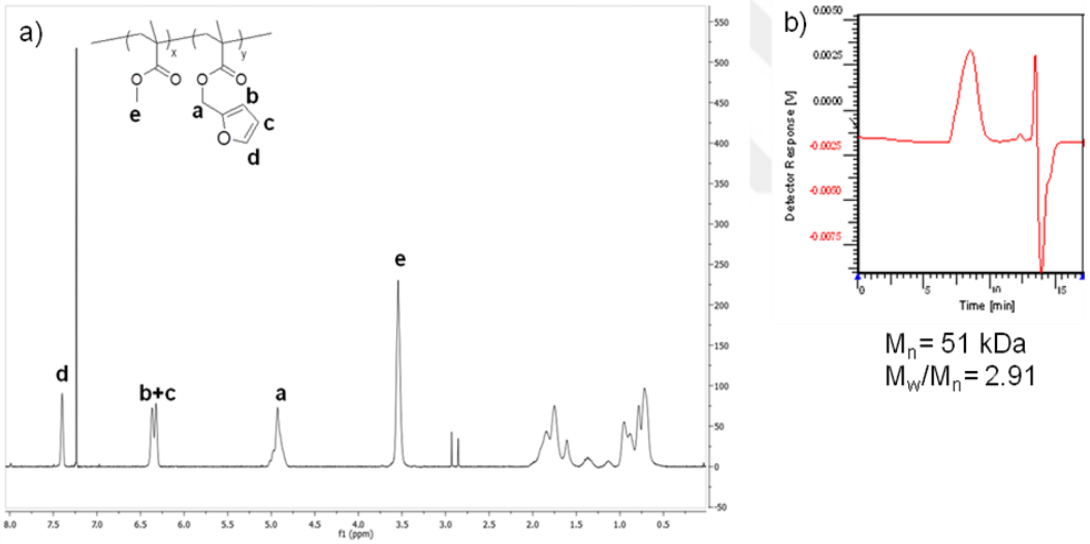

Figure 3.7. a)^{1}H-NMR spectrum b) Size exclusion chromatography trace of poly(MMA$_{60}$-FuMA$_{40}$).

3.3.2. Fabrication and Characterization of Furan-Containing Hydrophilic Non-Biodegradable Nanofibers

A variety of copolymers with different comonomer ratios were synthesized in order to investigate the importance of hydrophilic−hydrophobic balance on the fiber formation and their stability in aqueous medium. Furan-containing reactive nanofibers were prepared from poly(PEGMEMA$_x$-MMA$_y$-FuMA$_z$) by solution electrospinning method using

DMF/THF (3:2) solvent system at a concentration of 35 wt %. Optimal electrospinning conditions which provided nanofibers with minimal bead formation were found as an applied voltage of 11 kV, a flow rate of 0.008 mL/min, and a tip-to-collector distance of 20 cm. Copolymer with 50 % of PEGMEMA, (poly($PEGMEMA_{50}$-$FuMA_{50}$)) could not provide nanofibers through electrospinning but appeared as melted. An improvement in fiber formation was observed when the PEGMEMA content was decreased to 40 % and 30 % and MMA was integrated in the copolymer composition. Stable nanofibers could only be obtained when the hydrophilic PEGMEMA content was decreased to 20 %. As a result, the functionalization studies were performed on the poly($PEGMEMA_{20}$-MMA_{45}-$FuMA_{35}$) nanofibers.

The effect of electrospinning process parameters on the average fiber diameter of poly($PEGMEMA_{20}$-MMA_{45}-$FuMA_{35}$) nanofibers was explored by changing the tip-to-collector distance, applied voltage, and flow rate of the copolymer solution. A decrease in the tip-to-collector distance usually results in an increase in the average fiber diameter and bead formation as the time interval for solvent evaporation decreases. The influence of the distance was investigated by varying it to 5, 10, and 20 cm, while keeping the voltage as 11 kV and the flow rate as 0.008 mL/min. The average fiber diameters were found as 814 ± 444 nm, 404 ± 195 nm, and 280 ± 51 nm for the distances of 5, 10, and 20 cm, respectively (Figure 3.8). It was found that the increase in the distance resulted in a decrease both in bead formation and average fiber diameter while the uniformity of the fiber diameter was also improved. The applied voltage also affects the fiber morphology as the stretching and acceleration of the jet leads to rapid evaporation of solvent and decreases the fiber diameter. It was discovered that the average diameter decreased as 455 ± 165 nm, 375 ± 133 nm, 280 ± 51 nm when the applied voltage was increased as 5.5, 8 and 11 kV, respectively (Figure 3.9). It was observed that the bead formation and the mean fiber diameter decreased with increasing applied voltage. An increment in the average fiber diameter from 280 ± 51 to 506 ± 165 nm was also noticed when the flow rate increased from 0.008 to 0.024 mL/min since a higher flow rate does not give enough time for evaporation (Figure 3.10). Nanofibers for further experiments were electrospun on glass slides using the optimal conditions of 20 cm working distance, an operating voltage of 11 kV, and a flow rate of 0.008 mL/min.

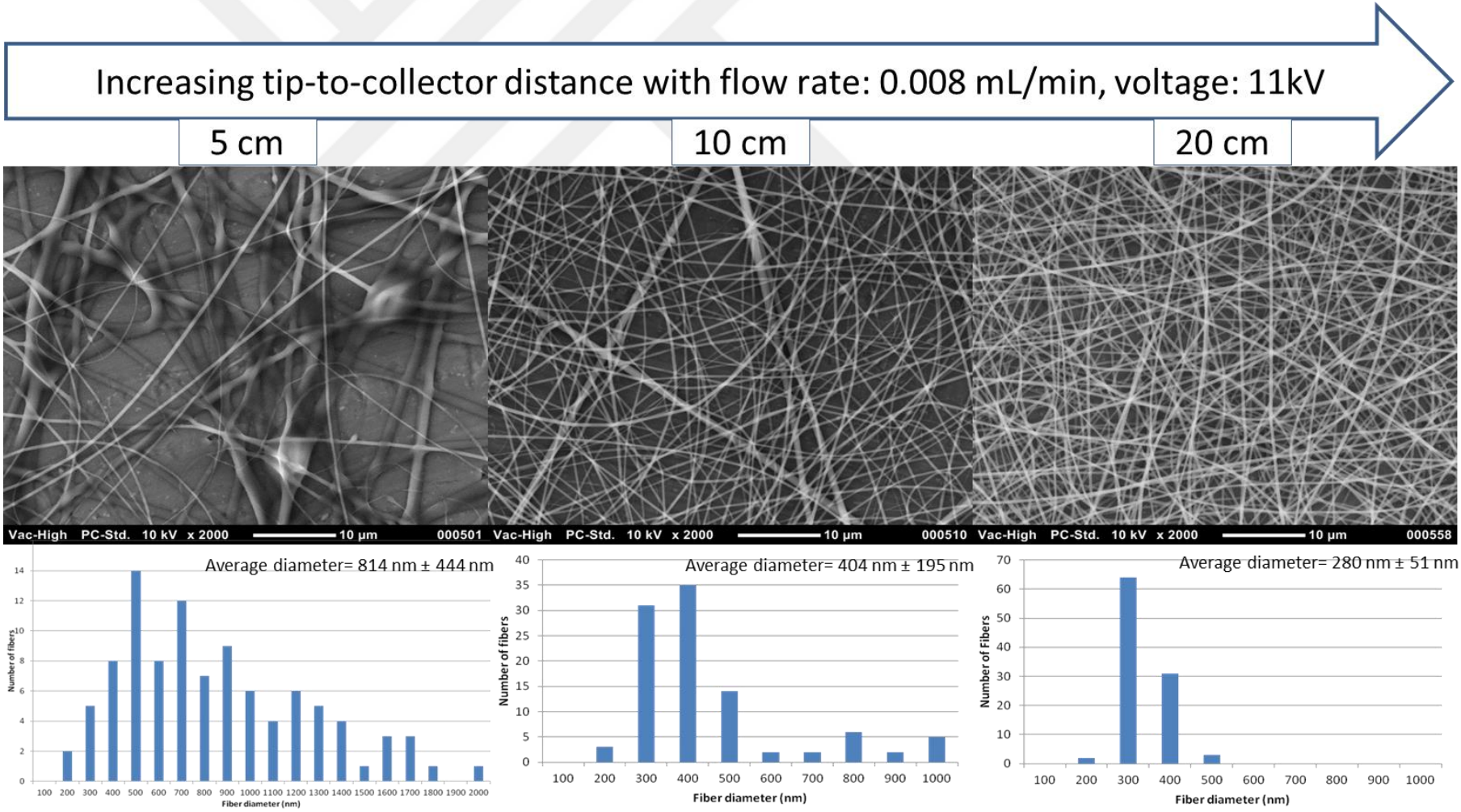

Figure 3.8. SEM images showing the effects of increasing tip-to-collector distance on the average fiber diameter.

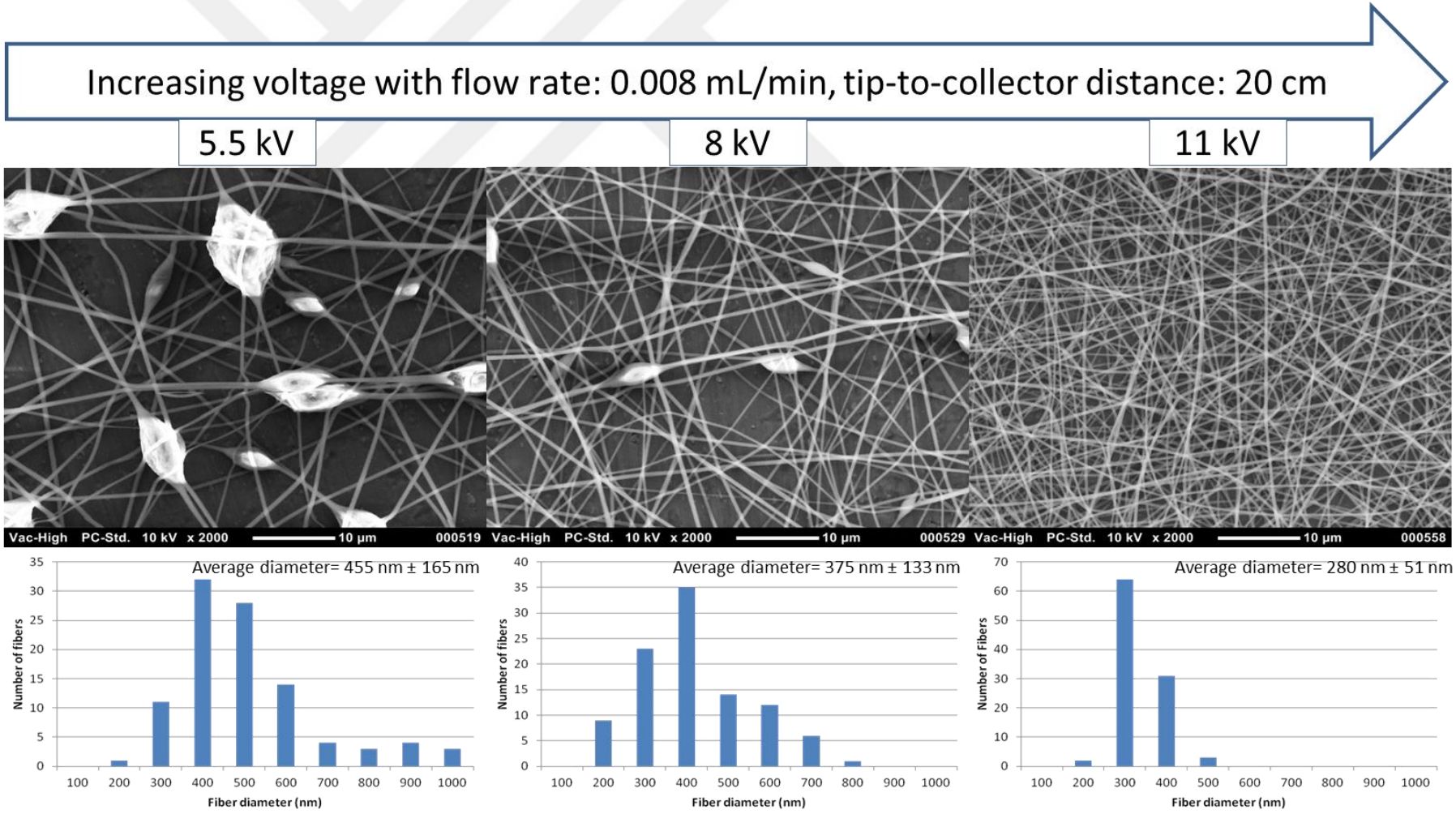

Figure 3.9. SEM images showing the effects of increasing applied voltage on the average fiber diameter.

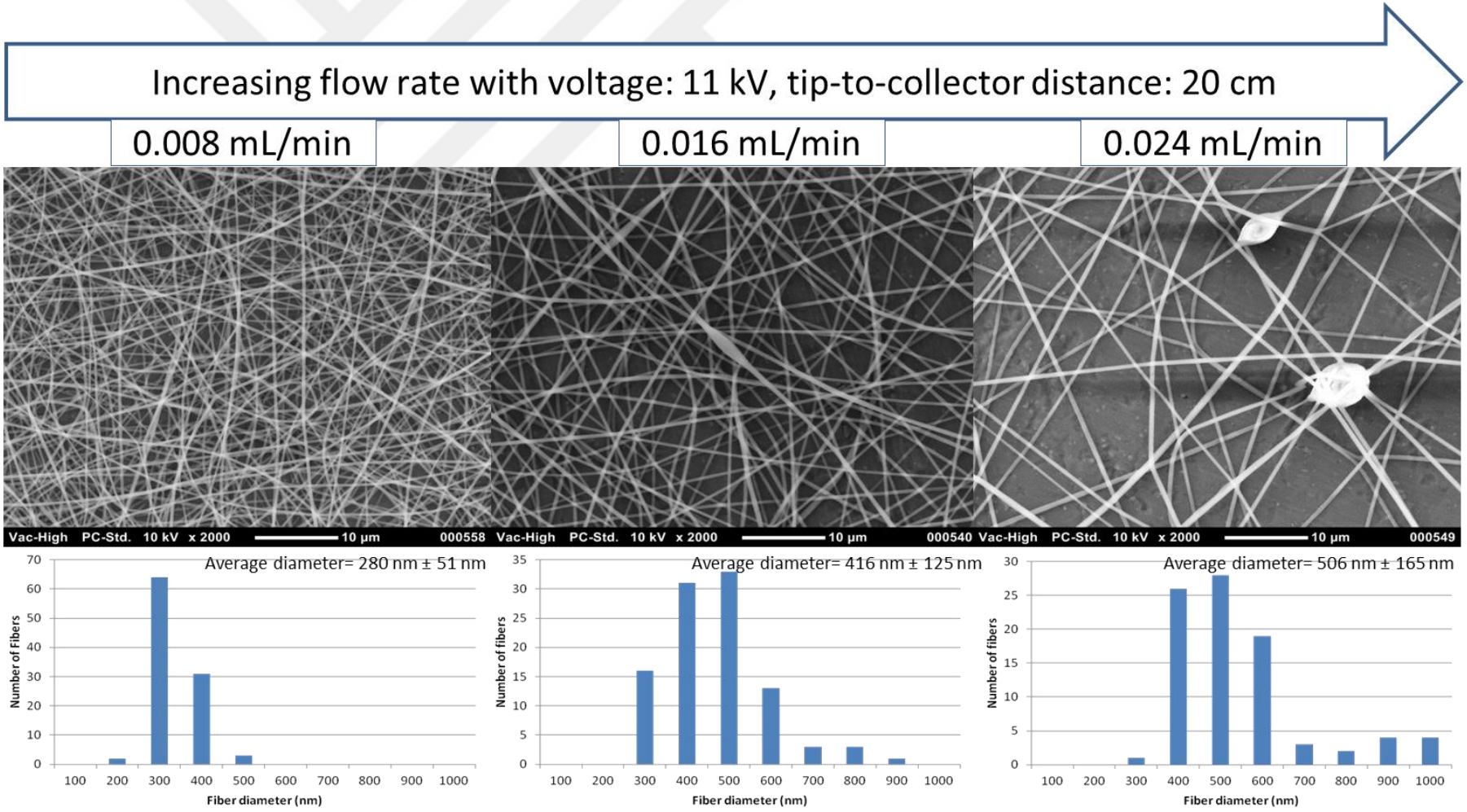

Figure 3.10. SEM images showing the effects of increasing flow rate on the average fiber diameter.

The stability of the nanofibers in aqueous environment was examined by immersing the nanofibrous scaffolds in water for 3 days followed by investigation using SEM. The poly(PEGMEMA$_{20}$-MMA$_{45}$-FuMA$_{35}$) nanofibers were stable with no significant change in their morphology, they were only swollen, the average diameter was increased to 581 nm ± 137 nm from 280 nm ± 51 nm (Figure 3.11). Poly(PEGMEMA$_{40}$-MMA$_{35}$-FuMA$_{25}$) and poly(PEGMEMA$_{30}$-MMA$_{30}$-FuMA$_{40}$) nanofibers were unstable in water and they lost their fibrillar structure. On the other hand, nanofibers with 50 % PEGMEMA content completely dissolved in water. As a result, it was seen that the hydrophilic/hidrophobic ratio both affected the nanofibrous structure and stability in water (Figure 3.12).

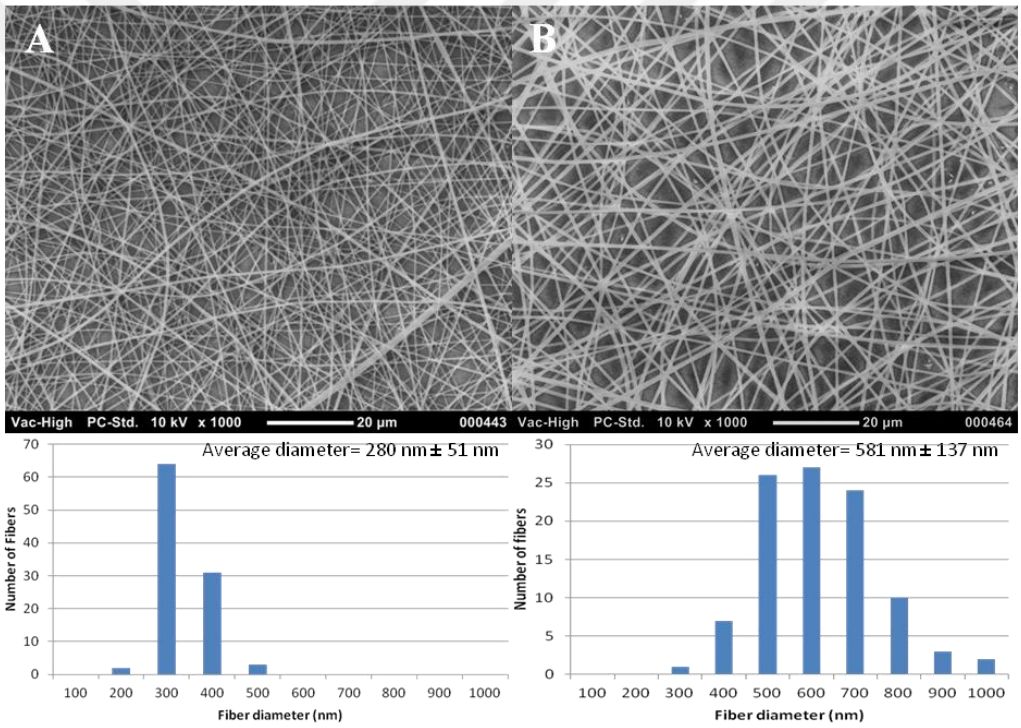

Figure 3.11. SEM images of poly(PEGMEMA$_{20}$-MMA$_{45}$-FuMA$_{35}$) nanofibers obtaining under optimal electrospinning conditions: (a) dry nanofibers and (b) after immersion in water for 3 days.

The hydrophilicity had also a role in the glass transition temperature (T_g) of the copolymers. Thermal analysis of the copolymers using differential scanning calorimetry (DSC) showed that the increase in PEGMEMA content lowered the T_g of the copolymers. The completely hydrophobic poly(MMA$_{60}$-FuMA$_{40}$) copolymer showed a T_g of 92.44 °C while the incorporation of 20 and 40 mol % PEGMEMA decreased the T_g to 31.08 and −24.22 °C, respectively (Figure 3.13).

The influence of PEGMEMA on the hydrophilicity of the polymeric nanofibers was examined through water contact angle measurement. The average contact angle for poly(MMA_{60}-$FuMA_{40}$) nanofibers without the hydrophilic PEG component was found as 105° while the average water contact angle for poly($PEGMEMA_{20}$-MMA_{45}-$FuMA_{35}$) nanofibers with 20 % PEGMEMA was 72° (Figure 3.14). This decrease in the water contact angle indicated that the PEG chains were on the surface of the nanofibers. It has been shown before that a relatively low amount of PEG-based hydrophilic component is sufficient to impart antibiofouling property to fibrous materials [121]. XPS studies also revealed that the ether type C−O linkages arising from the PEG chains were present on poly($PEGMEMA_{20}$-MMA_{45}-$FuMA_{35}$) nanofibers whereas they were not seen for the poly(MMA_{60}- $FuMA_{40}$) nanofibers.

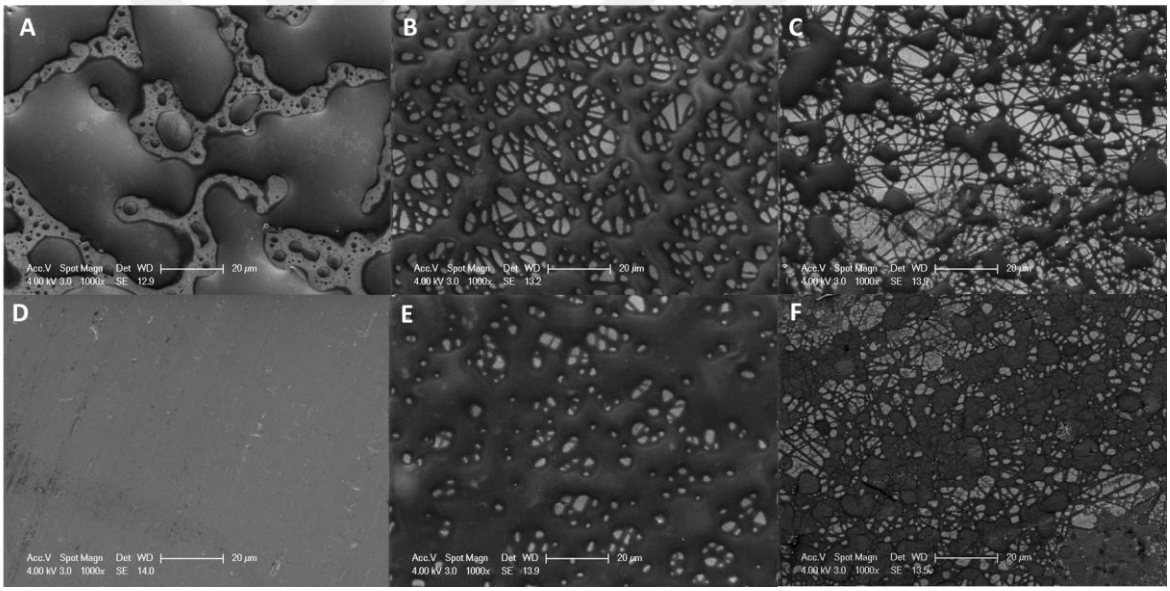

Figure 3.12. SEM images of nanofibers at dry state with compositional ratio of (a) $PEGMEMA_{50}$-$FuMA_{50}$ (b) $PEGMEMA_{40}$-MMA_{35}-$FuMA_{25}$ (c) $PEGMEMA_{30}$-MMA_{30}-$FuMA_{40}$, after immersion in water with compositional ratio (d) $PEGMEMA_{50}$-$FuMA_{50}$ (e) $PEGMEMA_{40}$-MMA_{35}-$FuMA_{25}$ (f) $PEGMEMA_{30}$-MMA_{30}-$FuMA_{40}$.

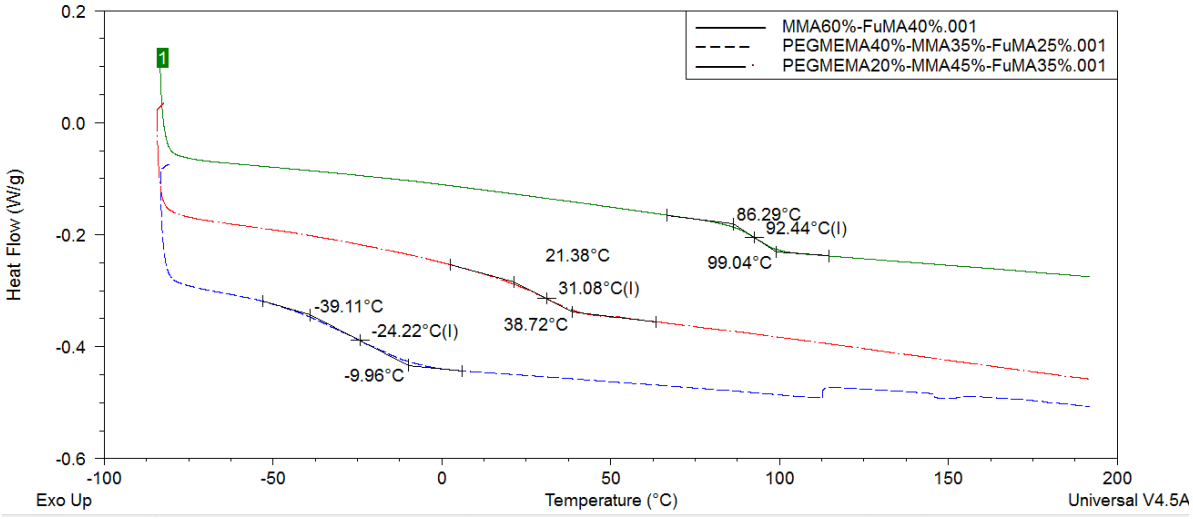

Figure 3.13. DSC measurements of MMA_{60}-$FuMA_{40}$, $PEGMEMA_{40}$-MMA_{35}-$FuMA_{25}$ and $PEGMEMA_{20}$-MMA_{45}-$FuMA_{35}$.

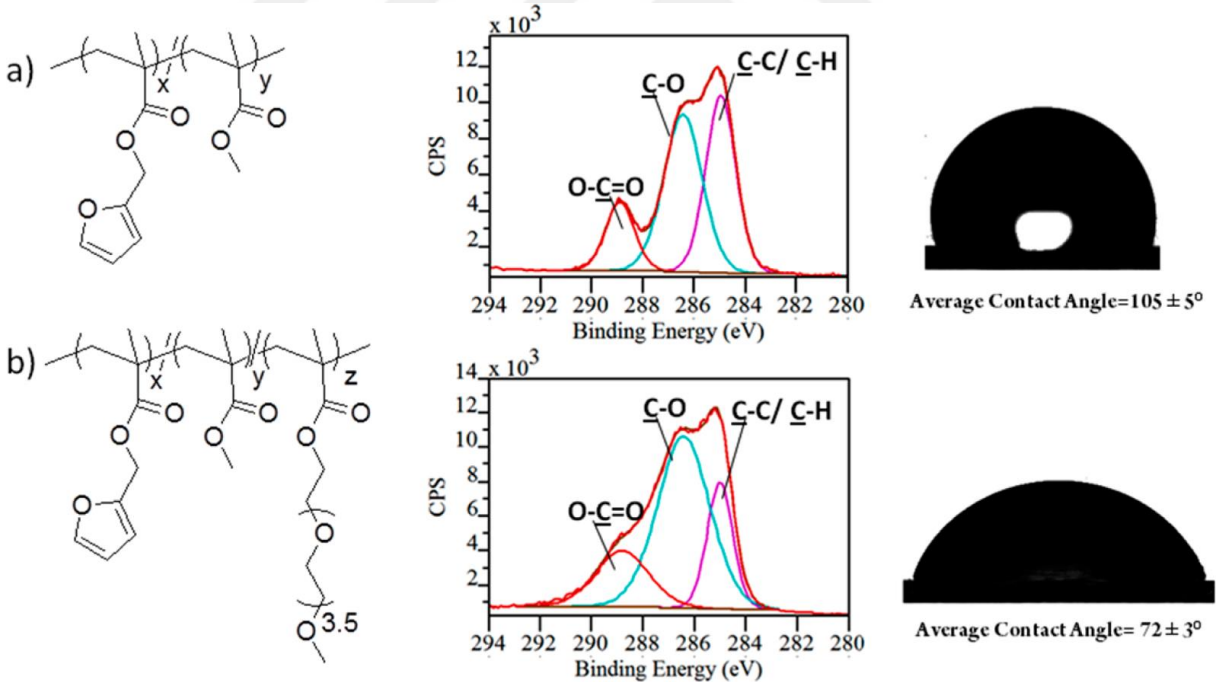

Figure 3.14. Contact angle measurement and elemental composition via XPS analysis on surface for (a) MMA_{60}-$FuMA_{40}$ nanofibers without PEG-based monomer and (b) $PEGMEMA_{20}$-MMA_{45}-$FuMA_{35}$ nanofibers containing PEG-based monomer.

3.3.3. (Bio)Functionalization of Furan Containing Nanofibers

In order to investigate the (bio)functionalization of furan-containing poly(PEGMEMA$_{20}$-MMA$_{45}$-FuMA$_{35}$) nanofibers via Diels−Alder cycloaddition reaction in aqueous environment, the nanofibers were initially functionalized with a maleimide-containing water-soluble fluorescent dye, namely, N-(5-fluoresceinyl)maleimide. The reaction proceeded for 4 h in the dark followed by the rinsing of the nanofibers with ample water in order to remove the excess dye. The conjugation was confirmed with the bright green fluorescence of these nanofibers under a fluorescence microscope (Figure 3.15). As a control experiment, the furan-containing nanofibers were also treated with an amine-bearing fluorescent probe, namely fluoresceinamine isomer I, for 4 h in the dark. Upon rinsing with excess water, the nanofibers were examined with fluorescence microscope and did not show any significant fluorescence in the absence of a maleimide-reactive dye (Figure 3.15, inset). As a result, it was proven that the conjugation was due to the specific Diels−Alder cycloaddition reaction between the furan and maleimide groups.

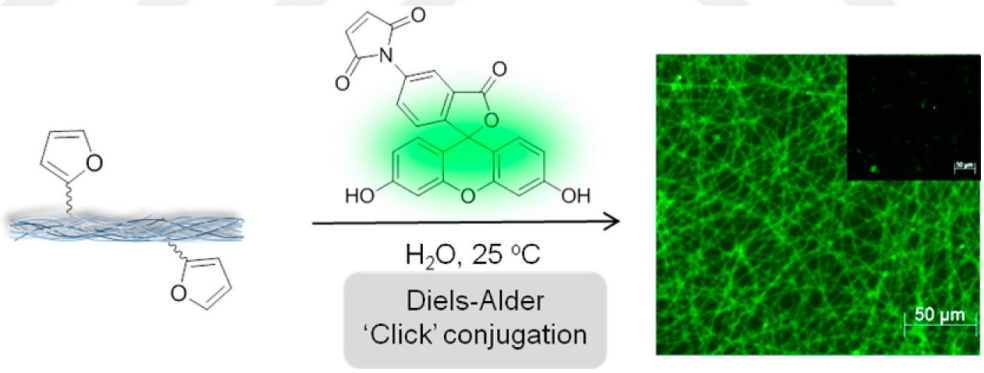

Figure 3.15. Fluorescence microscopy images for the functionalization of furan-containing nanofibers with maleimide-appended fluorescein (inset shows fibers after treatment with fluoresceinamine).

After the successful conjugation of the maleimide-containing fluorescent dye, biomolecule immobilization via the Diels-Alder chemistry was also studied. The biotin-avidin duo was chosen due to the strong biological interaction between them and the wide usage of streptavidin for the attachment of various peptides and oligonucleotides onto different surfaces [122]. Streptavin has four binding sites for biotin molecule, so up to three more biotinylated ligands can be bound on the remaning vacant pockets. For

biofunctionalization, the furan-containing nanofibers were firstly reacted with an aqueous solution of a maleimide-appended biotin ligand under ambient conditions through Diels−Alder reaction. After 4 h in the dark, the biotinylated scafolds were rinsed with ample water in order to remove the unbound biotin and the nanofibers were treated with an aqueous solution of FITC-labeled streptavidin for 30 min in the dark. After that, the nanofibers were again rinsed with water to remove the excess streptavidin adhered to the surface via nonspecific adsorption. The immobilization was examined using the fluorescence microscope and a bright green fluorescence confirmed the conjugation (Figure 3.16). The antibiofouling property of the nanofibers towards nonspecific protein binding gained by the PEG-chains was also investigated by treating the poly(MMA_{60}-$FuMA_{40}$) nanofibers with FITC-labeled streptavidin in the absence of PEG-based comonomer. A considerable amount of nonspecific protein attachment on the entirely hydrophobic nanofibers was confirmed by fluorescence microscopy analysis (Figure 3.17).

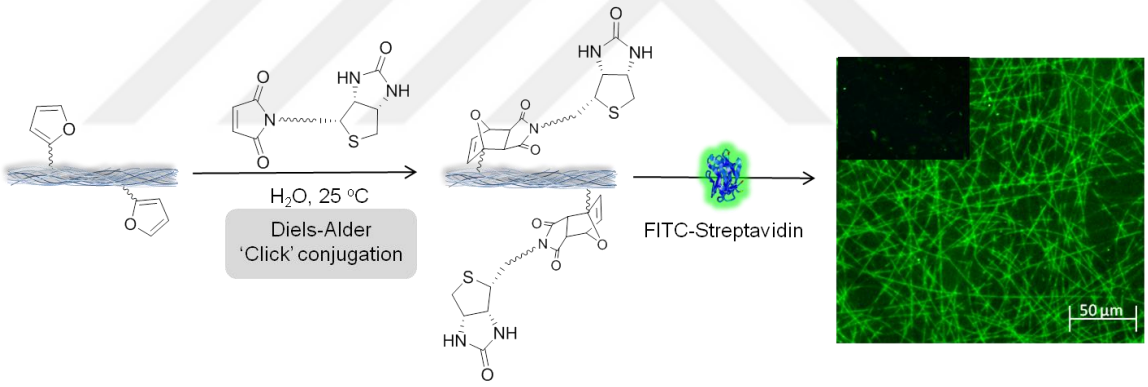

Figure 3.16. Fluorescence microscopy images for the functionalization of furan-containing nanofibers with maleimide-appended biotin followed by FITC-Streptavidin immobilization (inset shows fibers without biotinylation).

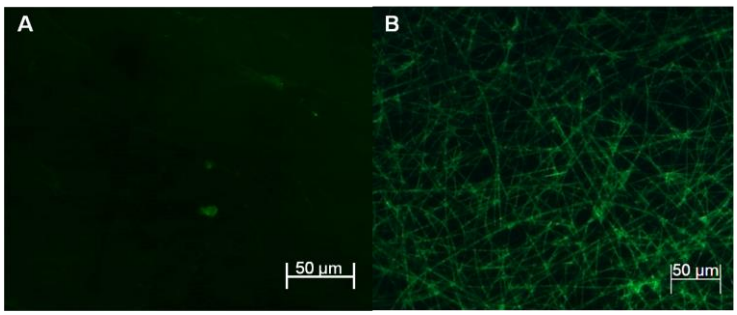

Figure 3.17. Fluorescence microscopy images of FITC-streptavidin exposed (a) non-biotinylated poly($PEGMEMA_{20}$-MMA_{45}-$FuMA_{35}$) nanofibers (b) non-biotinylated poly(MMA_{60}-$FuMA_{40}$) nanofibers to demonstrate anti-biofouling due to presence of PEG.

Furthermore, nanoparticle immobilization on the furan-containing nanofibers was also studied. For this purpose, the biotinylated poly(PEGMEMA$_{20}$-MMA$_{45}$-FuMA$_{35}$) nanofibers were treated with streptavidin-coated CdSe quantum dots solution in the dark for 30 min and washed with excess water. The nanoparticle immobilized nanofibers were investigated under fluorescence microscopy and the bright red fluorescence of the quantum dots upon excitation confirmed the successful conjugation of CdSe quantum dots on the fibers (Figure 3.18a). For the control experiment, the CdSe qdot solution was applied on non-biotinylated poly(PEGMEMA$_{20}$-MMA$_{45}$-FuMA$_{35}$) nanofibers under the same conditions which did not show any significant fluorescence (Figure 3.18a inset). Both surfaces were also examined with scanning transmission electron microscopy (STEM) and nanoparticles were observed on the biotinylated nanofibers while they were not present on the non-biotinylated nanofibers (Figure 3.18b).

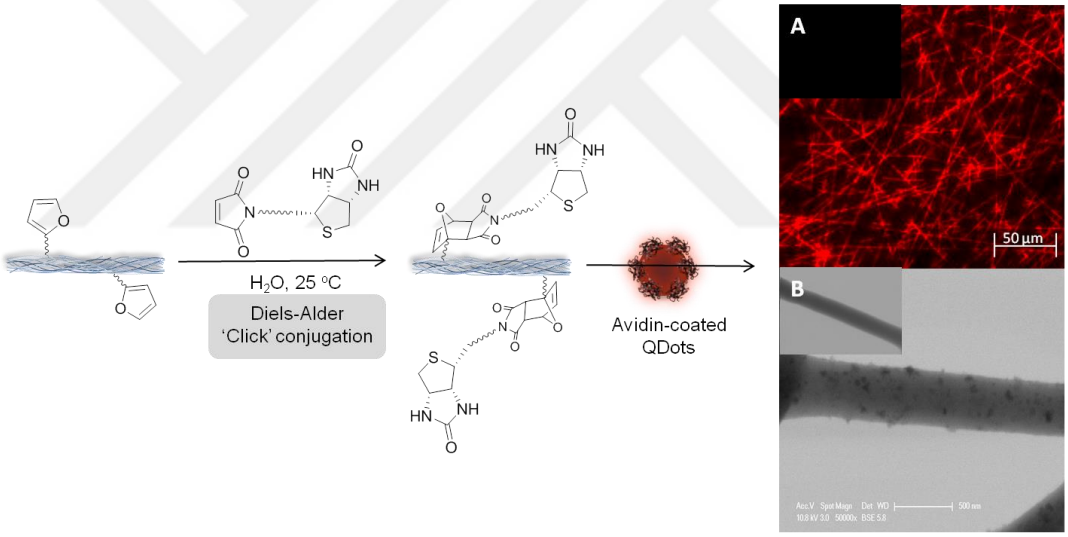

Figure 3.18. (a) Fluorescence microscopy images (b) STEM images for for the functionalization of furan-containing nanofibers with maleimide-appended biotin followed by avidin-coated qdots immobilization (inset shows fibers without biotinylation).

To conclude, a simple yet powerful methodology for the fabrication of reactive nanofibers that can be functionalized under metal-free conditions under aqueous conditions was established. Utilization of copolymers containing the electron- rich furan moiety as fiber precursors allows their modification via the Diels−Alder conjugation reaction that proceeds under mild and benign conditions. Nanofibers were electrospun using a copolymer containing MMA-based hydrophobic and PEG-based hydrophilic monomers,

where the former component provides the necessary stability to these fibers in aqueous environments and the later imparts antibiofouling characteristics. Efficient functionalization of these reactive fibers was demonstrated through immobilization of a small fluorescent dye, and ligand-mediated protein immobilization as well as nanoparticle attachment directed through ligand−biomolecule interactions. Ease of fabrication and efficiency of functionalization of these fibers under aqueous conditions makes them ideal platforms for various biomedical applications where scaffolds with high surface area are desirable.

4. BIOFUNCTIONALIZATION OF PATTERNED MALEIMIDE-CONTAINING NON-BIODEGRADABLE NANOFIBERS

4.1. Introduction

Recently, there has grown an increasing attention on the electrospinning technique for the fabrication of ultrafine fibers from various polymers including natural, synthetic and hybrid materials [4,5,123,124]. Besides being a simple, versatile and low-cost method, electrospinning can provide highly porous, interconnected fibrous matrices with high specific surface area. These nanofibers also mimic the fibrillar structure of the naturally-occuring extracellular matrix. These intrinsic fibrous properties enable the use of nanofiber-based materials in various applications including tissue engineering, drug delivery, (bio)sensors, filtration, electronics and protective clothing. Crosslinking of nanofibers have been widely studied using multi-step chemical crosslinking procedures. Chemical crosslinking agents such as glutaraldehyde, glyoxal, genipin and 1-ethyl-3-(3-dimethyl-aminopropyl)-1-carbodiimide hydrochloride (EDC), have been extensively used for the crosslinking of various natural and synthetic nanofibers such as collagen,[125] chitosan,[126] polyvinyl alcohol[127] and hybrid fibers such as polycaprolactone/gelatin nanofibers [128]. However, the remainings of these crosslinking agents may be harmful especially in medical applications as they may increase the cytotoxicity [129]. Crosslinking with UV radiation has also been prefarably used for the crosslinking of nanofibers. Sanyal, Hoogenboom and coworkers prepared *in situ* photocrosslinked alkene-containing polyoxazoline nanofibers using a photoinitiator and a tetrathiol as a crosslinking agent in the polymer solution [130]. Whittaker and coworkers used gamma irradiation for the crosslinking of acrylated L-lactide-co-trimethylene carbonate nanofibers [131]. Chang and coworkers introduced photocrosslinked poly[1-(4-vinylbenzyl uracil)] (PVBU) nanofibers using the $2\pi + 2\pi$ photodimerization property of uracil base [132]. The double bond of a maleimide group is also known to give efficient $2\pi + 2\pi$ cyclodimerization when exposed to UV irradiation. A maleimide-containing polymethacrylate was crosslinked under UV irradiation without a photoinitiator By Decker and Bianchi [133].

Materials with ordered structures and patterns favor some specific properties such as increased surface area which are particularly useful for various applications, foremost biomedical applications [134-136]. Cell and protein patterning are known to enhance biological responses, protein adsorption, cell attachment and proliferation which makes these ordered structures important for particular applications such as biosensors and tissue engineering. There have been used several methods to produce micropatterned nanofibers. One popular method is to use properly designed micropatterned conductive templates. Chang and Zhang produced PDLLA nanofibers with different patterned structures by varying the design of the electroconductive collectors [137]. However it is not easy to control the microstructure using the templates. Another method used for fabricating nanofibrous micropatterns is direct-write electrospinning on a movable conductive collector. Cho and coworkers produced three PCL nanofibrous mats with different rectangular lattice patterns using direct-write electrospinning method and performed successful cell-patterning [138]. One drawback of this technique is the need of complicated electrospinning design. Photolithographic patterning of nanofibers is another method which includes the photocrosslinking of the nanofibers using a photomask in the presence of a photoinitiator in the polymer solution. Koh and coworkers prepared micropatterned polycaptolactone/gelatin fibers by photopatterning of a PEG hydrogel on the nanofibers through a photomask which allowed sequential growth factor delivery [139]. The limitation of this technique is its applicability only to photo-crosslinkable materials. Ma and colleagues introduced a novel micropatterned alloy via pressing a polydimethylsiloxane template on molten alloy [140]. Nanofibers were electrospun on the micropatterned alloy followed by hydrogel casting to produce hydrogel micropatterns for cell encapsulation.

In the current study, a furan-protected maleimide-containing acrylate-based copolymer was synthesized via free radical polymerization, followed by the removal of furan group through retro Diels-Alder reaction. The solution of the obtained maleimide-containing copolymer was electrospun into maleimide-containing nanofibers which were crosslinked and patterned under UV irradiation in the presence of a photomask through 2-2 cyclodimerization (Figure 4.1). Recently, many researchers have extensively used click chemistry in order to functionalize electrospun nanofibers with bioactive species due to its advantageous properties such as mild reaction conditions [58,114]. The remaining free

maleimides on the patterned crosslinked nanofibers were used to immobilize thiol-bearing fluorescent dye, biotin and oligonucleotide. Hybridization was performed with a complementary Cy5-labeled oligonucleotide sequence. Nucleic acid hybridization on a patterned hydrogel was performed by Grinstaff and coworkers, [141] to our knowledge this is the first study that shows hybridization on a patterned clickable nanofibrous surface.

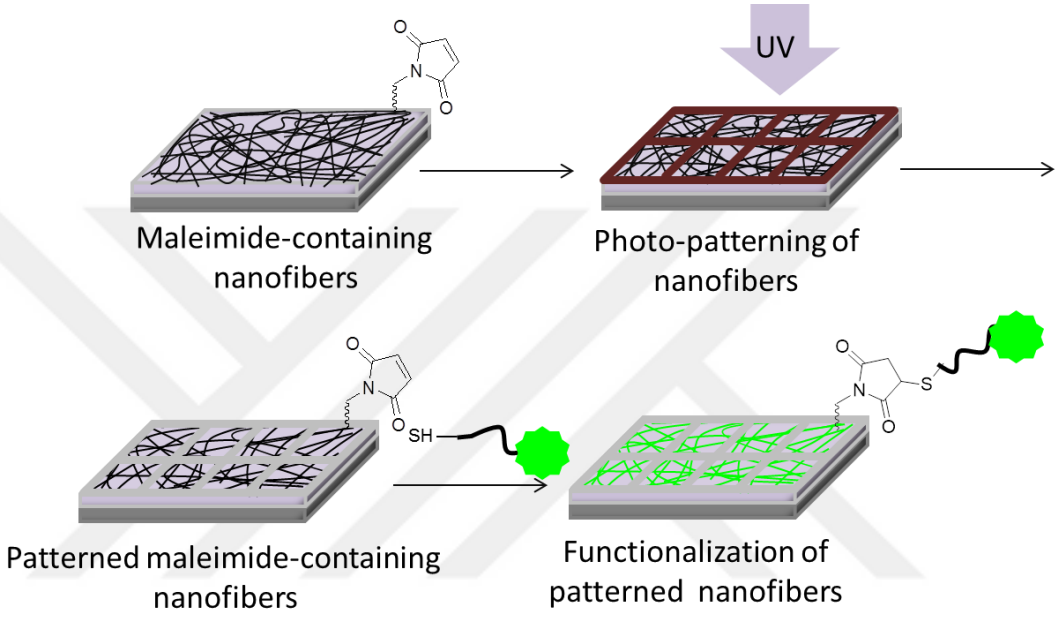

Figure 4.1. Schematic illustration of the functionalization of patterned nanofibers.

4.2. Experimental

4.2.1. Materials

Poly(ethylene glycol) monomethyl ether methacrylate (PEGMEMA) (average M_n = 300 g mol^{-1}) was obtained from Aldrich. Methyl methacrylate (MMA), dimethylformamide (DMF), and tetrahydrofuran (THF) were obtained from Merck. PEGMEMA and MMA were used after passing through neutral Al_2O_3 in order to remove inhibitors prior to use. FuMaMA was synthesized according to the literature procedure [142]. 4,4′-Azobis(4-cyanovaleric acid) (V-501) was purchased from Fluka. SAMSA (5-((2-(and-3)-S-(acetylmercapto) succinoyl) amino) was obtained from Invitrogen and activated prior to use according to the literature procedure. Biotinylated PEG alkane thiol and FITC-conjugated streptavidin were purchased from NanoScience Instruments and ThermoScientific, respectively.

4.2.2. Instrumentation

The NMR spectra were recorded on a Varian 400 MHz spectrometer with deuterated chloroform ($CDCl_3$) as the solvent at 25 ^oC. The molecular weight of the copolymer was estimated by gel permeation chromatography analysis using a Shimadzu PSSSDV (length/ID 8 × 300 mm, 10 μm particle size) mixed-C column calibrated with polystyrene standards (1−400 kDa) using a refractiveindex detector. THF was used as eluent at a flow rate of 1 mL/min at 30 °C. The morphology of electrospun nanofibers were observed with Jeol Neoscope JCM-5000 scanning electron microscopy. Fluorescence images of functionalized samples were recorded on a Zeiss Observer Z1 fluorescence microscope connected to Axiocam MRc5 using a Zeiss Filter set 38 (Excitation BP 470/40, Emission BP 525/50) for imaging the functionalized nanofibers. Static water contact angle were measured in air via the sessile-drop method using a goniometer (CAM 101 KSV instruments). Approximately 5 μL of deionized water was deposited on the surface and images were taken by an integrated digital camera. The software CAM2008 was used for image processing to determine the contact angle. Contact angle value for each sample was independently measured at three different locations and average values were measured.

4.2.3. Copolymerization of Reactive Copolymers

4.2.3.1. Synthesis of furan protected maleimide-containing copolymer (poly(PEGMEMA-MMA-FuMaMA)). PEGMEMA (average M_n = 300 g mol^{-1}), and MMA were passed through an aluminum oxide column in order to remove inhibitors. PEGMEMA (0.40 mL, 1.4 mmol), FuMaMA (407.5 mg, 1.4 mmol), MMA (0.44 mL, 4.2 mmol), and V-501 (9.8 mg, 0.035 mmol) were dissolved in THF (25 mL) in a 50 mL round-bottom flask equipped with a magnetic stir bar and degassed by bubbling nitrogen. Thereafter, the roundbottom flask was sealed and placed in a 65 °C oil bath and stirred for 20 h. At the end of the reaction, the solvent was evaporated under reduced pressure. The residue was dissolved in minimum amount of dichloromethane and purified by precipitation in cold diethyl ether. The polymer was obtained as a white powder (M_n=19.3 kDa, M_w/M_n=1.88), (500 mg, conversion 40%). ^{1}H-NMR (400 MHz, $CDCl_3$, δ): 6.51 (s, 2H, C*H*=C*H*), 5.24 (s, 2H, C*H*bridgehead protons), 4.07 (br s, 2H, –COOCH_2–PEG), 3.90 (br s, 2H, OCH_2), 3.63-

3.53 (m, 15H,–OCH_2CH_2O– and–COOCH_3), 3.35 (s, 3H, OCH_3), 2.85 (s, 2H, C*H*–C*H*, bridge protons).

4.2.3.2. Synthesis of maleimide-containing copolymer (poly(PEGMEMA-MMA-MaMA)). Poly(PEGMEMA-MMA-FuMaMA) was dissolved in toluene in a 250 mL round-bottom flask equipped with a magnetic stir bar and placed in a 110°C oil bath and stirred overnight. At the end of the reaction time, toluene was evaporated under reduced pressure. ^{1}H-NMR (400 MHz, $CDCl_3$, δ): 6.73 (s, 2H, C*H*=C*H*), 4.09 (br s, 2H, –COOCH_2–PEG), 3.96 (s, 2H, OCH_2), 3.63-3.54 (m, 15H,–OCH_2CH_2O– and–COOCH_3), 3.36 (s, 3H, OCH_3).

4.2.3.3. Synthesis of furan protected maleimide-containing copolymer (poly(MMA-FuMaMA)). MMA was passed through an aluminum oxide column in order to remove inhibitors. FuMaMA (300 mg, 1.03 mmol), MMA (0.44 mL, 4.14 mmol), and V-501 (7.35 mg, 0.026 mmol) were dissolved in THF (15 mL) in a 50 mL round-bottom flask equipped with a magnetic stir bar and degassed by bubbling nitrogen. Thereafter, the roundbottom flask was sealed and placed in a 65 °C oil bath and stirred for 20 h. At the end of the reaction, the solvent was evaporated under reduced pressure. The residue was dissolved in minimum amount of dichloromethane and purified by precipitation in cold diethyl ether. The polymer was obtained as a white powder (350 mg, conversion 48%). ^{1}H-NMR (400 MHz, $CDCl_3$, δ): 6.52 (s, 2H, C*H*=C*H*), 5.25 (s, 2H, C*H*bridgehead protons), 3.92 (br s, 2H, OCH_2), 3.57 (br s, 5H, OCH_3 and NCH_2), 2.86 (s, 2H, C*H*–C*H*, bridge protons).

4.2.3.4. Synthesis of maleimide-containing copolymer (poly(MMA-MaMA)). Poly(MMA-FuMaMA) was dissolved in toluene in a 250 mL round-bottom flask equipped with a magnetic stir bar and placed in a 110°C oil bath and stirred overnight. At the end of the reaction time, toluene was evaporated under reduced pressure. ^{1}H-NMR (400 MHz, $CDCl_3$, δ): 6.73 (s, 2H, C*H*=C*H*), 3.96 (s, 2H, OCH_2), 3.58 (br s, 5H, OCH_3 and NCH_2).

4.2.4. Electrospinning of Maleimide-Containing Copolymers

A copolymer solution was prepared with a concentration of 50 wt % using 1:1 (v/v) DMF/THF solvent mixture. In a typical experiment, the solution was delivered at a

constant flow rate of 0.01 mL/min to a needle connected to a high voltage power supply with an applied voltage of 13 kV and a the tip to collector distance of 15 cm. Fibers were collected on 22 × 22 mm glass slides and modified silicon surfaces sticked onto a grounded aluminum collector.

4.2.5. Photo-Patterning and Crosslinking of Maleimide-Containing Nanofibers

A photo-mask was placed on the maleimide-containing nanofibers electrospun on the modified silicon surface which was exposed to UV light (365 nm) for 3 min. Then, the surfaces were washed with organic solvent, dried under nitrogen stream and examined using SEM.

4.2.6. Dye Conjugation on Maleimide-Containing Patterned Nanofibers

A solution of activated SAMSA (1 mg/120 μL) was prepared in 1×PBS and 10 μL of this solution was dropped onto the patterned maleimide-containing nanofibers. After 6 h in the dark, the excess dye was rinsed with copious amounts of water. Modified nanofibers were investigated with fluorescence microscope.

4.2.7. Biofunctionalization of Maleimide-Containing Patterned Nanofibers

An aqueous solution of biotinylated PEG alkane thiol (1 mg/mL) was prepared and 20 μL of this solution was dropped onto the patterned maleimide-containing nanofibers. The reaction was carried out in the dark for 6 h at room temperature. Thereafter, the patterned fiber-coated surfaces were rinsed with copious amount of water in order to remove the unbound biotin. An aqueous solution of FITC-streptavidin (0.1 mg/mL) was prepared and 10 μL of this solution was dropped onto the biotinylated fibers. After 30 min in the dark, the fibers were washed with ample water to remove any unbound protein. The conjugation was analyzed with fluorescence microscopy.

For hybridization studies, a 16 base pair 5'-HS-AACGATCGAGCTGCAA (ThiolS1) modified at 5' end using the reagent 5'-thiol modifier C6 was used for the attachment of the thiol group on the oligonucleotide to the maleimide group on the patterned nanofibers. Complementary 16 base pair oligonucleotides used for hybridization

were modified with Cy5 on the 5'-end with sequences 5'-Cy5-TTGCAGCTCGATCGTT (Cy5S1, complementary to ThiolS1) and 5'-Cy5-TTGCTGCTCGATCGTT (Cy5-mismatch, complementary to ThiolS1 with a single-based mismatch). An aqueous solution of ThiolS1 with a concentration of 40 ng/μL was dropped on the patterned maleimide-containing nanofibers. After 6 h in the dark, the surfaces were washed with ample water to remove any unbound oligonucleotide and dried under nitrogen stream. Then, the resulting DNA-modified patterned nanofibers were hybridized with an aqueous solution of Cy5S1 with a concentration of 2 ng/μL. The hybridized surfaces were washed with water, dried under nitrogen stream and examined with fluorescence microscope. As a control experiment, the DNA-modified patterned nanofibers were hybridized with an aqueous solution of Cy5-mismatch. The surfaces were washed with water, dried with nitrogen and examined under fluorescence microscope.

4.3. Results and Discussion

4.3.1. Synthesis and Characterization of Maleimide-Containing Hydrophilic Non-Biodegradable Polymers

Furan-protected maleimide-containing reactive copolymers were synthesized by conventional free radical polymerization named as poly(PEGMEMA-MMA-FuMaMA). FuMaMA was used as the reactive group for functionalization, PEGMEMA was used for antibiofouling and MMA was used for fiber-producing propensity. Polymerizations were conducted under dilute conditions using THF as the solvent and V-501 as the initiator in order to prevent crosslinking. The obtained copolymers were purified by precipitation in cold diethyl ether (Figure 4.2).

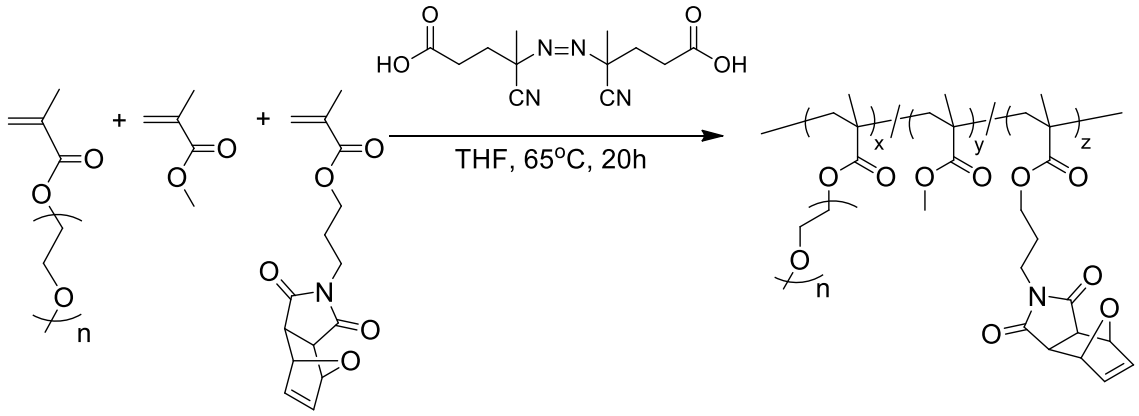

Figure 4.2. Synthesis of furan-protected maleimide-containing copolymer (poly(PEGMEMA-MMA-FuMaMA)).

The success of the copolymerization reactions were confirmed using ^{1}H-NMR spectrocopy (Figure 4.3).

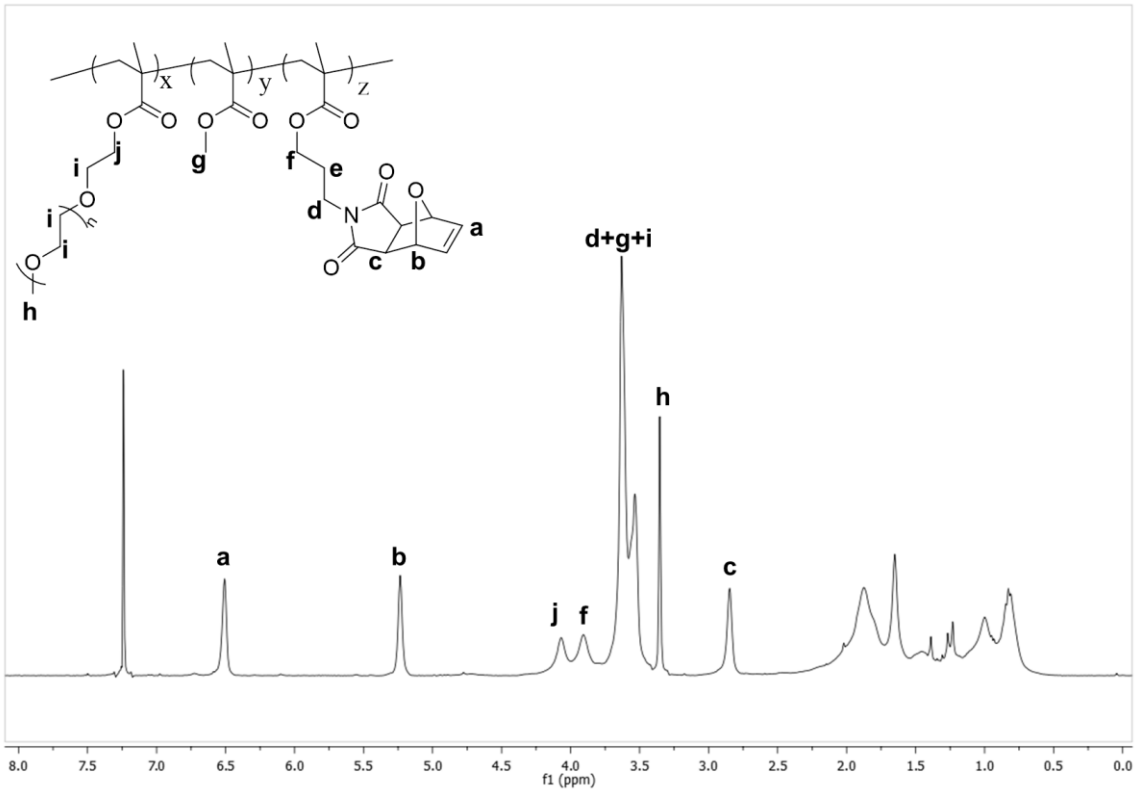

Figure 4.3. ^{1}H-NMR spectrum of poly(PEGMEMA-MMA-FuMaMA).

Prior to electrospinning, the furan protection of the copolymer was removed via retro-Diels Alder reaction at 110 °C in toluene (Figure 4.4). The appearance of the maleimide group was also confirmed by ^{1}H-NMR spectroscopy (Figure 4.5)

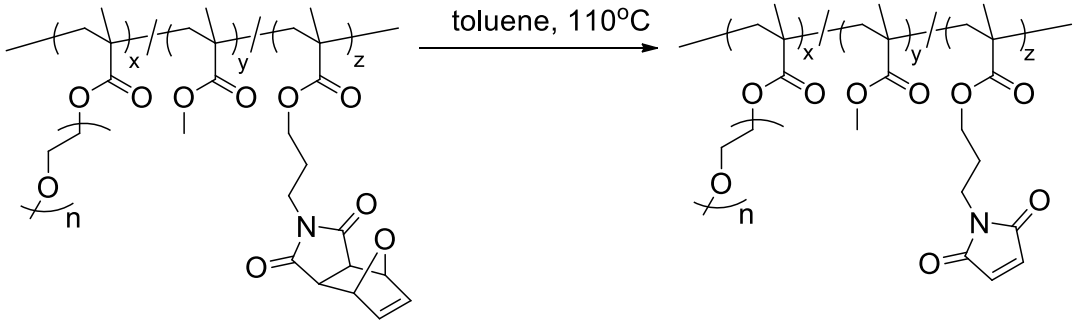

Figure 4.4. Synthesis of maleimide-containing copolymer (poly(PEGMEMA-MMA-MaMA)).

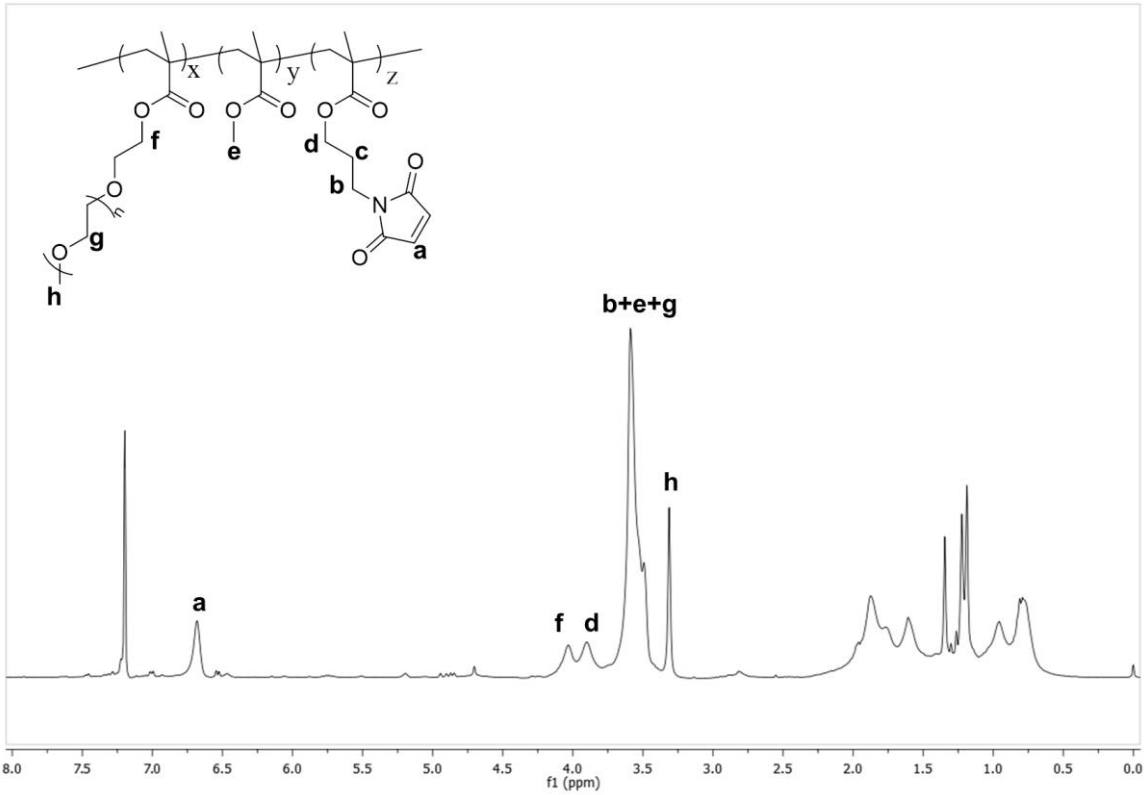

Figure 4.5. ^{1}H-NMR spectrum of poly(PEGMEMA-MMA-MaMA).

For control experiments, a polymer without PEG units poly(MMA-FuMaMA) was also synthesized under the same conditions (Figure 4.6) and confirmed with ^{1}H-NMR spectroscopy (Figure 4.7). A maleimide-containing copolymer without PEG units was also obtained through retro Diels-Alder reaction (Figure 4.8) and confirmed with ^{1}H-NMR spectroscopy (Figure 4.9).

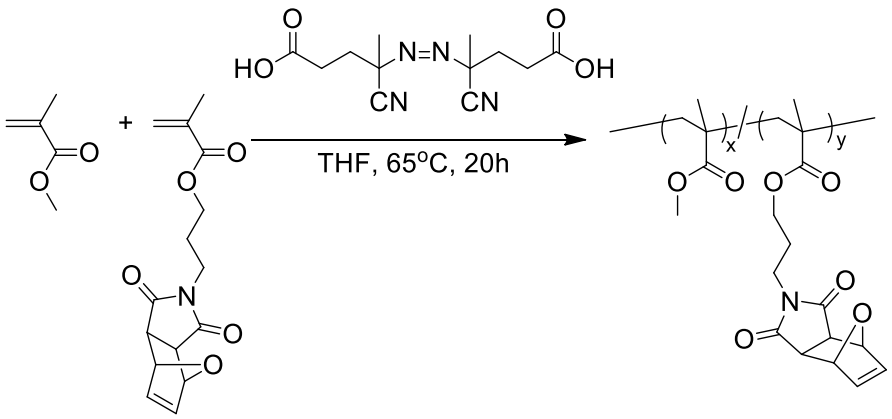

Figure 4.6. Synthesis of (poly(MMA-FuMaMA)).

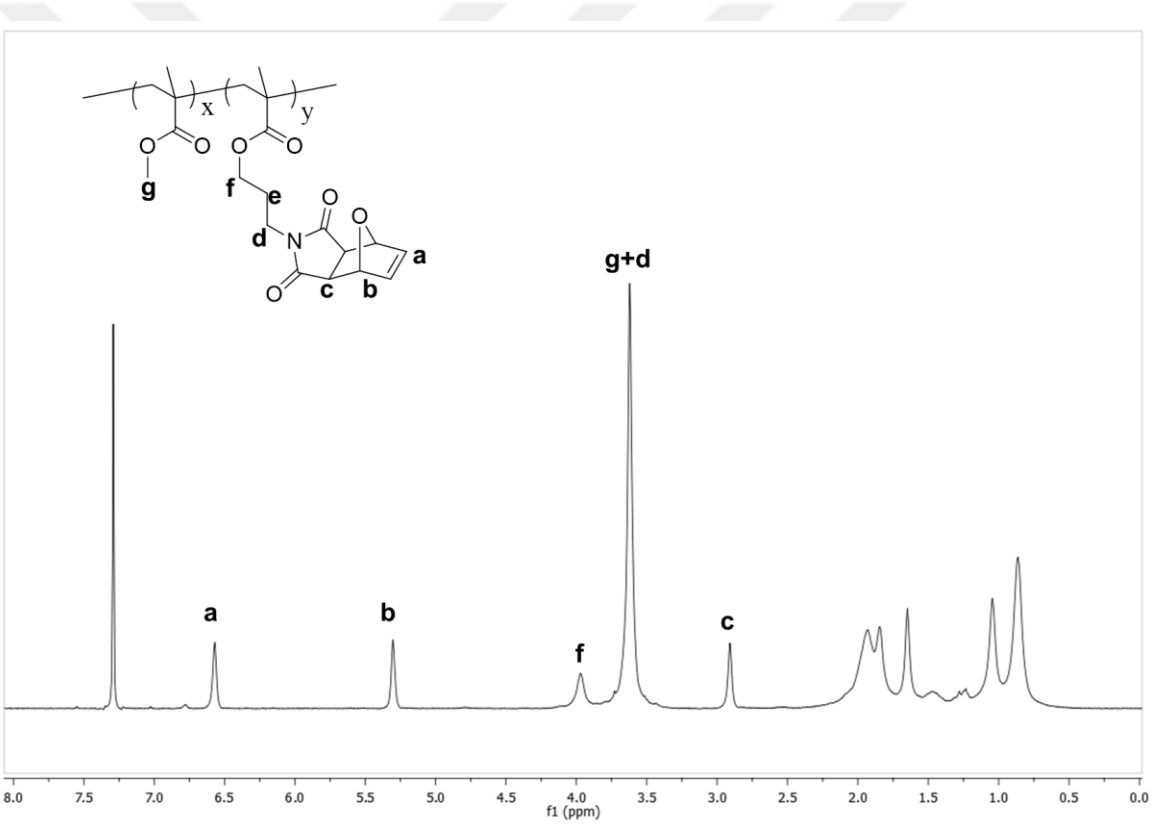

Figure 4.7. ^{1}H-NMR spectrum of poly(MMA-FuMaMA).

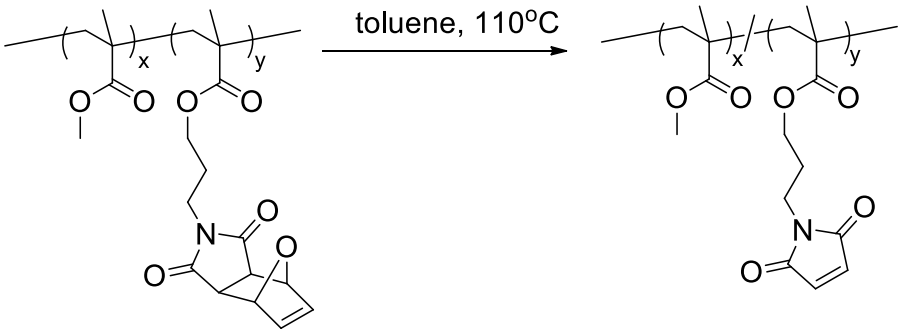

Figure 4.8. Synthesis of (poly(-MMA-MaMA)).

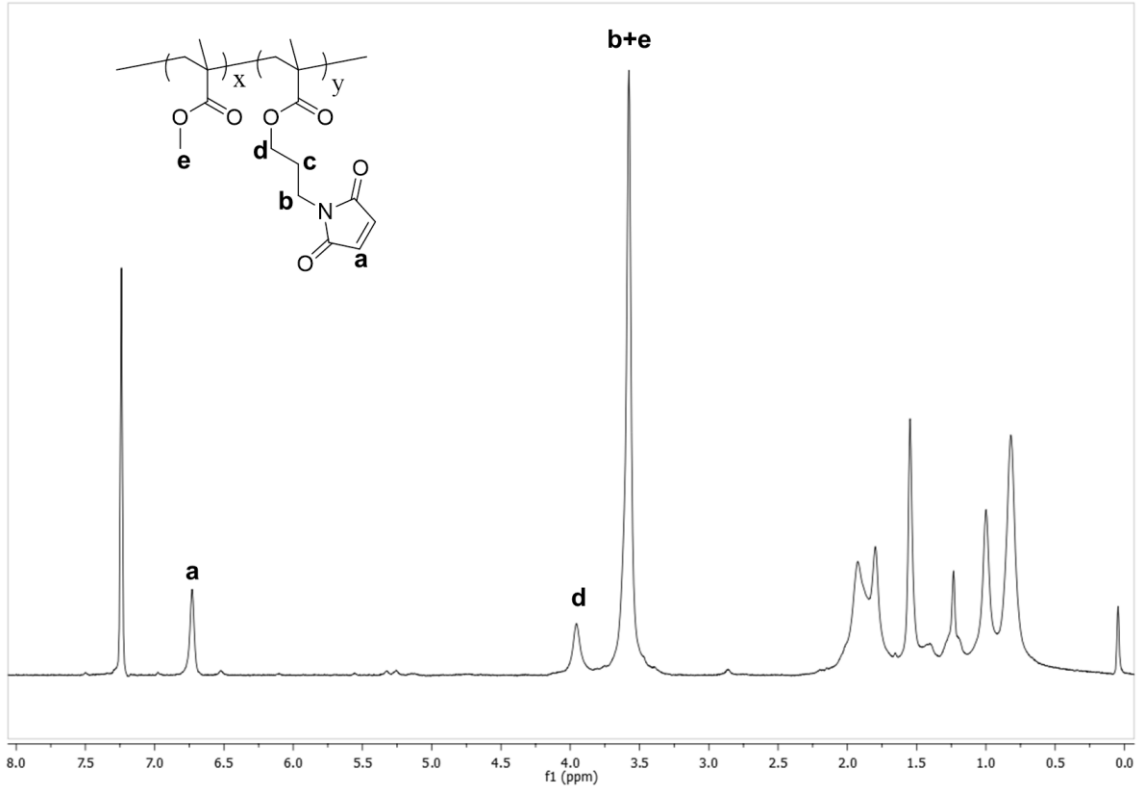

Figure 4.9. ^{1}H-NMR spectrum of poly(MMA-MaMA).

4.3.2. Fabrication and Photo-Patterning of Maleimide-Containing Nanofibers

The resulting maleimide-containing copolymers were electrospun into nanofibers from 50 wt % solutions in 1:1 DMF:THF with a flow rate of 0.01 mL/min, a tip-to-collector distance of 15 cm and an applied voltage of 13 kV onto modified silicon surfaces. The hydrophlic character of the copolymer was examined using average water contact

angle. For poly(PEGMEMA-MMA-MaMA) nanofibers, the average contact angle was found as 72.11° ± 7.59° while it was 114.60° ± 7.52 for poly(MMA-MaMA) nanofibers which was performed as a control experiment (Figure 4.10). These results indicated that the incorporation of PEG units it the copolymer structured increased the hydrophilicity of the nanofibers.

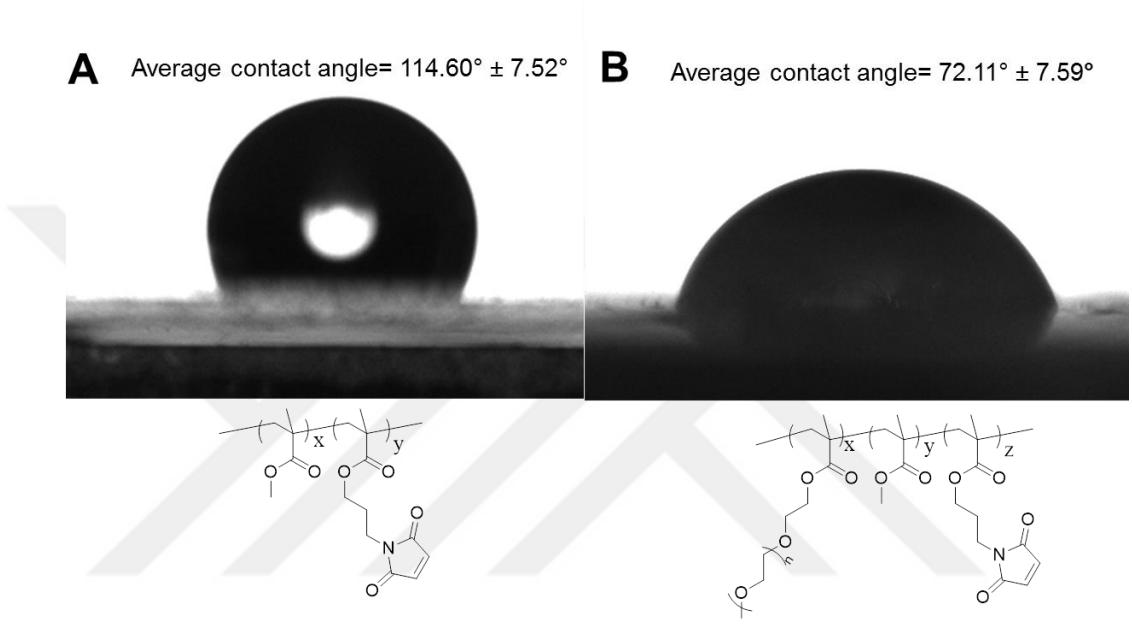

Figure 4.10. Average water contact angles of (a) poly(MMA-MaMA) (b) poly(PEGMEMA-MMA-MaMA) nanofibers.

A photo-mask was placed on the maleimide-containing nanofiber coated surfaces followed by UV (365 nm) exposure for 3 min. The surfaces were then rinsed with organic solvent leaving the crosslinked patterned nanofibers. It was observed that crosslinking did not cause any significant change in the fiber morphology. The average diameter of the nanofibers were 600 nm ± 203 nm before crosslinking and 650 nm ± 202 nm after crosslinking (Figure 4.11).

4.3.3. (Bio)Functionalization of Patterned Nanofibers

The remaining free maleimide groups on the patterned nanofibers were used for functionalization. A thiol-containing fluorescent dye, namely SAMSA, was used to functionalize the maleimide-bearing patterned nanofibers via Michael reaction. 10 μL of

the activated aqueous solution of SAMSA was dropped on the patterned nanofibers and the reaction between the thiol group on the dye and the maleimide group on the nanofibers proceeded for 6 h in the dark. After the reaction period, the surfaces were washed with ample water to remove the unbound dye, dried under nitrogen and examined under fluorescence microscope. The green colour on the patterned nanofibers confirmed the succes of the conjugation (Figure 4.12). As a control experiment, the patterned nanofibers were treated with an amine-bearing fluorescent dye under the same conditions which showed negligible fluorescence under fluorescence microscope. These results confirmed that the conjugation was due to the Michael reaction.

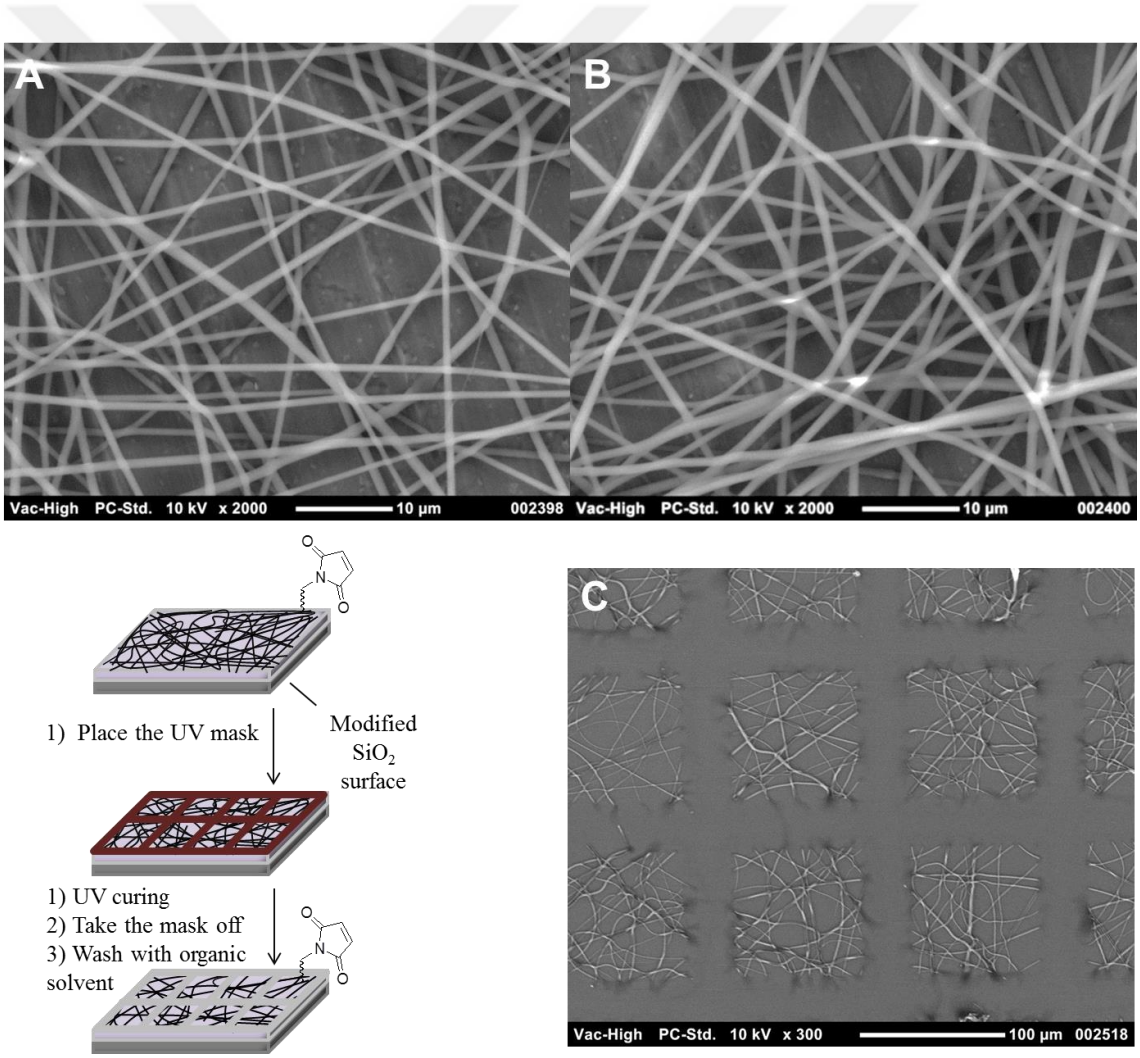

Figure 4.11. SEM images of poly(PEGMEMA-MMA-MaMA) nanofibers (a) before crosslinking (b) after crosslinking (c) after patterning.

After the succesful dye conjugation, bioimmobilization on the patterned nanofibers was studied. An aqueous solution of a biotinylated PEG alkane thiol was dropped on the patterned maleimide-containing nanofibers for modification via Michael reaction. After 6 h in the dark, the surfaces were washed with copious amount of water and dried under nitrogen. The biotinylated patterned nanofibers were treated with an aqueous solution of TRITC-extravidin for 30 min in the dark. The surfaces were washed with excess water, dried under nitrogen and examined with fluorescence microscope. The bright red colour on the patterned nanofibers indicated the extravidin immobilization via biotin-avidin interaction (Figure 4.13). As a control experiment, TRITC-extravidin was applied on non-biotinylated patterned nanofibers under the same conditions and the surfaces did not give any appreciable fluorescence.

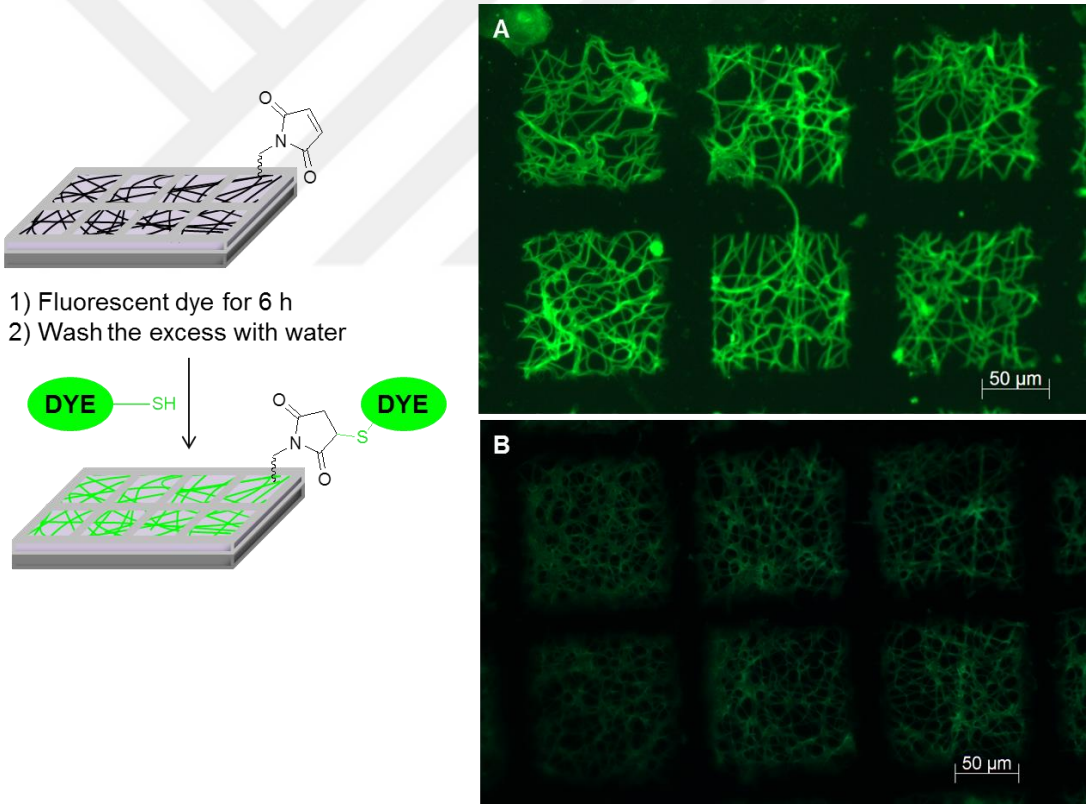

Figure 4.12. Fluorecence microscopy images of (a) thiol-containing fluorescent dye (b) amine-containing fluorescent dye immobilization on patterned nanofibers.

The patterned nanofibers were also used as a platform for DNA attachment. At first, thiol-containing fluorescently labeled DNA was immobilized on the patterned nanofibers. An aqueous solution of the FITC-DNA-SH was dropped on the maleimide-

containing patterned nanofibers for 6 h at ambient conditions. Then the surfaces were washed with copious amount of water, dried and monitored with fluorescence microscope. The green fluorescence indicated the successful conjugation (Figure 4.14).

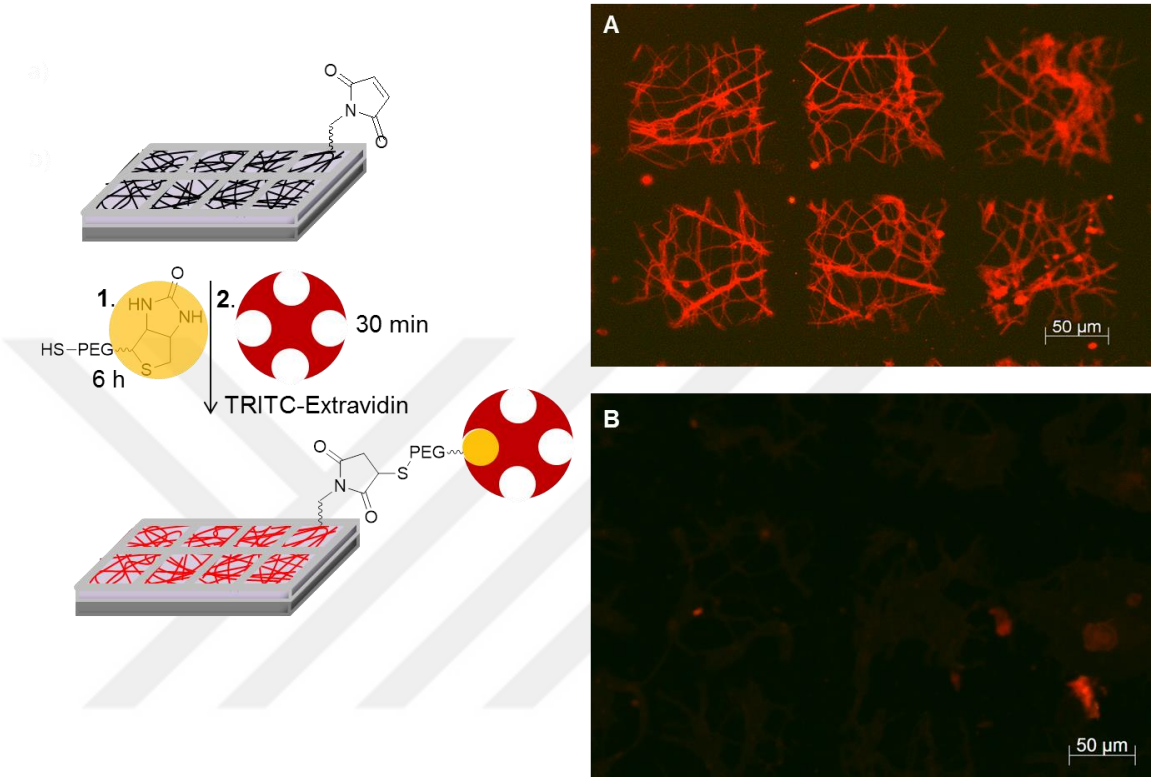

Figure 4.13. Fluorecence microscopy images of TRITC-Extravidin immobilization on (a) biotinylated (b) non-biotinylated patterned nanofibers.

Oligonucleotide hybridization was also studied with the patterned nanofibers. An aqueous solution of a 5' thiol modified oligonucleotide, ThiolS1, was applied on the maleimide-containing patterned nanofibers. After 6 h in the dark, the surfaces were washed with water and dried. The surface was then exposed to an aqueous solution containing the fluorescently labeled sequence Cy5S1, which is complementary to ThiolS1. After 30 min of hybridization, the surface was washed and the fluorescence signal from the surface was investigated. The bright red colour confirmed that the hybridization was succesful (Figure 4.15). A control experiment was performed using a mismatch of a single base pair, Cy5-mismatch, with the same hybridization conditions. Negligible fluorescence was observed under fluorescence microscope which proved that the hybridization was selective enough to distinguish the mismatch of only a single base pair.

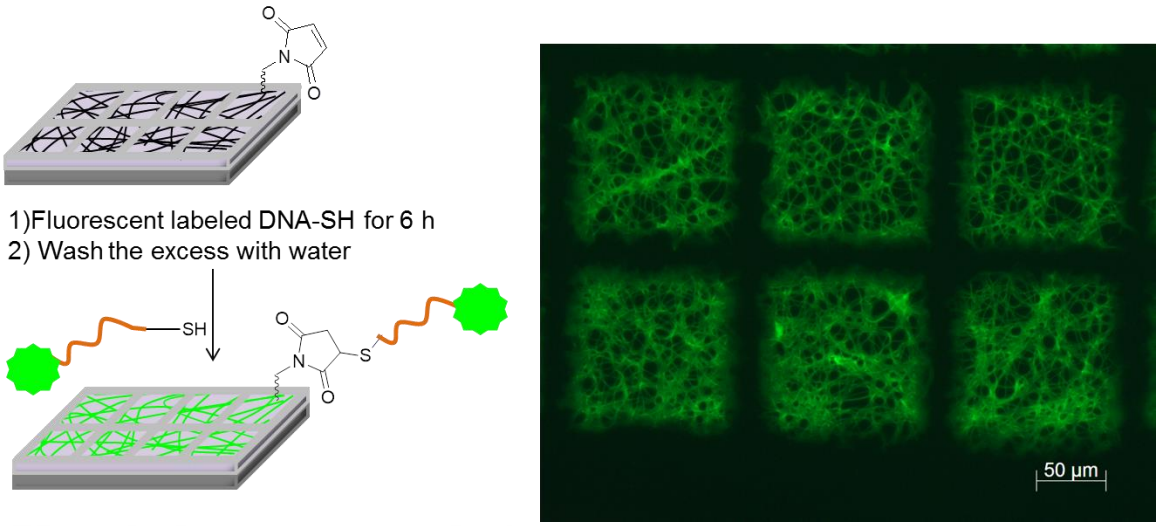

Figure 4.14. Fluorecence microscopy images of fluorescently-labeled DNA immobilization on patterned nanofibers.

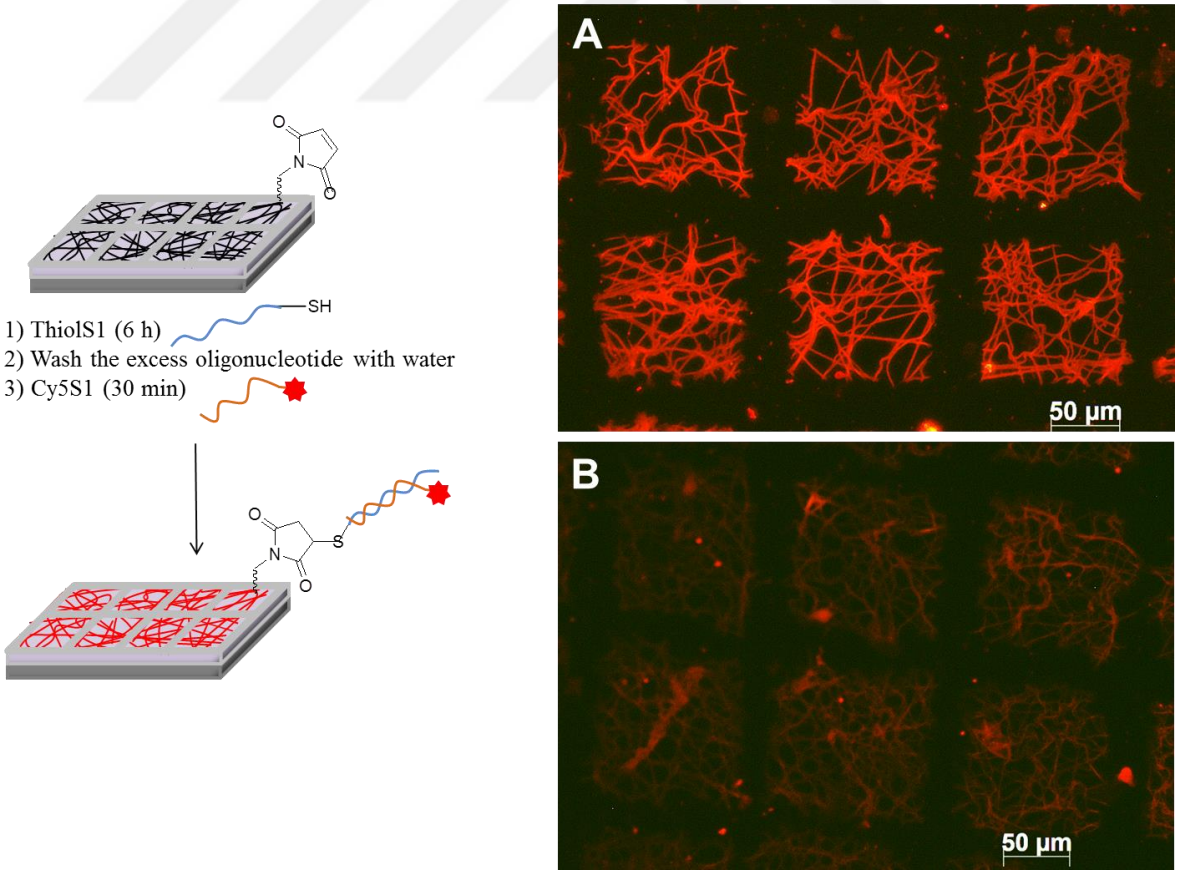

Figure 4.15. Fluorecence microscopy images of (a) Cy5S1 (b) Cy5-mismatch hybridization on ThiolS1 immobilized patterned nanofibers.

The hybridization of 1/10 and 1/100 dilutions of Cy5S1 on ThiolS1-immobilized patterned nanofibers was also examined. The confocal microscopy images showed that the sensing of the hybridization was sensitive to 1/10 dilution of Cy5S1 while there was negligible hybridization with 1/100 dilution (Figure 4.16).

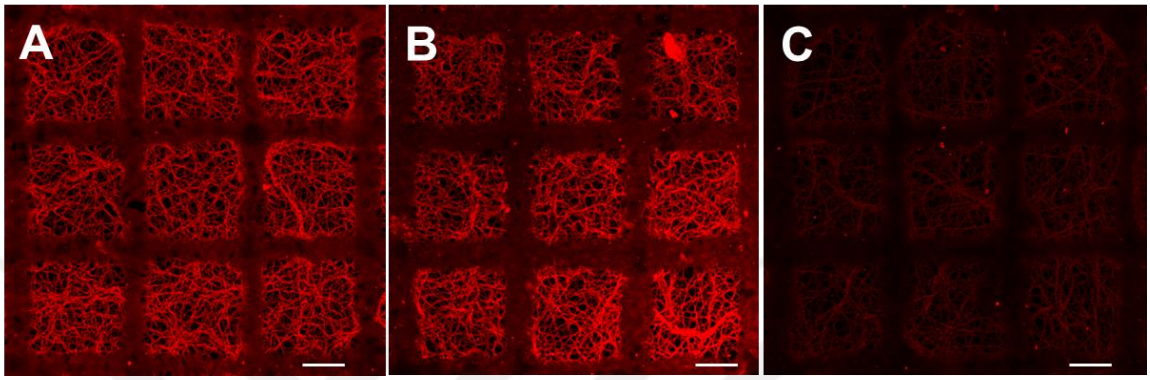

Figure 4.16. Confocal microscopy images of Cy5S1 hybridization with a concentration of (a) 2 ng/μL (b) 1/10 dilution (c) 1/100 diution on ThiolS1 immobilized patterned nanofibers (scalebar 50 μm).

In conclusion, the maleimide-containing nanofibers were efficiently photo-patterned and crosslinked using a single-step and reagent-free method. The obtained patterned nanofibers were used as scaffolds for thiol-bearing oligonucleotide immobilization via Michael reaction. The hybridization studies were also examined using the fluorescently labeled complementary sequence and it was observed that sensing was obtained at low concentrations. These patterned nanofibers are suitable to be used as DNA microarrays.

5. MODIFICATION OF *IN SITU* CROSSLINKED POLYOXAZOLINE NANOFIBERS

Published as the following paper: Kalaoglu-Altan, O.I., B. Verbraeken, K. Lava, T.N. Gevrek, R. Sanyal, T. Dargaville, K. De Clerck, R. Hoogenboom, and A. Sanyal, "Multireactive Poly(2-oxazoline) Nanofibers Through Electrospinning With Crosslinking On The Fly.", *ACS Macro Letters*, Vol. 5, pp. 676–681, 2016.

5.1. Introduction

Polymeric nanofibers have emerged as attractive building blocks for various functional materials that find applications in several areas of materials and biomedical sciences [5,143,144]. Unique properties of nanofibers such as very high surface to volume ratio, high porosity and structural similarity to the biological extracellular matrix render them with attractive attributes for various applications. Fabrication of polymeric nanofibers is readily achieved using electrospinning, a simple and robust technique [3,4]. A high electric field applied to the droplet of a polymer solution or melt extruded from the tip of a spinneret results in ejection of a charged jet to the collector, which is the counter electrode. Solvent evaporation and whipping of the jet during the flight leaves a nonwoven nanofibrous mesh on the collector. While the nanofibrous morphology provides advantages like increased surface area, it is often necessary to append functional moieties onto these nanofibers to tailor them for particular applications. This necessitates development of facile method- ologies for their efficient functionalization under mild conditions. Prior attempts at creating surface active nanofibers from nonreactive polymers involve plasma or wet chemical treatments to install carboxylic acids and alcohols [145,146]. These treatments are harsh, possess limited efficiency and cancompromise the mechanical stability of the nanofibers. An attractive alternative is electrospinning of nanofibers from polymers possessing reactive handles. Advances in "click" reaction based postpolymerization functionalization over the past several years have made such conjugations routine for accessing functional materials [58,62,147]. To date, click reactions such as copper catalyzed Huisgen azide−alkyne cycloaddition,[95] strain-promoted azide−alkyne cycloaddition [98,100], radical thiol−ene,[96] Michael

additions,[101] and the Diels−Alder cycloaddition reactions [120] have been employed for nanofiber modifications [115]. Until recently, multifunctional nanofibers remained largely unexplored beside the recent elegant example of “trifunctionalizable” nanofibers by the Becker group,[97] where they coelectrospun two different caprolactone-based copolymers containing three different reactive handles, and functionalized them with various dyes and peptides. While noteworthy advancements have been made in the area of functionalizable synthetic nanofibers, most studies have focused on fibers obtained using hydrophobic polymers.

Approaches toward fabrication of hydrophilic electrospun fibers are quite limited since as spun fibers will dissolve in aqueous media unless stabilized through physical or chemical cross-linking. Most of the studies in this direction have focused on poly(vinyl alcohol) which has been chemically crosslinked using treatment with glutaraldehyde [126]. More recently, Burdick and co-workers reported the electrospinning of norbornene-functionalized hyaluronic acid together with a dithiol and subsequent postelectrospinning UV-crosslinking [148]. The resulting crosslinked nanofibers could be further modified with thiols through thiol−ene chemistry. Given the significance of hydrophilic nanofibrous substrates in biological applications such as sensing or as scaffold materials, facile access to such fibers that can be functionalized in a modular fashion is quite important. Extension of various crosslinking methodologies to other classes of polymers than those mentioned above is also a must to expand the utility of these nanofibers in various biomedical areas. In recent years, poly(2-alkyl-2-oxazoline)s (PAOx), tertiary amide analogues of polypeptides, obtained using cationic ring-opening polymerization of the 2-oxazoline monomers have emerged as an important class of polymers suitable for various biomedical applications due to their resemblance to poly(ethylene glycol)s with regard to biocompatibility and “stealth” behavior [149-152]. Utilization of “clickable” functional group bearing initiators and monomers provides well-defined copolymers that can undergo both side chain and end group functionalization [153-156]. Among the various available “click”-type transformations, the radical thiol−ene reaction has been extensively employed due to its mild and metal catalyst-free conditions [68,69]. Thiol−ene chemistry in combination with PAOx was first reported by Schlaad and co-workers,[157] after which it has become a popular tool as the ene-group can be introduced in the monomer and does not interfere with the living cationic ring-opening polymerization [158-165]. Among the

limited number of reports on PAOx-based nanofibers, electro- spinning of poly(2-ethyl-2-oxazoline) (PEtOx) was reported by Iruin and co-workers to obtain noncrosslinked nanofibers [166]. Also, composite nanofibers were obtained by electrospinning an aqueous solution of PEtOx and $Co(CH_3COO)_2 \cdot 4H_2O$, which were then calcined to yield ceramic nanofibers [167]. Recently, Groll and co-workers reported the melt electrospinning of PEtOx resulting in fibers with diameters between 8 to 138 μm [168].

Here we report, for the first time, the fabrication of multifunctional hydrophilic nanofibers using *in situ* UV- crosslinking of poly(2-oxazoline) copolymers with a thiol-containing crosslinker during electrospinning [130]. The alkene moiety of poly(2-ethyl-2-oxazoline-co-2-(but-3-enyl)-2-oxazoline) (P(EtOx-co-ButEnOx)) was used for crosslinking via the photochemical radical thiol−ene reaction in the presence of a tetra-thiol and a photoinitiator (Figure 5.1). After their fabrication, multifunctionalization of these crosslinked fibers in a modular fashion by modification of the remaining thiol and ene groups from the crosslinker and the polymer, respectively, was probed through attachment of two different fluorescent dyes via the radical thiol−ene and Michael-type nucleophilic thiol−ene conjugation reactions using the residual alkene and thiol groups, respectively. Furthermore, spatially controlled functionalization of crosslinked nanofibers was also demon- strated via radical thiol−ene reaction in the presence of a thiol- appended fluorescent dye and photoinitiator upon irradiation through a photomask.

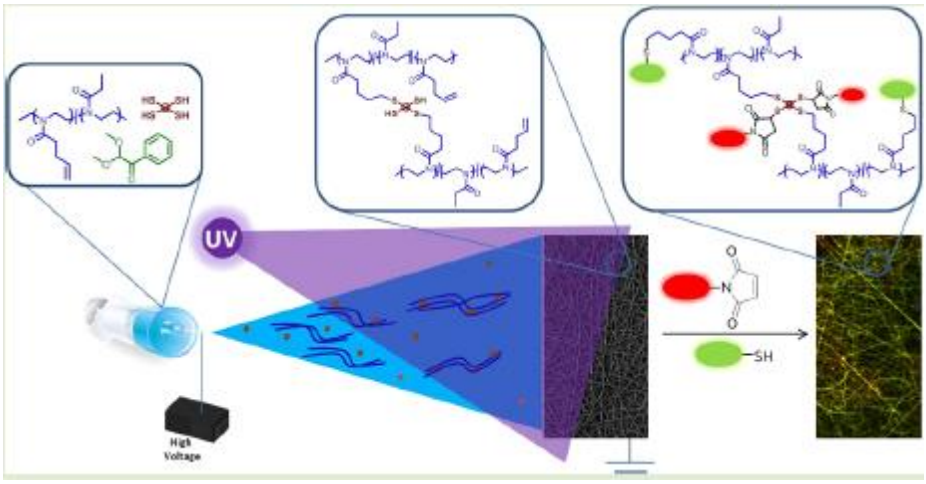

Figure 5.1. Schematic illustration showing the *in situ* crosslinking and functionalization of P(EtOx-co-ButEnOx) nanofibers.

5.2. Experimental

5.2.1. Materials

Pentaerythritol tetrakis(3-mercaptopropionate) (tetrathiol) and 2,2-dimethoxy-2-phenylacetophenone (DMPA) were purchased from Sigma Aldrich and Acros Organics, respectively. Tetramethylrhodamine-5-maleimide was purchased from Sigma. N-ethyl maleimide was purchased from Alfa Aesar. BODIPY-thiol was synthesized according to literature procedure [169]. Solvents were used as received.

5.2.2. Instrumentation

Scanning electron microscopy (SEM) images of the nanofibers were taken by Philips XL30 ESEMFEG/EDAX system at an operating voltage of 4 kV. Florescence Microscopy Fluorescence microscopy images of dry samples on nanofiber surfaces were recorded at room temperature using an LD-A-Plan 10×/0.30 objective in a Zeiss Observer Z1 fluorescence microscope (Zeiss Fluorescence Microscopy, Carl Zeiss Canada Ltd, Canada) connected to Axiocam MRc5 using a Zeiss Filter set 38 (Excitation BP 470/40, Emission BP 525/50) for imaging the functionalized nanofibers. Goniometer Static contact angle of a water droplet on nanofiber surfaces were measured under open-air condition using a goniometer (CAM 101 KSV instruments). Approximately 5 μL of deionized water was deposited on the surface and images were taken by an integrated digital camera. The software CAM2008 was used for image processing to determine the contact angle. The contact angle value for each sample was independently measured at three different locations and average values are reported.

5.2.3. Synthesis of P(EtOx-co-ButEnOx)

The ButenOx monomer was synthesized as first reported by Schlaad and coworkers [158]. The copolymer with an EtOx:ButenOx ratio of 190:10 and total degree of polymerization of 200 was reported following the microwave assisted polymerization protocol as described in ref [164]. The resulting polymer has 6.7 mol% ButenOx as

determined by ^{1}H-NMR spectroscopy (Bruker Avance 300 spectrometer, 300 MHz, $CDCl_3$), a number average molar mass of 30700 g/mol and a dispersity of 1.14 as determined by size exclusion chromatography (Agilent 1260-series HPLC system equipped with a 1260 online degasser, a 1260 ISO-pump, a 1260 automatic liquid sampler (ALS), a thermostated column compartment (TCC) at 50 °C equipped with two PLgel 5 μm mixed-D columns in series, a 1260 diode array detector (DAD) and a 1260 refractive index detector (RID). The used eluent was DMA containing 50mM of lithium chloride at an optimized flow rate of 0.593 mL/min). Mn value of the polymer was used as 18039 g/mol, calculated with the correction factor $M_{n,PEtOx}$=0.5876*$M_{n,PMMA}$.

5.2.4. Electrospinning and *In Situ* Crosslinking of P(EtOx-co-ButEnOx) Nanofibers

Electrospinning of crosslinked P(EtOx-co-ButEnOx) nanofibers P(EtOx-co-ButEnOx) nanofibers were crosslinked using pentaerythritol tetrakis(3- mercaptopropionate) under UV in the presence of DMPA as the photoinitiator. P(EtOx-co-ButEnOx) (200 mg, 0.011 mmol), pentaerythritol tetrakis(3-mercaptopropionate) (48.86 mg, 0.1 mmol) and DMPA (5.12 mg, 0.02 mmol) were stirred in 1:1 DMF:THF solvent system (0.2 mL). 3 The solution was placed in a 1 mL syringe with a needle and pumped with a flow rate of 0.01 mL/min. Nanofibers were electrospun under 13 kV voltage and 15 cm tip-to-collector distance on glass slides attached on a grounded aluminum collector. In-situ crosslinking was performed by UV during electrospinning.

5.2.5. Determination of Sulfhydryl Content

Determination of sulfhydryl content Free thiol group contents of the nanofibers were determined by Ellman's analysis [170]. The sulfhydryl groups were quantitated using the extinction coefficient of TNB^{2-} (2-nitro-5-thiobenzoic acid) ion as the reference. Ellman's reagent solution was prepared by dissolving 4 mg Ellman's reagent (5,5- dithio-bis-(2-nitrobenzoic acid) in 1 mL of reaction medium composed of 0.1 M sodium phosphate, pH 8.0, containing 1 mM EDTA buffer. A nanofibrous sample (2.1 mg) was placed in a vial and 3 mL of buffer and Ellman's reagent solution were added on the sample. The resultant mixture was incubated at 37 °C for 2 h. The absorbance at 412 nm was measured to

calculate the total sulfhydryl group content in the sample using the molar extinction coefficient of TNB^{2-} (14,150 $M^{-1}cm^{-1}$).

5.2.6. Fluorescent Dye Immobilization on Crosslinked P(EtOx-co-ButEnOx) Nanofibers via Thiol-Ene Reaction

A mixture of 10 µl of BODIPY-SH (1 mg/mL) and 1 µL of DMPA (2.4 mg/mL) solutions in THF was dropped on the glass slide covered with crosslinked nanofibers and the slide was placed under UV irradiation (365 nm at the distance of 10 cm) for 5 min. After the reaction, the sample was washed with excess THF to remove the unbound dye. For the control experiments, a solution of N-ethylmaleimide (5 mg/mL) in THF was dropped on P(EtOx-co-ButEnOx)) nanofiber-coated glass slides prior to BODIPY-SH immobilization and the slides were washed with ample THF after 4h. A mixture of 10 µl of BODIPY-SH (1 mg/mL) and 1 µl of DMPA (2.4 mg/mL) in THF were dropped on the glass slide covered with crosslinked nanofibers and a TEM grid as a UV mask was firmly placed onto the surface. The slide was placed under UV irradiation (365 nm at the distance of 10 cm) for 5 min. After the reaction, the sample was washed with excess THF to remove the unbound dye.

5.2.7. Fluorescent Dye Immobilization on Crosslinked P(EtOx-co-ButEnOx) Nanofibers via Michael Addition

5 µl of tetramethylrhodamine-5-maleimide solution (0.35 mg/mL) in methanol was dropped on a glass slide covered with crosslinked nanofibers and was left for 4 h in the dark. The sample was washed with ample methanol in order to remove the excess dye.

5.3. Results and Discussion

5.3.1. Fabrication of Crosslinked P(EtOx-co-ButEnOx) Nanofibers

Nanofibers were prepared by solution electrospinning of the alkene-side chain containing polymer P(EtOx-co-ButEnOx) in the presence of pentaerythritol tetrakis (3-mercapto propionate) as the thiol containing crosslinker and 2,2-dimethoxy-2-

phenylacetophenone (DMPA) as the photo initiator under irradiation with an UV lamp (365 nm) during electrospinning. It was envisioned that the alkene functionalized PAOx will undergo crosslinking via the radical thiol−ene reaction as the fibers are deposited on the collector. Following optimization experiments, a 52 wt % solution of the polymer in DMF/THF (1:1) was found to produce bead-free fibers with an average diameter of 542 nm ± 231 nm through electrospinning of the relatively low molar mass PAOx with a number-average molar mass of 18.0 kg/mol and a dispersity of 1.14 (Figure 5.2a). Nanofibers were produced using varying stoichiometry of alkene/tetrathiol/DMPA and, thereafter, subjected to rinsing with water to examine their stability due to crosslinking. When electrospun fibers obtained using molar ratios of 30:5:1, 30:10:1, 30:10:4 (alkene/tetrathiol/DMPA) were used, the fibers were not stable in aqueous environments and mostly underwent dissolution. It was only upon addition of a higher amount of the tetrathiol crosslinker (30:20:4) that robust nanofibers were obtained that were stable in water, and maintained their fibrous morphology, for prolonged periods of time (Figure 5.2b). We examined whether the surfaces coated with these nanofibers also show thermoresponsive wetting behavior. The contact angle of a droplet of water on these surfaces was 70° at 25 °C, while a significant increase to 90° was observed upon heating to 70 °C (Figure 5.2c). When the surfaces were cooled back to room temperature, the contact angle returned to 70°. These fibers could reversibly be cycled between these two wettability states by simple heating and cooling treatments (Figure 5.2d).

Requirement of a higher amount of the tetrathiol based crosslinker is not unexpected since this low molar mass component does not possess entanglements like the polymer chains and tends to partially evaporate after ejection from the nozzle during electrospinning. Interestingly, an alternative approach where a similar combination of polymer, tetrathiol, and DMPA was electrospun to yield fibers, followed by UV-irradiation after electrospinning did not yield fibers resistant to dissolution, perhaps due to inefficient crosslinking resulting from low chain mobility in the dry nanofiber. Stable nondissolving nanofibers were not achievable in the absence of either the tetrathiol or UV-irradiation. Furthermore, the presence of the ester carbonyl groups belonging to the tetrathiol in the crosslinked nanofibers was evidenced by FT-IR spectroscopy supporting that crosslinking takes place via chemical conjugation by thiol−ene reaction (Figure 5.3).

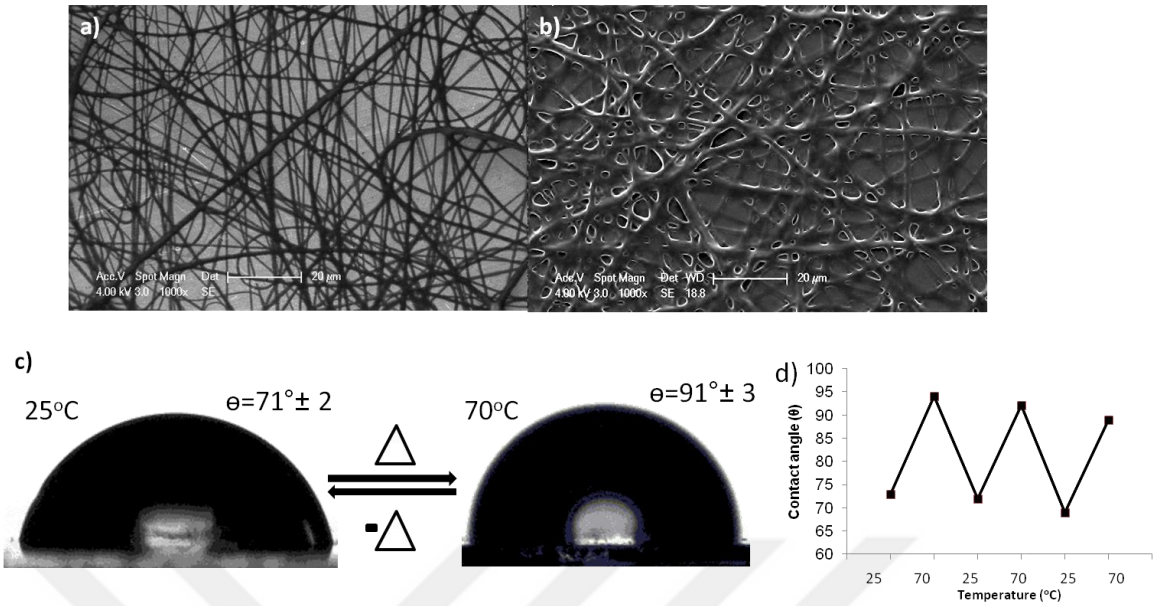

Figure 5.2. SEM images of nanofibers: (a) dry, (b) after immersion in water for 48 h, and (c) change in water contact angle, (d) graph showing the thermoresponsive behavior of the nanofibers probed with change in water contact angle with temperature.

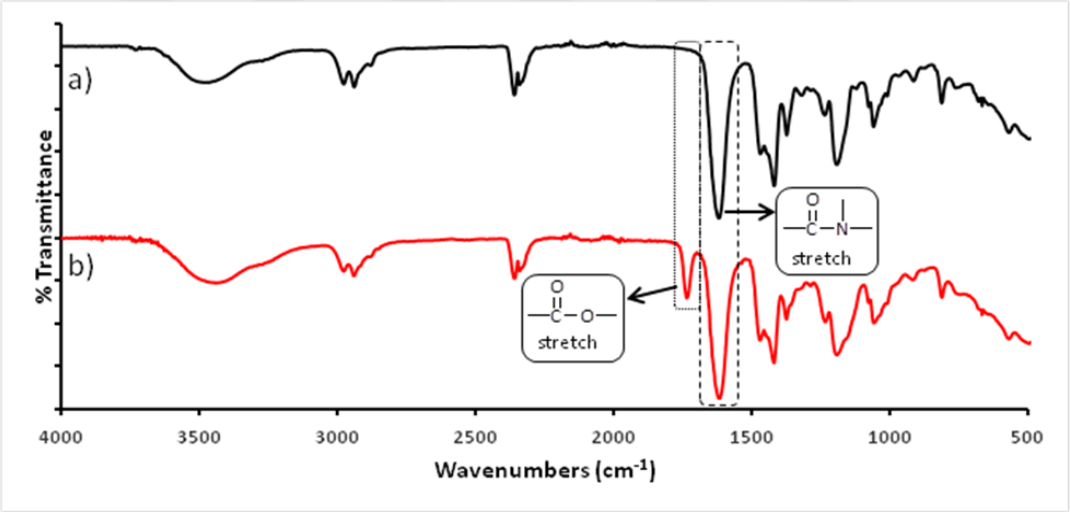

Figure 5.3. FT-IR spectra of (a) non-crosslinked (in black) and (b) crosslinked P(EtOx-co-ButEnOx) nanofibers.

In order to find the free thiol content on the crosslinked nanofibers, Ellman's analysis was performed. Using three different nanofiber samples thiol content was found as $4.65 \pm 0.45 \times 10^{-5}$ mmol/mg.

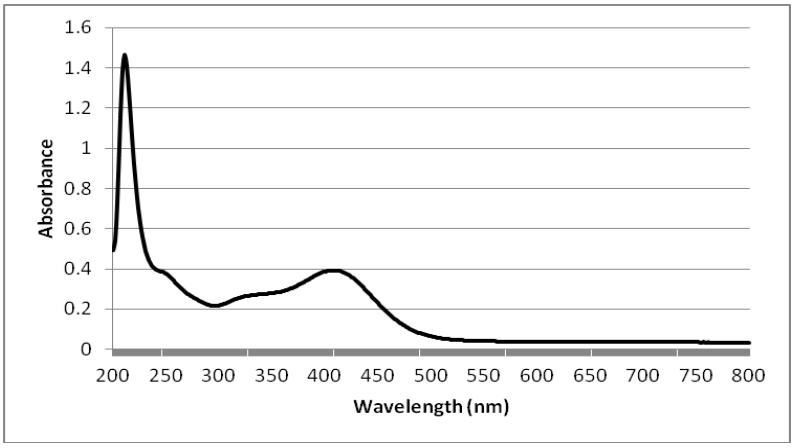

Figure 5.4. UV spectrum of Ellman's analysis.

5.3.2. Fluorescent Dye Immobilization on Crosslinked P(EtOx-co-ButEnOx) Nanofibers

Apart from tunable hydrophilicity, the PAOx are also known to exhibit thermoresponsive behavior dependent on their side chain functionality and composition [171]. The P(EtOx-co- ButEnOx) copolymer study here was found to exhibit a lower critical solution temperature and a cloud point temperature of 75 °C in a 5 mg/mL aqueous solution. A closer examination of the functionality of the polymer and crosslinker (Figure 5.5) suggests it is possible to obtain an insoluble network long before complete consumption of the alkene and thiol groups. The hypothetical availability of these two functional handles should allow attachment of different molecules through two different reactions. The residual alkenes can be conjugated with thiol containing molecules using the radical thiol−ene reaction (route A, Figure 5.5). Alternatively, nucleophilic thiol-maleimide conjugation can be used to attach desired molecules using the residual thiol groups arising from the crosslinker (route B, Figure 5.5). Furthermore, these fibers can be sequentially treated with maleimide and thiol containing molecules to accomplish multifunctionalization (route C, Figure 5.5).

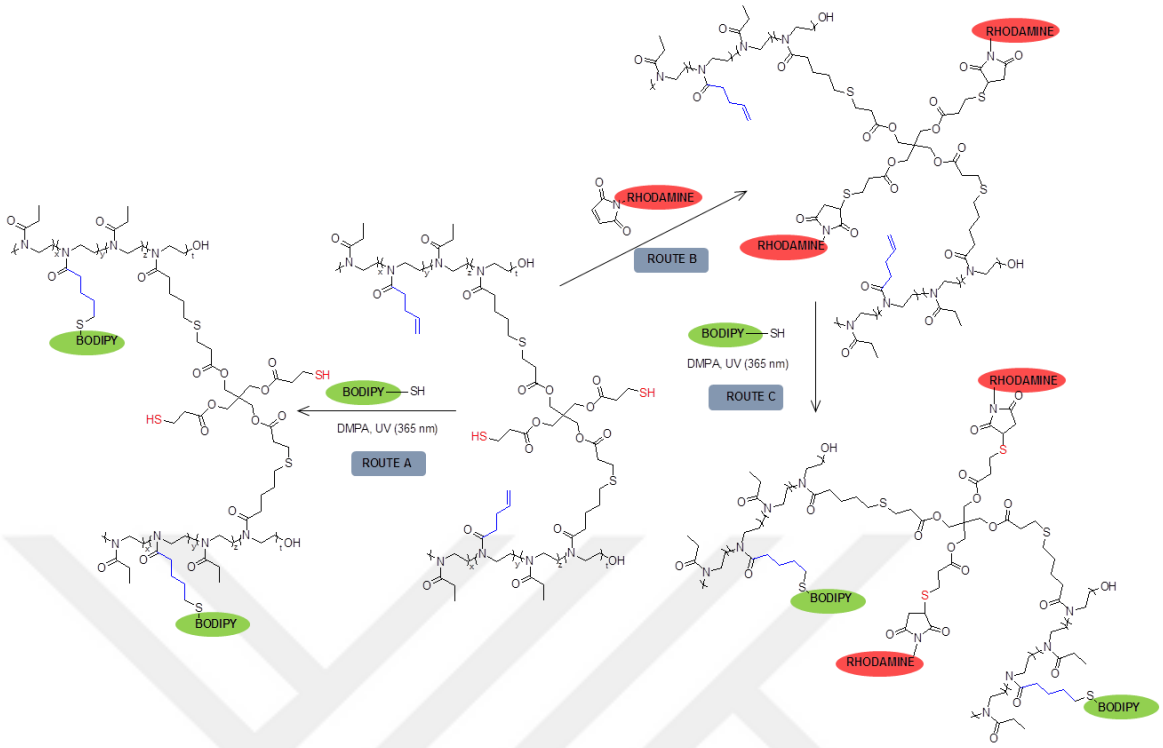

Figure 5.5. Functionalization of P(EtOx-co-ButEnOx) nanofibers.

First, functionalization of residual alkene groups was investigated. Nanofibers were exposed to a thiol-containing fluorescent dye, namely, BODIPY-SH, in the presence of DMPA under UV irradiation. After rinsing of the fibers with THF to remove residual unbound dye, fibers were examined via fluorescence microscopy. Bright green fluorescence of the dye functionalized fibers suggested efficient dye conjugation (Figure 5.6a). Not surprisingly, as a control experiment, when fibers were treated with the dye alone without any UV-exposure, a faint green fluorescence was clearly observable on the fibers indicating attachment of the thiol-containing dye, albeit in low efficiency (Figure 5.6b). It was likely that this occurs due to the presence of residual thiol groups on the fibers that form disulfide linkages with the thiol containing fluorescent dye. Indeed, the presence of residual thiol functional was confirmed using Ellman's reagent based on the appearance of a distinct absorbance at 412 nm belonging to the pyridothione fragment that is released into solution after reaction with the fibers (Figure 5.4). To probe this further, we treated the as spun nanofibers with N-ethylmaleimide to passivate the thiol groups before treatment with BODIPY-SH in the absence of UV irradiation. As anticipated, negligible fluorescence was observed for these fibers that only possessed the alkene groups (Figure 5.6a, inset).

Thiol groups on the crosslinked nanofibers were examined toward functionalization via Michael-type reaction using a maleimide-functionalized rhodamine dye. After incubation for 4 h, unbound dye was washed off with excess methanol. The red fluorescence of the nanofibers observed using fluorescence microscopy confirmed successful conjugation of the dye (Figure 5.6c). As a control, fibers were first treated with N- ethylmaleimide in order to passivate the free thiols and then treated with the maleimide-appended rhodamine dye. After incubation for 4 h, fiber-coated surfaces were washed with methanol. Inspection of the fluorescence images shows relatively weak signal when compared to the nonpassivated fibers (Figure 5.6c, inset).

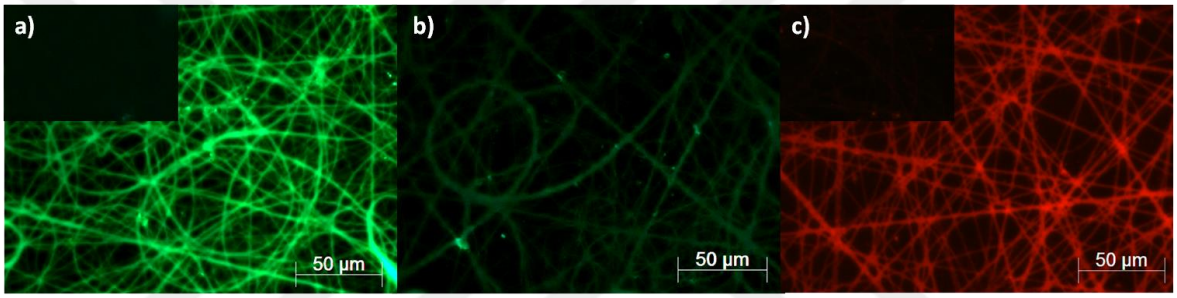

Figure 5.6. Fluorescence microscopy images of BODIPY-SH treated nanofibers (a) via thiol−ene reaction after, (b) without UV exposure, before N-ethylmaleimide conjugation and (c) rhodamine-maleimide treated nanofibers (insets are controls.

To demonstrate spatial control of the nanofiber functionalization, an exclusive advantage of using the photochemically promoted radical thiol−ene based conjugation strategy, attachment of BODIPY-SH under UV exposure through a photomask was probed. For this purpose, nanofibers were electrospun on silicon wafers and treated with N-ethylmaleimide to passivate the residual thiol groups. Thereafter, the fibers were imbibed with a mixture of BODIPY-SH and DMPA in THF and a photomask was placed on the fiber-coated surface. After exposure to UV irradiation, the photomask was peeled off, unbound dye was rinsed off with THF and the nanofiber coated surface was dried under nitrogen. Successful patterning was clearly observed with fluorescence microscopy (Figure 5.7).

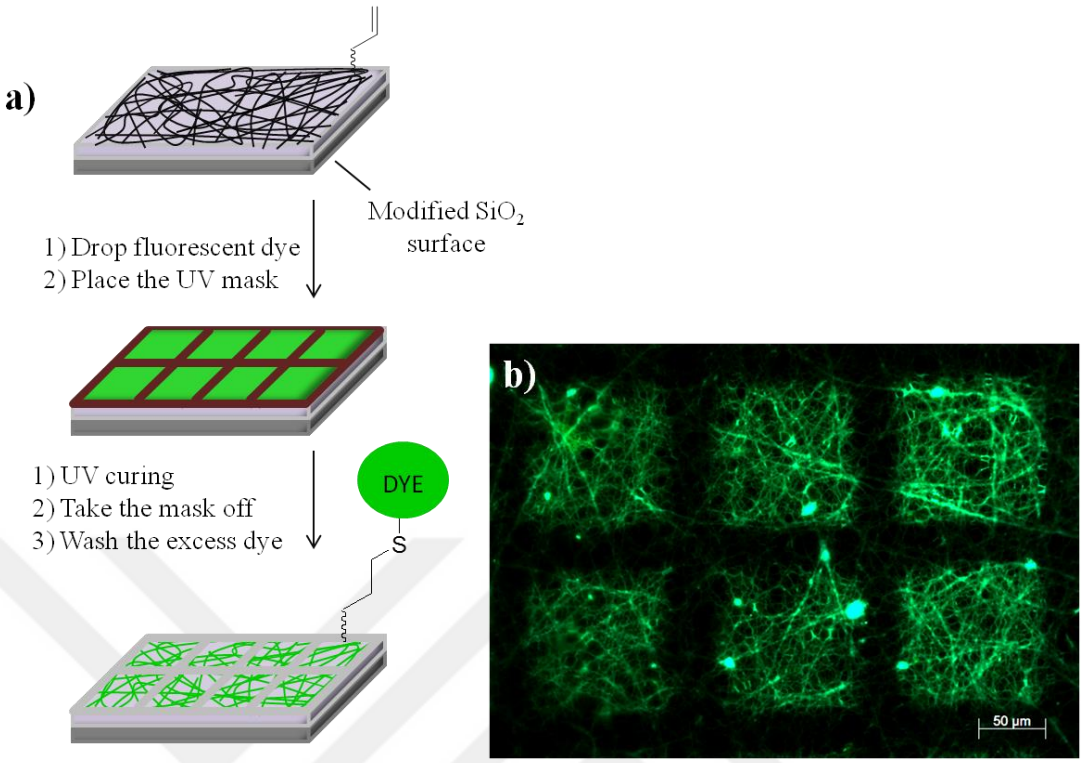

Figure 5.7. Photopatterning of P(EtOx-co-ButEnOx) nanofibers with BODIPY-SH.

The dual-functionalization demonstrate the capacity of these nanofibers, sequential conjugation of maleimide-rhodamine using thiol-maleimide coupling followed by attachment of BODIPY-SH under photochemical radical thiol−ene conditions was performed. After attachment of the first dye, unreacted dye was removed by thoroughly rinsing the fibers with methanol. Analysis of these fibers using fluorescence microscopy demonstrated that both dyes were efficiently attached onto the nanofibers, unambiguously demonstrating their multireactive nature (Figure 5.8).

In conclusion, fabrication of crosslinked hydrophilic nano-fibers that are amenable to facile multifunctionalization is accomplished in a single step using an *in situ* thiol−ene crosslinking during electrospinning. Hydrophilic polymers containing pendant alkene moieties are crosslinked using a tetra-thiol to provide robust electrospun fibers. These nanofibers readily undergo dual-functionalization under mild conditions using the nucleophilic thiol-maleimide and the photochemical radical thiol−ene conjugations. It can be envisioned that facile fabrication and functionalization of these PAOx-based materials, an upcoming surrogate of the widely utilized PEG-based biomaterials, will make these nanofibers attractive candidates for many applications.

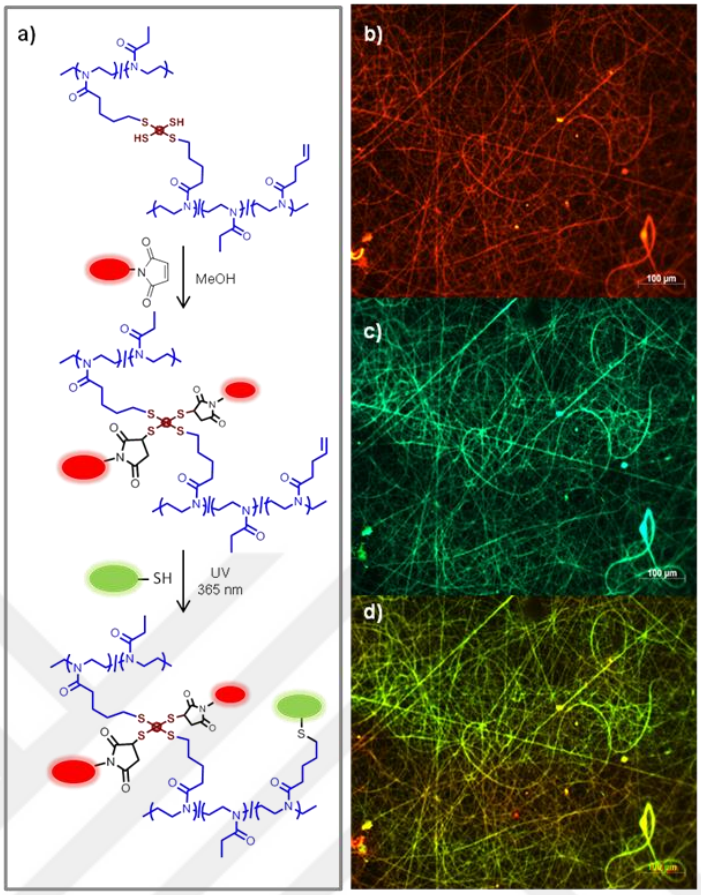

Figure 5.8. (a) Step-wise dual functionalization. Fluorescence images of sequentially functionalized nanofibers with (b) rhodamine maleimide, (c) BODIPY-SH, and (d) dual-functionalized (merged image) conditions.

6. BIOFUNCTIONALIZATION OF FURAN-CONTAINING BIODEGRADABLE NANOFIBERS VIA DIELS-ALDER REACTION

Published as the following paper: Kalaoglu-Altan, O.I., A. Kirac-Aydin, B. Sumer Bolu, R. Sanyal, and A. Sanyal, "Diels–Alder "Clickable" Biodegradable Nanofibers: Benign Tailoring Of Scaffolds For Biomolecular Immobilization And Cell Growth", *Bioconjugate Chemistry*, doi: 10.1021/acs.bioconjchem.7b00411, 2017.

6.1. Introduction

Polymeric nanofibers have been investigated widely for biological applications such as tissue engineering, regenerative medicine and drug delivery [172,173]. The tissue engineering scaffolds should mimic the native extracellular matrix (ECM) as it provides a physical support for cells and enhances cell adhesion, migration and proliferation. Polymeric nanofibers are promising materials as native ECM analogs with their physical resemblance to the ECM in addition to their high surface area, porosity and compositional variety with tunable fiber diameter and alignment [174].

Recently, electrospinning has become the most widely studied method to create the ECM-mimicking scaffolds due to the low cost equipment, simplicity of the operation, and the feasibility in scaling-up the production [2,5,175,176]. This method uses electrical forces to produce polymeric fibers with diameters in the range from several micrometers to less than 100nm. Synthetic polymers, such as polycaprolactone[177], polylactide[178], poly(lactide-co-glycolide)[179], poly(lactide-co-caprolactone)[180] have been widely electrospun into nanofibers for biological applications, which exhibit excellent mechanical properties, good processability and reproducibility. However, synthetic polymers are not as advantageous as natural polymers in cell attachment and proliferation due to the insufficient biocompatibility resulting from the hydrophobicity and the lack of bioactive sites for cell recognition [172,181-183]. Surface modification of the electrospun nanofibrous scaffolds is crucial, the incorporation of biomolecules onto the electrospun nanofibers could lead to a biofunctional scaffold, which would determine the efficiency of these fibers for regenerating biological functional tissues. These molecules such as

collagen, Arg-Gly-Asp (RGD), fibronectin and growth factors can be specifically recognized by various cellular constituents [88]. The bioactive molecules have been incorporated on the surface of the nanofibers using methods like plasma treatment, wet chemical methods, physical adsorption, surface graft polymerization which are disadvantageous because of the complicated and multi-step procedure, the destruction of the fiber structure, the limited penetration and applicability [87,88].

Recently, click chemistry, introduced by Sharpless, Kolb, and Finn in 2001,[52] is gaining attraction as it shows appreciable potential in the immobilization of various bioactive molecules onto fiber surfaces. Click reactions are favorable for surface modification as they are selective, highly efficient under mild reaction conditions giving no or inoffensive side products [58,184,185] One of the first examples of click chemistry in fiber modification was performed by Jing and coworkers where they attached an azide-bearing protein onto alkyne-bearing polylactide nanofibers using copper-catalyzed azide-alkyne cycloaddition (CuAAC) [95]. The usage of the toxic Cu catalyst in CuAAC has directed the interest to metal-free click reactions. Becker and coworkers have used various clickable groups on different nanofibers. Examples to their studies include an azide-containing GRGDS attachment onto DIBO-ended PCL nanofibers [186] and azide-containing gold nanoparticle immobilization onto DIBO-ended PBLG nanofibers [98] via strain-promoted azide-alkyne cycloaddition (SPAAC), (FITC)-conjugated RGD-thiol conjugation onto alkene-bearing poly(ester urea) nanofibers via thiol-ene reaction [96]. Diels-Alder reaction has also been investigated in areas such as macromolecular architectures, side-chain functionalization of polymers, side-chain functionalization of nanofibers and modification of biomolecules [76,77]. The importance of the Diels-Alder reaction in biomedical applications is being realized increasingly as it is an advantageous reaction as it can proceed in water and under mild reaction conditions, and the suitable diene-dienophile moieties, such as furan-maleimide, can easily be introduced to the desired system [187]. Furan-containing materials have been widely used for the functionalization of various types of polymeric interfaces such as thin films,[79] polymer brushes,[186] hydrogels,[189] nanoparticles,[190] nanofibers [120], as well as the synthesis of copolymers,[191] dendrimers,[77] and branched polymers [192]. One reason for the increasing attraction to the furan-maleimide pair is that the furan derivatives can be obtained from renewable resources which contributes to green chemistry [193].

Aliphatic polyesters synthesized via ring-opening polymerization of lactides are widely used in biomedical applications such as drug delivery and tissue engineering because of their biodegradable properties [194,195] Organocatalysts have become attractive for ROP recently as they have been rapidly replacing the conventional metal catalyst [196,197]. Although the polylactide-based materials have been used for various biomedical application, there are not many examples showing their functionality. Aliphatic carbonates are also preferred for biological applications due to their excellent biocompatibility [198]. Cyclic carbonate monomers such as trimethylene carbonate (TMC) have been widely copolymerized with lactide, [199] ε-caprolactone [200] and glycolide [201]. However, their high hydrophobicity and absence of reactive sites for biomolecule immobilization limited their biomedical applications. Recently, functional cyclic carbonate monomers with various reactive groups such as alkyne [202], azide[203], maleimide,[74] anthracene[83] have been investigated in order to obtain various functional (co)polymers with enhanced hydrophilicity, biodegradability and bioactive molecule immobilization. A furan-bearing cyclic carbonate was also used by Nelson and coworkers for the nanoimprinting of biodegradable polycarbonate based thin films crosslinked via the Diels-Alder reaction [204]. Malkoch and coworkers investigated the cytotoxicity of several polycarbonates with various functional-groups, including furan, and highlighted the suitability of these polymers in biomedical applications [205].

In this study, we synthesized a furan-functional polylactide based copolymer with anti-biofouling property and produced furan-containing biodegradable nanofibers using the electrospinning method [206]. In our previous works, we studied non-biodegradable furan-containing nanofibers. The novelty of this study comes from the biodegradable nature of the nanofibers. The obtained nanofibers were then functionalized with maleimide-bearing fluorescent dye, biotin and RGD peptide.

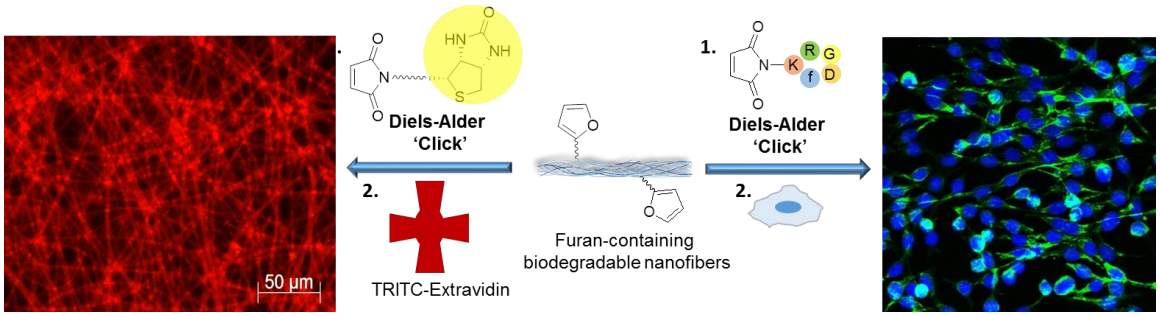

Figure 6.1. General scheme for the modification of furan-containing biodegradable nanofiber.

6.2. Experimental

6.2.1. Materials

L-Lactide (Aldrich) was recrystallized from toluene three times, dried in vacuo at room temperature for 6 h and stored in glovebox. 1,8-Diazabicyclo[5.4.0]undec-7-ene (DBU; Fluka) and benzyl alcohol (Merck) was dried over activated 4 Å molecular sieves and stored in a nitrogen filled glovebox. 1-(3,5-bis(trifluoromethyl)phenyl)-3-cyclohexylthiourea (TU) was synthesized according to the literature procedure [207]. Polymerizations were done in the glovebox using anhydrous dichloromethane (DCM) from SciMatCo purification system. Chloroform was purchased from VWR Chemicals and used as received. N-(5-Fluoresceinyl)maleimide and fluoresceinamine isomer I were obtained from Aldrich. Biotin-PEG2-maleimide was purchased from ThermoScientific and FITC-labeled streptavidin was obtained from Pierce. TRITC-conjugated extravidin and DAPI were purchased from Sigma. Cyclo[Arg-Gly-Asp-D-Phe-Lys(3-Maleimide propionic acid)] (cRGDfK(Mal)) was purchased from Peptides International. Alexa Fluor 488® phalloidin was obtained from Invitrogen.

6.2.2. Instrumentation

^{1}H-NMR spectra of the polymers were recorded on a Bruker 400 MHz spectrometer using trimethylsilane as an internal reference and deuterated chloroform as a solvent. The molecular weights of the copolymers were estimated by gel permeation chromatography (GPC) using a Shimadzu PSS-SDV (length/ID 8 × 300 mm, 10 µm particle size) mixed-C

column calibrated with polystyrene standards (1–150 kDa) using a refractive-index detector. Tetrahydrofuran (THF) was used as the eluent at a flow rate of 1 $mLmin^{-1}$ at 30 °C. The morphology of electrospun nanofibers was observed with Jeol Neoscope JCM-5000 scanning electron microscope (SEM) and Philips XL30 ESEM-FEG/EDAX system SEM. Fluorescence images of samples were recorded at room temperature on a Zeiss Observer Z1 fluorescence microscope. Static water contact angle were measured in air via the sessile-drop method using a goniometer (CAM 101 KSV instruments). Approximately 5 μL of deionized water was deposited on the surface and images were taken by an integrated digital camera. The software CAM2008 was used for image processing to determine the contact angle. Contact angle value for each sample was independently measured at three different locations and average values were measured. Differential scanning calorimeter (DSC) experiments were performed on a TA Instruments Q-2000 DSC apparatus at a heating rate of 10 °C/min. The X-ray source employed was a monochromatic Al Kα (1486.6 eV) at 72 W and 10^{-9} mbar. All XPS spectra were calibrated on the aliphatic carbon signal at 285.0 eV. Confocal microscopy images were taken by Leica TCS SP5 Confocal Microscope.

6.2.3. Synthesis of TEG-containing Cyclic Carbonate Monomer (MTC-TEG)

6.2.3.1 Synthesis of TEG containing acetal. To a solution of G1 anhydride (2.91 g, 0.008 mol) and DMAP (0.75 g, 6.1 mmol) in anhydrous CH_2Cl_2 (40 mL), triethylene glycol monomethyl ether (0.8 mL, 5.3 mmol) and pyridine (0.65 mL, 0.008 mol) were added under N_2. The reaction proceeded at room temperature for 24 h. Then, distilled H_2O (0.65 mL) was added to the reaction mixture and stirred for 5 h. Solution was extracted with 1M $NaHSO_4$ (50 mL x 3), 10 % Na_2CO_3 (50 mL x 3) and brine (50 mL x 1) solutions, respectively. The organic layer was dried over Na_2SO_4, filtered and evaporated under vacuo. The final compound was purified via column chromatography (hexane/ethyl acetate) to obtain a viscous colorless liquid (1.0 g, 86% yield).

6.2.3.2. Synthesis of TEG containing diol. At first, DOWEX-H^+ was washed with methanol (x 3). TEG containing acetal (1.0 g, 4.3 mmol) and DOWEX-H^+ (a tip of a spoon) were put in a round bottom flask in methanol ant the raction was carried out at 40 °C in oil bath under N_2. After 24 h, DOWEX-H^+ was filtered and methanol was evaporated

under vacuo. The obtained oily compound was purified with column chromatography (hexane/ethyl acetate) to yield a colorless liquid (0.8 g, 80% yield).

6.2.3.3. Synthesis of TEG containing cyclic carbonate monomer (MTC-TEG). The TEG-containing cyclic carbonate monomer was synthesized according to the literature procedure. TEG containing diol (430 mg, 1.5 mmol) and pyridine (1.142 mL, 2.3 mmol) were dissolved in anhydrous CH_2Cl_2 (6 mL). Reaction solution was cooled to -80 °C in dry ice bath and triphosgene solution (230 mg, 0.78 mmol) in CH_2Cl_2 was added dropwise to reaction mixture over 1 h under N_2. Reaction was stirred for 2 h at room temperature. After 2 h, saturated NH_4Cl solution (15 mL) was added to quench the reaction. Then, the organic layer was extracted with 1N HCl (x 3) and saturated $NaHCO_3$ solutions. Organic layer was dried with anhydrous Na_2SO_4, filtered and evaporated under vacuo. Final compound was purified with column chromatography (hexane/ethyl acetate) to yield a clear colorless liquid (270 mg, 80% yield). ^{1}H-NMR (400 MHz, $CDCl_3$, ppm): δ = 4.66 (d, 2H, C(CH_3)CH_2O)), 4.34 (t, 2H, CH_2OCO), 4.19 (d, 2H, C(CH_3)CH_2O)), 3.61 (m, 10H, CH_2O), 3.34 (s, 3H, –OCH_3) 1.32 (s, 3H, C(CH_3)). ^{13}C NMR (400 MHz, $CDCl_3$, ppm): δ = 171.0, 147.4, 72.9, 71.9, 70.6, 70.5, 68.6, 64.9, 59.0, 40.1, 17.6.

6.2.4. Synthesis of Furan-Containing Cyclic Carbonate Monomer (MTC-F)

6.2.4.1. Synthesis of furan containing acetal. To a solution of G1 anhydride (5 g, 0.022 mol) and DMAP (0.73 g, 6 mmol) in anhydrous CH_2Cl_2 (80 mL), furfuryl alcohol (1.3 mL, 0.015 mol) and pyridine (3.5 mL, 0.045 mol) were added under N_2. The reaction proceeded at room temperature for 24 h. Then, distilled H_2O (3.5 mL) was added to the reaction mixture and stirred for 5 h. Solution was extracted with 1 M $NaHSO_4$ (50 mL x 3), 10 % Na_2CO_3 (50 mL x 3) and brine (50 mL x 1) solutions, respectively. The organic layer was dried over Na_2SO_4, filtered and evaporated under vacuo. (2 g, 83 %).

6.2.4.2. Synthesis of furan containing diol. Furan-containing acetal (2.5 g) was dissolved in THF (6 mL) and 1N HCl (6 mL) at room temperature and stirred for 4 h. Then the THF was evaporated under *vacuo* and the diol was purified via extraction with CH_2Cl_2. (1.9 g, 90 %).

6.2.4.3. Synthesis of furan containing cyclic carbonate monomer (MTC-F). Furan-containing diol (2 g, 0.0093 mol) was dissolved in anhydrous THF (50 mL) in a round bottom flask and cooled to 0 °C. Then, a solution of ethyl chloroformate (1.77 mL, 0.019 mol) in THF (5 mL) and triethylamine (3.9 mL, 0.028 mol) in THF (5 mL) was added to the solution dropwise. The reaction was stirred for 2 h at 0 °C and then overnight at room temperature. Then, the ammonium salt was filtered and the solvent was evaporated under reduced pressure. Pure compound was obtained by recrystallization from anhydrous THF (1.56 g, 70 %). ^{1}H-NMR (400 MHz, $CDCl_3$, ppm): δ = 7.43 (s, 1H furan), 6.44 (s, 1H furan), 6.37 (s, 1H furan), 5.17 (s, 2H, –OCH_2–furan) , 4.70 (d, 2H, *J=10.8 Hz*, C(CH_3)CH_2O)), 4.17 (d, 2H, *J=10.8 Hz*, C(CH_3)CH_2O)), 1.32 (s, 3H, C(CH_3)). ^{13}C NMR (400 MHz, $CDCl_3$, ppm): δ = 170.7, 148.2, 147.3, 143.7, 111.4, 110.6, 72.8, 59.3, 40.1, 17.4.

6.2.5. Synthesis of Furan and TEG-Containing PLLA Copolymers

In a typical experiment, MTC-F (157 mg, 0.65 mmol), MTC-TEG (75 mg, 0.25 mmol), L-lactide (348 mg, 2.42 mmol), TU (15.4 mg, 0.042 mmol) and benzyl alcohol (1.7 µL, 0.017 mmol) were added in a glass vial equipped with magnetic stirring bar and dissolved in anhydrous dichloromethane (3 mL) in a nitrogen-filled glovebox. Under rapid stirring, DBU (12.5 µL, 0.084 mmol) was added to the reaction mixture. The reaction was carried out at room temperature and quenched with benzoic acid (51.29 mg, 0.42 mmol) after 20 h. The resulting copolymer was purified by precipitation in 1:1 methanol/ether solution, followed by filtration and drying under *vacuo* to yield a white powder (360 mg, conversion 65 %).

6.2.6. Electrospinning of Furan and TEG-Containing PLLA Copolymers

MTC-TEG-F/PLA copolymers were dissolved in $CHCl_3$ at a concentration of 40 wt % and stirred for 6 h in order to obtain a homogenous solution. The solution was delivered at a constant flow rate to a needle connected to a high-voltage power supply. For a typical experiment, the tip to collector distance was 15 cm, the applied voltage was 15 kV and the flow rate was 0.01 mL min^{-1}. Fibers were collected on 22 x 22 mm glass slides attached on a grounded aluminum collector.

6.2.7. Conjugation of Fluorescent Dye to Furan and TEG-Containing PLLA Nanofibers

The MTC-$TEG_{7.5}$-F/PLA nanofibers were treated with a water-soluble fluorescent dye, namely *N*-(5-fluoresceinyl)maleimide. The dye was dissolved in 1x PBS (1 mg/mL) and the solution (50 μL) was dropped on the nanofibers at room temperature. After 4 h in the dark, the surfaces were washed with ample amount of water, dried under nitrogen stream and examined under fluorescence microscope. As a control experiment, a solution of fluorescein amine isomer I was prepared in 1× PBS solution (1 mg/mL) and this solution (50 μL) was dropped on the glass slide covered with furan-containing nanofibers. After 4 h in the dark, the nanofibers were gently rinsed with excess PBS solution. Subsequently, modified nanofibers were analyzed with fluorescence microscope.

6.2.8. Ligand-Directed Immobilization of Protein on Furan and TEG-Containing PLLA Nanofibers

An aqueous solution of biotin-PEG2-maleimide (50 μL, 1 mg/mL) was dropped onto MTC-$TEG_{7.5}$-F/PLA nanofibers. After incubating 4 h at room temperature in the dark, the coated-fiber surfaces were washed with copious amount of water. Aqueous solution of TRITC-Extravidin (0.1 mg/mL) was prepared and this solution (10 μL) was dropped onto the biotinylated nanofibers. After 30 min in the dark, the fibers were gently rinsed with ample amount of water to remove any unbound protein. The immobilization of protein was analyzed using fluorescence microscopy.

6.2.9. Degradation Studies of Furan and TEG-Containing PLLA Nanofibers

Electrospun nanofibrous samples were incubated in closed vials containing 2 mL of 1× PBS at 37 °C for different periods of time. The specimens were washed with ample water and dried under nitrogen stream at the end of each degradation period and examined using SEM.

6.2.10. Bicinchoninic Acid Protein Quantification of Furan and TEG-Containing PLLA Nanofibers

An aqueous solution of cRGDfK(Mal) (1 mg/mL, 30 µL) was dropped onto MTC-$TEG_{7.5}$-F/PLA nanofibers at room temperature. After 4 h, nanofiber surfaces were washed with water and dried. The peptide (cRGDfK(Mal)) amount conjugated onto the furan-containing PLLA nanofibers was quantified using a bicinchoninic acid (BCA) kit (ThermoScientific, U.S.A.) according to manufacturer's instructions.

6.2.11. Cell Culture on Furan and TEG-Containing PLLA Nanofibers

L929 mouse fibroblasts were seeded onto prepared nanofiber coated slides with a density of 2×10^4 cells/cm^2 using a stock solution 2×10^5 cells/mL. After dropping the cell suspensions onto coated slides, they were incubated at 37 °C in 5% CO_2 containing atmosphere for 3 h. Afterwards, cell media (1 mL) was added into each well containing nanofiber coated slides. After incubation (24 or 72 h), cell media was removed, slides were washed with 1× PBS and cells were fixed with 3.7% formaldehyde solution at room temperature. For staining filamentous actins (F-actins), first, cells were incubated in 0.1% Triton X-100 in PBS for 5 min, then after washing with 1× PBS, they were incubated in Alexa Fluor 488® phalloidin solution (5 units/mL concentration containing 1 % bovine serum albumin (BSA) in 1× PBS) for 20 min at room temperature. Subsequently, cell nuclei were stained with DAPI. Resulting images of cells attached onto nanofibers were taken and processed via AxioVision software.

6.2.12. Cytotoxicity of Furan and TEG-Containing PLLA Nanofibers

In this study, L929 mouse fibroblast cells were used, which were grown in 5% CO_2 containing atmosphere at 37 °C. Cells were cultured in RPMI 1640 media supplemented with 10% fetal bovine serum (FBS) (PAN Biotech). For all experiments, cells were seeded at their exponential growth phase. For cytotoxicity assay, L929 cells were seeded into 96 well plates in quadruplicates. Nanofibers were pulverized and after addition of 1× PBS, they were sonicated for 20 min to obtain a cloudy solution with a final concentration of 10 mg/mL. Dilutions were made to obtain final polymer solutions with different

concentrations. Cells were treated with polymer solutions at various concentrations and they were incubated continuously for 48 h in incubator. To determine cell viability CCK-8 assay was employed according to manufacturer's recommendations and viability values were calculated via GraphPad Prism software.

6.3. Results and Discussions

6.3.1. Synthesis of TEG-Containing Cyclic Carbonate Monomer

TEG-containing cyclic carbonate monomer was synthesized from a TEG-containing diol in the presence of triphosgene (Figure 6.2).

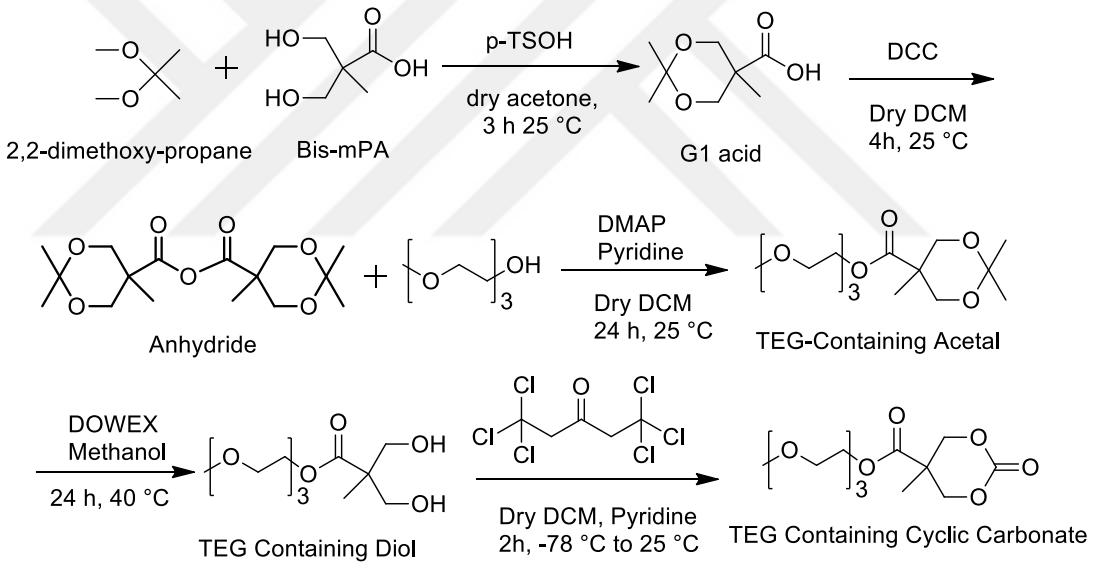

Figure 6.2. General scheme for the synthesis of the TEG-containing cyclic carbonate.

The structure of the TEG-containing cyclic carbonate monomer was confimed with ^{1}H-NMR and ^{13}C-NMR spectra (Figure 6.3,6.4).

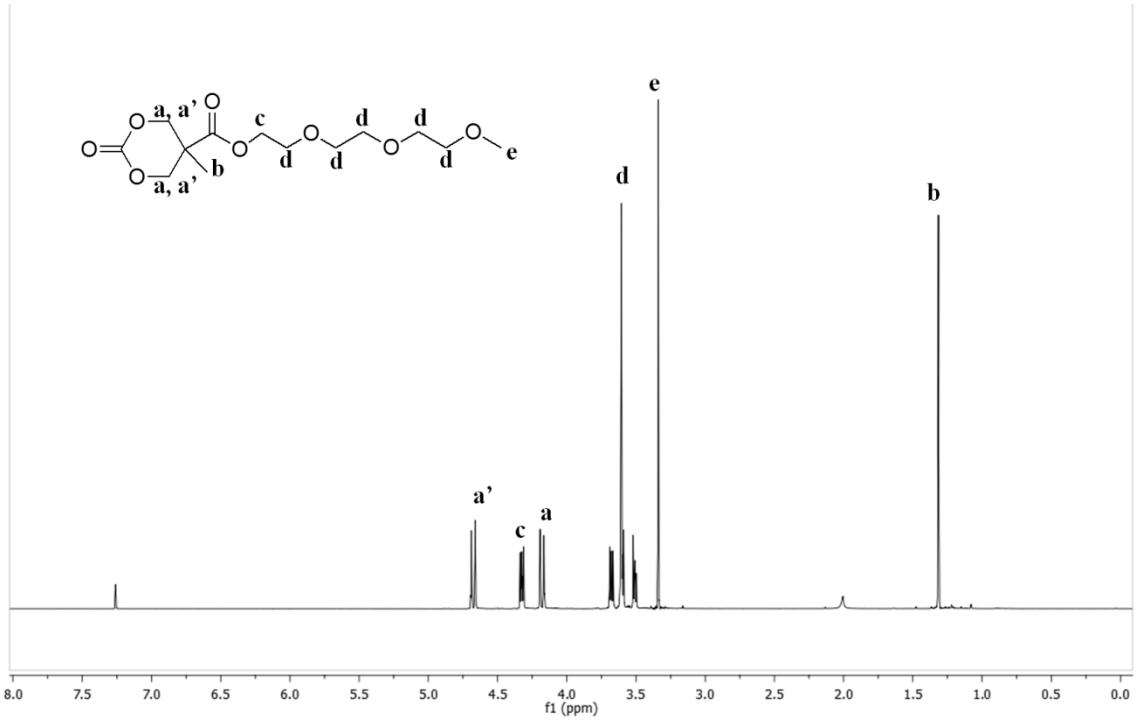

Figure 6.3. ^{1}H-NMR spectrum of TEG-containing cyclic carbonate.

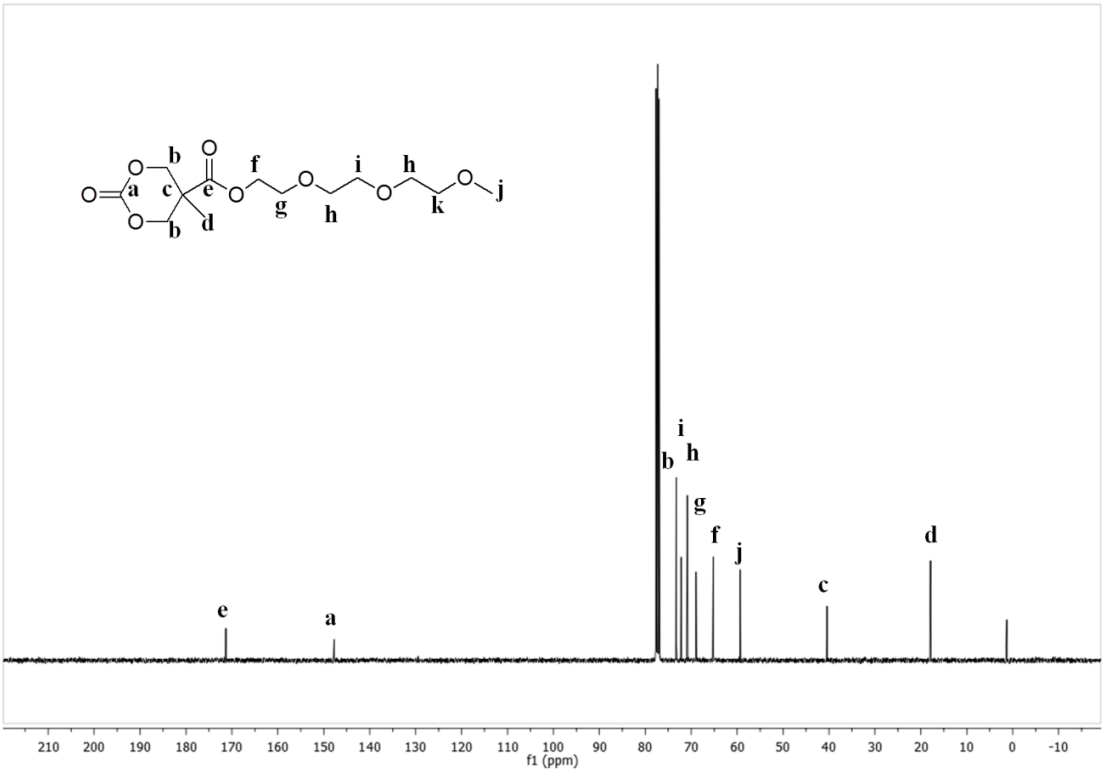

Figure 6.4. ^{13}C-NMR spectrum of TEG-containing cyclic carbonate.

6.3.2. Synthesis of Furan-Containing Cyclic Carbonate Monomer

Furan-containing cyclic carbonate monomer was synthesized from a furan-containing diol in the presence of ethyl chloroformate (Figure 6.5).

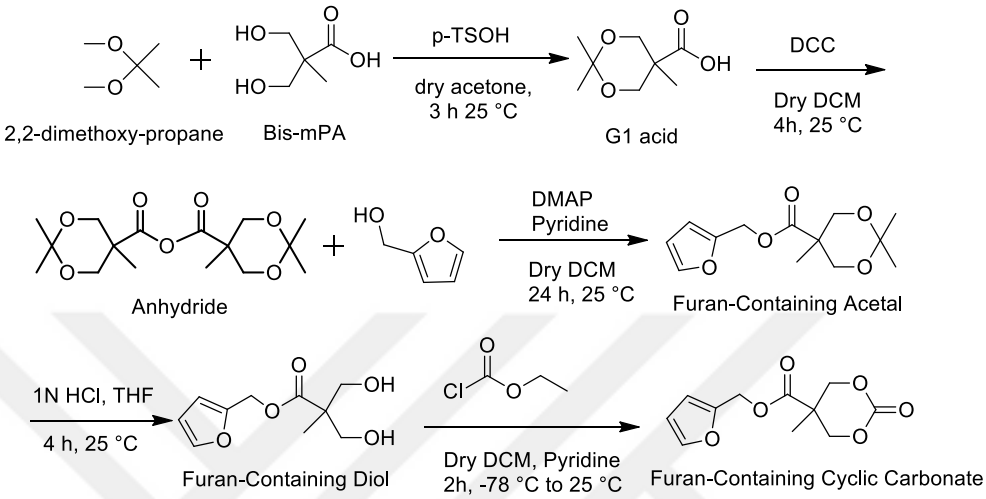

Figure 6.5. General scheme for the synthesis of the furan-containing cyclic carbonate.

The structure of the furan-containing cyclic carbonate monomer was confimed with ^{1}H-NMR and ^{13}C-NMR spectra (Figure 6.6,6.7).

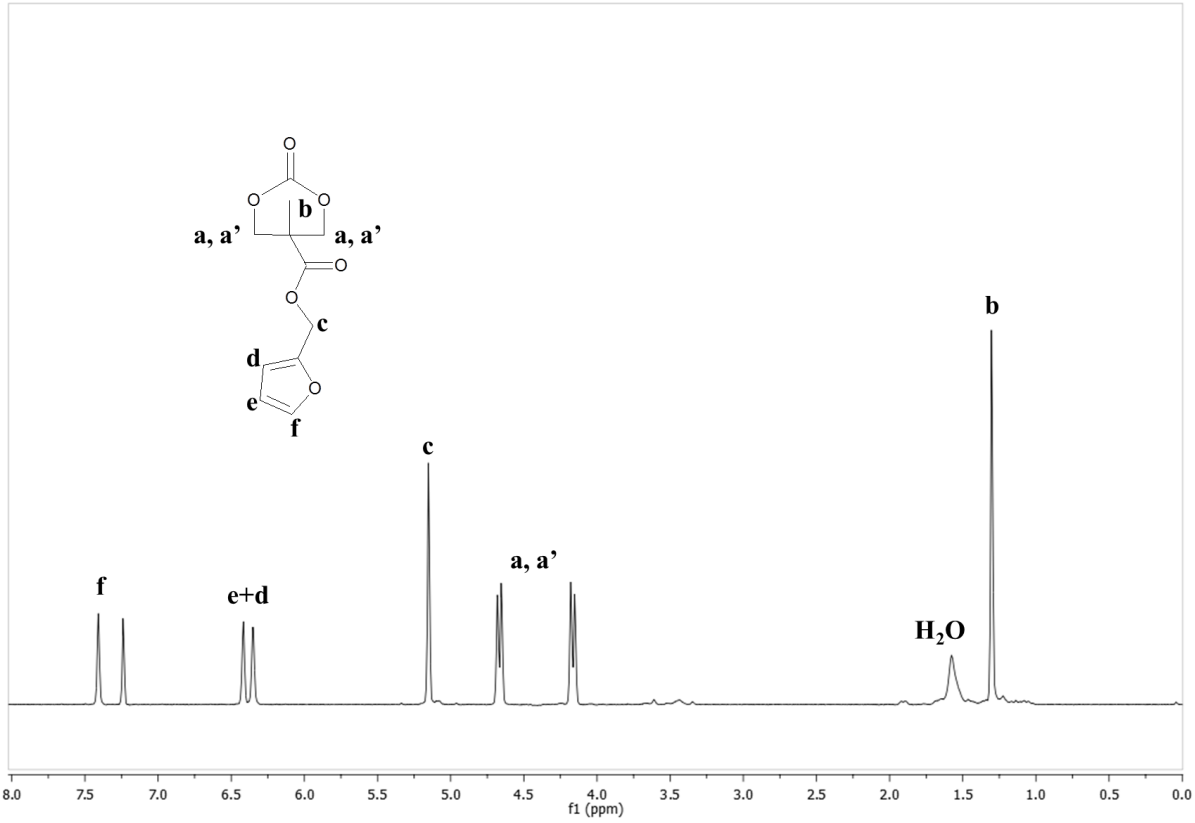

Figure 6.6. ^{1}H-NMR spectrum of furan-containing cyclic carbonate.

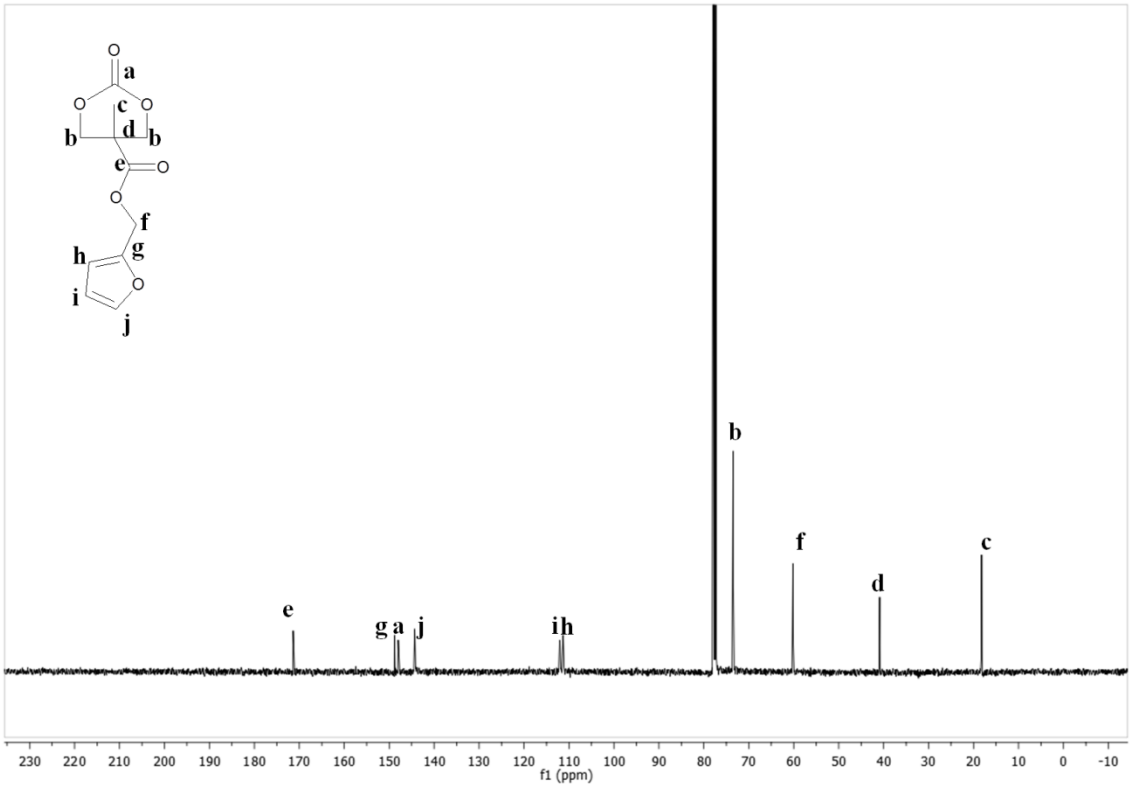

Figure 6.7. ^{13}C-NMR spectrum of furan-containing cyclic carbonate.

6.3.3. Synthesis of Furan and TEG-Containing PLLA Copolymers

Synthesis of side-chain furan-containing polylactides was performed using ring opening polymerization of L-lactide with furan (MTC-F) and TEG-bearing (MTC-TEG) cyclic carbonate monomers catalyzed by DBU/TU co-catalyst system using benzyl alcohol as an initiator (Figure 6.8). The furan containing cyclic carbonate monomer was obtained by reaction of furfuryl alcohol with a bis-MPA based anhydride. Subsequent deprotection of the acetal group to the diol, followed by condensation with ethylchloroformate yielded the furan-containing carbonate monomer with high yield and purity. Likewise, the triethylene glycol (TEG) containing carbonate monomer was synthesized from triethylene glycol momnomethyl ether using a simiar protocol. The hydrophilic TEG-based monomer was incorporated into the copolymers to provide the polymeric nanofibers with anti-biofouling characteristics. To understand what is the minimal amount of the TEG-based monomer that will impart the nanofibers with desirable level of anti-biofouling ability, while preserving fiber formation ability, a series of copolymers containing varying amount

of the MTC-TEG monomer were synthesized using ROP (Table 6.1). Polymerizations were confimed using ^{1}H-NMR spectrum (Figure 6.9-6.12)

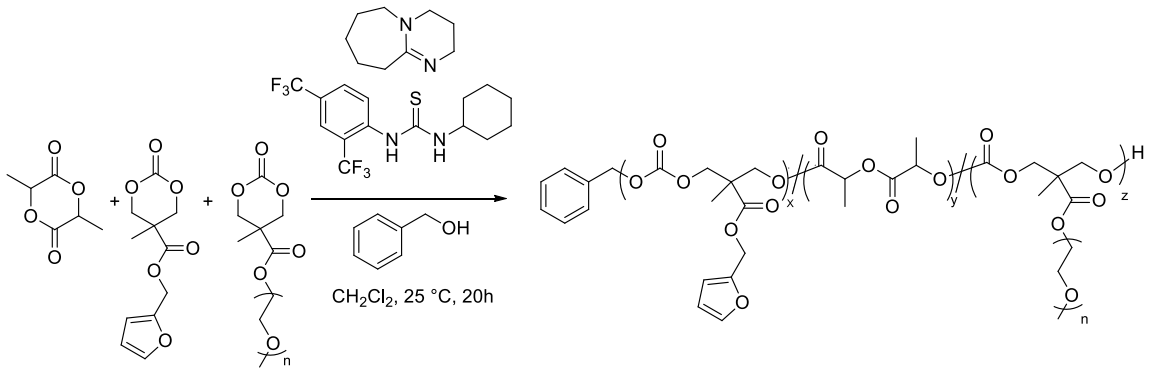

Figure 6.8. Synthesis of TEG and furan-containing hydrophilic biodegradable PLA copolymers.

Table 6.1. Summary of size exclusion chromatography results for synthesized furan-containing PLAs.

Polymers	**[TEG]/[Furan]/[LA]**[a]	**[M]/[I]**[b]	**M_n**[c]	**M_w**[c]	**PDI**[c]
MTC-TEG_5-F/PLA	10/40/150	200	12189	16893	1.39
MTC-$TEG_{7.5}$-F/PLA	15/40/145	200	13045	18492	1.42
MTC-TEG_{10}-F/PLA	20/40/140	200	7100	9758	1.37
MTC-F/PLA	0/40/160	200	13306	16053	1.23

[a]Molar feed ratio; [b]I=benzyl alcohol; [c]Determined using SEC using polystyrene standards (1-150 kDa) in THF.

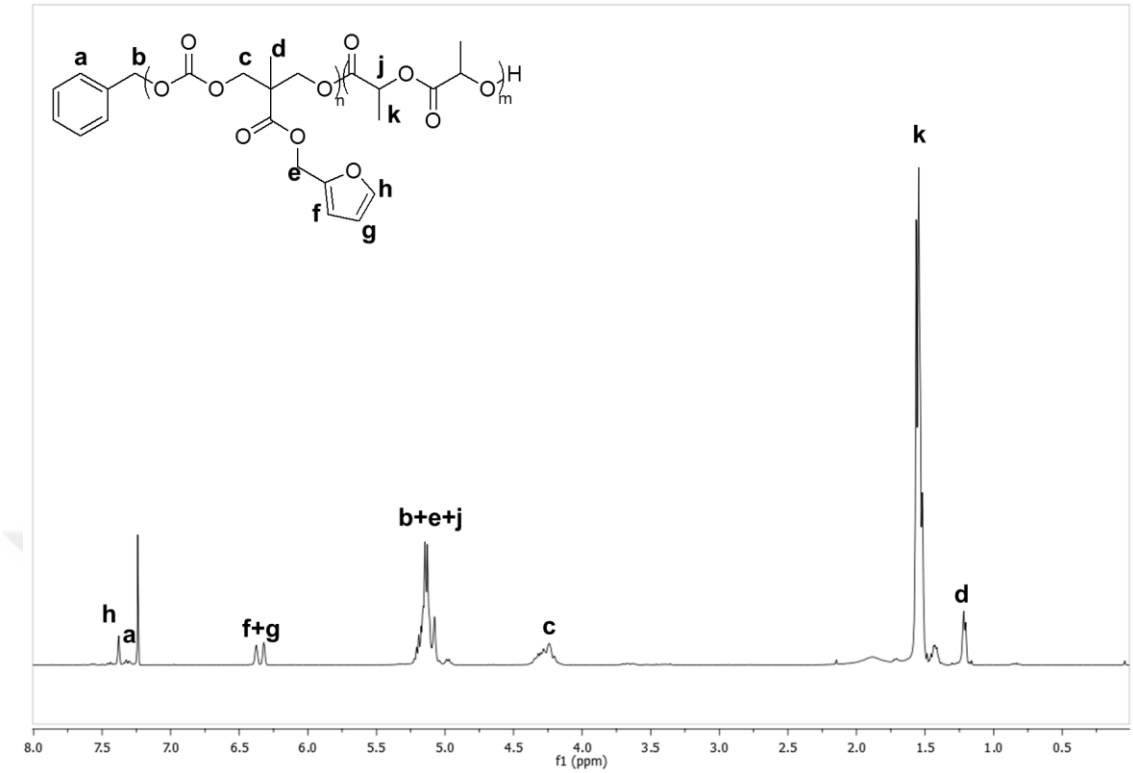

Figure 6.9. ^{1}H-NMR spectrum of furan-containing copolymer.

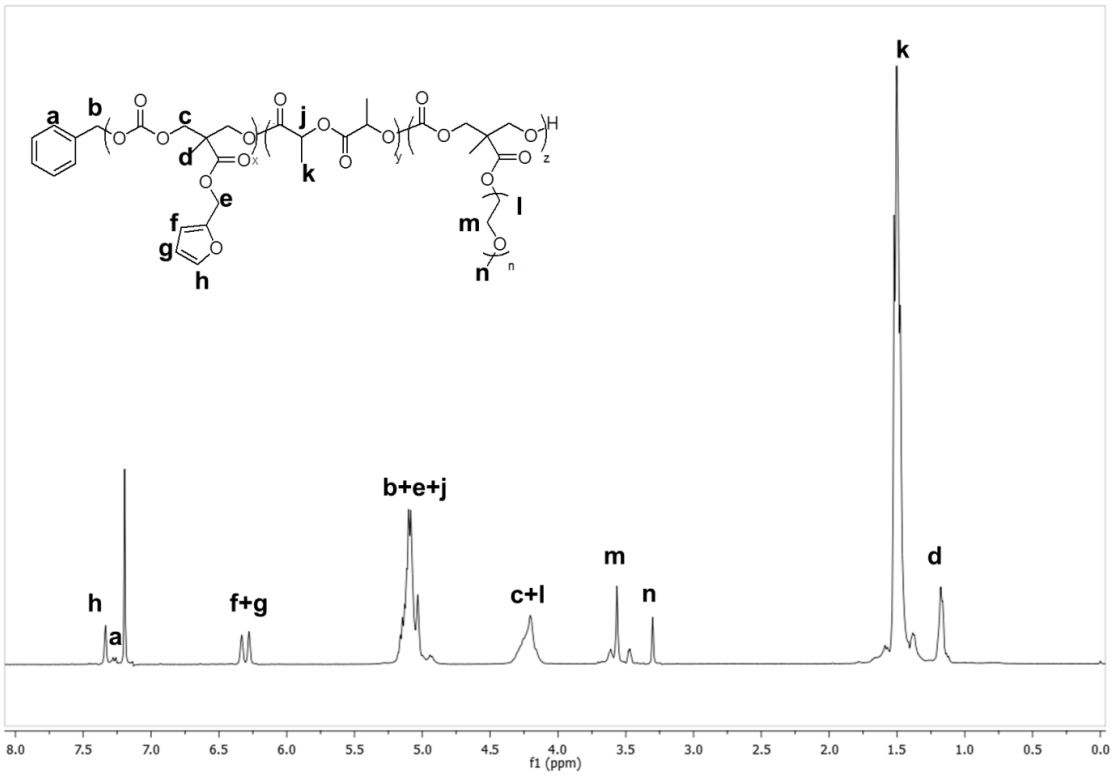

Figure 6.10. ^{1}H-NMR spectrum of furan and 5% TEG-containing copolymer.

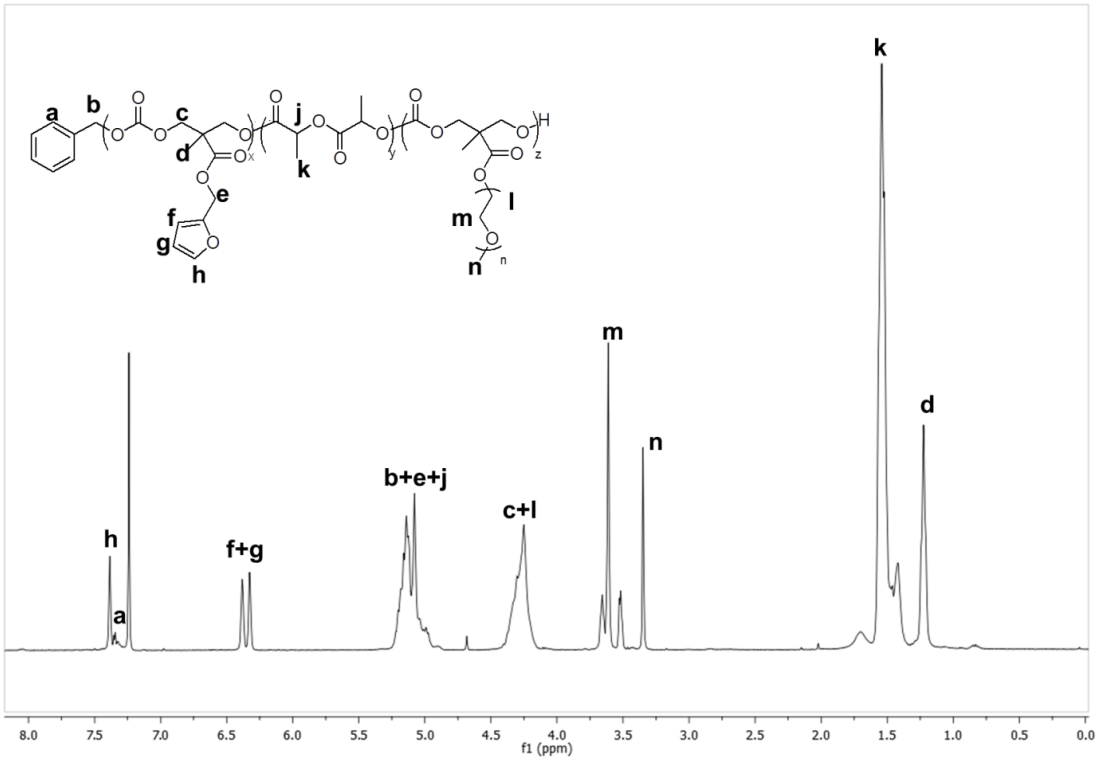

Figure 6.11. ^{1}H-NMR spectrum of furan and 7.5% TEG-containing copolymer.

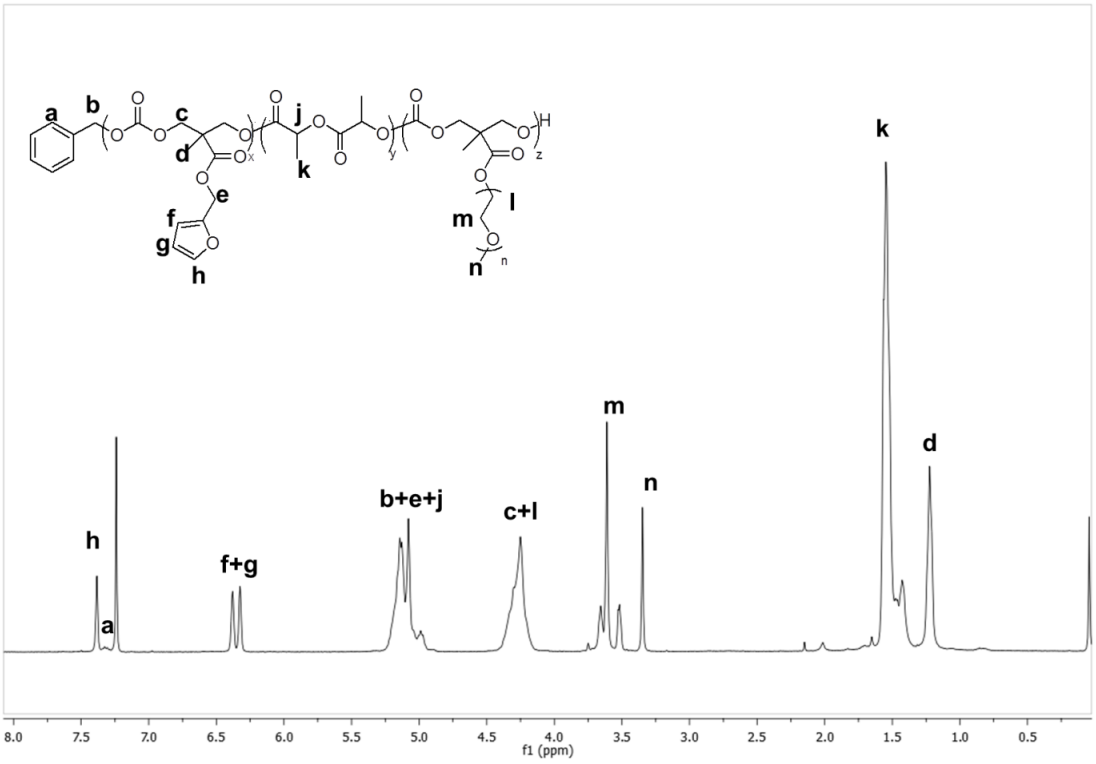

Figure 6.12. ^{1}H-NMR spectrum of furan and 10 % TEG-containing copolymer.

6.3.4. Fabrication of Furan and TEG-Containing PLLA Nanofibers

With the polymeric precursors at hand, furan-containing nanofibers were prepared using the solution electrospinning method. Bead-free nanofibers were successfully prepared from solutions of furan-containing copolymers using chloroform as a solvent with a concentration of 40 wt % and electrospun with an applied voltage of 15 kV, a tip-to-collector distance of 15 cm and a flow rate of 0.01mL/min. The scanning electron microscopy images of nanofibers indicated that while bead-free uniform fibers were obtained using the copolymer devoid of TEG-groups and those containing 5% and 7.5% TEG groups, the 10 % TEG-monomer containing copolymers did not give stable nanofibers (Figure 6.13). The fibers obtained using the higher TEG content appeared to be in a melted state rather than stable nanofibers. Differential scanning calorimetric analysis of the copolymers revealed that increasing amount of TEG in the copolymers lowered the glass transition temperature (T_g) from 35.1 °C to 5.8 °C which explains the poor nanofiber formation from copolymers with high TEG content (Figure 6.14).

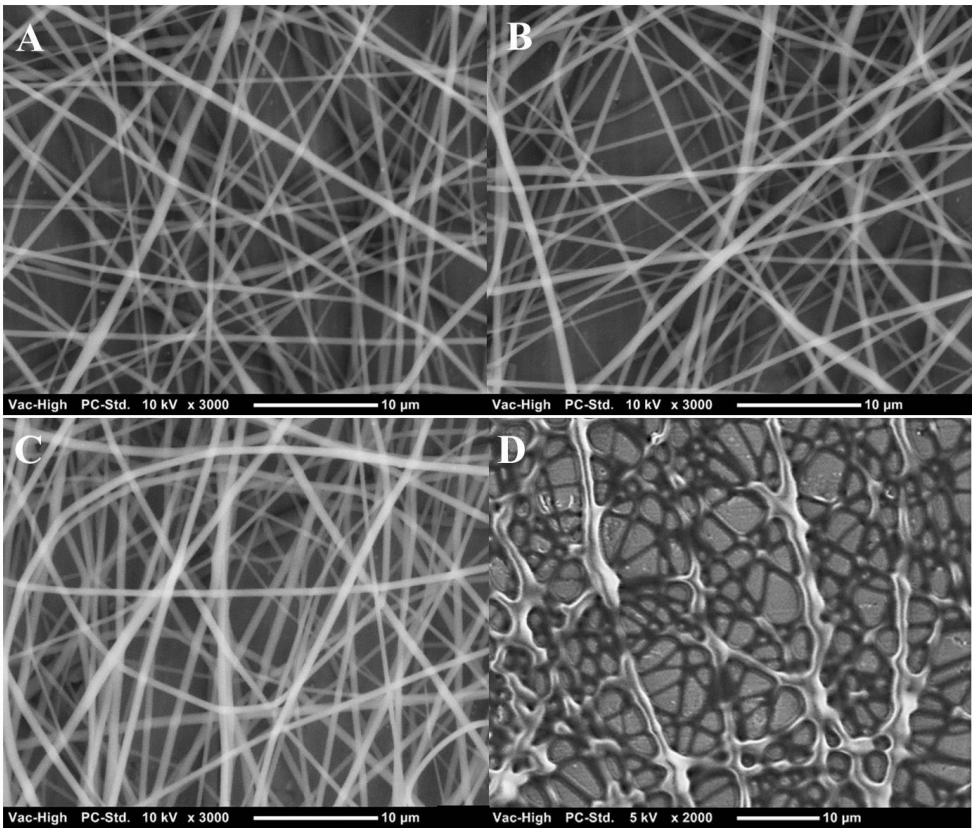

Figure 6.13. SEM images of (a) 0% (b) 5% (c) 7.5% (d) 10 % TEG-containing MTC-F/PLA nanofibers.

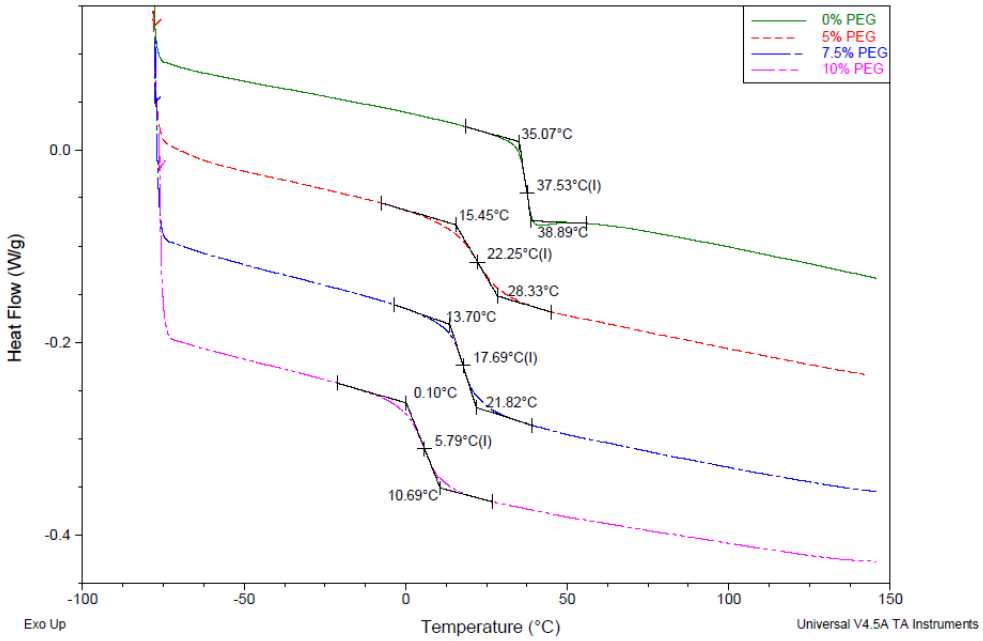

Figure 6.14. DSC thermograms of furan-containing PLLA copolymers with various TEG comonomer ratios.

The three nanofibers with stable fiber morphlogies containing TEG moeities ranging from 0-7.5 mol% were evaluated for their anti-biofouling characteristics. The fibers were treated with FITC-labelled Streptavidin (0.1 mg/mL in PBS) and after incubating for 30 min in the dark, were rinsed with copious amount of PBS (1×). While the nanofibers devoid of TEG groups adsorbed and retained high amount of protein, comparatively less amount of protein adsorbed onto fibers with 5 % TEG groups (Figure 6.15). Finally, it was only when the TEG content was increased to 7.5 mol%, nanofibers with significant antibiofouling character were obtained with an average diameter of 472 nm ± 160 nm. It is well established that hydrophilicity of the TEG units plays a role in providing anti-biofouling characteristics to the materials surface. Hence to correlate the observations here with surface hydrophilicity of nanofibers, water contact angle measurements were undertaken. An average of water contact angle for the furan-containing nanofibers (MTC-F/PLA) without TEG units was obtained as 128°, while the value for the 7.5 mol% TEG-containing nanofibers was obtained as 84°. Additionally, XPS analysis also supported presence of the TEG units on nanofiber surface through an increase in ether type C-O linkages for nanofibers containing the TEG comonomer (Figure 6.16).

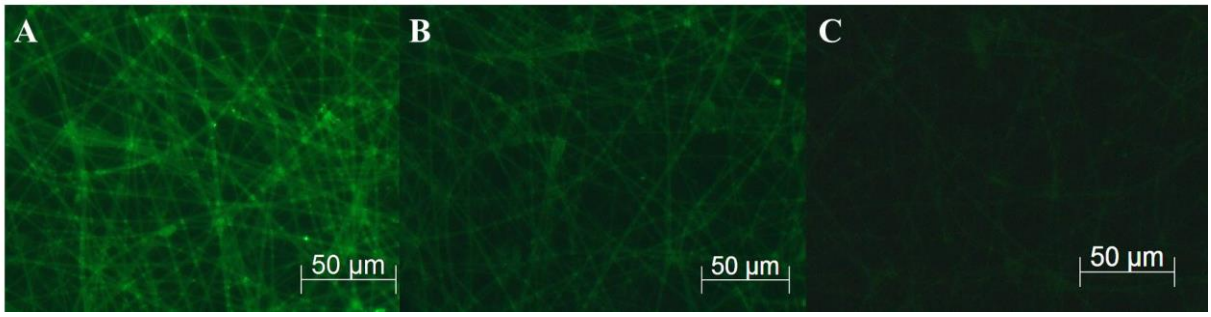

Figure 6.15. Fluorescence microscopy images of FITC-labelled Streptavidin immobilization on non-biotinylated (a) 0 % TEG-containing (b) 5 % TEG-containing (c) 7.5 % TEG-containing MTC-F/PLA nanofibers.

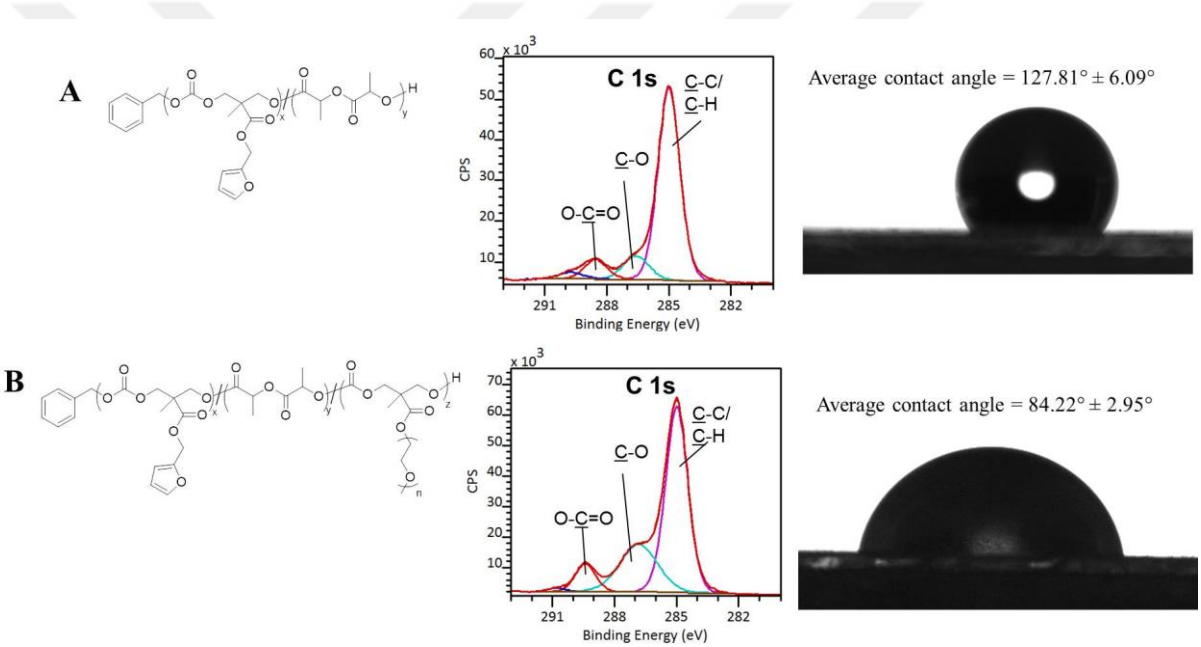

Figure 6.16. XPS and water contant angle measurements of (a) MTC-F/PLA (b) MTC-$TEG_{7.5}$-F/PLA nanofibers.

6.3.5. (Bio)Functionalization, Degradation and Cell Culture Studies of Furan and TEG-Containing PLLA Nanofibers

The MTC-$TEG_{7.5}$-F/PLA nanofibers were first treated with a maleimide-containing fluorescent dye in order to investigate the feasibility of the conjugation through the Diels-Alder cycloaddition reaction (Figure 6.17). An aqueous solution of the fluorescent dye was dropped on the nanofibers in the dark at room temperature. After 4 h, the nanofibers were washed with PBS solution in order to remove unbound dye. The conjugation was confirmed with the bright green colour observed under fluorescence microscope. A control

experiment was performed using an amine-containing fluorescent dye under the same conditions and negligible fluorescence was observed (Figure 6.17inset). These results suggest that the conjugation was a result of Diels-Alder reaction between the furan-containing nanofibers and maleimide-containing fluorescent dye.

After establishing that succesful functionalization of nanofibers occur through the Diels-Alder cycloaddition reaction, we focused on functionalization of these nanofibers with biomolecules. First, the feasability of a ligand directed bioconjugation was evaluated by conjugation of biotin onto these nanofibers. The MTC-TEG$_{7.5}$-F/PLA nanofibers were treated with an aqueous solution of a maleimide-bearing biotin and thus biotinylated nanofibers were washed with ample amount of water and then treated with an aqueous solution of TRITC-Extravidin. After incubation for 30 min, the nanofibers were washed with water to remove any unbound enzyme, followed by analysis using fluorescence microscopy. The bright red fluorescence indicated the successful immobilization of TRITC-Extravidin onto the nanofibers (Figure 6.18). As a control experiment, an aqueous solutions of TRITC-Extravidin was dropped on the non-biotinylated MTC-TEG$_{7.5}$-F/PLA nanofibers under the same conditions. Negligible fluorescence observed for these nanofibers suggested that the immobilization was indeed specific and occured through ligand-mediated pathway (Figure 6.18inset).

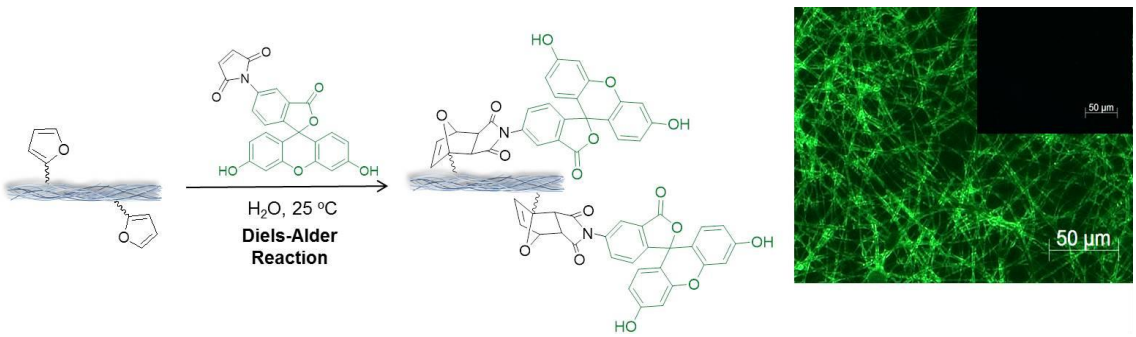

Figure 6.17. Fluorescence microscopy images of MTC-TEG$_{7.5}$-F/PLA nanofibers treated with maleimide-containing fluorescent dye (inset shows fibers after treatment with fluoresceinamine).

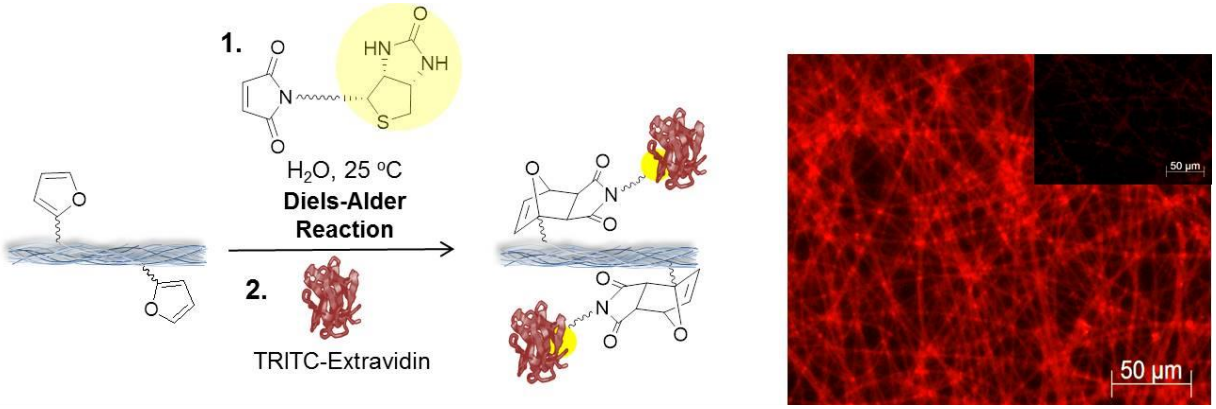

Figure 6.18. Ligand-directed TRITC-Extravidin immobilization on MTC-$TEG_{7.5}$-F/PLA nanofibers and fluorescence microscopy images (Control experiment on nonbiotinylated nanofibers is shown as inset).

The furan-containing polyester fibers with and without the hydrophilic TEG groups were evaluated for their biodegradability in PBS (1×) solution. It can be expected that the difference in their hydrophilicity will play a role in the extent of their degradation. After immersion in PBS for 20 days, the samples were analyzed with SEM (Figure 6.19). While the nanofibers devoid of any TEG units seemed to retain most of their structure, the nanofibers contaning TEG fragments appeared to lose their intact fibrous structure. This difference in stability suggests that attachment of hydrophilic TEG groups promotes their biodegradability. Due to presence of biodegradable ester and carbonate linkages throughout their backbone, both of these nanofibers can be expected to undergo degradation with time, albeit at different rates.

Appropriately functionalized electrospun fibers can act as suitable substrate for cell adhesion and proliferation. To evaluate this aspect, L929 mouse fibroblasts were seeded on nonfunctionalized and RGD-functionalized MTC-$TEG_{7.5}$-F/PLA nanofibers. The cell adhesion promoting peptide fragment cRGDfK was conjugated to the MTC-$TEG_{7.5}$-F/PLA nanofibers via Diels-Alder reaction of cRGDfK(Mal). The fibers were incubated with an aqueous solution (1 mg/mL) of the maleimide bearing peptide for 4 h at room temperature. After rinsing with copious amount of water to remove any unbound peptide, the peptide amount conjugated onto the nanofiber was quantified as 8.84 µg/mg using the BCA assay (Figure 6.20).

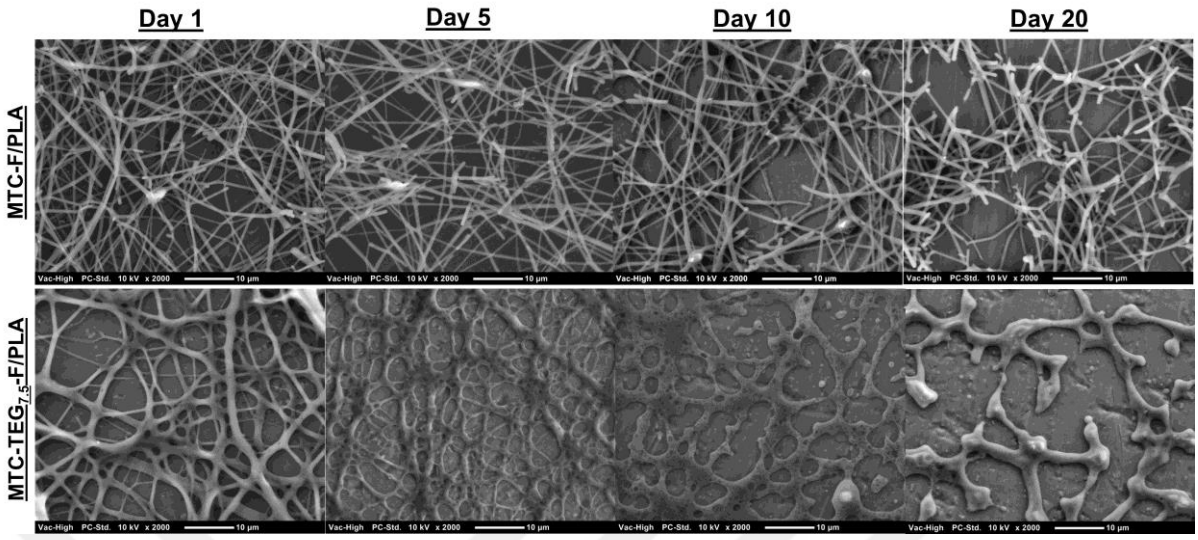

Figure 6.19. SEM micrographs indicating change in morphology of nanofibers with and without TEG units after immersion in PBS at 37 °C for 20 days.

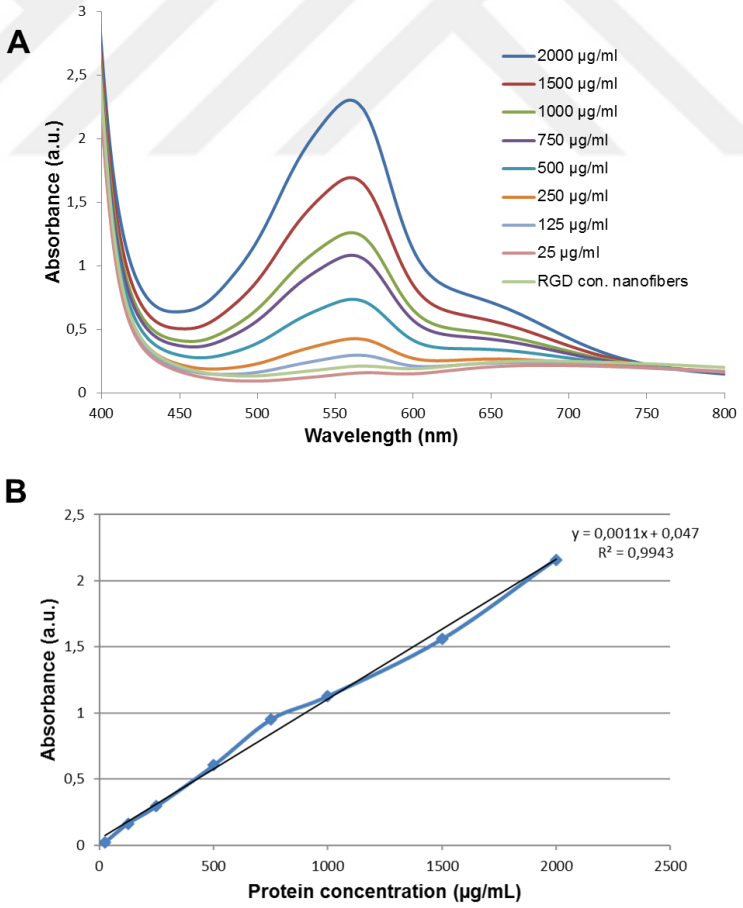

Figure 6.20. (a) UV-vis spectra of BCA assay standards and cRGD conjugated MTC-$TEG_{7.5}$-F/PLA nanofibers (b) BCA assay calibration curve.

Each nanofiber coated surface was used as substrate for cells cultured for 3 days, and cell adhered surfaces were analyzed with confocal microscopy. The cells were fixed and stained with Alexa Fluor 488® phalloidin solution (green) in PBS (1×) to investigate their morphology and the patterns of filamentous actin (F-actin) on the 1st and 3rd day with DAPI (blue) staining. It was observed that the spherical shapes of the fibroblast cells tend to transform into spindle-like in all cases, indicating stronger binding on to the nanofiber coated platforms (Figure 6.21a). Non-functionalized nanofibers showed shorter F-actin bundles while the peptide-functionalized fibers showed cells with stretched morphology and longer F-actin fibers. It can be deduced that the functionalization of nanofibers with the cell adhesive peptide fragment enhanced the cell spreading and proliferation as expected. The cytotoxicity experiments indicated that both non-functionalized and RGD-functionalized nanofibers were not cytotoxic even at high polymer concentrations (Figure 6.21b). The cells seeded remained highly viable even at high concentration up to 1 mg/mL as indicated by almost unaffected cell viability levels. Furthermore, seeded fibroblast displayed spreading and proliferation on nanofiber surfaces over the course of 3 days which also suggested that the polymeric fibers were not only biocompatible but also provided a highly cyto-compatible environment.

Biodegradable nanofibers fabricated using copolymers containing pendant furan groups and anti-biofouling polyether groups undergo facile functionalization with maleimide-containing small molecules and ligands through the Diels-Alder cycloaddition reaction at ambient temperature in aqueous media without the need of any additional catalyst. Conjugation of ligands onto nanofiber surface enables immobilization of proteins in an efficient manner. The immobilization of protein occurs in a specific manner because of the anti-biofouling characteristics of these materials due to the presence of ethylene glycol based side chains. These non-toxic biodegradable nanofibers can be easily modified with appropriately functionalized cell adhesive peptides to promote cellular attachment and proliferation. Overall, the facile synthesis of these reactive yet anti-biofouling biodegradable nanofibers, coupled with their efficient functionalization in a benign manner to render them suitable for biomolecular immobilization, as well as cell proliferation, make them attractive substrates for a variety of biomedical applications.

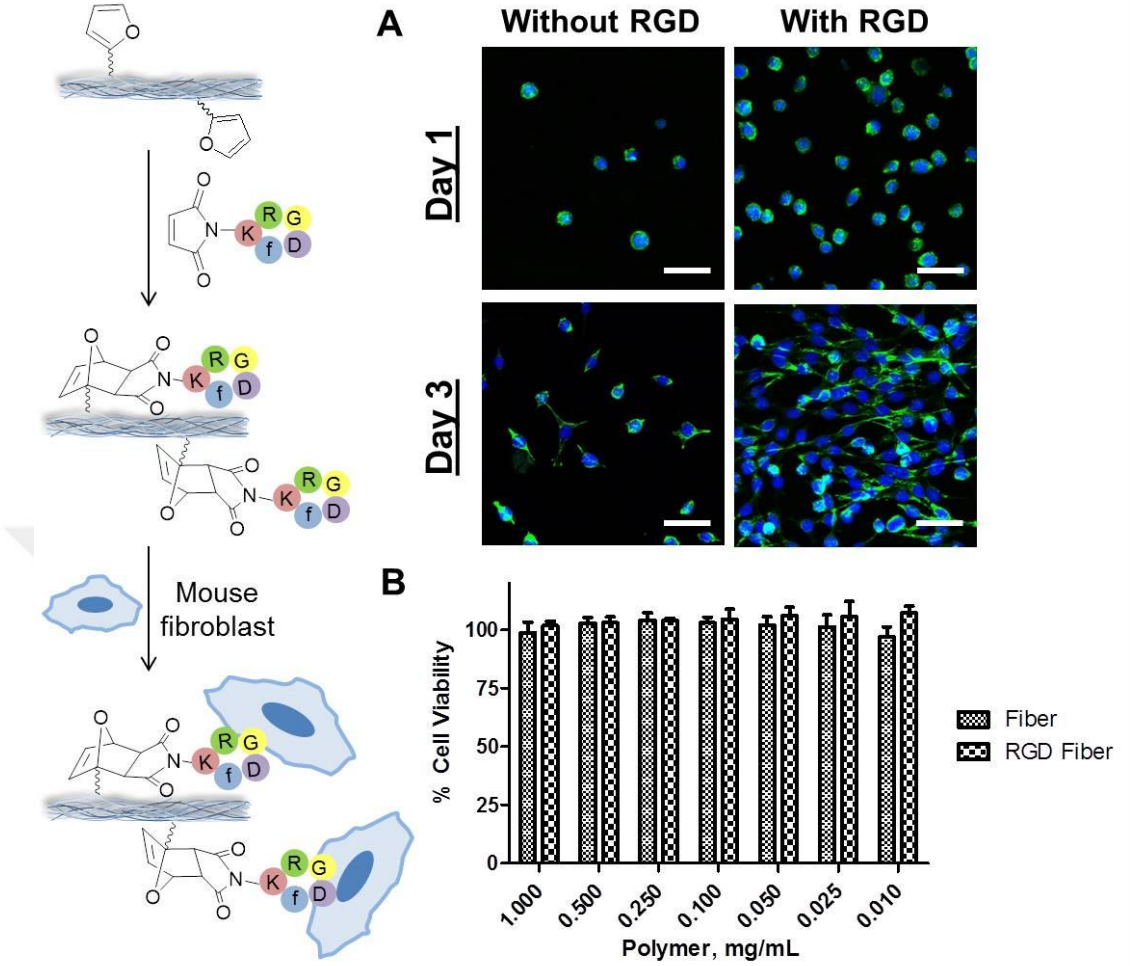

Figure 6.21. (a) Confocal microscopy images of scaffolds showing L929 mouse fibroblasts after 1 and 3 days on (scalebar 50 μm); (b) Cytotoxicity of, non-functionalized and RGD-functionalized nanofibers.

7. MODIFICATION OF DUAL FUNCTIONAL BIODEGRADABLE POLYLACTIDE NANOFIBERS

7.1. Introduction

Nanofiber technology has also become an appealing area in the last decade as they are promising materials to overcome the deficiencies in biomedical field with their unique properties among other nanomaterials. Nanofibers possess high surface area and porosity allowing the enhanced adhesion of bioactive agents, cells, etc. They physically resemble to the fibrillar structure of extracellular matrix (ECM) encouraging cellular organization, survival and function. Besides the flexibility in the composition of nanofibers which can be designed using a wide range of polymers, fiber morphology can also be controlled according to the desired properties. However, these nanofibers still need the attachment of various bioactive molecules in order to improve their properties such as biocompatibility, cell-adhesivity and stimuli-responsivity. The lack of reactive sites on the fiber surface causes to be directed towards multi-step, insufficient and harsh procedures such as plasma treatment, wet chemical methods or physical adsorption [87,88,208]. Degradable polymers need a conjugation method with a solvent compatible with their solubility parameters, which cause a limitation in the conjugation chemistry. Recently, click chemistry has emerged as a fascinating biofunctionalization method due to its high efficiency, orthogonality, and mild reaction conditions. Cu(I) catalyzed Huisgen 1,3-dipolar azide-alkyne cycloaddition which has gained great attention previously, is now being depreciated because of the toxic metal impurities. On the other hand, metal-free click reactions such as thiol−ene reaction, strain promoted azide−alkyne cycloaddition (SPAAC) and Diels−Alder addition are gaining recognition increasingly for the surface modification of nanofibers. SPAAC has been used extensively for hydrogel fabrication, as a labeling method for biological systems, nanofiber, surface, and polymer functionalization due to its efficiency and bio-orthoganality since its development by Bertozzi's and Boons' groups. In a recent work by Becker and coworkers, chain-end reactive PLA nanofibers were prepared using 4-dibenzyocyclooctynol as the initiator for the ring opening polymerization of L-lactide, which were post-functionalized with N_3-GYIGSR peptide via strain-promoted azide-alkyne cycloaddition (SPAAC) [100]. The same group also studied multifunctionality of

nanofibers by sequentially functionalizing the poly(ε-caprolactone) nanofibers with Gly-Arg-Gly-Asp-Ser (GRGDS), BMP-2 peptide, and dopamine via SPAAC, oxime ligation and CuAAC, respectively [97].

Reactive degradable polymers have become frequently used materials in biomedical applications as their multivalent nature improves the efficacy by the multiple attachment of biomolecules such as drugs, proteins, enzymes, growth factors, etc. In recent years, environmentally friendly thermoplastics and biomaterials have gained increasing attraction [35,209]. Aliphatic polyesters such as poly(glycolide) (PGA), poly(lactide) (PLA), and poly(-caprolactone) (PCL), are among the polymeric materials used in biomedical applications as a result of their biocompatibility and biodegradability properties [197][198] PLA has received particular interest as its raw material, L-lactic acid, can be obtained through the fermentation of renewable resources such as corn and sugars [210]. Besides these advantages, PLA also possesses good mechanical properties. Consequently, PLA is widely used for biomedical applications such as drug delivery, absorbable sutures, medical implants, scaffolds for tissue engineering, etc. [211,212]. PLA can be obtained via the ring-opening polymerization (ROP) of lactide initiated by an alcohol in the presence of a catalyst, preferably metal-free organocatalyst which also supports the green chemistry. Copolymers composing of both PEG and aliphatic polyester constituents have become particularly attractive for biomedical applications because PEGylation enhances the biocompatibility, hydrophilicity and anti-biofouling property of the materials [213].

In this study, a chain-end functional polylactide was synthesized via organo-catalyzed ring opening polymerization using a furan-protected maleimide alcohol as an initiator. Then the furan protection was removed in order to obtain maleimide end functional polymer. Thirdly, the end hydroxyl group of the furan protected-maleimide end group-containing polylactide was converted to azide group in order to provide dual-functionality. These polymers were electrospun into nanofibers. The dual-functionality was examined using DIBO and tetrazine-containing fluorescent dyes via SPAAC and iedDA reactions. Then, the dual functional PLA nanofibers were PEGylated using the strain-promoted alkene containing end and a tetrazine-containing PEG via iedDA reaction. The azide end was functionalized with a DIBO-containing biotin through SPAAC reaction, followed by FITC-labeled streptavidin and CY5-labeled biotin immobilization. The

novelty in this dual-functional study comes from its anti-biofouling nature as a result of the PEGylation and reagent-free functionalization.

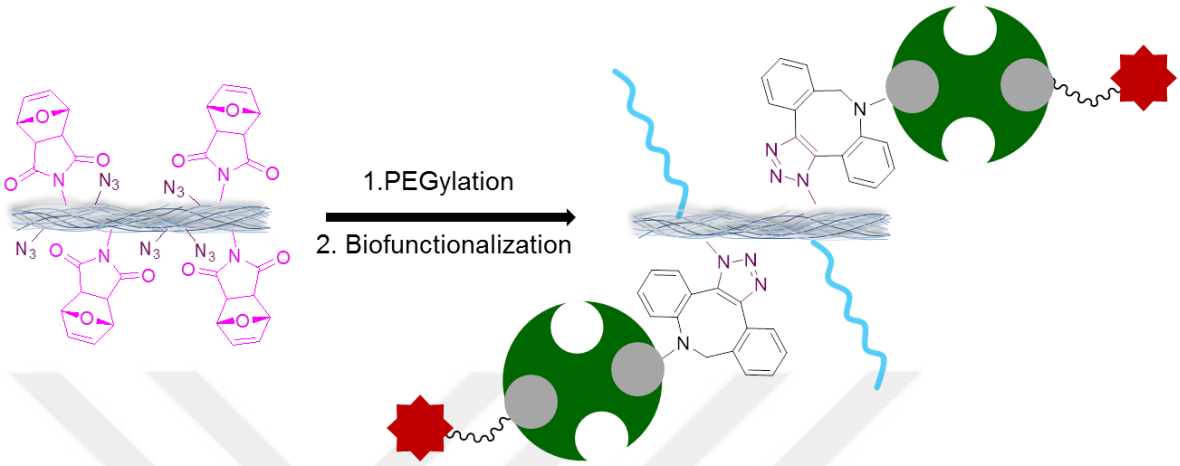

Figure 7.1. Schematic illustration of dual functionalization of nanofibers.

7.2. Experimental

7.2.1. Materials

L-Lactide (Aldrich) was recrystallized from toluene twice, dried in vacuo at room temperature for 24 h and stored in glovebox. 1,8-Diazabicyclo[5.4.0]undec-7-ene (DBU; Fluka) was dried over activated 4 Å molecular sieves and stored in a nitrogen filled glovebox. Furan-protected maleimide-containing alcohol was synthesized according to the literature procedure [142]. Polymerizations were done using dry dichloromethane (DCM) from dry solvent system in glovebox. Toluene (VWR chemicals), 4-(Dimethylamino)pyridine (DMAP; Aldrich) and 1-(3-Dimethylaminopropyl)-3-ethylcarbodiimide hydrochloride (EDCI; Alfa Aesar) were used as received. 5-((2-(and-3)-S-(acetylmercapto) succinoyl)amino) fluorescein (SAMSA fluorescein; Invitrogen) was activated according to the literature procedure prior to use. Cy5-tetrazine, DBCO-PEG4-carboxyrhodamine 110, tetrazine-mPEG (5 kDa), DBCO-PEG4-biotin and Cy5-biotin were purchased from Click Chemistry Tools. FITC-streptavidin was purchased from Thermo Fisher Scientific.

7.2.2. Instruments

^{1}H-NMR spectra of the polymers were recorded on a Bruker 400 MHz spectrometer using trimethylsilane as an internal reference and deuterated chloroform as a solvent. The molecular weights of the copolymers were estimated by gel permeation chromatography (GPC) using a Shimadzu PSS-SDV (length/ID 8 × 300 mm, 10 μm particle size) mixed-C column calibrated with polystyrene standards (1–150 kDa) using a refractive-index detector. Tetrahydrofuran (THF) was used as the eluent at a flow rate of 1 mLmin^{-1} at 30 °C. The morphology of electrospun nanofibers was observed with Jeol Neoscope JCM-5000 scanning electron microscope (SEM). Fluorescence images of samples were recorded at room temperature on a Zeiss Observer Z1 fluorescence microscope. UV light (365 nm) was used for thiol-ene reactions. Static water contact angle were measured in air via the sessile-drop method using a goniometer (CAM 101 KSV instruments). Approximately 5 μL of deionized water was deposited on the surface and images were taken by an integrated digital camera. The software CAM2008 was used for image processing to determine the contact angle. Contact angle value for each sample was independently measured at three different locations and average values were measured.

7.2.3. Synthesis of Alkene-Ended PLA (A-PLA) Polymers

L-lactide (400 mg, 2.78 mmol), furan protected maleimide-containing alcohol (4.1 mg, 0.018 mmol) and TU (34.08 mg, 0.092 mmol) were placed in a vial under nitrogen atmosphere in a glove box and dissolved in anhydrous dichloromethane (3 mL). DBU (13.68 μl, 0.092 mmol) was added under rapid stirring and the reaction proceeded for 20 h at room temperature. The resulting polymer was purified by precipitation in 1:1 methanol:ether. The polymer was dried in vacuo for 24 h at room temperature ($[M]_0/[I]_0$ = 150, $M_{n,SEC}$ = 14.7 kg/mol, M_w/M_n = 1.31, conversion 70 %). ^{1}H-NMR (400 MHz, $CDCl_3$,δ): 6.49 (s, 2H, C*H*=C*H*), 5.28 (s, 2H, C*H* bridgehead protons), 5.13 (q, 1H, C*H* protons of lactide), 4.34 (q, 1H, C*H*OH), 4.07 (t, 2H, –OCH_2), 3.53 (t, 2H,–NCH_2), 2.81 (s, 2H, bridge protons), 1.91 (m, 2H, –NCH$_2$CH_2CH$_2$O), 1.55 (s, 3H, CH_3 protons of lactide).

7.2.4. Synthesis of Maleimide-Ended PLA (M-PLA) Polymers

Furan protection of A-PLA was removed by refluxing at 100 °C in toluene via retro Diels-Alder reaction. After 20 h, toluene was evaporated under reduced pressure and the resulting polymer was dried in vacuo at room temperature. ^{1}H-NMR analysis proved the deprotection of the maleimide group was achieved. ^{1}H-NMR (400 MHz, $CDCl_3$,δ): 6.68 (s, 2H, C*H*=C*H*), 5.13 (q, 1H, C*H* protons of lactide), 4.34 (q, 1H, C*H*OH), 4.07 (t, 2H, –OCH_2), 3.53 (t, 2H,–NCH_2), 1.91 (m, 2H, –NCH_2CH_2CH_2O), 1.55 (s, 3H, CH_3 protons of lactide).

7.2.5. Synthesis of Alkene-PLA-Azide (A-PLA-N_3) Bifunctional Polymers

A-PLA (20 mg, 1.4x10^{-3} mmol), 4-azidobutanoicacid (0.546 mg, 4.2x10^{-3} mmol), DMAP (0.171 mg, 1.4x10^{-3} mmol) and EDCI (0.268 mg, 1.4x10^{-3} mmol) were placed in a 10 mL round bottom flask with a stir bar at room temperature using DCM as the solvent. After 16 h, the solution was extracted with water, saturated aqueous sodium bicarbonate, 0.1 M HCl and again with water. The organic solution was dried with Na_2SO_4 and concentrated using *vacuo.* ^{1}H-NMR (400 MHz, $CDCl_3$,δ): 6.49 (s, 2H, C*H*=C*H*), 5.28 (s, 2H, C*H* bridgehead protons), 5.13 (q, 1H, C*H* protons of lactide), 4.34 (q, 1H, C*H*OH), 4.07 (t, 2H, –OCH_2), 3.53 (t, 2H,–NCH_2), 3.32 (t, 2H, –COOCH_2–), 2.46 (t, 2H, –CH_2N_3) 2.81 (s, 2H, bridge protons), 1.91 (m, 4H, –NCH_2CH_2CH_2O and –OCH_2CH_2CH_2N_3), 1.55 (s, 3H, CH_3 protons of lactide). This compound needs to be further purified to obtain better quality analytical data. Removal of any free azide was ensured by thorough precipitation. At this point, for electrospinning, the polymer obtained here was utilized.

7.2.6. Electrospinning of PLA Polymers

Polymer solutions were prepared in chloroform (1 g/1.2 mL). The solution was delivered at a constant flow rate to a needle connected to a high-voltage power supply. For a typical experiment, the tip to collector distance was 12 cm, the applied voltage was 14 kV and the flow rate was 0.01 mL min^{-1}. Fibers were collected on 22 x 22 mm glass slides attached on a grounded aluminum collector.

7.2.7. Fluorescent Dye Conjugation on A-PLA Nanofibers via Thiol-ene Reaction

SAMSA was activated according to the literature procedure prior to use [214]. 5 µl of the activated SAMSA solution (1 mg/120 µL) in distilled water was dropped on A-PLA nanofiber containing glass slide using 2-hydroxy-4′-(2-hydroxyethoxy)-2-methylpropiophenone (1.1 µL, 1.4 mg/1.1 mL) as the photoinitiator and exposed to UV light (365 nm) for 5 min. The slides were washed with ample water to remove the unbound dye. The conjugation was controlled with fluorescence microscopy.

7.2.8. Fluorescent Dye Conjugation on M-PLA Nanofibers via Michael Reaction

5 µl of the activated SAMSA solution (1 mg/120 µL) in distilled water was dropped on M-PLA nanofiber containing glass slide. The reaction proceeded for 6 h at room temperature in the dark. After, the slide was washed with ample amount of water to remove the excess dye. The conjugation was controlled with fluorescence microscopy.

7.2.9. Dual Fluorescent Dye Conjugation on A-PLA-N_3 Nanofibers

Cy5-tetrazine solution (10 µL, 1 mg/mL) in distilled water was dropped on A-PLA-N_3 nanofiber containing glass slide. After 6 h at room temperature in the dark, the glass slide was washed with water to remove any unbound dye. Then, the aqueous of DBCO-PEG4-carboxyrhodamine 110 (10 µL, 1 mg/mL) was dropped on the Cy5-tetrazine immobilized nanofibers. The reaction was carried out for 6 h in the dark at room temperature. The slide was washed with ample amount of water to remove the excess dye and dried under nitrogen stream. The conjugations were analyzed using the fluorescence microscopy.

7.2.10. PEGylation and Enzyme Immobilization on A-PLA-N_3 Nanofibers

At first, A-PLA-N_3 nanofibers were PEGylated using an aqueous solution of tetrazine-mPEG (5 kDa). 10 µl of tetrazine-mPEG solution (1 mg/mL) was dropped on the A-PLA-N_3 nanofiber containing glass. After 6 h, the slide was washed with water and dried under nitrogen stream. Then, the fibers were biotinylated by applying aqueous

DBCO-PEG4-biotin solution (20 μL, 1 mg/mL) on the nanofibers for 6 h at room temperature. The surface was washed with ample water to remove excess biotin and dried under nitrogen stream. Aqueous of FITC-streptavidin solution (10 μl, 0.1 mg/mL) was dropped on the biotinylated nanofibers at room temperature in the dark. Excess streptavidin was washed with water after 30 min and the surface was dried using nitrogen. Lastly, aqueous Cy5-biotin solution (10 μL, 0.1 mg/mL) was dropped on the streptavidin-immobilized nanofibers at room temperature. After 30 min in the dark, the fibers were washed with ample amount of water and dried under nitrogen stream. The conjugations were analyzed using fluorescence microscopy.

7.3. Results and Discussions

7.3.1. Synthesis of (Dual)Functional PLA Polymers

A-PLA polymers were synthesized using furan-protected maleimide-containing alcohol as the initiator and DBU/TU as the catalyst system via ring-opening polymerization in order to provide good control over molecular weights and polydispersities (Figure 7.1). Polymerizations were carried out in DCM at room-temperature under nitrogen atmosphere in a glove box. The functional group was converted to maleimide (M-PLA) by removing the furan protection through retro Diels-Alder reaction at 110 °C. In order to obtain bifunctional PLA nanofibers, the end hydroxyl group of A-PLA was converted to azide group (A-PLA-N_3) using 4-azidobutanoicacid in the presence of EDCI and DMAP. Structures were confirmed by ^{1}H-NMR spectroscopy (Figure 7.3-7.5). FT-IR spectra of A-PLA and A-PLA-N_3 also showed that –OH peak disappeared and –N_3 appeared upon azide conjugation to A-PLA (Figure 7.6).

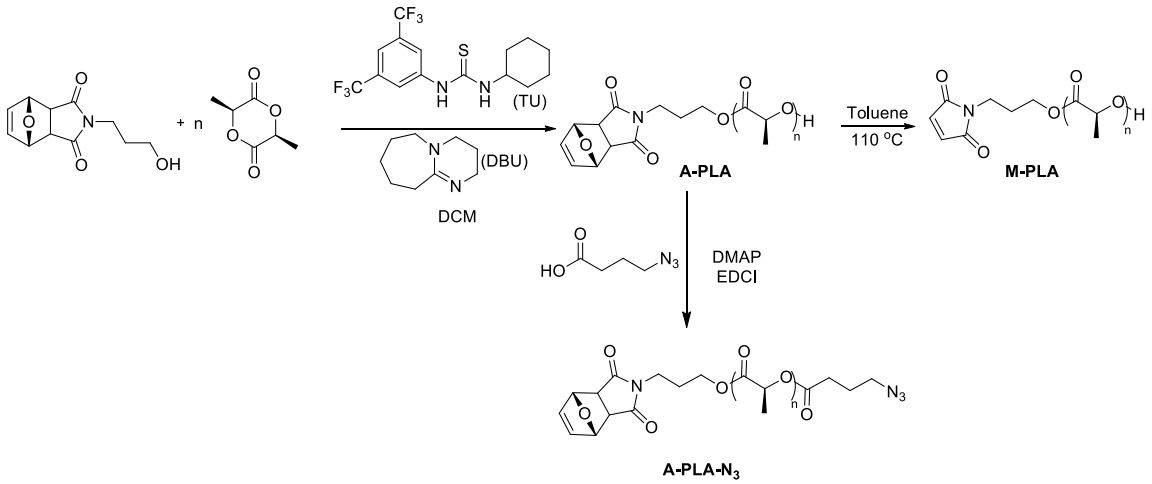

Figure 7.2. Synthesis of PLA polymers.

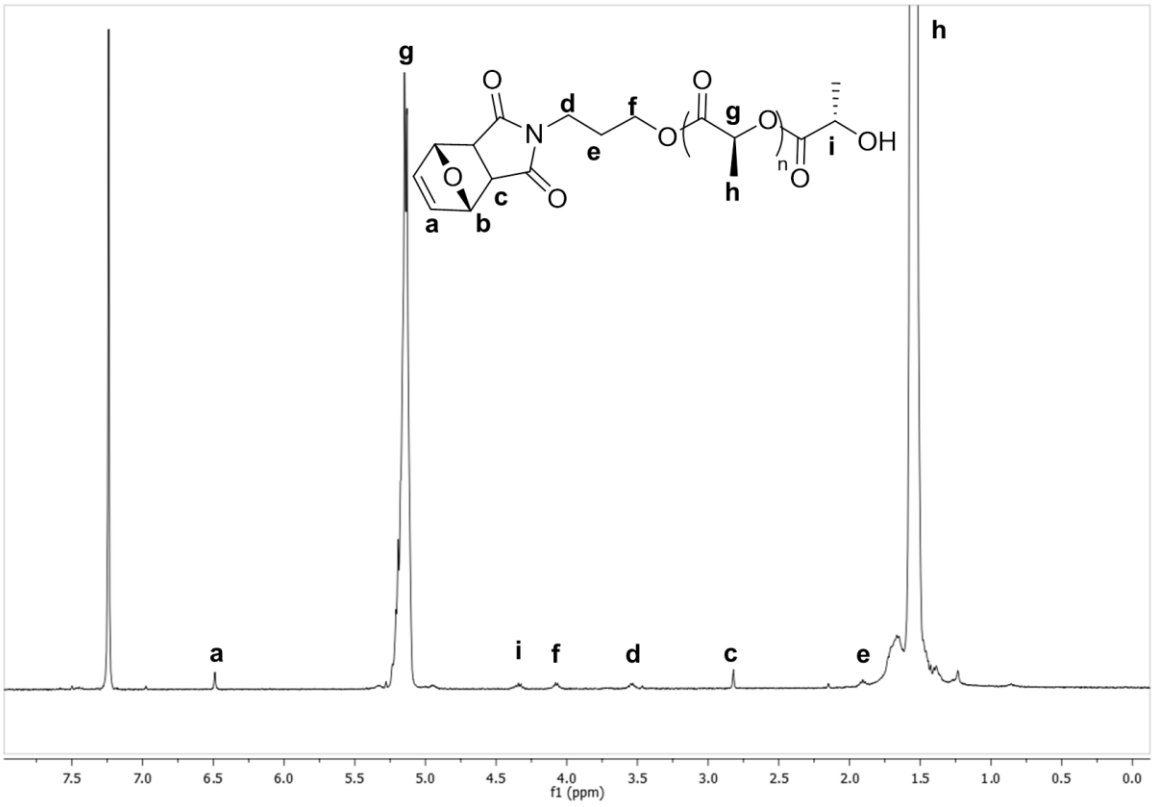

Figure 7.3. ^{1}H-NMR spectrum of A-PLA.

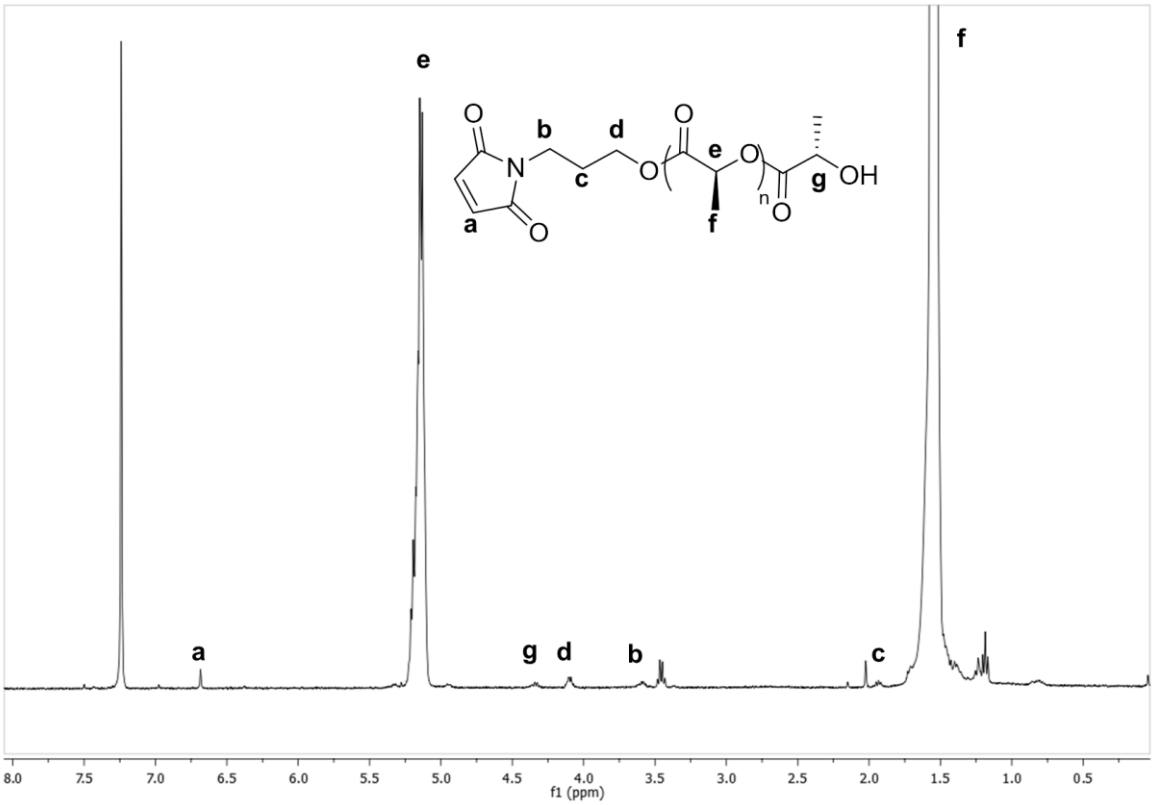

Figure 7.4. ^{1}H-NMR spectrum of M-PLA.

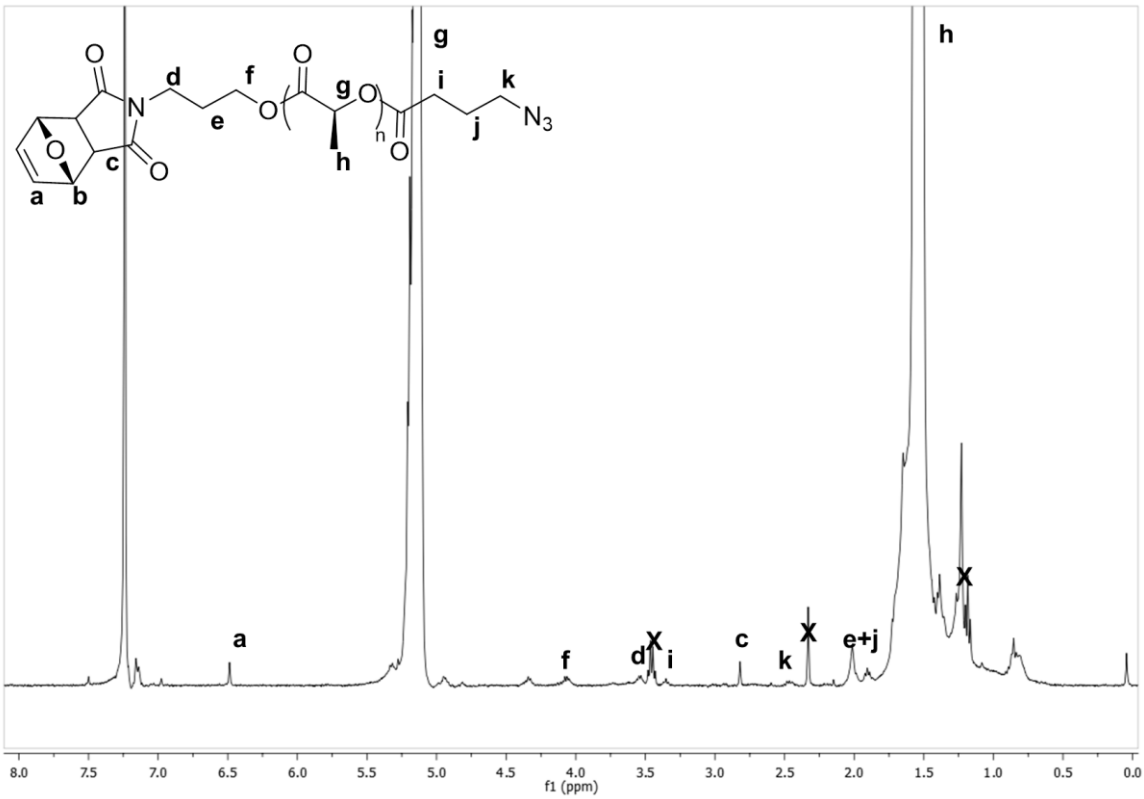

Figure 7.5. ^{1}H-NMR spectrum of A-PLA-N_3 ('X' denotes residual solvent peaks).

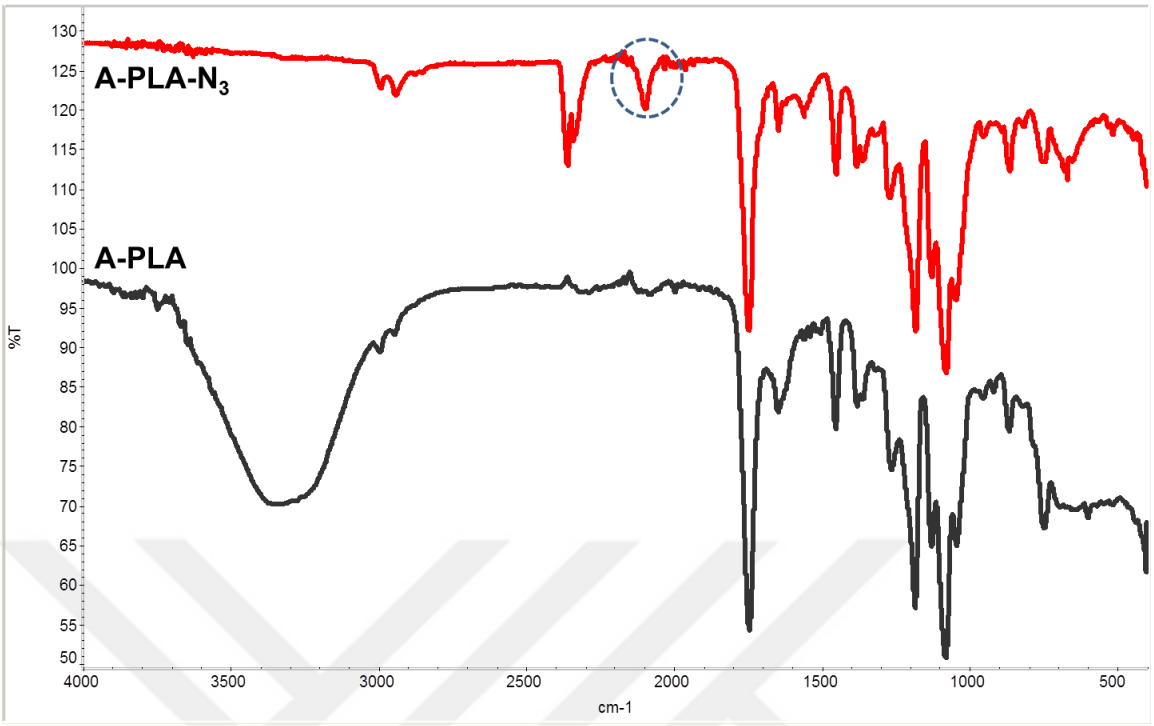

Figure 7.6. FT-IR spectra of A-PLA and A-PLA-N_3.

7.3.2. Fabrication of (Dual)Functional Nanofibers

Nanofibers from PLA based polymers were obtained using solution electrospinning method, from 35 wt % solutions in chloroform. SEM image of the obtained A-PLA nanofiber indicated the formation of uniform nanofibers (Figure 7.7). A-PLA nanofibers has an average diameter of 276 nm ± 112 nm, M-PLA nanofibers had an average diameter of 277 nm ± 131 nm and A-PLA-N_3 nanofibers had an average diameter of 297 nm ± 128 nm. It can be said that three of the polymers gave stable nanofibers with similar average diameters. A-PLA nanofibers were functionalized with thiol-ene reaction, M-PLA nanofibers were functionalized with Michael reaction and A-PLA-N_3 nanofibers were functionalized through iedDA and SPAAC reactions.

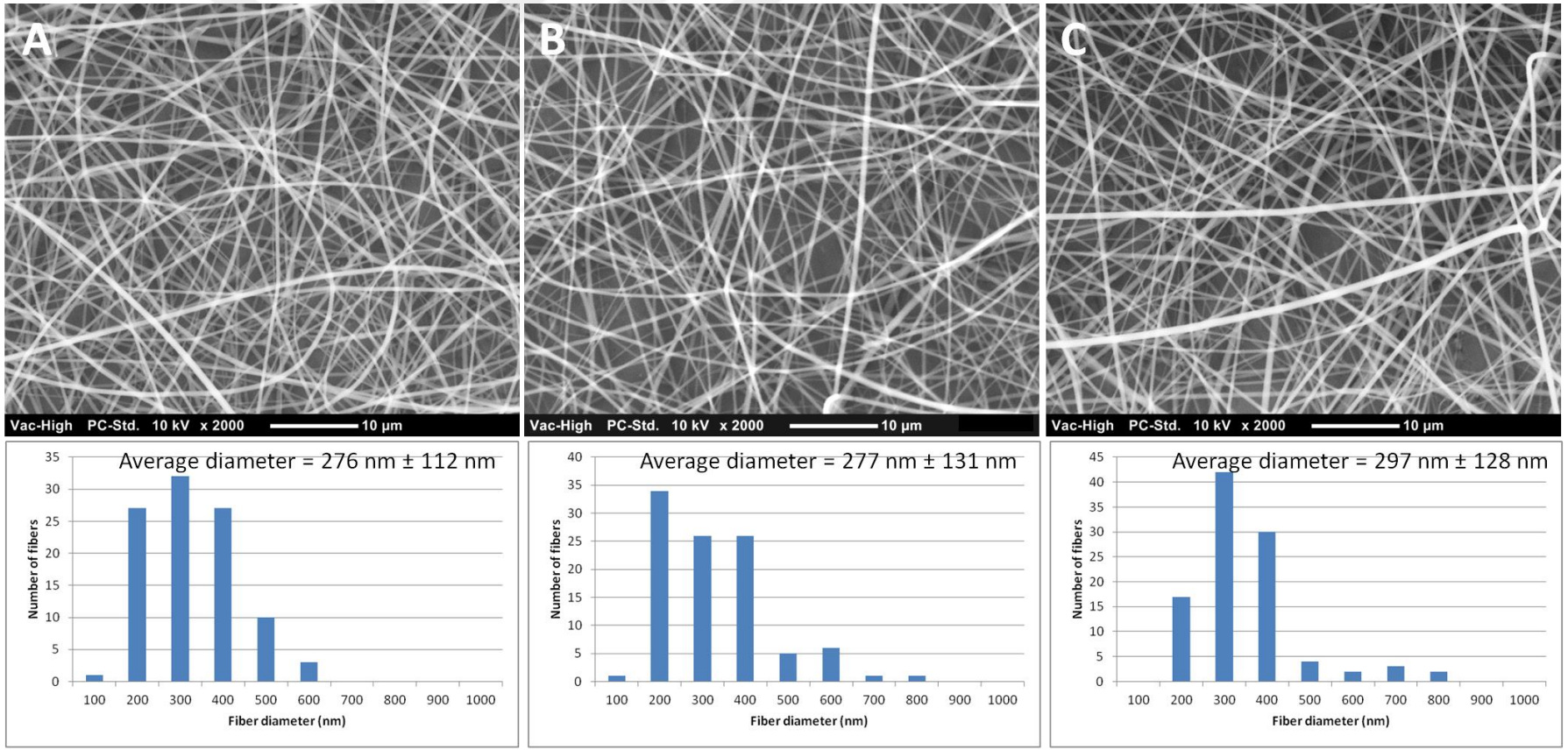

Figure 7.7. SEM images of (a) A- PLA (b) M-PLA (c) A-PLA-N_3 nanofibers.

7.3.3. Fluorescent Dye Immobilization on (Dual)Functional Nanofibers

Initial functionalization of A-PLA nanofibers was examined by immobilization of a thiol-containing fluorescent dye, SAMSA via thiol-ene reaction. An aqueous solution containing SAMSA and 2-hydroxy-4′-(2-hydroxyethoxy)-2-methylpropiophenone as the photoinitiator was dropped on the glass slide covered with A-PLA nanofibers which was then placed under UV (365 nm) irradiation for 5 min. The surface was washed with excess water to remove the excess dye and dried under nitrogen stream. Using fluorescence microscopy, it was clearly showed that the thiol-containing fluorescence probe reacted with the alkene groups on the surface of nanofibers (Figure 7.8a). Control experiment was carried out with a similar procedure, only with the lack of UV light in order to prove the conjugation was as a result of thiol-ene reaction. The feasibility of Michael reaction on the functional nanofibers were examined by the maleimide-group on M-PLA nanofibers after retro Diels-Alder reaction. The thiol-containing fluorescent dye, SAMSA was immobilized on the M-PLA nanofiber containing glass slide in the dark for 6 h. The unbound dye was washed with ample water and the slide was dried under nitrogen. According to fluorescence microscopy, the green color present on the functionalized nanofibers indicated the success of the Michael reaction. As the control experiment, SAMSA was also applied on A-PLA nanofibers under the same conditions.

The bifunctional nanofibers were prepared by converting the terminal hydroxyl group of A-PLA to azide via esterification using 4-azidobutanoicacid in the presence of EDCI and DMAP, which was followed by the electrospinning of the 35 wt % $CHCl_3$ solution of the resulting A-PLA-N_3. An aqueous solution of a tetrazine-appended fluorescent dye, Cy5-tetrazine, was immobilized on the alkene chain-end functionality of A-PLA-N_3 nanofibers via a type of iedDA reaction, strain-promoted alkene-tetrazine click chemistry (Figure 7.9a). The reaction proceeded at room temperature for 8 h in the dark. Any unbound dye was washed with excess water and the functionalized nanofibers were examined under fluorescence microscopy. The red color confirmed the immobilization was as a result of the chemical reaction. Then, an aqueous solution of a DBCO-appended fluorescent dye was dropped on the Cy5-tetrazine immobilized A-PLA-N_3 nanofibers and the reaction between the azide-end group of the nanofibers and DBCO group was carried out for 8 h at room temperature in the dark. The functionalization was monitored by

fluorescence microscopy and the green color confirmed that the immobilization was via strain-promoted alkyne-azide cycloaddition (SPAAC).

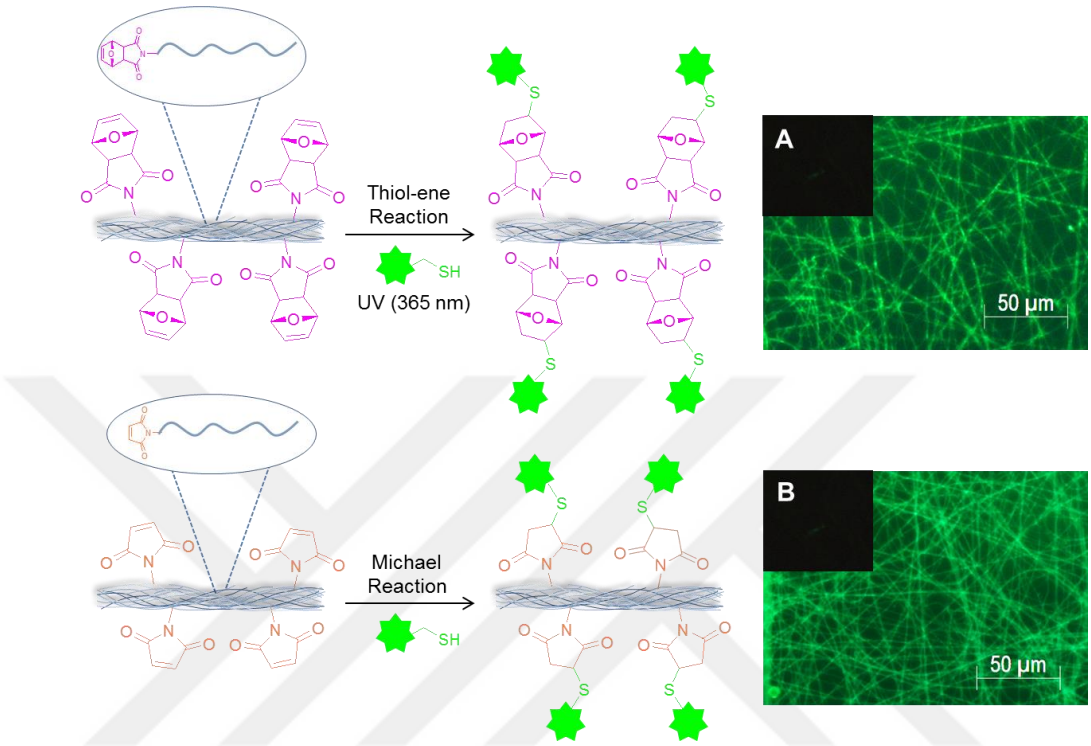

Figure 7.8. Fluorescence microscopy images of SAMSA dye conjugation on (a) A-PLA nanofibers via thiol-ene (b) M-PLA nanofibers via Michael reaction (control experiments are shown as insets).

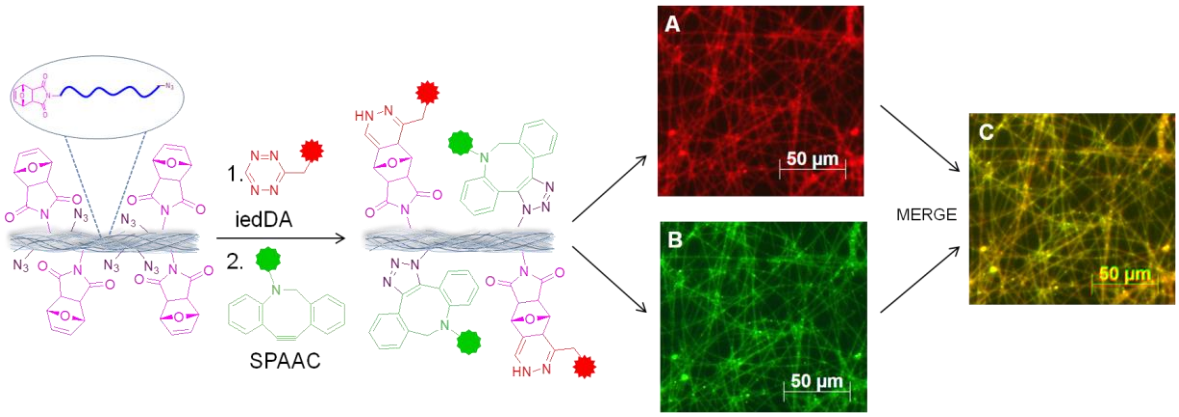

Figure 7.9. Fluorescence microscopy images of (a) Cy5-tetrazine immobilized via iedDA (b) DBCO-appended dye conjugation on Cy5-tetrazine immobilized via SPAAC on A-PLA-N_3 nanofibers (c) Merged image of A and B.

7.3.4. PEGylation and Biomolecule Immobilization on Dual Functional Nanofibers

The anti-biofouling character of A-PLA-N_3 nanofibers were evaluated through controlling if there was non-specific biomolecule immobilization. An aqueous solution of FITC-Streptavidin was dropped on the non-biotinylated A-PLA-N_3 nanofibers, followed by examination under fluorescence microscopy after 30 min. Some green fluorescence showed that there was non-specific binding of FITC-Streptavidin on non-biotinylated nanofibers (Figure 7.10a). Therefore, the A-PLA-N_3 nanofibers were PEGylated in order to increase the anti-biofouling property using tetrazine-mPEG via iedDA reaction. An aqueous tetrazine-mPEG solution was applied on the A-PLA-N_3 nanofibers for 6 h and washed with excess water. Upon drying under nitrogen, the same experiment was performed on the PEGylated and non-biotinylated A-PLA-N_3 nanofibers and it was observed that there was negligible fluorescence showing that PEGylation increased the anti-biofouling property (Figure 7.10b). The contact angle measurements showed that the average contact angle decreased from 120° ± 4.44 to 85° ± 10.17 after PEGylation which also indicated the increased hydrophilicity and anti-biofouling character of A-PLA-N_3 nanofibers (Figure 7.10c, d).

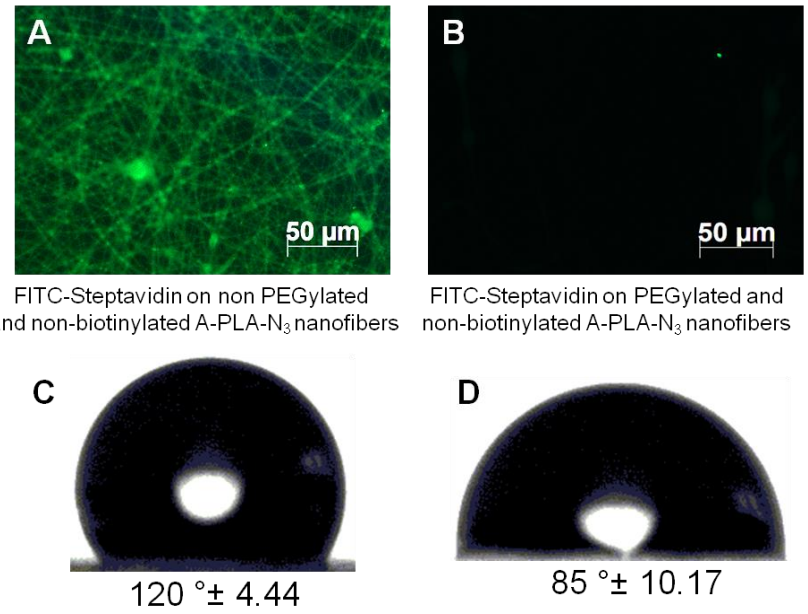

Figure 7.10. Fluorescence microscopy images of FITC-Streptavidin immobilization on non-biotinylated (a) non-PEGylated (b) PEGylated A-PLA-N_3 nanofibers. Water contact angles of (c) non-PEGylated (d) PEGylated A-PLA-N_3 nanofibers.

Then, the PEGylated nanofibers were biotinylated using a DBCO-appended biotin via SPAAC. Biotin-streptavidin pair was chosen as a result of the high biological interaction between biotin and avidin molecules. Streptavidin contains four binding sites for biotin which allows the utilization of the remaining three vacant sites fort he immobilizarion of other biotinylated biomolecules such as peptides and oligonucleotides. An aqueous solution of DBCO-PEG4-biotin was dropped on the PEGylated fibers at room temperature. After 6 h, the fibers were washed with ample water and dried. An aqueous solution of FITC-streptavidin was dropped on the biotinylated nanofibers at room temperature in the dark. After 30 min, the fibers were washed with water in order to remove any nonspecifically bound streptavidin. The green color present under fluorescence microscopy indicated the success of the conjugation (Fig 7.11a). The remaining vacant sites of the streptavidin were used for the immobilization of another biotin molecule, Cy5-biotin. An aqueous solution of Cy5-biotin was dropped on the streptavidin-immobilized nanofibers in the dark at room temperature. 30 min later, the surface was washed with water and dried under nitrogen stream. The nanofibers were examined using fluorescence microscopy and the bright red color confirmed the immobilization of the Cy5-biotin (Figure 7.11b).

To conclude, a polylactide initiated with a furan-protected malemide alcohol was synthesized using organo-catalyzed ring opening polymerization. The end-hydroxy group was converted into an azide group, followed byelectrospinning. The dual functionality was used to conjugate tetrazine and DIBO-containing fluorescent dyes via iedDA and SPAAC reactions. The nanofibers were also gained antibiofouling character via PEGylation using a tetrazine-PEG and a DIBO-containing biotin was conjugated onto the PEGylated via SPAAC. The biotinylated surfaces were immobilized with FITC-Streptavidin and Cy5-Biotin. These are promising materials for biomedical applications such as biosensing and cell scaffolding as they allow biofunctionalization under mild reaction conditions with high efficiency in aqueous media, as well as their anti-biofouling character.

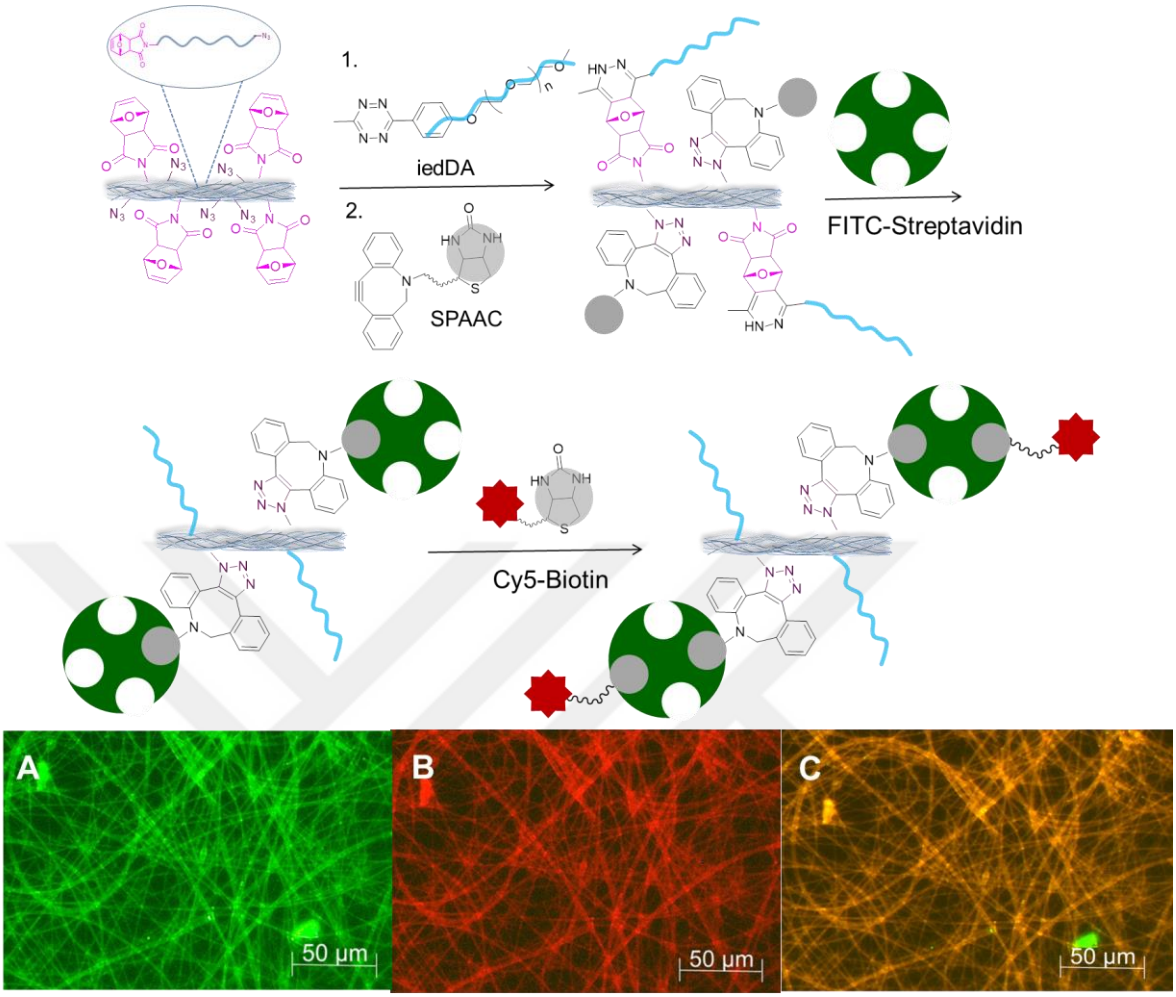

Figure 7.11. Fluorescence microscopy images of (a) FITC-streptavidin immobilization on biotinylated (b) Cy5-Biotin conjugation on FITC-streptavidin immobilized, A-PLA-N_3 nanofibers (c) Merged image of A and B.

8. CONCLUSIONS

This thesis includes the design of clickable polymers with various reactive groups that can be electrospun into reactive nanofibers. These reactive sites on the nanofibers are aimed to be used for the reagent-free (bio)functionalization of nanofibers. Both biodegradable and non-biodegradable polymers with different reactive groups such as furan, maleimide and alkene were synthesized using organo-catalyzed ring-opening polymerization and free radical polymerization. After electrospinning them into reactice nanofibers, efficient conjugations were performed via Diels-Alder, thiol-ene, Michael, SPAAC and iedDiels-Alder reactions.

The first project in this thesis describes the biofunctionalization of furan-containing non-biodegradable nanofibers. Furfuryl methacrylate, PEGMEMA and MMA were copolymerized using free radical polymerization. The copolymer was electrospun into furan-containing non-biodegradable nanofibers. Efficiency of functionalization was obtained by seperate conjugations of a maleimide-containing fluorescent dye and a maleimide-containing biotin molecule via Diels-Alder reaction. Then, FITC-Streptavidin and CdSe Qdots were immobilized on the biotinylated nanofibers.

The second project is related to the biofunctionalization of maleimide-containing non-biodegradable nanofibers. A copolymers was synthesized using a furan-protected maleimide bearing acrylate-based monomer, PEGMEMA and MMA, followed by the Retro Diels-Alder reaction, leaving the reactive maleimide group. The maleimide-bearing copolymer was electrospun into maleimide-containing nanofibers which were photo-crosslink and patterned using a photomask and UV light. The maleimide-containing patterned nanofibers were functionalized with thiol-bearing fluorescent dye, biotin and fluorescently labeled-DNA. TRITC-Extravidin was immobilized on the biotinylated nanofibers. Lastly, a thiol-bearing oligonucleotide was conjugated on the maleimide-containing patterned nanofibers and hybridized with its complementary fluorescently labelled oligonucletiode sequence.

The third project includes the *in situ* crosslinking and functionalization of polyoxazoline-based nanofibers. The alkene-bearing polyoxazoline based polymer was dissolved with a tetrathiol and a photoinitiator and photocrosslinked during elecrospinninh. The remaining alkene moiety on the nanofibers were used fort he immobilization of a thiol-bearing fluorescent dye via thiol-ene reaction. The free thiol groups from the tetrathiol were also used for the immobilization of a maleimide-bearing fluorescent dye via Michael reaction. Patterning was also studied while fluorescent dye immobilization via thiol-ene reaction.

The fourth project involves the biofunctionalization of furan-containing biodegradable nanofibers. Lactide was copolymerized with furan and TEG-containing cyclic carbonate monomers via organo-catalyzed ring opening polymerization. The resuting furan containing-PLA based copolymer was electrospun into furan containing biodegradable nanofibers which were functionalized with maleimide-bearing fluorescent dye and biotin via Diels-Alder reaction. TRITC-Extravidin was immobilized on the biotinylated nanofibers. Lastly, a maleimide-bearing RGD peptide was immobilized on the furan containing biodegradable nanofibers and the nanofibers were used for cell culture.

The last project is also based on the biofunctionalization of biodegradable nanofibers. A furan-protected malemide alcohol was used to initiate the organo-catalyzed ring opening polymerization of lactide followed by electrospinning. The alkene group was used to immobilized a thiol-bearing fluorescent dye via thiol-ene reaction. Then, the furan protection was removed by retro Diels-Alder reaction and the resulting maleimide unit was used for the immobilization of a thiol-bearing fluorescent dye via Michael reaction. Lastly, the chain-end hydroxyl group of the furan-protected malemide alcohol initiated lactide was converted into azide group. The dual functionality was used to conjugate tetrazine and DIBO-containing fluorescent syes via iedDA and SPAAC reactions. Lastly, these nanofibers were PEGylayed using a tetrazine-PEG via iedDA and conjugated to a DIBO-containing biotin via SPAAC. The biotinylated surfaces were immobilized with FITC-Streptavidin and Cy5-Biotin.

In general, this thesis involves the design of clickable group-bearing nanofibers which can be reagent-free (bio)functionalized for various biomedical applications.

REFERENCES

1. Leung, V., and F. Ko, “Biomedical Applications Of Nanofibers.”, *Polymers for Advanced Technologies*, Vol. 22, pp. 350–365, 2011.

2. Xie, J., X. Li, and Y. Xia, “Putting Electrospun Nanofibers To Work For Biomedical Research.”, *Macromolecular Rapid Communications*, Vol. 29, pp. 1775–1792, 2008.

3. Greiner, A., and J.H. Wendorff, “Electrospinning: A Fascinating Method For The Preparation Of Ultrathin Fibers.”, *Angewandte Chemie - International Edition*, Vol. 46, pp. 5670–5703, 2007.

4. Huang, Z.M., Y.Z. Zhang, M. Kotaki, and S. Ramakrishna, “A Review On Polymer Nanofibers By Electrospinning And Their Applications In Nanocomposites.”, *Composites Science and Technology*, Vol. 63, pp. 2223–2253, 2003.

5. Bhardwaj, N., and S.C. Kundu, “Electrospinning: A Fascinating Fiber Fabrication Technique.”, *Biotechnology Advances*, Vol. 28, pp. 325–347, 2010.

6. Persano, L., A. Camposeo, C. Tekmen, and D. Pisignano, “Industrial Upscaling Of Electrospinning And Applications Of Polymer Nanofibers: A Review.”, *Macromolecular Materials and Engineering*, Vol. 298, pp. 504–520, 2013.

7. Ki, C.S., D.H. Baek, K.D. Gang, K.H. Lee, I.C. Um, and Y.H. Park, “Characterization Of Gelatin Nanofiber Prepared From Gelatin-formic Acid Solution.”, *Polymer*, Vol. 46, pp. 5094–5102, 2005.

8. Jun, Z., H. Hou, A. Schaper, J.H. Wendorff, and A. Greiner, “Poly-L-lactide Nanofibers By Electrospinning – Influence Of Solution Viscosity And Electrical Conductivity On Fiber Diameter And Fiber Morphology.”, *e-Polymers*, pp. 1–9, 2003.

9. Darko, G., S. Chigome, S. Lillywhite, Z. Tshentu, J. Darkwa, and N. Torto, “Sorption

Of Toxic Metal Ions In Aqueous Environment Using Electrospun Polystyrene Fibres Incorporating Diazole Ligands.", *Water SA*, Vol. 39, pp. 39–46, 2013.

10. Haghi, A. K., and M. Akbari, "Trends In Electrospinning Of Natural Nanofibers.", *Physica Status Solidi (A) Applications and Materials Science*, Vol. 204, pp. 1830–1834, 2007.

11. Celebioglu, A., and T. Uyar, "Cyclodextrin Nanofibers By Electrospinning.", *Chemical Communications*, Vol. 46, pp. 6903-6905, 2010.

12. Deitzel, J., J. Kleinmeyer, D. Harris, and N. Beck Tan, "The Effect Of Processing Variables On The Morphology Of Electrospun Nanofibers And Textiles.", *Polymer*, Vol. 42, pp. 261–272, 2001.

13. Fong, H., I. Chun, and D.H. Reneker, "Beaded Nanofibers Formed During Electrospinning.", *Polymer*, Vol. 40, pp. 4585–4592, 1999.

14. Park, J.-C., T. Ito, K.-O. Kim, K.-W. Kim, B.-S. Kim, M.-S. Khil, H.-Y. Kim, and I.-S. Kim, "Electrospun Poly(vinyl Alcohol) Nanofibers: Effects Of Degree Of Hydrolysis And Enhanced Water Stability.", *Polymer Journal*, Vol. 42, pp. 273–276, 2010.

15. Pham, Q.P., U. Sharma, and A.G. Mikos, "Electrospinning Of Polymeric Nanofibers For Tissue Engineering Applications: A Review.", *Tissue engineering*, Vol. 12, pp. 1197–1211, 2006.

16. Zuo, W., M. Zhu, W. Yang, H. Yu, Y. Chen, and Y. Zhang, "Experimental Study On Relationship Between Jet Instability And Formation Of Beaded Fibers During Electrospinning.", *Polymer Engineering and Science*, Vol. 45, pp. 704–709, 2005.

17. Lee, J.S., K.H. Choi, H. Do Ghim, S.S. Kim, D.H. Chun, H.Y. Kim, and W.S. Lyoo, "Role Of Molecular Weight Of Atactic Poly(vinyl Alcohol) (PVA) In The Structure And Properties Of PVA Nanofabric Prepared By Electrospinning.", *Journal of Applied Polymer Science*, Vol. 93, pp. 1638–1646, 2004.

18. Li, D., and Y. Xia, “Electrospinning Of Nanofibers: Reinventing The Wheel?”, *Advanced Materials*, Vol. 16, pp. 1151–1170, 2004.

19. Zhang, Z., J. Hu, and P.X. Ma, “Nanofiber-based Delivery Of Bioactive Agents And Stem Cells To Bone Sites.”, *Advanced Drug Delivery Reviews*, Vol. 64, pp. 1129–1141, 2012.

20. Mazoochi, T., M. Hamadanian, M. Ahmadi, and V. Jabbari, “Investigation On The Morphological Characteristics Of Nanofiberous Membrane As Electrospun In The Different Processing Parameters.”, *International Journal of Industrial Chemistry*, Vol. 3, pp. 1–8, 2012.

21. De Vrieze, S., T. Van Camp, a. Nelvig, B. Hagström, P. Westbroek, and K. De Clerck, “The Effect Of Temperature And Humidity On Electrospinning.”, *Journal of Materials Science*, Vol. 44, pp. 1357–1362, 2009.

22. Li, Z., and C. Wang, “Effects Of Working Parameters On Electrospinning.”, *One-Dimensional Nanostructures*, pp. 15–29, 2013.

23. Agarwal, S., A. Greimer, and J.H. Wendorff, “Electrospinning Of Manmade And Biopolymer Nanofibers-Progress In Techniques, Materials, And Applications.”, *Advanced Functional Materials*, Vol. 19, pp. 2863–2879, 2009.

24. Hu, X., S. Liu, G. Zhou, Y. Huang, Z. Xie, and X. Jing, “Electrospinning Of Polymeric Nanofibers For Drug Delivery Applications.”, *Journal of Controlled Release*, Vol. 185, pp. 12–21, 2014.

25. Chew, S.Y., Y. Wen, Y. Dzenis, and K.W. Leong, “The Role Of Electrospinning In The Emerging Field Of Nanomedicine.”, *Current Pharmaceutical Design*, Vol. 12, pp. 4751–4770, 2006.

26. Abrigo, M., S.L. McArthur, and P. Kingshott, “Electrospun Nanofibers As Dressings For Chronic Wound Care: Advances, Challenges, And Future Prospects.”,

Macromolecular Bioscience, Vol. 14, pp. 772–792, 2014.

27. Xu, H., H. Li, Q. Ke, and J. Chang, "An Anisotropically And Heterogeneously Aligned Patterned Electrospun Scaffold With Tailored Mechanical Property And Improved Bioactivity For Vascular Tissue Engineering.", *ACS Applied Materials & Interfaces*, Vol. 7, pp. 8706–8718, 2015.

28. Bao, M., X. Lou, Q. Zhou, W. Dong, H. Yuan, and Y. Zhang, "Electrospun Biomimetic Fibrous Scaffold From Shape Memory Polymer Of PDLLA-co-TMC For Bone Tissue Engineering.", *ACS Applied Materials & Interfaces*, Vol. 6, pp. 2611–21, 2014.

29. Lim, S.H., and H.Q. Mao, "Electrospun Scaffolds For Stem Cell Engineering.", *Advanced Drug Delivery Reviews*, Vol. 61, pp. 1084–1096, 2009.

30. Dvir, T., B.P. Timko, D.S. Kohane, and R. Langer, "Complex Tissues.", *Nature Publishing Group*, Vol. 6, pp. 13–22, 2010.

31. Lee, C., M. Hsieh, S. Chang, Y. Lin, S. Liu, T. Lin, K. Hung, J.S. Pang, and J. Juang, "Enhancement Of Diabetic Wound Repair Using Biodegradable Nano Fibrous Metformin-Eluting Membranes: In Vitro And In Vivo.", *ACS Applied Materials & Interfaces,*Vol. 6, pp. 10–17, 2014.

32. GhavamiNejad, A., A. Rajan Unnithan, A. Ramachandra Kurup Sasikala, M. Samarikhalaj, R.G. Thomas, Y.Y. Jeong, S. Nasseri, P. Murugesan, D. Wu, C. Hee Park, and C.S. Kim, "Mussel-Inspired Electrospun Nanofibers Functionalized With Size Controlled Silver Nanoparticles For Wound Dressing Application.", *ACS Applied Materials & Interfaces*, Vol. 7, pp.12176–12183, 2015.

33. Li, W., T. Luo, Y. Yang, X. Tan, and L. Liu, "Formation Of Controllable Hydrophilic/Hydrophobic Drug Delivery Systems By Electrospinning Of Vesicles.", *Langmuir*, Vol. 31, pp. 5141–5146, 2015.

34. El-Fiqi, A., J.-H. Kim, and H.-W. Kim, "Osteoinductive Fibrous Scaffolds Of Biopolymer/Mesoporous Bioactive Glass Nanocarriers With Excellent Bioactivity And Long-Term Delivery Of Osteogenic Drug.", *ACS Applied Materials & Interfaces*, Vol. 7, pp. 1140–1152, 2015.

35. He, C., W. Nie, and W. Feng, "Engineering Of Biomimetic Nanofibrous Matrices For Drug Delivery And Tissue Engineering.", *Journal of Materials Chemistry B*, Vol. 2, pp. 7828–7848, 2014.

36. Luo, J., A.S. Meyer, R. V Mateiu, D. Kalyani, and M. Pinelo, "Functionalization Of A Membrane Sublayer Using Reverse Filtration Of Enzymes And Dopamine Coating.", *ACS Applied Materials & Interfaces*, Vol. 6, pp. 22894–22904, 2014.

37. Lian, G., X. Zhang, H. Si, J. Wang, D. Cui, and Q. Wang, "Boron Nitride Ultrathin Fibrous Nanonets: One-step Synthesis And Applications For Ultrafast Adsorption For Water Treatment And Selective Filtration Of Nanoparticles.", *ACS Applied Materials and Interfaces*, Vol. 5, pp. 12773–12778, 2013.

38. Desai, K., K. Kit, J. Li, P. Michael Davidson, S. Zivanovic, and H. Meyer, "Nanofibrous Chitosan Non-wovens For Filtration Applications.", *Polymer*, Vol. 50, pp. 3661–3669, 2009.

39. Wang, X., X. Wang, X. Wang, F. Chen, K. Zhu, Q. Xu, and M. Tang, "Novel Electrochemical Biosensor Based On Functional Composite Nanofibers For Sensitive Detection Of P53 Tumor Suppressor Gene.", *Analytica Chimica Acta*, Vol. 765, pp. 63–69, 2013.

40. Wang, X., G. Shu, C. Gao, Y. Yang, Q. Xu, and M. Tang, "Electrochemical Biosensor Based On Functional Composite Nanofibers For Detection Of K-ras Gene Via Multiple Signal Amplification Strategy.", *Analytical Biochemistry*, Vol. 466, pp. 51–58, 2014.

41. Seong, D.Y., M.S. Choi, and Y.J. Kim, "Fluorescent Chemosensor For The Detection

Of Histamine Based On Dendritic Porphyrin-incorporated Nanofibers.", *European Polymer Journal*, Vol. 48, pp. 1988–1996, 2012.

42. Wang, H., W. Tang, H. Wei, Y. Zhao, S. Hu, Y. Guan, W. Pan, B. Xia, N. Li, and F. Liu, "Integrating Dye-intercalated DNA Dendrimers With Electrospun Nanofibers: A New Fluorescent Sensing Platform For Nucleic Acids, Proteins, And Cells.", *Journal of Materials Chemistry B*, Vol. 3, pp. 3541–3547, 2015.

43. Zhou, C., Y. Shi, X. Ding, M. Li, J. Luo, Z. Lu, and D. Xiao, "Development Of A Fast And Sensitive Glucose Biosensor Using Iridium Complex-doped Electrospun Optical Fibrous Membrane.", *Analytical Chemistry*, Vol. 85, pp. 1171–1176, 2013.

44. Wang, H., D. Wang, Z. Peng, W. Tang, N. Li, and F. Liu, "Assembly Of DNA-functionalized Gold Nanoparticles On Electrospun Nanofibers As A Fluorescent Sensor For Nucleic Acids.", *Chemical Communications*, Vol. 49, pp. 5568–5570, 2013.

45. Zhu, F., Q. Xin, Q. Feng, Y. Zhou, and R. Liu, "Novel Poly(vinylidene Fluoride)/thermoplastic Polyester Elastomer Composite Membrane Prepared By The Electrospinning Of Nanofibers Onto A Dense Membrane Substrate For Protective Textiles.", *Journal of Applied Polymer Science*, Vol. 132, pp.42170–42180, 2015.

46. Homaeigohar, S., and M. Elbahri, "Nanocomposite Electrospun Nanofiber Membranes For Environmental Remediation.", *Materials*, Vol. 7, pp. 1017–1045, 2014.

47. Ma, Z., M. Kotaki, and S. Ramakrishna, "Electrospun Cellulose Nanofiber As Affinity Membrane.", *Journal of Membrane Science*, Vol. 265, pp. 115–123, 2005.

48. Thavasi, V., G. Singh, and S. Ramakrishna, "Electrospun Nanofibers In Energy And Environmental Applications.", *Energy & Environmental Science*, Vol. 1, pp. 205, 2008.

49. Persano, L., A. Camposeo, and D. Pisignano, "Active Polymer Nanofibers For

Photonics, Electronics, Energy Generation And Micromechanics.", *Progress in Polymer Science*, Vol. 43, pp. 48–95, 2014.

50. Chang, J., M. Dommer, C. Chang, and L. Lin, "Piezoelectric Nanofibers For Energy Scavenging Applications.", *Nano Energy*, Vol. 1, pp. 356–371, 2012.

51. Tanaka, M., "Development Of Ion Conductive Nanofibers For Polymer Electrolyte Fuel Cells.", *Polymer Journal*, Vol. 48, pp. 51–58, 2015.

52. Kolb, H.C., M.G. Finn, and K.B. Sharpless, "Click Chemistry: Diverse Chemical Function from a Few Good Reactions", *Angewandte Chemie-International Edition*, Vol. 40, pp. 2004-2021, 2001.

53. Tornøe, C.W., C. Christensen, and M. Meldal, "Peptidotriazoles On Solid Phase: [1,2,3]-Triazoles By Regiospecific Copper(I)-catalyzed 1,3-dipolar Cycloadditions Of Terminal Alkynes To Azides.", *Journal of Organic Chemistry*, Vol. 67, pp. 3057–3064, 2002.

54. Rostovtsev, V. V., L.G. Green, V. V. Fokin, and K.B. Sharpless, "A Stepwise Huisgen Cycloaddition Process: Copper(I)-catalyzed Regioselective 'ligation' of Azides And Terminal Alkynes.", *Angewandte Chemie-International Edition*, Vol. 41, pp. 2596–2599, 2002.

55. Binder, W.H., and R. Sachsenhofer, "'Click' Chemistry In Polymer And Material Science: An Update.", *Macromolecular Rapid Communications*, Vol. 29, pp. 952–981, 2008.

56. Hein, J.E., and V. V Fokin, "Copper-Catalyzed Azide-Alkyne Cycloaddition (CuAAC) And Beyond: New Reactivity Of Copper(I) Acetylides", *Chemical Society Reviews*, Vol. 39, pp. 1302–1315, 2011.

57. Meldal, M., and C.W. Tomøe, "Cu-catalyzed Azide-Alkyne Cycloaddition.", *Chemical Reviews*, Vol. 108, pp. 2952–3015, 2008.

58. Becer, C.R, R. Hoogenboom, and U.S. Schubert, “Click Chemistry Beyond Metal-catalyzed Cycloaddition.”, *Angewandte Chemie-International Edition*, Vol. 48, pp. 4900–4908, 2009.

59. Worrell, B.T., J. A. Malik, and V. V. Fokin, “Direct Evidence Of A Dinuclear Copper Intermediate in Cu(I)-Catalyzed Azide-Alkyne Cycloadditions.”, *Science*, Vol. 340, pp. 457–460, 2013.

60. Parrish, B., R.B. Breitenkamp, and T. Emrick, “PEG- And Peptide-Grafted Aliphatic Polyesters By Click Chemistry PEG- And Peptide-Grafted Aliphatic Polyesters By Click Chemistry.”, *Biomaterials*, Vol. 127, pp. 7404–7410, 2005.

61. Parrish, B., and T. Emrick, “Soluble Camptothecin Derivatives Prepared By Click Cycloaddition Chemistry On Functional Aliphatic Polyesters.”, *Bioconjugate Chemistry*, Vol. 18, pp. 263–267, 2007.

62. Lutz, J.F., “Copper-free Azide-alkyne Cycloadditions: New Insights And Perspectives.”, *Angewandte Chemie-International Edition*, Vol. 47, pp. 2182–2184, 2008.

63. Wittig, G., and A. Krebs, “Zur Existenz Niedergliedriger Cycloalkine, I.”, *Chemische Berichte*, Vol. 94, pp. 3260–3275, 1961.

64. Baskin, J.M., and C.R. Bertozzi, “Bioorthogonal Click Chemistry: Covalent Labeling In Living Systems.”, *QSAR & Combinatorial Science*, Vol. 26, pp. 1211–1219, 2007.

65. Agard, N.J., Baskin, J.M., Prescher, J.A, Lo, A. and C.R. Bertozzi, “A Comparative Study Of Bioorthogonal Reactions With Azides”, *ACS Chemical Biology*, Vol. 1, pp. 644–648, 2006.

66. Agard, N.J., J.A. Prescher, and C.R. Bertozzi, “A Strain-promoted [3 + 2] Azide-alkyne Cycloaddition For Covalent Modification Of Biomolecules In Living Systems.”, *Journal of the American Chemical Society*, Vol. 126, pp. 15046–7, 2004.

67. Isaacman, M.J., E.M. Corigliano, and L.S. Theogarajan, “Stealth Polymeric Vesicles Via Metal-Free Click Coupling.”, *Biomacromolecules*, Vol. 14, pp. 2996–3000, 2013.

68. Lowe, A.B., “Thiol-ene ‘Click’ Reactions And Recent Applications In Polymer And Materials Synthesis.”, *Polymer Chemistry*, Vol. 1, pp. 17, 2010.

69. Hoyle, C.E., and C.N. Bowman, “Thiol-ene Click Chemistry.”, *Angewandte Chemie-International Edition*, Vol. 49, pp. 1540–1573, 2010.

70. Tempelaar, S., L. Mespouille, P. Dubois, and A.P. Dove, “Organocatalytic Synthesis And Postpolymerization Functionalization Of Allyl-functional Poly(carbonate)s.”, *Macromolecules*, Vol. 44, pp. 2084–2091, 2011.

71. Allen, C.F.H., and G.P. Happ, “The Thermal Reversibility Of The Michael Reaction: I. Nitriles.”, *Canadian Journal of Chemistry*, Vol. 42, pp. 641–649, 1964.

72. Gauthier, M., M. Gibson, and H.-A. Klok, “Synthesis Of Functional Polymers By Post-Polymerization Modification.”, *Angewandte Chemie-International Edition*, Vol. 48, pp. 48–58, 2009.

73. Nair, D.P., M. Podgórski, S. Chatani, T. Gong, W. Xi, C.R. Fenoli, and C.N. Bowman, “The Thiol-Michael Addition Click Reaction: A Powerful And Widely Used Tool In Materials Chemistry.”, *Chemistry of Materials*, Vol. 26, pp. 724–744, 2014.

74. Onbulak, S., S. Tempelaar, R.J. Pounder, O. Gok, R. Sanyal, A.P. Dove, and A. Sanyal, “Synthesis And Functionalization Of Thiol-reactive Biodegradable Polymers.”, *Macromolecules*, Vol. 45, pp. 1715–1722, 2012.

75. Diels, O., and K. Alder, “Synthesen In Der Hydroaromatischen Reihe.”, *Justus Liebig’s Annalen der Chemie*, Vol. 460, pp. 98–122, 1928.

76. Sanyal, A., “Diels-alder Cycloaddition-Cycloreversion: A Powerful Combo In Materials Design.”, *Macromolecular Chemistry and Physics*, Vol. 211, pp. 1417–

1425, 2010.

77. Tasdelen, M.A., "Diels–Alder 'Click' Reactions: Recent Applications In Polymer And Material Science.", *Polymer Chemistry*, Vol. 2, pp. 2133–2145, 2011.

78. Hizal, G., U. Tunca, and A. Sanyal, "Discrete Macromolecular Constructs Via The Diels-Alder 'Click' reaction.", *Journal of Polymer Science, Part A: Polymer Chemistry*, Vol. 49, pp. 4103–4120, 2011.

79. Gevrek, T.N., R.N. Ozdeslik, G.S. Sahin, G. Yesilbag, S. Mutlu, and A. Sanyal, "Functionalization Of Reactive Polymeric Coatings Via Diels-alder Reaction Using Microcontact Printing.", *Macromolecular Chemistry and Physics*, Vol. 213, pp. 166–172, 2012.

80. Gacal, B., H. Durmaz, M. A. Tasdelen, G. Hizal, U. Tunca, Y. Yagci, and A. L. Demirel, "Anthracene-maleimide-based Diels-Alder 'click Chemistry' as A Novel Route To Graft Copolymers.", *Macromolecules*, Vol. 39, pp. 5330–5336, 2006.

81. Barker, I. A., D.J. Hall, C.F. Hansell, F.E. Du Prez, R.K. O'Reilly, and A.P. Dove, "Tetrazine-norbornene Click Reactions To Functionalize Degradable Polymers Derived From Lactide.", *Macromolecular Rapid Communications*, Vol. 32, pp. 1362–1366, 2011.

82. Williams, R.J., I. A. Barker, R.K. O'Reilly, and A.P. Dove, "Orthogonal Modification Of Norbornene-Functional Degradable Polymers." *ACS Macro Letters*, Vol. 1, pp. 1285–1290, 2012.

83. Dag, A., M. Aydin, H. Durmaz, G. Hizal, and U. Tunca, "Various Polycarbonate Graft Copolymers Via Diels-Alder Click Reaction.", *Journal of Polymer Science, Part A: Polymer Chemistry*, Vol. 50, pp. 4476–4483, 2012.

84. Batz, H.-G., G. Franzmann, and H. Ringsdorf, "Model Reactions For Synthesis Of Pharmacologically Active Polymers By Way Of Monomeric And Polymeric Reactive

Esters.", *Angewandte Chemie-International Edition*, Vol. 11, pp. 1103–1104, 1972.

85. Ferruti, P., A. Bettelli, and A. Feré, "High Polymers Of Acrylic And Methacrylic Esters Of N-hydroxysuccinimide As Polyacrylamide And Polymethacrylamide Precursors.", *Polymer*, Vol. 13, pp. 462–464, 1972.

86. Theato, P., "Synthesis Of Well-Defined Polymeric Activated Esters.", *Journal of Polymer Science, Part A: Polymer Chemistry*, Vol. 46, pp. 6677–6687, 2008.

87. Yoo, H.S., T.G. Kim, and T.G. Park, "Surface-functionalized Electrospun Nanofibers For Tissue Engineering And Drug Delivery.", *Advanced Drug Delivery Reviews*, Vol. 61, pp. 1033–1042, 2009.

88. Zhao, W., J. Li, K. Jin, W. Liu, X. Qiu, and C. Li, "Fabrication Of Functional PLGA-based Electrospun Scaffolds And Their Applications In Biomedical Engineering.", *Materials Science and Engineering C*, Vol. 59, pp. 1181–1194, 2016.

89. Chen, J.P., and C.H. Su, "Surface Modification Of Electrospun PLLA Nanofibers By Plasma Treatment And Cationized Gelatin Immobilization For Cartilage Tissue Engineering.", *Acta Biomaterialia*, Vol. 7, pp. 234–243, 2011.

90. Van Hong Thien, D., M.H. Ho, S.W. Hsiao, and C.H. Li, "Wet Chemical Process To Enhance Osteoconductivity Of Electrospun Chitosan Nanofibers.", *Journal of Materials Science*, Vol. 50, pp. 1575–1585, 2015.

91. Liu, H., Y. Zheng, P. V. Gurgel, and R.G. Carbonell, "Affinity Membrane Development From PBT Nonwoven By Photo-induced Graft Polymerization, Hydrophilization And Ligand Attachment.", *Journal of Membrane Science*, Vol. 428, pp. 562–575, 2013.

92. Gentsch, R., F. Pippig, S. Schmidt, P. Cernoch, J. Polleux, and H.G. Börner, "Single-step Electrospinning To Bioactive Polymer Nanofibers.", *Macromolecules*, Vol. 44, pp. 453–461, 2011.

93. Casper, C.L., N. Yamaguchi, K.L. Kiick, and J.F. Rabolt, “Functionalizing Electrospun Fibers With Biologically Relevant Macromolecules.”, *Biomacromolecules*, Vol. 6, pp. 1998–2007, 2005.

94. Jiang, L., Y. Lu, X. Liu, H. Tu, J. Zhang, X. Shi, H. Deng, and Y. Du, “Layer-by-layer Immobilization Of Quaternized Carboxymethyl Chitosan/organic Rectorite And Alginate Onto Nanofibrous Mats And Their Antibacterial Application.”, *Carbohydrate Polymers*, Vol. 121, pp. 428–435, 2015.

95. Shi, Q., X. Chen, T. Lu, and X. Jing, “The Immobilization Of Proteins On Biodegradable Polymer Fibers Via Click Chemistry.”, *Biomaterials*, Vol. 29, pp. 1118–1126, 2008.

96. Lin, F., J. Yu, W. Tang, J. Zheng, S. Xie, and M.L. Becker, “Postelectrospinning ‘Click’ Modification Of Degradable Amino Acid-Based Poly(ester Urea) Nanofibers.” *Macromolecules*, Vol. 46, pp.9515–9525, 2013.

97. Zheng, J., G. Hua, J. Yu, F. Lin, M.B. Wade, D.H. Reneker, and M.L. Becker, “Post-Electrospinning ‘Triclick’ Functionalization Of Degradable Polymer Nanofibers.”, *ACS Macro Letters*, Vol. 4, pp. 207–213, 2015.

98. Zheng, J., K. Liu, D.H. Reneker, and M.L. Becker, “Post-assembly Derivatization Of Electrospun Nanofibers Via Strain-promoted Azide Alkyne Cycloaddition.”, *Journal of the American Chemical Society*, Vol. 134, pp. 17274–17277, 2012.

99. Zheng, J., S. Xie, F. Lin, G. Hua, T. Yu, D.H. Reneker, and M.L. Becker, “4-Dibenzocyclooctynol (DIBO) As An Initiator For Poly(ε-caprolactone): Copper-free Clickable Polymer And Nanofiber-based Scaffolds.”, *Polymer Chemistry*, Vol. 4, pp. 2215, 2013.

100. Smith Callahan, L. A., S. Xie, I. A Barker, J. Zheng, D.H. Reneker, A.P. Dove, and M.L. Becker, “Directed Differentiation And Neurite Extension Of Mouse Embryonic Stem Cell On Aligned Poly(lactide) Nanofibers Functionalized With YIGSR

Peptide.", *Biomaterials*, Vol. 34, pp. 9089–9095, 2013.

101. Yang, H., Q. Zhang, B. Lin, G. Fu, X. Zhang, and L. Guo, "Thermo-sensitive Electrospun Fibers Prepared By A Sequential Thiol-ene Click Chemistry Approach.", *Journal of Polymer Science, Part A: Polymer Chemistry*, Vol. 50, pp. 4182–4190, 2012.

102. Zhao, H., W. Gu, M.W. Thielke, E. Sterner, T. Tsai, T.P. Russell, E.B. Coughlin, and P. Theato, "Functionalized Nanoporous Thin Films And Fibers From Photocleavable Block Copolymers Featuring Activated Esters.", *Macromolecules*, Vol. 46, pp. 5195–5201, 2013.

103. Shi, J., L. Wang, F. Zhang, H. Li, L. Lei, L. Liu, and Y. Chen, "Incorporating Protein Gradient Into Electrospun Nanofibers As Scaffolds For Tissue Engineering.", *ACS Applied Materials and Interfaces*, Vol. 2, pp. 1025–1030, 2010.

104. Leung, M., A. Cooper, and S. Jana, "Nanofiber-Based In Vitro System For High Myogenic Differentiation Of Human Embryonic Stem Cells.", *Biomacromolecules*, Vol. 14 pp. 4207–4216, 2013.

105. Liu, J., H. Nie, Z. Xu, F. Guo, S. Guo, J. Yin, Y. Wang, and C. Zhang, "Construction Of PRP-containing Nanofibrous Scaffolds For Controlled Release And Their Application To Cartilage Regeneration.", *Journal of Materials Chemistry B*, Vol. 3, pp. 581–591, 2015.

106. Uzun, S.D., F. Kayaci, T. Uyar, S. Timur, and L. Toppare, "Bioactive Surface Design Based On Functional Composite Electrospun Nanofibers For Biomolecule Immobilization And Biosensor Applications." *ACS Applied Materials and Interfaces*, Vol. 6,pp.5235–5243, 2014.

107. Oliveira, C., A.R. Costa-Pinto, R.L. Reis, A. Martins, and N.M. Neves, "Biofunctional Nanofibrous Substrate Comprising Immobilized Antibodies And Selective Binding Of Autologous Growth Factors.", *Biomacromolecules*, Vol. 15, pp.

2196–2205, 2014.

108. Chen, P.-C., X.-J. Huang, and Z.-K. Xu, “Kinetics-bolstered Catalytic Study Of A High Performance Lipase-immobilized Nanofiber Membrane Bioreactor.”, *RSC Advances*, Vol. 4, pp. 6151–6158, 2014.

109. Agarwal, S., J.H. Wendorff, and A. Greiner, “Progress In The Field Of Electrospinning For Tissue Engineering Applications.”, *Advanced Materials*, Vol. 21, pp. 3343–3351, 2009.

110. Kim, B.J., Y.S. Choi, and H.J. Cha, “Reinforced Multifunctionalized Nanofibrous Scaffolds Using Mussel Adhesive Proteins.”, *Angewandte Chemie-International Edition*, Vol. 51, pp. 675–678, 2012.

111. Rim, N.G., C.S. Shin, and H. Shin, “Current Approaches To Electrospun Nanofibers For Tissue Engineering.”, *Biomedical Materials*, Vol. 8, pp. 14102, 2013.

112. Celebioglu, A., S. Demirci, and T. Uyar, “Cyclodextrin-grafted Electrospun Cellulose Acetate Nanofibers Via 'Click' Reaction For Removal Of Phenanthrene.”, *Applied Surface Science*, Vol. 305, pp. 581–588, 2014.

113. Lancuški, A., S. Fort, and F. Bossard, “Electrospun Azido-PCL Nanofibers For Enhanced Surface Functionalization By Click Chemistry.” *ACS Applied Materials and Interfaces*, Vol. 4, pp. 6499–6504, 2012.

114. Kalaoglu-Altan, O.I., R. Sanyal, and A. Sanyal, “Reactive And 'Clickable' Electrospun Polymeric Nanofibers.”, *Polymer Chemistry*, Vol. 6, pp. 3372–3381, 2015.

115. Kose, M.M., G. Yesilbag, and A. Sanyal, “Segment Block Dendrimers Via Diels-Alder Cycloaddition.”, *Organic Letters*, Vol. 10, pp. 2353–2356, 2008.

116. Shi, M., K. Ho, A. Keating, and M.S. Shoichet, “Doxorubicin-Conjugated Immuno-

Nanoparticles For Intracellular Anticancer Drug Delivery.", *Advanced Functional Materials*, Vol. 19, pp. 1689–1696, 2009.

117. Castonguay, A., E. Wilson, N. Al-Hajaj, L. Petitjean, J. Paoletti, D. Maysinger, and A. Kakkar, "Thermosensitive Dendrimer Formulation For Drug Delivery At Physiologically Relevant Temperatures.", *Chemical Communications*, Vol. 47, pp. 12146–12148, 2011.

118. Rideout, D.C., and R. Breslow, "Hydrophobic Acceleration Of Diels-Alder Reactions.", *Journal of the American Chemical Society,* Vol. 102, pp. 7816–7817, 1980.

119. Wei, H.L., Z. Yang, L.M. Zheng, and Y.M. Shen, "Thermosensitive Hydrogels Synthesized By Fast Diels-Alder Reaction In Water.", *Polymer*, Vol. 50, pp. 2836–2840, 2009.

120. Kalaoglu-Altan, O.I., R. Sanyal, and A. Sanyal, "'Clickable' Polymeric Nanofibers Through Hydrophilic−Hydrophobic Balance : Fabrication Of Robust Biomolecular Immobilization Platforms." *Biomacromolecules*, Vol. 16, pp. 1590−1597, 2015.

121.Heath, D.E., and S.L. Cooper, "Design And Characterization Of PEGylated Terpolymer Biomaterials.", *Journal of Biomedical Materials Research-Part A*, Vol. 94, pp. 1294–1302, 2010.

122. Moss, J. and M. D.Lane, "The Biotin-Dependent Enzymes.", *Advances in Enzymology and Related Areas of Molecular Biology*, Vol. 35, pp. 321−442, 1971.

123. Agarwal, S., A. Greiner, and J.H. Wendorff, "Functional Materials By Electrospinning Of Polymers.", *Progress in Polymer Science*, Vol. 38, pp. 963–991, 2013.

124. Barnes, C.P., S.A. Sell, E.D. Boland, D.G. Simpson, and G.L. Bowlin, "Nanofiber Technology: Designing The Next Generation Of Tissue Engineering Scaffolds.",

Advanced Drug Delivery Reviews, Vol. 59, pp. 1413–1433, 2007.

125. Torres-Giner, S., J. V. Gimeno-Alcañiz, M.J. Ocio, and J.M. Lagaron, "Comparative Performance Of Electrospun Collagen Nanofibers Cross-linked By Means Of Different Methods.", *ACS Applied Materials and Interfaces*, Vol. 1, pp. 218–223, 2009.

126. Schiffman, J.D., and C.L. Schauer, "Cross-Linking Chitosan Nanofibers." *Biomacromolecules,* Vol. 8, pp. 594–601, 2006.

127. Tang, C., C.D. Saquing, J.R. Harding, and S.A. Khan, "In Situ Cross-linking Of Electrospun Poly(vinyl Alcohol) Nanofibers.", *Macromolecules*, Vol. 43, pp. 630–637, 2010.

128. Kim, M.S., I. Jun, Y.M. Shin, W. Jang, S.I. Kim, and H. Shin, "The Development Of Genipin-crosslinked Poly(caprolactone) (PCL)/Gelatin Nanofibers For Tissue Engineering Applications.", *Macromolecular Bioscience*, Vol. 10, pp. 91–100, 2010.

129. Zhang, X., K. Tang, and X. Zheng, "Electrospinning And Crosslinking Of COL/PVA Nanofiber-microsphere Containing Salicylic Acid For Drug Delivery.", *Journal of Bionic Engineering*, Vol. 13, pp. 143–149, 2016.

130. Kalaoglu-Altan, O.I., B. Verbraeken, K. Lava, T.N. Gevrek, R. Sanyal, T. Dargaville, K. De Clerck, R. Hoogenboom, and A. Sanyal, "Multireactive Poly(2-oxazoline) Nanofibers Through Electrospinning With Crosslinking On The Fly.", *ACS Macro Letters*, Vol. 5, pp. 676–681, 2016.

131. Dargaville, B.L., C. Vaquette, F. Rasoul, J.J. Cooper-White, J.H. Campbell, and A.K. Whittaker, "Electrospinning And Crosslinking Of Low-molecular-weight Poly(trimethylene Carbonate-co-l-lactide) As An Elastomeric Scaffold For Vascular Engineering.", *Acta Biomaterialia*, Vol. 9, pp. 6885–6897, 2013.

132. Wang, Y.S., C.C. Cheng, Y.S. Ye, Y.C. Yen, and F.C. Chang, "Bioinspired Photo-

cross-linked Nanofibers From Uracil-functionalized Polymers.", *ACS Macro Letters*, Vol. 1, pp. 159–162, 2012.

133. Decker, C., and C. Bianchi, "Photocrosslinking Of A Maleimide Functionalized Polymethacrylate.", *Polymer International*, Vol. 52, pp. 722–732, 2003.

134. Zhao, S., Q. Zhou, Y.-Z. Long, G.-H. Sun, Y. Zhang, W.-J. Li, T.-X. Xu, F. Kim, and H. Yan, "Nanofibrous Patterns By Direct Electrospinning Of Nanofibers Onto Topographically Structured Non-conductive Substrates.", *Nanoscale*, Vol. 5, pp. 4993, 2013.

135. Prabhakaran, M.P., E. Vatankhah, D. Kai, and S. Ramakrishna, "Methods For Nano/Micropatterning Of Substrates: Toward Stem Cells Differentiation.", *International Journal of Polymeric Materials and Polymeric Biomaterials*, Vol. 64, pp. 338–353, 2015.

136. Jia, C., D. Yu, M. Lamarre, P.L. Leopold, Y.D. Teng, and H. Wang, "Patterned Electrospun Nanofiber Matrices Via Localized Dissolution: Potential For Guided Tissue Formation.", *Advanced Materials*, Vol. 26, pp. 8192–8197, 2014.

137. Zhang, D., and J. Chang, "Patterning Of Electrospun Fibers Using Electroconductive Templates.", *Advanced Materials*, Vol. 19, pp. 3662–3667, 2007.

138. Lee, J., S.Y. Lee, J. Jang, Y.H. Jeong, and D.W. Cho, "Fabrication Of Patterned Nanofibrous Mats Using Direct-Write Electrospinning.", *Langmuir*, Vol. 28, pp. 7267–7275, 2012.

139. Lee, H.J., and W.G. Koh, "Hydrogel Micropattern-incorporated Fibrous Scaffolds Capable Of Sequential Growth Factor Delivery For Enhanced Osteogenesis Of HMSCs.", *ACS Applied Materials and Interfaces*, Vol. 6, pp. 9338–9348, 2014.

140. Song, W., D. An, D.-I. Kao, Y.-C. Lu, G. Dai, S. Chen, and M. Ma, "Nanofibrous Microposts And Microwells Of Controlled Shapes And Their Hybridization With

Hydrogels For Cell Encapsulation.” *ACS Applied Materials and Interfaces*, Vol. 6, pp. 7038–7044, 2014.

141. Dominguez, M.M., M. Wathier, M.W. Grinstaff, and S.E. Schaus, “Immobilized Hydrogels For Screening Of Molecular Interactions.”, *Analytical Chemistry*, Vol. 79, pp. 1064–1066, 2007.

142. Dispinar, T., R. Sanyal, and A. Sanyal., “A Diels-Alder/Retro Diels-Alder Strategy To Synthesize Polymers Bearing Maleimide Side Chains.”, *Journal of Polymer Science: Part A: Polymer Chemistry*, Vol. 45, pp. 4545–4551, 2007.

143. Teo, W.E., and S. Ramakrishna, “A Review On Electrospinning Design And Nanofibre Assemblies.”, *Nanotechnology*, Vol. 17, pp. R89–R106, 2006.

144. Wu, J., N. Wang, Y. Zhao, and L. Jiang, “Electrospinning Of Multilevel Structured Functional Micro-/nanofibers And Their Applications.”, *Journal of Materials Chemistry A*, Vol. 1, pp. 7290, 2013.

145. Yang, F., J.G.C. Wolke, and J. A. Jansen, “Biomimetic Calcium Phosphate Coating On Electrospun Poly(ε-caprolactone) Scaffolds For Bone Tissue Engineering.”, *Chemical Engineering Journal*, Vol. 137, pp. 154–161, 2008.

146. Chen, F., C.N. Lee, and S.H. Teoh, “Nanofibrous Modification On Ultra-thin Poly(e-caprolactone) Membrane Via Electrospinning.”, *Materials Science and Engineering C*, Vol. 27, pp. 325–332, 2007.

147. Durmaz, H., A. Sanyal, G. Hizal, and U. Tunca, “Double Click Reaction Strategies For Polymer Conjugation And Post-functionalization Of Polymers.” *Polymer Chemistry*, Vol.3, pp. 34−45,2012.

148. Wade, R.J., E.J. Bassin, W.M. Gramlich, and J.A. Burdick, “Nanofibrous Hydrogels With Spatially Patterned Biochemical Signals To Control Cell Behavior.”, *Advanced Materials*, Vol. 27, pp. 1356–1362, 2015.

149. Sedlacek, O., B.D. Monnery, S.K. Filippov, R. Hoogenboom, and M. Hruby, “Poly(2-oxazoline)s - Are They More Advantageous For Biomedical Applications Than Other Polymers?”, *Macromolecular Rapid Communications*, Vol. 33, pp. 1648–1662, 2012.

150. Luxenhofer, R., Y. Han, A. Schulz, J. Tong, Z. He, A. V Kabanov, and R. Jordan, “Poly (2-oxazoline)s As Polymer Therapeutics.”, *Macromolecular Rapid Communications*, Vol. 33, pp. 1613–1631, 2012.

151. Adams, N., and U.S. Schubert, “Poly(2-oxazolines) In Biological And Biomedical Application Contexts.”, *Advanced Drug Delivery Reviews*, Vol. 59, pp. 1504–1520, 2007.

152. Barz, M., R. Luxenhofer, R. Zentel, and M.J. Vicent, “Overcoming The PEG-addiction: Well-defined Alternatives To PEG, From Structure–Property Relationships To Better Defined Therapeutics.”, *Polymer Chemistry*, Vol. 2, pp. 1900, 2011.

153. Hoogenboom, R., “Poly(2-oxazoline)s: A Polymer Class With Numerous Potential Applications.”, *Angewandte Chemie-International Edition*, Vol. 48, pp. 7978–7994, 2009.

154. Le Fer, G., C. Amiel, and G. Volet, “Copolymers Based On Azidopentyl-2-oxazoline: Synthesis, Characterization And LCST Behavior.”, *European Polymer Journal*, Vol. 71, pp. 523–533, 2015.

155. Rossegger, E., V. Schenk, and F. Wiesbrock, “Design Strategies For Functionalized Poly(2-oxazoline)s And Derived Materials.”, *Polymers*, Vol. 5, pp. 956–1011, 2013.

156. Lava, K., B. Verbraeken, and R. Hoogenboom, “Poly(2-oxazoline)s And Click Chemistry: A Versatile Toolbox Toward Multi-functional Polymers.”, *European Polymer Journal*, Vol. 65, pp. 98–111, 2015.

157. Gress, A., A. Völkel, and H. Schlaad, “Thio-click Modification Of Poly[2-(3-butenyl)-2-oxazoline].”, *Macromolecules*, Vol. 40, pp. 7928–7933, 2007.

158. Diehl, C., and H. Schlaad, “Thermo-responsive Polyoxazolines With Widely Tuneable LCST.”, *Macromolecular Bioscience*, Vol. 9, pp. 157–161, 2009.

159. Cortez, M.A., and S.M. Grayson, “Thiol-ene Click Functionalization And Subsequent Polymerization Of 2-oxazoline Monomers.”, *Macromolecules*, Vol. 43, pp. 4081–4090, 2010.

160. Kempe, K., R. Hoogenboom, and U.S. Schubert, “A Green Approach For The Synthesis And Thiol-ene Modification Of Alkene Functionallized Poly(2-oxazoline)s.”, *Macromolecular Rapid Communications*, Vol. 32, pp. 1484–1489, 2011.

161. Schenk, V., L. Ellmaier, E. Rossegger, M. Edler, T. Griesser, G. Weidinger, and F. Wiesbrock, “Water-Developable Poly(2-oxazoline)-Based Negative Photoresists.”, *Macromolecular Rapid Communications*, Vol. 33, pp. 396–400, 2012.

162. Tauhardt, L., D. Pretzel, K. Kempe, M. Gottschaldt, D. Pohlers, and U.S. Schubert, “Zwitterionic Poly(2-oxazoline)s As Promising Candidates For Blood Contacting Applications.”, *Polymer Chemistry*, Vol. 5, pp. 5751, 2014.

163. Schenk, V., E. Rossegger, C. Ebner, F. Bangerl, K. Reichmann, B. Hoffmann, M. Höpfner, and F. Wiesbrock, “RGD-Functionalization Of Poly(2-oxazoline)-based Networks For Enhanced Adhesion To Cancer Cells.”, *Polymers*, Vol. 6, pp. 264–279, 2014.

164. Dargaville, T.R., R. Forster, B.L. Farrugia, K. Kempe, L. Voorhaar, U.S. Schubert, and R. Hoogenboom, “Poly(2-oxazoline) Hydrogel Monoliths Via Thiol-ene Coupling.”, *Macromolecular Rapid Communications*, Vol. 33, pp. 1695–1700, 2012.

165. Farrugia, B.L., K. Kempe, U.S. Schubert, R. Hoogenboom, and T.R. Dargaville, “Poly(2-oxazoline) Hydrogels For Controlled Fibroblast Attachment.”, *Biomacromolecules*, Vol. 14, pp. 2724–2732, 2013.

166. Buruaga, L., A. Gonzalez, and J.J. Iruin, “Electrospinning Of Poly(2-ethyl-2-oxazoline).”, *Journal of Materials Science*, Vol. 44, pp. 3186–3191, 2009.

167. George, G., and S. Anandhan, “Structural Characterization Of Nano-crystalline Co3O4 Ultra-fine Fibers Obtained By Sol-gel Electrospinning.”, *Journal of Sol-Gel Science and Technology*, Vol. 67, pp. 256–266, 2013.

168. Hochleitner, G., J.F. Hümmer, R. Luxenhofer, and J. Groll, “High Definition Fibrous Poly(2-ethyl-2-oxazoline) Scaffolds Through Melt Electrospinning Writing.”, *Polymer*, Vol. 55, pp. 5017–5023, 2014.

169. Shepherd, J.L., A. Kell, E. Chung, C.W. Sinclar, M.S. Workentin, and D. Bizzotto, “Selective Reductive Desorption Of A SAM-coated Gold Electrode Revealed Using Fluorescence Microscopy.”, *Journal of the American Chemical Society*, Vol. 126, pp. 8329–8335, 2004.

170. Ellman, G.L., “Tissue Sulfhydryl Groups.”, *Archives of Biochemistry and Biophysics*, Vol. 82, pp. 70–77, 1959.

171. Kempe, K., T. Neuwirth, J. Czaplewska, M. Gottschaldt, R. Hoogenboom, and U.S. Schubert, " Poly(2-oxazoline) Glycopolymers With Tunable LCST Behavior", *Polymer Chemistry*, Vol. 2, pp. 1737−1743, 2011.

172. Duque Sánchez, L., N. Brack, A. Postma, P.J. Pigram, and L. Meagher, “Surface Modification Of Electrospun Fibres For Biomedical Applications: A Focus On Radical Polymerization Methods.”, *Biomaterials*, Vol. 106, pp. 24–45, 2016.

173. Zhang, Z., J. Hu, and P.X. Ma, “Nanofiber-based Delivery Of Bioactive Agents And Stem Cells To Bone Sites.”, *Advanced Drug Delivery Reviews*, Vol. 64, pp. 1129–1141, 2012.

174. Nisbet, D.R., J.S. Forsythe, W. Shen, D.I. Finkelstein, and M.K. Horne, “A Review Of The Cellular Response On Electrospun Nanofibers For Tissue Engineering.”,

Journal of Biomaterials Applications, Vol. 24, pp. 7–29, 2009.

175. Quirós, J., K. Boltes, and R. Rosal, "Bioactive Applications For Electrospun Fibers.", *Polymer Reviews*, Vol. 56, pp. 631–667, 2016.

176. Kai, D., G. Jin, M.P. Prabhakaran, and S. Ramakrishna, "Electrospun Synthetic And Natural Nanofibers For Regenerative Medicine And Stem Cells.", *Biotechnology Journal*, Vol. 8, pp. 59–72, 2013.

177. Jing, X., H.Y. Mi, X.C. Wang, X.F. Peng, and L.S. Turng, "Shish-Kebab-structured Poly(ε-caprolactone) Nanofibers Hierarchically Decorated With Chitosan-Poly(ε-caprolactone) Copolymers For Bone Tissue Engineering.", *ACS Applied Materials and Interfaces*, Vol. 7, pp. 6955–6965, 2015.

178. Madhurakkat Perikamana, S.K., J. Lee, T. Ahmad, Y. Jeong, D.G. Kim, K. Kim, and H. Shin, "Effects Of Immobilized BMP-2 And Nanofiber Morphology On In Vitro Osteogenic Differentiation Of HMSCs And In Vivo Collagen Assembly Of Regenerated Bone.", *ACS Applied Materials and Interfaces*, Vol. 7, pp. 8798–8808, 2015.

179. Li, D., H. Sun, L. Jiang, K. Zhang, W. Liu, Y. Zhu, J. Fangteng, C. Shi, L. Zhao, H. Sun, and B. Yang, "Enhanced Biocompatibility Of PLGA Nanofibers With Gelatin/nano- Hydroxyapatite Bone Biomimetics Incorporation.", *ACS Applied Materials and Interfaces*, Vol. 6, pp. 9402–9410, 2014.

180. Zhu, Y., M.F. Leong, W.F. Ong, M.B. Chan-Park, and K.S. Chian, "Esophageal Epithelium Regeneration On Fibronectin Grafted Poly(l-lactide-co-caprolactone) (PLLC) Nanofiber Scaffold.", *Biomaterials*, Vol. 28, pp. 861–868, 2007.

181. Ku, S.H., and C.B. Park, "Human Endothelial Cell Growth On Mussel-inspired Nanofiber Scaffold For Vascular Tissue Engineering.", *Biomaterials*, Vol. 31, pp. 9431–9437, 2010.

182. Liang, D., B.S. Hsiao, and B. Chu, “Functional Electrospun Nanofibrous Scaffolds For Biomedical Applications.”, *Advanced Drug Delivery Reviews*, Vol. 59, pp. 1392–1412, 2007.

183. Wu, J., L. Xie, W. Zhi, Y. Lin, and Q. Chen, “Biomimetic Nanofibrous Scaffolds For Neural Tissue Engineering And Drug Development.”, *Drug Discovery Today*, doi.org/10.1016/j.drudis.2017.03.007, 2017.

184. Barner-Kowollik, C., F.E. Du Prez, P. Espeel, C.J. Hawker, T. Junkers, H. Schlaad, and W. Van Camp, “‘Clicking’ polymers Or Just Efficient Linking: What Is The Difference?”, *Angewandte Chemie-International Edition*, Vol. 50, pp. 60–62, 2011.

185. Espeel, P., and F.E. Du Prez, “‘Click’-Inspired Chemistry In Macromolecular Science: Matching Recent Progress And User Expectations.” *Macromolecules*, Vol. 48, pp. 2–14, 2015.

186. Zheng, J., D. Kontoveros, F. Lin, G. Hua, D.H. Reneker, M.L. Becker, and R.K. Willits, “Enhanced Schwann Cell Attachment And Alignment Using One-Pot ‘Dual Click’ GRGDS And YIGSR Derivatized Nanofibers.”, *Biomacromolecules*, Vol. 16, pp. 357–363, 2015.

187. Gregoritza, M., and F.P. Brandl, “The Diels–Alder Reaction: A Powerful Tool For The Design Of Drug Delivery Systems And Biomaterials.”, *European Journal of Pharmaceutics and Biopharmaceutics*, Vol. 97, pp. 438–453, 2015.

188. Yuksekdag, Y.N., T.N. Gevrek, and A. Sanyal, “Diels-Alder ‘Clickable’ Polymer Brushes: A Versatile Catalyst-Free Conjugation Platform.”, *ACS Macro Letters*, pp. 415–420, 2017.

189. Altinbasak, I., R. Sanyal, and A. Sanyal, “Best Of Both Worlds: Diels–Alder Chemistry Towards Fabrication Of Redox-responsive Degradable Hydrogels For Protein Release.”, *RSC Advances*, Vol. 6, pp. 74757–74764, 2016.

190. Owen, S.C., N. Patel, J. Logie, G. Pan, H. Persson, J. Moffat, S.S. Sidhu, and M.S. Shoichet, “Targeting HER2 + Breast Cancer Cells: Lysosomal Accumulation Of Anti-HER2 Antibodies Is Influenced By Antibody Binding Site And Conjugation To Polymeric Nanoparticles.”, *Journal of Controlled Release*, Vol. 172, pp. 395–404, 2013.

191. Liu, Y.-L., T.-W. Chuo, N.R. Sottos, K.S. Anseth, C.N. Bowman, P. V. Braun, N.R. Sottos, S.R. White, and J.S. Moore, “Self-healing Polymers Based On Thermally Reversible Diels–Alder Chemistry.”, *Polymer Chemistry*, Vol. 4, pp. 2194, 2013.

192. Sun, H., C.P. Kabb, and B.S. Sumerlin, “Thermally-labile Segmented Hyperbranched Copolymers: Using Reversible-covalent Chemistry To Investigate The Mechanism Of Self-condensing Vinyl Copolymerization.”, *Chemical Science*, Vol. 5, pp. 4646–4655, 2014.

193. Gandini, A., “The Furan/Maleimide Diels–Alder Reaction: A Versatile Click–Unclick Tool In Macromolecular Synthesis.”, *Progress in Polymer Science*, Vol. 38, pp. 1–29, 2013.

194. Jérôme, C., and P. Lecomte, “Recent Advances In The Synthesis Of Aliphatic Polyesters By Ring-opening Polymerization.”, *Advanced Drug Delivery Reviews*, Vol. 60, pp. 1056–1076, 2008.

195. Seyednejad, H., A.H. Ghassemi, C.F. Van Nostrum, T. Vermonden, and W.E. Hennink, “Functional Aliphatic Polyesters For Biomedical And Pharmaceutical Applications.”, *Journal of Controlled Release*, Vol. 152, pp. 168–176, 2011.

196. Pounder, R.J., and A.P. Dove, “Towards Poly(ester) Nanoparticles: Recent Advances In The Synthesis Of Functional Poly(ester)s By Ring-opening Polymerization.”, *Polymer Chemistry*, Vol. 1, pp. 260–271, 2010.

197. Tian, H., Z. Tang, X. Zhuang, X. Chen, and X. Jing, “Biodegradable Synthetic Polymers: Preparation, Functionalization And Biomedical Application.”, *Progress in*

Polymer Science, Vol. 37, pp. 237–280, 2012.

198. Chen, W., F. Meng, R. Cheng, C. Deng, J. Feijen, and Z. Zhong, "Advanced Drug And Gene Delivery Systems Based On Functional Biodegradable Polycarbonates And Copolymers.", *Journal of Controlled Release*, Vol. 190, pp. 398–414, 2014.

199. Darensbourg, D.J., W. Choi, O. Karroonnirun, and N. Bhuvanesh, "Ring-opening Polymerization Of Cyclic Monomers By Complexes Derived From Biocompatible Metals. Production Of Poly(lactide), Poly(trimethylene Carbonate), And Their Copolymers.", *Macromolecules*, Vol. 41, pp. 3493–3502, 2008.

200. Bat, E., J.A. Plantinga, M.C. Harmsen, M.J.A. Van Luyn, Z. Zhang, D.W. Grijpma, and J. Feijen, "Trimethylene Carbonate And ε-caprolactone Based (Co)polymer Networks: Mechanical Properties And Enzymatic Degradation.", *Biomacromolecules*, Vol. 9, pp. 3208–3215, 2008.

201. Davachi, S.M., B. Kaffashi, and J.M. Roushandeh, "Synthesis And Characterization Of A Novel Terpolymer Based On L-lactide, Glycolide, And Trimethylene Carbonate For Specific Medical Applications.", *Polymers for Advanced Technologies*, Vol. 23, pp. 565–573, 2012.

202. Pretula, J., K. Kaluzynski, B. Wisniewski, R. Szymanski, T. Loontjens, and S. Penczek, "Formation Of Poly(ethylene Phosphates) In Polycondensation Of H3PO4 With Ethylene Glycol. Kinetic And Mechanistic Study.", *Journal of Polymer Science Part A-Polymer Chemistry*, Vol. 46, pp. 830–843, 2008.

203. Xu, J., T.M. Filion, F. Prifti, and J. Song, "Cytocompatible Poly(ethylene Glycol)-co-polycarbonate Hydrogels Cross-linked By Copper-free, Strain-promoted Click Chemistry.", *Chemistry-An Asian Journal*, Vol. 6, pp. 2730–2737, 2011.

204. Thongsomboon, W., M. Sherwood, N. Arellano, and A. Nelson, "Thermally Induced Nanoimprinting Of Biodegradable Polycarbonates Using Dynamic Covalent Crosslinks.", *ACS Macro Letters*, Vol. 2, pp. 17–20, 2013.

205. Olsson, J. V., D. Hult, Y. Cai, S. García-Gallego, and M. Malkoch, "Reactive Imidazole Intermediates: Simplified Synthetic Approach To Functional Aliphatic Cyclic Carbonates.", *Polymer Chemistry*, Vol. 5, pp. 6651–6655, 2014.

206. Kalaoglu-Altan,O.I., A. Kirac-Aydin, B. Sumer Bolu, R. Sanyal, and A. Sanyal, "Diels–Alder "Clickable" Biodegradable Nanofibers: Benign Tailoring Of Scaffolds For Biomolecular Immobilization And Cell Growth", *Bioconjugate Chemistry*, doi: 10.1021/acs.bioconjchem.7b00411, 2017.

207. Pratt, R.C., B.G.G. Lohmeijer, D. A. Long, P.N.P. Lundberg, A.P. Dove, H. Li, C.G. Wade, R.M. Waymouth, and J.L. Hedrick, "Exploration, Optimization, And Application Of Supramolecular Thiourea-amine Catalysts For The Synthesis Of Lactide (Co)polymers.", *Macromolecules*, Vol. 39, pp. 7863–7871, 2006.

208. Agarwal, S., J.H. Wendorff, and A. Greiner, "Chemistry On Electrospun Polymeric Nanofibers: Merely Routine Chemistry Or A Real Challenge?", *Macromolecular Rapid Communications*, Vol. 31, pp. 1317–1331, 2010.

209. Riva, R., S. Schmeits, C. Jerome, R. Jerome, and P. Lecomte, "Combination Of Ring-Opening Polymerization And 'Click Chemistry'; Toward Functionalization And Grafting Of Poly(ε-caprolactone).", *Macromolecules*, Vol. 40, pp. 796–803, 2007.

210. Tokiwa, Y., and B.P. Calabia, "Biodegradability And Biodegradation Of Polyesters.", *Journal of Polymers and the Environment*, Vol. 15, pp. 259–267, 2007.

211. Albertsson, A.-C., and I.K. Varma, "Recent Developments In Ring-opening Polymerization Of Lactones For Biomedical Applications.", *Biomacromolecules*, Vol. 4, pp. 1466–1486, 2003.

212. Ashammakhi, N., A. Ndreu, Y. Yang, H. Ylikauppila, and L. Nikkola, "Nanofiber-based Scaffolds For Tissue Engineering.", *European Journal of Plastic Surgery*, Vol. 35, pp. 135–149, 2012.

213. Yu, Y., J. Zou, L. Yu, W. Ji, Y. Li, W. Law, and C. Cheng, “Functional Polylactide-g-Paclitaxel-Poly(Ethylene Glycol) By Azide-Alkyne Click Chemistry.”, *Macromolecules*, Vol. 44, pp. 4793–4800, 2011.

214. Chamow, S.M., T.P. Kogan, D.H. Peers, R.C. Hastings, R.A. Byrn, and A. Ashkenazi, “Conjugation of Soluble CD4 without Loss Of Biological Activity Via A Novel Carbohydrate-Directed Cross-Linking Reagent.”, *The Journal of Biological Chemistry*, Vol. 267, pp. 15916–15922, 1992.

APPENDIX A: COPYRIGHT NOTICES

JOHN WILEY AND SONS LICENSE TERMS AND CONDITIONS

Sep 01, 2017

This Agreement between Ozlem Ipek Kalaoglu Altan ("You") and John Wiley and Sons ("John Wiley and Sons") consists of your license details and the terms and conditions provided by John Wiley and Sons and Copyright Clearance Center.

License Number	4180010792005
License date	Sep 01, 2017
Licensed Content Publisher	John Wiley and Sons
Licensed Content Publication	Angewandte Chemie International Edition
Licensed Content Title	Electrospinning: A Fascinating Method for the Preparation of Ultrathin Fibers
Licensed Content Author	Andreas Greiner,Joachim H. Wendorff
Licensed Content Date	Jun 22, 2007
Licensed Content Pages	34
Type of use	Dissertation/Thesis
Requestor type	University/Academic
Format	Print and electronic
Portion	Figure/table
Number of figures/tables	1
Original Wiley figure/table number(s)	Figure 1
Will you be translating?	No
Title of your thesis / dissertation	Reactive and Clickable Hydrophilic Nanofibers as Novel Biomaterials
Expected completion date	Sep 2017
Expected size (number of pages)	170
Requestor Location	Ozlem Ipek Kalaoglu Altan Bogazici University Department of Chemistry Bebek Istanbul, 34342 Turkey Attn: Ozlem Ipek Kalaoglu Altan
Publisher Tax ID	EU826007151
Billing Type	Invoice
Billing Address	Ozlem Ipek Kalaoglu Altan Bogazici University Department of Chemistry Bebek Istanbul, Turkey 34342 Attn: Ozlem Ipek Kalaoglu Altan
Total	0.00 USD
Terms and Conditions	

TERMS AND CONDITIONS

This copyrighted material is owned by or exclusively licensed to John Wiley & Sons, Inc. or one of its group companies (each a"Wiley Company") or handled on behalf of a society with

Figure A.1. Copyright permission.

JOHN WILEY AND SONS LICENSE TERMS AND CONDITIONS

Sep 01, 2017

This Agreement between Ozlem Ipek Kalaoglu Altan ("You") and John Wiley and Sons ("John Wiley and Sons") consists of your license details and the terms and conditions provided by John Wiley and Sons and Copyright Clearance Center.

License Number	4180020958960
License date	Sep 01, 2017
Licensed Content Publisher	John Wiley and Sons
Licensed Content Publication	Macromolecular Materials & Engineering
Licensed Content Title	Industrial Upscaling of Electrospinning and Applications of Polymer Nanofibers: A Review
Licensed Content Author	Luana Persano,Andrea Camposeo,Cagri Tekmen,Dario Pisignano
Licensed Content Date	Jan 8, 2013
Licensed Content Pages	17
Type of use	Dissertation/Thesis
Requestor type	University/Academic
Format	Print and electronic
Portion	Figure/table
Number of figures/tables	2
Original Wiley figure/table number(s)	Figure 3, Figure 7
Will you be translating?	No
Title of your thesis / dissertation	Reactive and Clickable Hydrophilic Nanofibers as Novel Biomaterials
Expected completion date	Sep 2017
Expected size (number of pages)	170
Requestor Location	Ozlem Ipek Kalaoglu Altan Bogazici University Department of Chemistry Bebek Istanbul, 34342 Turkey Attn: Ozlem Ipek Kalaoglu Altan
Publisher Tax ID	EU826007151
Billing Type	Invoice
Billing Address	Ozlem Ipek Kalaoglu Altan Bogazici University Department of Chemistry Bebek Istanbul, Turkey 34342 Attn: Ozlem Ipek Kalaoglu Altan
Total	0.00 USD
Terms and Conditions	

TERMS AND CONDITIONS

This copyrighted material is owned by or exclusively licensed to John Wiley & Sons, Inc. or one of its group companies (each a"Wiley Company") or handled on behalf of a society with

Figure A.1. Copyright permission (cont.).

ELSEVIER LICENSE
TERMS AND CONDITIONS

Sep 01, 2017

This Agreement between Ozlem Ipek Kalaoglu Altan ("You") and Elsevier ("Elsevier") consists of your license details and the terms and conditions provided by Elsevier and Copyright Clearance Center.

License Number	4180021346261
License date	Sep 01, 2017
Licensed Content Publisher	Elsevier
Licensed Content Publication	Polymer
Licensed Content Title	Beaded nanofibers formed during electrospinning
Licensed Content Author	H Fong,I Chun,D.H Reneker
Licensed Content Date	Jul 1, 1999
Licensed Content Volume	40
Licensed Content Issue	16
Licensed Content Pages	8
Start Page	4585
End Page	4592
Type of Use	reuse in a thesis/dissertation
Intended publisher of new work	other
Portion	figures/tables/illustrations
Number of figures/tables/illustrations	1
Format	both print and electronic
Are you the author of this Elsevier article?	No
Will you be translating?	No
Original figure numbers	Figure 1
Title of your thesis/dissertation	Reactive and Clickable Hydrophilic Nanofibers as Novel Biomaterials
Expected completion date	Sep 2017
Estimated size (number of pages)	170
Requestor Location	Ozlem Ipek Kalaoglu Altan Bogazici University Department of Chemistry Bebek Istanbul, 34342 Turkey Attn: Ozlem Ipek Kalaoglu Altan
Total	0.00 USD
Terms and Conditions	

INTRODUCTION

1. The publisher for this copyrighted material is Elsevier. By clicking "accept" in connection with completing this licensing transaction, you agree that the following terms and conditions apply to this transaction (along with the Billing and Payment terms and conditions

Figure A.1. Copyright permission (cont.).

ELSEVIER LICENSE
TERMS AND CONDITIONS

Sep 01, 2017

This Agreement between Ozlem Ipek Kalaoglu Altan ("You") and Elsevier ("Elsevier") consists of your license details and the terms and conditions provided by Elsevier and Copyright Clearance Center.

License Number	4180030002367
License date	Sep 01, 2017
Licensed Content Publisher	Elsevier
Licensed Content Publication	Biotechnology Advances
Licensed Content Title	Electrospinning: A fascinating fiber fabrication technique
Licensed Content Author	Nandana Bhardwaj,Subhas C. Kundu
Licensed Content Date	May–June 2010
Licensed Content Volume	28
Licensed Content Issue	3
Licensed Content Pages	23
Start Page	325
End Page	347
Type of Use	reuse in a thesis/dissertation
Intended publisher of new work	other
Portion	figures/tables/illustrations
Number of figures/tables/illustrations	1
Format	both print and electronic
Are you the author of this Elsevier article?	No
Will you be translating?	No
Original figure numbers	Table 3
Title of your thesis/dissertation	Reactive and Clickable Hydrophilic Nanofibers as Novel Biomaterials
Expected completion date	Sep 2017
Estimated size (number of pages)	170
Requestor Location	Ozlem Ipek Kalaoglu Altan Bogazici University Department of Chemistry Bebek Istanbul, 34342 Turkey Attn: Ozlem Ipek Kalaoglu Altan
Total	0.00 USD
Terms and Conditions	

INTRODUCTION

1. The publisher for this copyrighted material is Elsevier. By clicking "accept" in connection with completing this licensing transaction, you agree that the following terms and conditions apply to this transaction (along with the Billing and Payment terms and conditions

Figure A.1. Copyright permission (cont.).

JOHN WILEY AND SONS LICENSE TERMS AND CONDITIONS

Sep 01, 2017

This Agreement between Ozlem Ipek Kalaoglu Altan ("You") and John Wiley and Sons ("John Wiley and Sons") consists of your license details and the terms and conditions provided by John Wiley and Sons and Copyright Clearance Center.

License Number	4180030230325
License date	Sep 01, 2017
Licensed Content Publisher	John Wiley and Sons
Licensed Content Publication	Journal of Applied Polymer Science
Licensed Content Title	Role of molecular weight of atactic poly(vinyl alcohol) (PVA) in the structure and properties of PVA nanofabric prepared by electrospinning
Licensed Content Author	Joon Seok Lee,Kyu Ha Choi,Han Do Ghim,Sam Soo Kim,Du Hwan Chun,Hak Yong Kim,Won Seok Lyoo
Licensed Content Date	May 24, 2004
Licensed Content Pages	9
Type of use	Dissertation/Thesis
Requestor type	University/Academic
Format	Print and electronic
Portion	Figure/table
Number of figures/tables	1
Original Wiley figure/table number(s)	Figure 5
Will you be translating?	No
Title of your thesis / dissertation	Reactive and Clickable Hydrophilic Nanofibers as Novel Biomaterials
Expected completion date	Sep 2017
Expected size (number of pages)	170
Requestor Location	Ozlem Ipek Kalaoglu Altan Bogazici University Department of Chemistry Bebek Istanbul, 34342 Turkey Attn: Ozlem Ipek Kalaoglu Altan
Publisher Tax ID	EU826007151
Billing Type	Invoice
Billing Address	Ozlem Ipek Kalaoglu Altan Bogazici University Department of Chemistry Bebek Istanbul, Turkey 34342 Attn: Ozlem Ipek Kalaoglu Altan
Total	0.00 USD
Terms and Conditions	

TERMS AND CONDITIONS

Figure A.1. Copyright permission (cont.).

JOHN WILEY AND SONS LICENSE TERMS AND CONDITIONS

Sep 01, 2017

This Agreement between Ozlem Ipek Kalaoglu Altan ("You") and John Wiley and Sons ("John Wiley and Sons") consists of your license details and the terms and conditions provided by John Wiley and Sons and Copyright Clearance Center.

License Number	4180030461264
License date	Sep 01, 2017
Licensed Content Publisher	John Wiley and Sons
Licensed Content Publication	Macromolecular Bioscience
Licensed Content Title	Electrospun Nanofibers as Dressings for Chronic Wound Care: Advances, Challenges, and Future Prospects
Licensed Content Author	Martina Abrigo,Sally L. McArthur,Peter Kingshott
Licensed Content Date	Mar 28, 2014
Licensed Content Pages	21
Type of use	Dissertation/Thesis
Requestor type	University/Academic
Format	Print and electronic
Portion	Figure/table
Number of figures/tables	2
Original Wiley figure/table number(s)	Figure 1, Figure 2
Will you be translating?	No
Title of your thesis / dissertation	Reactive and Clickable Hydrophilic Nanofibers as Novel Biomaterials
Expected completion date	Sep 2017
Expected size (number of pages)	170
Requestor Location	Ozlem Ipek Kalaoglu Altan Bogazici University Department of Chemistry Bebek Istanbul, 34342 Turkey Attn: Ozlem Ipek Kalaoglu Altan
Publisher Tax ID	EU826007151
Billing Type	Invoice
Billing Address	Ozlem Ipek Kalaoglu Altan Bogazici University Department of Chemistry Bebek Istanbul, Turkey 34342 Attn: Ozlem Ipek Kalaoglu Altan
Total	0.00 USD
Terms and Conditions	

TERMS AND CONDITIONS

This copyrighted material is owned by or exclusively licensed to John Wiley & Sons, Inc. or one of its group companies (each a"Wiley Company") or handled on behalf of a society with

Figure A.1. Copyright permission (cont.).

ROYAL SOCIETY OF CHEMISTRY LICENSE TERMS AND CONDITIONS

Sep 01, 2017

This Agreement between Ozlem Ipek Kalaoglu Altan ("You") and Royal Society of Chemistry ("Royal Society of Chemistry") consists of your license details and the terms and conditions provided by Royal Society of Chemistry and Copyright Clearance Center.

License Number	4180040431836
License date	Sep 01, 2017
Licensed Content Publisher	Royal Society of Chemistry
Licensed Content Publication	Journal of Materials Chemistry B
Licensed Content Title	Engineering of biomimetic nanofibrous matrices for drug delivery and tissue engineering
Licensed Content Author	Chuanglong He,Wei Nie,Wei Feng
Licensed Content Date	Sep 22, 2014
Licensed Content Volume	2
Licensed Content Issue	45
Type of Use	Thesis/Dissertation
Requestor type	academic/educational
Portion	figures/tables/images
Number of figures/tables/images	1
Format	print and electronic
Distribution quantity	1000
Will you be translating?	no
Order reference number	
Title of the thesis/dissertation	Reactive and Clickable Hydrophilic Nanofibers as Novel Biomaterials
Expected completion date	Sep 2017
Estimated size	170
Requestor Location	Ozlem Ipek Kalaoglu Altan Bogazici University Department of Chemistry Bebek Istanbul, 34342 Turkey Attn: Ozlem Ipek Kalaoglu Altan
Billing Type	Invoice
Billing Address	Ozlem Ipek Kalaoglu Altan Bogazici University Department of Chemistry Bebek Istanbul, Turkey 34342 Attn: Ozlem Ipek Kalaoglu Altan
Total	0.00 USD

Terms and Conditions

This License Agreement is between {Requestor Name} (“You”) and The Royal Society of Chemistry (“RSC”) provided by the Copyright Clearance Center (“CCC”). The license consists of

Figure A.1. Copyright permission (cont.).

ROYAL SOCIETY OF CHEMISTRY LICENSE TERMS AND CONDITIONS

Sep 01, 2017

This Agreement between Ozlem Ipek Kalaoglu Altan ("You") and Royal Society of Chemistry ("Royal Society of Chemistry") consists of your license details and the terms and conditions provided by Royal Society of Chemistry and Copyright Clearance Center.

License Number	4180040774691
License date	Sep 01, 2017
Licensed Content Publisher	Royal Society of Chemistry
Licensed Content Publication	Chemical Communications (Cambridge)
Licensed Content Title	Assembly of DNA-functionalized gold nanoparticles on electrospun nanofibers as a fluorescent sensor for nucleic acids
Licensed Content Author	Huaming Wang,Dingzhong Wang,Zhou Peng,Wei Tang,Na Li,Feng Liu
Licensed Content Date	Apr 30, 2013
Licensed Content Volume	49
Licensed Content Issue	49
Type of Use	Thesis/Dissertation
Requestor type	academic/educational
Portion	figures/tables/images
Number of figures/tables/images	1
Format	print and electronic
Distribution quantity	1000
Will you be translating?	no
Order reference number	
Title of the thesis/dissertation	Reactive and Clickable Hydrophilic Nanofibers as Novel Biomaterials
Expected completion date	Sep 2017
Estimated size	170
Requestor Location	Ozlem Ipek Kalaoglu Altan Bogazici University Department of Chemistry Bebek Istanbul, 34342 Turkey Attn: Ozlem Ipek Kalaoglu Altan
Billing Type	Invoice
Billing Address	Ozlem Ipek Kalaoglu Altan Bogazici University Department of Chemistry Bebek Istanbul, Turkey 34342 Attn: Ozlem Ipek Kalaoglu Altan
Total	0.00 USD

Terms and Conditions

This License Agreement is between {Requestor Name} (“You”) and The Royal Society of Chemistry (“RSC”) provided by the Copyright Clearance Center (“CCC”). The license consists of

Figure A.1. Copyright permission (cont.).

THE AMERICAN ASSOCIATION FOR THE ADVANCEMENT OF SCIENCE LICENSE TERMS AND CONDITIONS

Sep 06, 2017

This Agreement between Ozlem Ipek Kalaoglu Altan ("You") and The American Association for the Advancement of Science ("The American Association for the Advancement of Science") consists of your license details and the terms and conditions provided by The American Association for the Advancement of Science and Copyright Clearance Center.

License Number	4183120481372
License date	Sep 06, 2017
Licensed Content Publisher	The American Association for the Advancement of Science
Licensed Content Publication	Science
Licensed Content Title	Direct Evidence of a Dinuclear Copper Intermediate in Cu(I)-Catalyzed Azide-Alkyne Cycloadditions
Licensed Content Author	B. T. Worrell,J. A. Malik,V. V. Fokin
Licensed Content Date	Apr 26, 2013
Licensed Content Volume	340
Licensed Content Issue	6131
Volume number	340
Issue number	6131
Type of Use	Thesis / Dissertation
Requestor type	Scientist/individual at a research institution
Format	Print and electronic
Portion	Figure
Number of figures/tables	1
Order reference number	
Title of your thesis / dissertation	Reactive and Clickable Hydrophilic Nanofibers as Novel Biomaterials
Expected completion date	Sep 2017
Estimated size(pages)	170
Requestor Location	Ozlem Ipek Kalaoglu Altan Bogazici University Department of Chemistry Bebek Istanbul, 34342 Turkey Attn: Ozlem Ipek Kalaoglu Altan
Billing Type	Invoice
Billing Address	Ozlem Ipek Kalaoglu Altan Bogazici University Department of Chemistry Bebek Istanbul, Turkey 34342 Attn: Ozlem Ipek Kalaoglu Altan
Total	0.00 USD
Terms and Conditions	

American Association for the Advancement of Science TERMS AND CONDITIONS

Figure A.1. Copyright permission (cont.).





Title: PEG- and Peptide-Grafted Aliphatic Polyesters by Click Chemistry

Author: Bryan Parrish, Rebecca B. Breitenkamp, Todd Emrick

Publication: Journal of the American Chemical Society

Publisher: American Chemical Society

Date: May 1, 2005

Copyright © 2005, American Chemical Society

Logged in as:
Ozlem Ipek Kalaoglu Altan
Account #:
3000650649
LOGOUT

PERMISSION/LICENSE IS GRANTED FOR YOUR ORDER AT NO CHARGE

This type of permission/license, instead of the standard Terms & Conditions, is sent to you because no fee is being charged for your order. Please note the following:

- Permission is granted for your request in both print and electronic formats, and translations.
- If figures and/or tables were requested, they may be adapted or used in part.
- Please print this page for your records and send a copy of it to your publisher/graduate school.
- Appropriate credit for the requested material should be given as follows: "Reprinted (adapted) with permission from (COMPLETE REFERENCE CITATION). Copyright (YEAR) American Chemical Society." Insert appropriate information in place of the capitalized words.
- One-time permission is granted only for the use specified in your request. No additional uses are granted (such as derivative works or other editions). For any other uses, please submit a new request.

If credit is given to another source for the material you requested, permission must be obtained from that source.

BACK CLOSE WINDOW

Copyright © 2017 Copyright Clearance Center, Inc. All Rights Reserved. Privacy statement. Terms and Conditions.
Comments? We would like to hear from you. E-mail us at customercare@copyright.com

Figure A.1. Copyright permission (cont.).





Title: Soluble Camptothecin Derivatives Prepared by Click Cycloaddition Chemistry on Functional Aliphatic Polyesters

Author: Bryan Parrish, Todd Emrick

Publication: Bioconjugate Chemistry

Publisher: American Chemical Society

Date: Jan 1, 2007

Copyright © 2007, American Chemical Society

Logged in as:
Ozlem Ipek Kalaoglu Altan
Account #:
3000650649

LOGOUT

PERMISSION/LICENSE IS GRANTED FOR YOUR ORDER AT NO CHARGE

This type of permission/license, instead of the standard Terms & Conditions, is sent to you because no fee is being charged for your order. Please note the following:

- Permission is granted for your request in both print and electronic formats, and translations.
- If figures and/or tables were requested, they may be adapted or used in part.
- Please print this page for your records and send a copy of it to your publisher/graduate school.
- Appropriate credit for the requested material should be given as follows: "Reprinted (adapted) with permission from (COMPLETE REFERENCE CITATION). Copyright (YEAR) American Chemical Society." Insert appropriate information in place of the capitalized words.
- One-time permission is granted only for the use specified in your request. No additional uses are granted (such as derivative works or other editions). For any other uses, please submit a new request.

If credit is given to another source for the material you requested, permission must be obtained from that source.

BACK CLOSE WINDOW

Copyright © 2017 Copyright Clearance Center, Inc. All Rights Reserved. Privacy statement. Terms and Conditions.
Comments? We would like to hear from you. E-mail us at customercare@copyright.com

Figure A.1. Copyright permission (cont.).

JOHN WILEY AND SONS LICENSE TERMS AND CONDITIONS

Sep 06, 2017

This Agreement between Ozlem Ipek Kalaoglu Altan ("You") and John Wiley and Sons ("John Wiley and Sons") consists of your license details and the terms and conditions provided by John Wiley and Sons and Copyright Clearance Center.

License Number	4183151300011
License date	Sep 06, 2017
Licensed Content Publisher	John Wiley and Sons
Licensed Content Publication	Angewandte Chemie International Edition
Licensed Content Title	Copper-Free Azide–Alkyne Cycloadditions: New Insights and Perspectives
Licensed Content Author	Jean-François Lutz
Licensed Content Date	Feb 8, 2008
Licensed Content Pages	3
Type of use	Dissertation/Thesis
Requestor type	University/Academic
Format	Print and electronic
Portion	Figure/table
Number of figures/tables	2
Original Wiley figure/table number(s)	scheme 1, scheme 2
Will you be translating?	No
Title of your thesis / dissertation	Reactive and Clickable Hydrophilic Nanofibers as Novel Biomaterials
Expected completion date	Sep 2017
Expected size (number of pages)	170
Requestor Location	Ozlem Ipek Kalaoglu Altan Bogazici University Department of Chemistry Bebek Istanbul, 34342 Turkey Attn: Ozlem Ipek Kalaoglu Altan
Publisher Tax ID	EU826007151
Billing Type	Invoice
Billing Address	Ozlem Ipek Kalaoglu Altan Bogazici University Department of Chemistry Bebek Istanbul, Turkey 34342 Attn: Ozlem Ipek Kalaoglu Altan
Total	0.00 USD
Terms and Conditions	

TERMS AND CONDITIONS

This copyrighted material is owned by or exclusively licensed to John Wiley & Sons, Inc. or one of its group companies (each a"Wiley Company") or handled on behalf of a society with

Figure A.1. Copyright permission (cont.).





Title:	Stealth Polymeric Vesicles via Metal-Free Click Coupling
Author:	Michael J. Isaacman, Eleonora M. Corigliano, Luke S. Theogarajan
Publication:	Biomacromolecules
Publisher:	American Chemical Society
Date:	Sep 1, 2013

Logged in as:
Ozlem Ipek Kalaoglu Altan
Account #: 3000650649
LOGOUT

Copyright © 2013, American Chemical Society

PERMISSION/LICENSE IS GRANTED FOR YOUR ORDER AT NO CHARGE

This type of permission/license, instead of the standard Terms & Conditions, is sent to you because no fee is being charged for your order. Please note the following:

- Permission is granted for your request in both print and electronic formats, and translations.
- If figures and/or tables were requested, they may be adapted or used in part.
- Please print this page for your records and send a copy of it to your publisher/graduate school.
- Appropriate credit for the requested material should be given as follows: "Reprinted (adapted) with permission from (COMPLETE REFERENCE CITATION). Copyright (YEAR) American Chemical Society." Insert appropriate information in place of the capitalized words.
- One-time permission is granted only for the use specified in your request. No additional uses are granted (such as derivative works or other editions). For any other uses, please submit a new request.

If credit is given to another source for the material you requested, permission must be obtained from that source.

BACK CLOSE WINDOW

Copyright © 2017 Copyright Clearance Center, Inc. All Rights Reserved. Privacy statement. Terms and Conditions.
Comments? We would like to hear from you. E-mail us at customercare@copyright.com

Figure A.1. Copyright permission (cont.).

ROYAL SOCIETY OF CHEMISTRY LICENSE TERMS AND CONDITIONS

Sep 06, 2017

This Agreement between Ozlem Ipek Kalaoglu Altan ("You") and Royal Society of Chemistry ("Royal Society of Chemistry") consists of your license details and the terms and conditions provided by Royal Society of Chemistry and Copyright Clearance Center.

License Number	4183130141531
License date	Sep 06, 2017
Licensed Content Publisher	Royal Society of Chemistry
Licensed Content Publication	Polymer Chemistry
Licensed Content Title	Thiol–ene "click" reactions and recent applications in polymer and materials synthesis: a first update
Licensed Content Author	Andrew B. Lowe
Licensed Content Date	May 1, 2014
Licensed Content Volume	5
Licensed Content Issue	17
Type of Use	Thesis/Dissertation
Requestor type	academic/educational
Portion	figures/tables/images
Number of figures/tables/images	1
Format	print and electronic
Distribution quantity	10
Will you be translating?	no
Order reference number	
Title of the thesis/dissertation	Reactive and Clickable Hydrophilic Nanofibers as Novel Biomaterials
Expected completion date	Sep 2017
Estimated size	170
Requestor Location	Ozlem Ipek Kalaoglu Altan Bogazici University Department of Chemistry Bebek Istanbul, 34342 Turkey Attn: Ozlem Ipek Kalaoglu Altan
Billing Type	Invoice
Billing Address	Ozlem Ipek Kalaoglu Altan Bogazici University Department of Chemistry Bebek Istanbul, Turkey 34342 Attn: Ozlem Ipek Kalaoglu Altan
Total	0.00 USD

Terms and Conditions

This License Agreement is between {Requestor Name} ("You") and The Royal Society of Chemistry ("RSC") provided by the Copyright Clearance Center ("CCC"). The license consists of

Figure A.1. Copyright permission (cont.).

ROYAL SOCIETY OF CHEMISTRY LICENSE TERMS AND CONDITIONS

Sep 06, 2017

This Agreement between Ozlem Ipek Kalaoglu Altan ("You") and Royal Society of Chemistry ("Royal Society of Chemistry") consists of your license details and the terms and conditions provided by Royal Society of Chemistry and Copyright Clearance Center.

License Number	4183130141531
License date	Sep 06, 2017
Licensed Content Publisher	Royal Society of Chemistry
Licensed Content Publication	Polymer Chemistry
Licensed Content Title	Thiol–ene "click" reactions and recent applications in polymer and materials synthesis: a first update
Licensed Content Author	Andrew B. Lowe
Licensed Content Date	May 1, 2014
Licensed Content Volume	5
Licensed Content Issue	17
Type of Use	Thesis/Dissertation
Requestor type	academic/educational
Portion	figures/tables/images
Number of figures/tables/images	1
Format	print and electronic
Distribution quantity	10
Will you be translating?	no
Order reference number	
Title of the thesis/dissertation	Reactive and Clickable Hydrophilic Nanofibers as Novel Biomaterials
Expected completion date	Sep 2017
Estimated size	170
Requestor Location	Ozlem Ipek Kalaoglu Altan Bogazici University Department of Chemistry Bebek Istanbul, 34342 Turkey Attn: Ozlem Ipek Kalaoglu Altan
Billing Type	Invoice
Billing Address	Ozlem Ipek Kalaoglu Altan Bogazici University Department of Chemistry Bebek Istanbul, Turkey 34342 Attn: Ozlem Ipek Kalaoglu Altan
Total	0.00 USD

Terms and Conditions

This License Agreement is between {Requestor Name} ("You") and The Royal Society of Chemistry ("RSC") provided by the Copyright Clearance Center ("CCC"). The license consists of

Figure A.1. Copyright permission (cont.).





Title: Organocatalytic Synthesis and Postpolymerization Functionalization of Allyl-Functional Poly(carbonate)s

Author: Sarah Tempelaar, Laetitia Mespouille, Philippe Dubois, et al

Publication: Macromolecules

Publisher: American Chemical Society

Date: Apr 1, 2011

Copyright © 2011, American Chemical Society

Logged in as:
Ozlem Ipek Kalaoglu Altan
Account #:
3000650649

LOGOUT

PERMISSION/LICENSE IS GRANTED FOR YOUR ORDER AT NO CHARGE

This type of permission/license, instead of the standard Terms & Conditions, is sent to you because no fee is being charged for your order. Please note the following:

- Permission is granted for your request in both print and electronic formats, and translations.
- If figures and/or tables were requested, they may be adapted or used in part.
- Please print this page for your records and send a copy of it to your publisher/graduate school.
- Appropriate credit for the requested material should be given as follows: "Reprinted (adapted) with permission from (COMPLETE REFERENCE CITATION). Copyright (YEAR) American Chemical Society." Insert appropriate information in place of the capitalized words.
- One-time permission is granted only for the use specified in your request. No additional uses are granted (such as derivative works or other editions). For any other uses, please submit a new request.

If credit is given to another source for the material you requested, permission must be obtained from that source.

BACK CLOSE WINDOW

Copyright © 2017 Copyright Clearance Center, Inc. All Rights Reserved. Privacy statement. Terms and Conditions.
Comments? We would like to hear from you. E-mail us at customercare@copyright.com

Figure A.1. Copyright permission (cont.).

NRC RESEARCH PRESS LICENSE
TERMS AND CONDITIONS

Sep 06, 2017

This Agreement between Ozlem Ipek Kalaoglu Altan ("You") and NRC Research Press ("NRC Research Press") consists of your license details and the terms and conditions provided by NRC Research Press and Copyright Clearance Center.

License Number	4183131382957
License date	Sep 06, 2017
Licensed Content Publisher	NRC Research Press
Licensed Content Publication	Canadian Journal of Chemistry
Licensed Content Title	THE THERMAL REVERSIBILITY OF THE MICHAEL REACTION: I. NITRILES
Licensed Content Author	C. F. H. Allen, G. P. Happ
Licensed Content Date	Mar 1, 1964
Licensed Content Volume	42
Licensed Content Issue	3
Type of Use	Thesis/Dissertation
Requestor type	Academic
Format	Print and electronic
Portion	Figure/table
Number of figures/tables	2
Order reference number	
Title of your thesis / dissertation	Reactive and Clickable Hydrophilic Nanofibers as Novel Biomaterials
Expected completion date	Sep 2017
Estimated size(pages)	170
Requestor Location	Ozlem Ipek Kalaoglu Altan Bogazici University Department of Chemistry Bebek Istanbul, 34342 Turkey Attn: Ozlem Ipek Kalaoglu Altan
Billing Type	Invoice
Billing Address	Ozlem Ipek Kalaoglu Altan Bogazici University Department of Chemistry Bebek Istanbul, Turkey 34342 Attn: Ozlem Ipek Kalaoglu Altan
Total	0.00 USD
Terms and Conditions	

General Terms & Conditions

Permission is granted upon the requester's compliance with the following terms and conditions:

1. A credit line will be prominently placed in your product(s) and include: for books the author, book title, editor, copyright holder, year of publication; for journals the author, title of article, title of journal, volume number, issue number, and the inclusive pages. The credit

Figure A.1. Copyright permission (cont.).





Title: Synthesis and Functionalization of Thiol-Reactive Biodegradable Polymers

Author: Sebla Onbulak, Sarah Tempelaar, Ryan J. Pounder, et al

Publication: Macromolecules

Publisher: American Chemical Society

Date: Feb 1, 2012

Copyright © 2012, American Chemical Society

Logged in as:
Ozlem Ipek Kalaoglu Altan
Account #:
3000650649

LOGOUT

PERMISSION/LICENSE IS GRANTED FOR YOUR ORDER AT NO CHARGE

This type of permission/license, instead of the standard Terms & Conditions, is sent to you because no fee is being charged for your order. Please note the following:

- Permission is granted for your request in both print and electronic formats, and translations.
- If figures and/or tables were requested, they may be adapted or used in part.
- Please print this page for your records and send a copy of it to your publisher/graduate school.
- Appropriate credit for the requested material should be given as follows: "Reprinted (adapted) with permission from (COMPLETE REFERENCE CITATION). Copyright (YEAR) American Chemical Society." Insert appropriate information in place of the capitalized words.
- One-time permission is granted only for the use specified in your request. No additional uses are granted (such as derivative works or other editions). For any other uses, please submit a new request.

If credit is given to another source for the material you requested, permission must be obtained from that source.

BACK CLOSE WINDOW

Copyright © 2017 Copyright Clearance Center, Inc. All Rights Reserved. Privacy statement. Terms and Conditions.
Comments? We would like to hear from you. E-mail us at customercare@copyright.com

Figure A.1. Copyright permission (cont.).





Title: Orthogonal Modification of Norbornene-Functional Degradable Polymers

Author: Rebecca J. Williams, Ian A. Barker, Rachel K. O'Reilly, et al

Publication: ACS Macro Letters

Publisher: American Chemical Society

Date: Nov 1, 2012

Copyright © 2012, American Chemical Society

Logged in as:
Ozlem Ipek Kalaoglu Altan
Account #:
3000650649

LOGOUT

PERMISSION/LICENSE IS GRANTED FOR YOUR ORDER AT NO CHARGE

This type of permission/license, instead of the standard Terms & Conditions, is sent to you because no fee is being charged for your order. Please note the following:

- Permission is granted for your request in both print and electronic formats, and translations.
- If figures and/or tables were requested, they may be adapted or used in part.
- Please print this page for your records and send a copy of it to your publisher/graduate school.
- Appropriate credit for the requested material should be given as follows: "Reprinted (adapted) with permission from (COMPLETE REFERENCE CITATION). Copyright (YEAR) American Chemical Society." Insert appropriate information in place of the capitalized words.
- One-time permission is granted only for the use specified in your request. No additional uses are granted (such as derivative works or other editions). For any other uses, please submit a new request.

If credit is given to another source for the material you requested, permission must be obtained from that source.

BACK CLOSE WINDOW

Copyright © 2017 Copyright Clearance Center, Inc. All Rights Reserved. Privacy statement. Terms and Conditions.
Comments? We would like to hear from you. E-mail us at customercare@copyright.com

Figure A.1. Copyright permission (cont.).

JOHN WILEY AND SONS LICENSE TERMS AND CONDITIONS

Sep 06, 2017

This Agreement between Ozlem Ipek Kalaoglu Altan ("You") and John Wiley and Sons ("John Wiley and Sons") consists of your license details and the terms and conditions provided by John Wiley and Sons and Copyright Clearance Center.

License Number	4183140664307
License date	Sep 06, 2017
Licensed Content Publisher	John Wiley and Sons
Licensed Content Publication	Journal of Polymer Science Part A: Polymer Chemistry
Licensed Content Title	Various polycarbonate graft copolymers via diels–alder click reaction
Licensed Content Author	Aydan Dag,Mehtap Aydin,Hakan Durmaz,Gurkan Hizal,Umit Tunca
Licensed Content Date	Jul 30, 2012
Licensed Content Pages	8
Type of use	Dissertation/Thesis
Requestor type	University/Academic
Format	Print and electronic
Portion	Figure/table
Number of figures/tables	2
Original Wiley figure/table number(s)	scheme 1, scheme 2
Will you be translating?	No
Title of your thesis / dissertation	Reactive and Clickable Hydrophilic Nanofibers as Novel Biomaterials
Expected completion date	Sep 2017
Expected size (number of pages)	170
Requestor Location	Ozlem Ipek Kalaoglu Altan Bogazici University Department of Chemistry Bebek Istanbul, 34342 Turkey Attn: Ozlem Ipek Kalaoglu Altan
Publisher Tax ID	EU826007151
Billing Type	Invoice
Billing Address	Ozlem Ipek Kalaoglu Altan Bogazici University Department of Chemistry Bebek Istanbul, Turkey 34342 Attn: Ozlem Ipek Kalaoglu Altan
Total	0.00 USD
Terms and Conditions	

TERMS AND CONDITIONS

This copyrighted material is owned by or exclusively licensed to John Wiley & Sons, Inc. or one of its group companies (each a"Wiley Company") or handled on behalf of a society with which a Wiley Company has exclusive publishing rights in relation to a particular work

Figure A.1. Copyright permission (cont.).

ELSEVIER LICENSE
TERMS AND CONDITIONS

Sep 06, 2017

This Agreement between Ozlem Ipek Kalaoglu Altan ("You") and Elsevier ("Elsevier") consists of your license details and the terms and conditions provided by Elsevier and Copyright Clearance Center.

License Number	4183140888716
License date	Sep 06, 2017
Licensed Content Publisher	Elsevier
Licensed Content Publication	Biomaterials
Licensed Content Title	The immobilization of proteins on biodegradable polymer fibers via click chemistry
Licensed Content Author	Quan Shi,Xuesi Chen,Tiancheng Lu,Xiabin Jing
Licensed Content Date	Mar 1, 2008
Licensed Content Volume	29
Licensed Content Issue	8
Licensed Content Pages	9
Start Page	1118
End Page	1126
Type of Use	reuse in a thesis/dissertation
Intended publisher of new work	other
Portion	figures/tables/illustrations
Number of figures/tables/illustrations	3
Format	both print and electronic
Are you the author of this Elsevier article?	No
Will you be translating?	No
Original figure numbers	Figure 1 , scheme 1, scheme 2
Title of your thesis/dissertation	Reactive and Clickable Hydrophilic Nanofibers as Novel Biomaterials
Expected completion date	Sep 2017
Estimated size (number of pages)	170
Requestor Location	Ozlem Ipek Kalaoglu Altan Bogazici University Department of Chemistry Bebek Istanbul, 34342 Turkey Attn: Ozlem Ipek Kalaoglu Altan
Total	0.00 USD
Terms and Conditions	

INTRODUCTION

1. The publisher for this copyrighted material is Elsevier. By clicking "accept" in connection with completing this licensing transaction, you agree that the following terms and conditions

Figure A.1. Copyright permission (cont.).





Title: Postelectrospinning "Click" Modification of Degradable Amino Acid-Based Poly(ester urea) Nanofibers

Author: Fei Lin, Jiayi Yu, Wen Tang, et al

Publication: Macromolecules

Publisher: American Chemical Society

Date: Dec 1, 2013

Copyright © 2013, American Chemical Society

Logged in as:
Ozlem Ipek Kalaoglu Altan
Account #:
3000650649

LOGOUT

PERMISSION/LICENSE IS GRANTED FOR YOUR ORDER AT NO CHARGE

This type of permission/license, instead of the standard Terms & Conditions, is sent to you because no fee is being charged for your order. Please note the following:

- Permission is granted for your request in both print and electronic formats, and translations.
- If figures and/or tables were requested, they may be adapted or used in part.
- Please print this page for your records and send a copy of it to your publisher/graduate school.
- Appropriate credit for the requested material should be given as follows: "Reprinted (adapted) with permission from (COMPLETE REFERENCE CITATION). Copyright (YEAR) American Chemical Society." Insert appropriate information in place of the capitalized words.
- One-time permission is granted only for the use specified in your request. No additional uses are granted (such as derivative works or other editions). For any other uses, please submit a new request.

If credit is given to another source for the material you requested, permission must be obtained from that source.

BACK CLOSE WINDOW

Copyright © 2017 Copyright Clearance Center, Inc. All Rights Reserved. Privacy statement. Terms and Conditions.
Comments? We would like to hear from you. E-mail us at customercare@copyright.com

Figure A.1. Copyright permission (cont.).

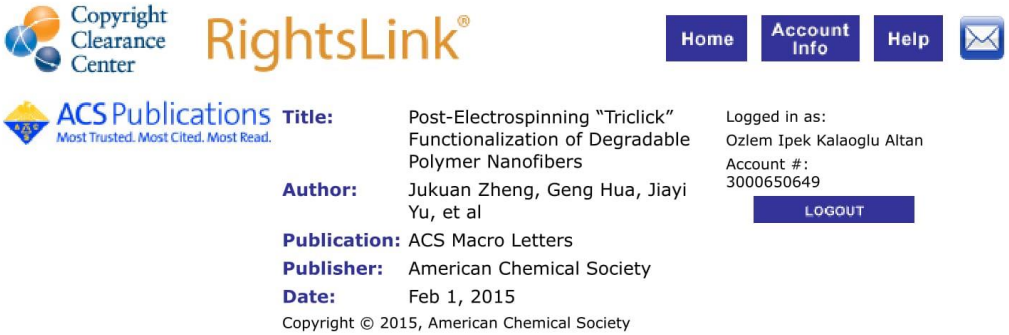

PERMISSION/LICENSE IS GRANTED FOR YOUR ORDER AT NO CHARGE

This type of permission/license, instead of the standard Terms & Conditions, is sent to you because no fee is being charged for your order. Please note the following:

- Permission is granted for your request in both print and electronic formats, and translations.
- If figures and/or tables were requested, they may be adapted or used in part.
- Please print this page for your records and send a copy of it to your publisher/graduate school.
- Appropriate credit for the requested material should be given as follows: "Reprinted (adapted) with permission from (COMPLETE REFERENCE CITATION). Copyright (YEAR) American Chemical Society." Insert appropriate information in place of the capitalized words.
- One-time permission is granted only for the use specified in your request. No additional uses are granted (such as derivative works or other editions). For any other uses, please submit a new request.

If credit is given to another source for the material you requested, permission must be obtained from that source.

BACK CLOSE WINDOW

Copyright © 2017 Copyright Clearance Center, Inc. All Rights Reserved. Privacy statement. Terms and Conditions.
Comments? We would like to hear from you. E-mail us at customercare@copyright.com

Figure A.1. Copyright permission (cont.).



Home | Account Info | Help



Title:	Post-Assembly Derivatization of Electrospun Nanofibers via Strain-Promoted Azide Alkyne Cycloaddition	Logged in as: Ozlem Ipek Kalaoglu Altan Account #: 3000650649 LOGOUT
Author:	Jukuan Zheng, Kaiyi Liu, Darrell H. Reneker, et al	
Publication:	Journal of the American Chemical Society	
Publisher:	American Chemical Society	
Date:	Oct 1, 2012	

Copyright © 2012, American Chemical Society

PERMISSION/LICENSE IS GRANTED FOR YOUR ORDER AT NO CHARGE

This type of permission/license, instead of the standard Terms & Conditions, is sent to you because no fee is being charged for your order. Please note the following:

- Permission is granted for your request in both print and electronic formats, and translations.
- If figures and/or tables were requested, they may be adapted or used in part.
- Please print this page for your records and send a copy of it to your publisher/graduate school.
- Appropriate credit for the requested material should be given as follows: "Reprinted (adapted) with permission from (COMPLETE REFERENCE CITATION). Copyright (YEAR) American Chemical Society." Insert appropriate information in place of the capitalized words.
- One-time permission is granted only for the use specified in your request. No additional uses are granted (such as derivative works or other editions). For any other uses, please submit a new request.

If credit is given to another source for the material you requested, permission must be obtained from that source.

BACK | CLOSE WINDOW

Copyright © 2017 Copyright Clearance Center, Inc. All Rights Reserved. Privacy statement. Terms and Conditions.
Comments? We would like to hear from you. E-mail us at customercare@copyright.com

Figure A.1. Copyright permission (cont.).

ELSEVIER LICENSE
TERMS AND CONDITIONS

Sep 06, 2017

This Agreement between Ozlem Ipek Kalaoglu Altan ("You") and Elsevier ("Elsevier") consists of your license details and the terms and conditions provided by Elsevier and Copyright Clearance Center.

License Number	4183150733196
License date	Sep 06, 2017
Licensed Content Publisher	Elsevier
Licensed Content Publication	Biomaterials
Licensed Content Title	Directed differentiation and neurite extension of mouse embryonic stem cell on aligned poly(lactide) nanofibers functionalized with YIGSR peptide
Licensed Content Author	Laura A. Smith Callahan,Sibai Xie,Ian A. Barker,Jukuan Zheng,Darrell H. Reneker,Andrew P. Dove,Matthew L. Becker
Licensed Content Date	Dec 1, 2013
Licensed Content Volume	34
Licensed Content Issue	36
Licensed Content Pages	7
Start Page	9089
End Page	9095
Type of Use	reuse in a thesis/dissertation
Intended publisher of new work	other
Portion	figures/tables/illustrations
Number of figures/tables/illustrations	3
Format	both print and electronic
Are you the author of this Elsevier article?	No
Will you be translating?	No
Original figure numbers	Figure 1, Figure 2 Figure 3
Title of your thesis/dissertation	Reactive and Clickable Hydrophilic Nanofibers as Novel Biomaterials
Expected completion date	Sep 2017
Estimated size (number of pages)	170
Requestor Location	Ozlem Ipek Kalaoglu Altan Bogazici University Department of Chemistry Bebek Istanbul, 34342 Turkey Attn: Ozlem Ipek Kalaoglu Altan
Total	0.00 USD
Terms and Conditions	

INTRODUCTION

Figure A.1. Copyright permission (cont.).





Title: Functionalized Nanoporous Thin Films and Fibers from Photocleavable Block Copolymers Featuring Activated Esters

Author: Hui Zhao, Weiyin Gu, Michael W. Thielke, et al

Publication: Macromolecules

Publisher: American Chemical Society

Date: Jul 1, 2013

Copyright © 2013, American Chemical Society

Logged in as:
Ozlem Ipek Kalaoglu Altan
Account #:
3000650649

LOGOUT

PERMISSION/LICENSE IS GRANTED FOR YOUR ORDER AT NO CHARGE

This type of permission/license, instead of the standard Terms & Conditions, is sent to you because no fee is being charged for your order. Please note the following:

- Permission is granted for your request in both print and electronic formats, and translations.
- If figures and/or tables were requested, they may be adapted or used in part.
- Please print this page for your records and send a copy of it to your publisher/graduate school.
- Appropriate credit for the requested material should be given as follows: "Reprinted (adapted) with permission from (COMPLETE REFERENCE CITATION). Copyright (YEAR) American Chemical Society." Insert appropriate information in place of the capitalized words.
- One-time permission is granted only for the use specified in your request. No additional uses are granted (such as derivative works or other editions). For any other uses, please submit a new request.

If credit is given to another source for the material you requested, permission must be obtained from that source.

BACK CLOSE WINDOW

Copyright © 2017 Copyright Clearance Center, Inc. All Rights Reserved. Privacy statement. Terms and Conditions.
Comments? We would like to hear from you. E-mail us at customercare@copyright.com

Figure A.1. Copyright permission (cont.).

ROYAL SOCIETY OF CHEMISTRY LICENSE TERMS AND CONDITIONS

Sep 06, 2017

This Agreement between Ozlem Ipek Kalaoglu Altan ("You") and Royal Society of Chemistry ("Royal Society of Chemistry") consists of your license details and the terms and conditions provided by Royal Society of Chemistry and Copyright Clearance Center.

License Number	4183160280500
License date	Sep 06, 2017
Licensed Content Publisher	Royal Society of Chemistry
Licensed Content Publication	Polymer Chemistry
Licensed Content Title	Diels–Alder "click" reactions: recent applications in polymer and material science
Licensed Content Author	Mehmet Atilla Tasdelen
Licensed Content Date	May 27, 2011
Licensed Content Volume	2
Licensed Content Issue	10
Type of Use	Thesis/Dissertation
Requestor type	academic/educational
Portion	figures/tables/images
Number of figures/tables/images	1
Format	print and electronic
Distribution quantity	10
Will you be translating?	no
Order reference number	
Title of the thesis/dissertation	Reactive and Clickable Hydrophilic Nanofibers as Novel Biomaterials
Expected completion date	Sep 2017
Estimated size	170
Requestor Location	Ozlem Ipek Kalaoglu Altan Bogazici University Department of Chemistry Bebek Istanbul, 34342 Turkey Attn: Ozlem Ipek Kalaoglu Altan
Billing Type	Invoice
Billing Address	Ozlem Ipek Kalaoglu Altan Bogazici University Department of Chemistry Bebek Istanbul, Turkey 34342 Attn: Ozlem Ipek Kalaoglu Altan
Total	0.00 USD

Terms and Conditions

This License Agreement is between {Requestor Name} ("You") and The Royal Society of Chemistry ("RSC") provided by the Copyright Clearance Center ("CCC"). The license consists of

Figure A.1. Copyright permission (cont.).



Home | Create Account | Help



Title: "Clickable" Polymeric Nanofibers through Hydrophilic–Hydrophobic Balance: Fabrication of Robust Biomolecular Immobilization Platforms

Author: Ozlem I. Kalaoglu-Altan, Rana Sanyal, Amitav Sanyal

Publication: Biomacromolecules

Publisher: American Chemical Society

Date: May 1, 2015

Copyright © 2015, American Chemical Society

LOGIN

If you're a copyright.com user, you can login to RightsLink using your copyright.com credentials. Already **a RightsLink user** or want to learn more?

PERMISSION/LICENSE IS GRANTED FOR YOUR ORDER AT NO CHARGE

This type of permission/license, instead of the standard Terms & Conditions, is sent to you because no fee is being charged for your order. Please note the following:

- Permission is granted for your request in both print and electronic formats, and translations.
- If figures and/or tables were requested, they may be adapted or used in part.
- Please print this page for your records and send a copy of it to your publisher/graduate school.
- Appropriate credit for the requested material should be given as follows: "Reprinted (adapted) with permission from (COMPLETE REFERENCE CITATION). Copyright (YEAR) American Chemical Society." Insert appropriate information in place of the capitalized words.
- One-time permission is granted only for the use specified in your request. No additional uses are granted (such as derivative works or other editions). For any other uses, please submit a new request.

BACK | CLOSE WINDOW

Copyright © 2017 Copyright Clearance Center, Inc. All Rights Reserved. Privacy statement. Terms and Conditions.
Comments? We would like to hear from you. E-mail us at customercare@copyright.com

Figure A.1. Copyright permission (cont.).

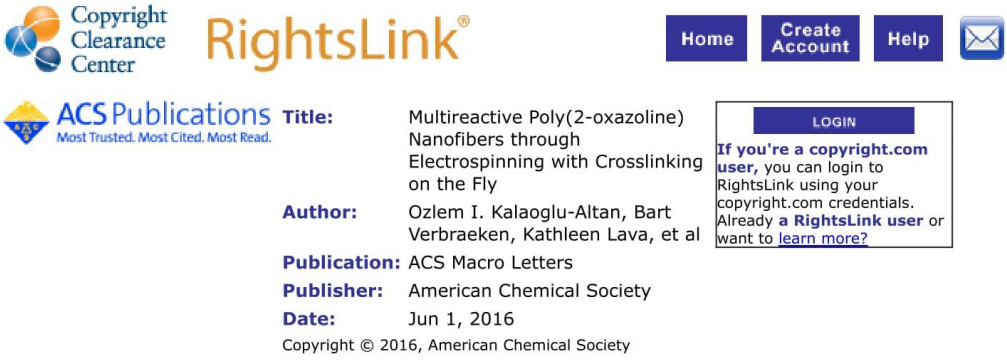

PERMISSION/LICENSE IS GRANTED FOR YOUR ORDER AT NO CHARGE

This type of permission/license, instead of the standard Terms & Conditions, is sent to you because no fee is being charged for your order. Please note the following:

- Permission is granted for your request in both print and electronic formats, and translations.
- If figures and/or tables were requested, they may be adapted or used in part.
- Please print this page for your records and send a copy of it to your publisher/graduate school.
- Appropriate credit for the requested material should be given as follows: "Reprinted (adapted) with permission from (COMPLETE REFERENCE CITATION). Copyright (YEAR) American Chemical Society." Insert appropriate information in place of the capitalized words.
- One-time permission is granted only for the use specified in your request. No additional uses are granted (such as derivative works or other editions). For any other uses, please submit a new request.

BACK CLOSE WINDOW

Copyright © 2017 Copyright Clearance Center, Inc. All Rights Reserved. Privacy statement. Terms and Conditions.
Comments? We would like to hear from you. E-mail us at customercare@copyright.com

Figure A.1. Copyright permission (cont.).

Copyright Clearance Center RightsLink®

Home Create Account Help

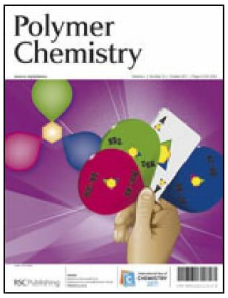

Title: Reactive and 'clickable' electrospun polymeric nanofibers

Author: Ozlem I. Kalaoglu-Altan,Rana Sanyal,Amitav Sanyal

Publication: Polymer Chemistry

Publisher: Royal Society of Chemistry

Date: Jan 1, 0023

Copyright © 2015, Royal Society of Chemistry

LOGIN

If you're a copyright.com user, you can login to RightsLink using your copyright.com credentials. Already **a RightsLink user** or want to learn more?

This reuse request is free of charge. Please review guidelines related to author permissions here: http://www.rsc.org/AboutUs/Copyright/Permissionrequests.asp

BACK CLOSE WINDOW

Copyright © 2017 Copyright Clearance Center, Inc. All Rights Reserved. Privacy statement. Terms and Conditions.
Comments? We would like to hear from you. E-mail us at customercare@copyright.com

Figure A.1. Copyright permission (cont.).





Title: Diels–Alder "Clickable" Biodegradable Nanofibers: Benign Tailoring of Scaffolds for Biomolecular Immobilization and Cell Growth

Author: Ozlem Ipek Kalaoglu-Altan, Azize Kirac-Aydin, Burcu Sumer Bolu, et al

Publication: Bioconjugate Chemistry

Publisher: American Chemical Society

Date: Sep 1, 2017

Copyright © 2017, American Chemical Society

LOGIN

If you're a copyright.com user, you can login to RightsLink using your copyright.com credentials. Already **a RightsLink user** or want to learn more?

PERMISSION/LICENSE IS GRANTED FOR YOUR ORDER AT NO CHARGE

This type of permission/license, instead of the standard Terms & Conditions, is sent to you because no fee is being charged for your order. Please note the following:

- Permission is granted for your request in both print and electronic formats, and translations.
- If figures and/or tables were requested, they may be adapted or used in part.
- Please print this page for your records and send a copy of it to your publisher/graduate school.
- Appropriate credit for the requested material should be given as follows: "Reprinted (adapted) with permission from (COMPLETE REFERENCE CITATION). Copyright (YEAR) American Chemical Society." Insert appropriate information in place of the capitalized words.
- One-time permission is granted only for the use specified in your request. No additional uses are granted (such as derivative works or other editions). For any other uses, please submit a new request.

BACK CLOSE WINDOW

Copyright © 2017 Copyright Clearance Center, Inc. All Rights Reserved. Privacy statement. Terms and Conditions.
Comments? We would like to hear from you. E-mail us at customercare@copyright.com

Figure A.1. Copyright permission (cont.).